VNIVERSITAT DE VALÈNCIA

Programa de Doctorat en Biomedicina i Biotecnologia

Línea d'investigació en Biotecnologia de la Reproducció Humana Assistida

INTERNATIONAL PhD THESIS

LH administration as a potential strategy for ovarian protection and female fertility preservation against highly gonadotoxic chemotherapy

Author:

Luis Miguel del Castillo Lima

Supervised by:

Dr. Sonia Herraiz Raya

Prof. Antonio Pellicer Martínez

Valencia, October 2022

Dra. Sonia Herraiz Raya, Doctora en Biología, Investigadora principal del área de Rejuvenecimiento ovárico y Preservación de la fertilidad en Fundación IVI (FIVI) y miembro del grupo de Investigación en Medicina Reproductiva del Instituto de Investigación Sanitaria (IIS) La Fe.

CERTIFICA:

Que el trabajo de investigación titulado: **"LH administration as a potential strategy for ovarian protection and female fertility preservation against highly gonadotoxic chemotherapy"** ha sido realizado íntegramente por Luis Miguel del Castillo Lima bajo mi dirección. Dicha memoria está concluida y reúne todos los requisitos para su presentación y defensa como TESIS DOCTORAL ante un tribunal.

Y para que así conste a los efectos oportunos, firmo la presente certificación en Valencia a 9 de mayo de 2022.

Fdo. Dra. Sonia Herraiz Raya

Prof. Antonio Pellicer Martínez, Catedràtic en Ginecologia, Doctor en Medicina i Cirurgia, Professor titular del Departament de Pediatria, Obstetrícia i Ginecologia de la Facultat de Medicina i Odontologia de la Universitat de València, fundador del Instituto Valenciano de Infertilidad y presidente de la Fundación IVI.

CERTIFICA:

Que el trabajo de investigación titulado: **"LH administration as a potential strategy for ovarian protection and female fertility preservation against highly gonadotoxic chemotherapy"** ha sido realizado íntegramente por Luis Miguel del Castillo Lima bajo mi dirección. Dicha memoria está concluida y reúne todos los requisitos para su presentación y defensa como TESIS DOCTORAL ante un tribunal.

Y para que así conste a los efectos oportunos, firmo la presente certificación en Valencia a 9 de mayo de 2022.

Fdo. Prof. Antonio Pellicer Martínez

El presente trabajo de tesis doctoral ha sido realizado en los laboratorios de Fundación IVI, así como en los laboratorios del Departament de Pediatria, Obstetrícia i Ginecologia, en el Servei de Microscòpia de la Unitat Central d'Investigació de Medicina, y en el animalario de la Facultat de Medicina i Odontologia de la Universitat de València.

Gracias a la ayuda de un proyecto de investigación con la Universitat de València en la Facultat de Medicina i Odontologia, Departament de Pediatria, Obstetrícia i Ginecologia, que ha sido financiado por la ayuda PROMETEO de la Generalitat Valenciana para la realización de proyectos I+D para grupos de investigación (PROMETEO/2018/137), por el programa de ayudas para la formación de profesorado universitario (FPU) del Ministerio de Universidades (FPU16/05264), y por la ayuda Acción Estratégica de Salud (ISCIII, CP19/00141) del Instituto de Salud Carlos III.

Agradecimientos

Ya está, finalmente he terminado mi tesis doctoral. Muchas veces he pensado, incluso deseado, que llegara el momento en el que pudiera agradecer a todas las personas que han participado en esta aventura. Como toda gran historia que se precie, no puedo negar que esta andadura se ha visto expuesta a numerosos obstáculos que han hecho peligrar su final. ¿Quién diría que fuera a acabar bien? ¿Cómo creerías que terminaría el viaje cuando estás inmerso en la oscuridad? Al final te das cuenta que todo es pasajero, todo lo malo se deja atrás para dar paso a un nuevo día. Y cuando el sol brilla, lo hace más radiante que antes. Es entonces cuando te das cuenta que esas malas experiencias son igual, o incluso más útiles que los buenos momentos porque son las que te enseñan realmente a entender cómo eres. Estas historias en las que sus protagonistas no se rinden, y siguen constantemente adelante hasta el final porque persiguen una meta, son las que llenan el corazón de los lectores. Del mismo modo, en la mayoría de historias nos encontramos con varios protagonistas acompañados de uno o varios grupos de personajes, cuyos destinos se entrelazan para alcanzar un objetivo común. Es por ello que en las siguientes líneas quiero agradecer a todos y cada uno de los actores que me han seguido en esta etapa para conseguir alcanzar este día.

En primer lugar, quisiera darles las gracias a mis directores de tesis, ya que sin ellos esto no habría sido posible. Al doctor Antonio Pellicer, por haberme dado la oportunidad de realizar esta tesis doctoral en su equipo, así como por sus sugerencias e ideas. A la doctora Sonia Herraiz, gracias por todos tus consejos y comentarios a lo largo de estos años que me han ayudado a tener un pensamiento más crítico, reflexivo, y enriquecedor desde el punto de vista científico. También me gustaría agradecer al doctor Nicolás Garrido que me haya dejado formar parte de esa gran familia que es Fundación IVI y de su confianza durante todos estos años. Nico, gracias de verdad. No puedo terminar este párrafo sin incluir al resto de investigadores principales: César, Horten, Irene, Paco y Patri; quienes además de haber sido fantásticos profesores durante el máster, sois también grandes personas en el ámbito personal. Querría destacar en especial a Irene, gracias por darme tu apoyo, consejo, sinceridad y ayuda en los momentos en los que lo he necesitado.

Ahora me gustaría dar las gracias a los compañeros de viaje, a quienes les debo infinitamente esta tesis. Una cosa positiva de no haber tenido un despacho fijo durante todos estos años es que me ha dado la oportunidad de conoceros un poquito mejor a cada uno de vosotros, y con ello valorar lo que cuesta encontrar tan buenas personas. A Anna, has sido imprescindible en todos los aspectos. Has sido mi tutora en los primeros años, quien me ha enseñado realmente gran parte de lo que he aprendido en el laboratorio durante esta etapa, y quien me ha ayudado en todos los ámbitos. Has sido un pilar, alguien que me ha escuchado, aconsejado y consolado, alguien a quien me he mostrado como soy, y con quien he reído dentro y fuera del trabajo. En definitiva, eres una amiga. A Jessica, gracias por ser como eres y por tus locuras con las que nos hemos reído tantas veces, pero también gracias por tu comprensión en muchas ocasiones y tus consejos. Eres una auténtica crack. A María, por las charlas y buenos momentos en el gran despacho que hicimos a partir de un comedor. A Lucía, mi “negra” favorita y compañera de cervezas, gracias por darme tus consejos y ser una amiga dentro y fuera del trabajo. A Rober, mi hombre infusiones, gracias por dejarme aprender de ti y por tener tan buen corazón. Sabes que mi ludoteca estará siempre disponible para ti. A Pepi, por el buen rollo y salero que llevas contigo a todas partes, aunque no estés bien. Gracias por escucharme y apoyarme en todo lo que hemos hablado, por tu humildad y la confianza que nos hemos demostrado. Tienes un amigo para todo lo que necesites. A Almu, junto con Majo seremos siempre los pollitos de la ESHRE que no pueden ir separados. Gracias por tu ayuda estos años con los papeleos y tu confianza. A Rosalba, gracias por escucharme y enseñarme un poquito tu Canadá. A MC, gracias por tus consejos y conversaciones en momentos en los que más falta han hecho. A Yassmin, por tu positividad y sinceridad, gracias por dejarme conocerte cómo eres y tus preocupaciones, ya sabes que siempre podrás contar conmigo para lo que necesites. A Emilio, gracias por llamarme jefe, pero aquí el único jefe que hay eres tú. Gracias por dejarme conocerte y por tu humildad. A Elena, por los buenos momentos fuera del trabajo. Ahora es el momento de darle las gracias al alma de Fundación IVI. Sin estas dos personas, ni esta tesis ni el resto serían igual. Gracias a A&A. Gracias Ali por tus conocimientos y ayuda en todo lo que he necesitado. A Amparo, sobran las palabras. Eres de esas personas con las que no hace falta decir nada para saber lo que piensa. Has sido otro pilar durante estos años, una de las razones por las que hoy esté

escribiendo estos agradecimientos. Gracias por escuchar y dejar contarte mis sentimientos. Gracias por ayudarme en todo lo que he necesitado y por haberte preocupado por mí.

También querría agradecer a mis otros compañeros que, si bien no he podido compartir muchos momentos juntos, formáis también parte de esta historia: Noe, Patri Sebastián, Pablo, Marina, Andrea, Anita, María Gil, Irene, Adolfo, Antonio, Ismael, Diana, y Pedro. Mil gracias a todos.

A todo el equipo de la UAGI por su apoyo para el desarrollo de esta investigación. En especial gracias a Leo por su ayuda con los problemitas informáticos, y a Marcos por las gestiones administrativas y consejos.

Also, thanks to IVI London's people for kindly hosting me. I would like to give special thanks to Charlotte, Christina, Rebecca, Dorien, Eleanor, Salonika, Taslima, Noreen, and Fred for making my 3-months stay an unbeatable experience. Mil gracias a Lourdes y Patricia por vuestra acogida y darle a la clínica ese toque español que me ha hecho sentirme como en casa. A César, gracias por permitirme formar parte de tu equipo, por mostrarme la visión clínica, por tu apoyo, consejos, y por descubrirme la pasión por la medicina. Gracias de verdad.

Especial mención a mis veteranos, a quienes les debo mis primeros pasos en la empresa y que, sin su guía, habría sido todo mucho más difícil. Gracias a Ana Corachán, mi compi de siempre pase lo que pase, gracias por las risas y los buenos momentos que hemos compartido. A Hannes, gracias por ser como eres, las conversaciones sobre tecnología y, sobre todo, por cómo te has comportado conmigo durante este viaje. Siempre me tendrás como amigo. A Silvia, la RAE personificada, gracias por tu dulzura y los buenos momentos. A Nuria, por haber sido una piña en los primeros años, y por tu sentido del humor.

No puedo olvidar a aquellos compañeros que, si bien ya han completado su etapa en Fundación IVI, han sido muy importantes en esta aventura. A Sarita, por ser siempre transparente y fiel a tus principios. Gracias por ser una amiga dentro y fuera del trabajo. A Alfredo, por tus clases magistrales de estadística y sacarnos siempre una sonrisa. A Víctor y Guille, por las charlas en el comedor que nos ayudaron a sobrellevar los malos días. A Álex, por escucharme, animarme y compartir planes de futuro afines. Seguro que nuestros caminos se cruzarán en el futuro. A Indra, por tu sinceridad, humildad y consejos. También quiero destacar a mi pareja de italianos.

A Mauro, por escucharme, y por transmitirme su positividad y buen rollo. A Livia, por ser como eres, por tu apoyo y ánimos en los momentos que más lo he necesitado, por tu energía, y por las risas que hemos compartido.

A todo el personal técnico y veterinario del animalario de la Facultat de Medicina i Odontologia de la Universitat de València. Especialmente me gustaría agradecer a Ana y Eva por enseñarme los secretos del manejo de animales en la experimentación animal y la confianza depositada en mí. Del mismo modo, gracias a Sonia y Toni del Servei de Microscòpia de la Unitat Central d'Investigació de Medicina por sus consejos, opiniones, y hacer tan amenas los maratones que nos hemos pegado en cada sesión.

También querría dar a las personas que he conocido en el Departament de Pediatria, Obstetrícia i Ginecologia. Gracias a Ana y Miguel por las discusiones sobre la vida y amenizar el trabajo. A ti Miguel también te quiero dar las gracias por escucharme y aconsejarme desde la más profunda sinceridad. A Víctor, ¿qué puedo decir de ti?, gracias por tus bromas y tonterías que han hecho todo más fácil, y han permitido tener muchos buenos momentos, tanto dentro como fuera del laboratorio. Gracias guapetón. Del mismo modo, querría agradecer a otras personas que he podido conocer en el Instituto de Investigación Sanitaria La Fe. A José Vicente, por darme tus consejos y opiniones de la investigación que me han ayudado en varias ocasiones. Al doctor Sandoval, por escucharme en los momentos en los que lo he necesitado y guiarme. No puedo darte el jamón que tanto hemos hablado, pero sí mi confianza y cariño.

No puedo dejar de lado a aquellas personas que me inculcaron en el pasado el interés por la ciencia y la reproducción asistida, gracias a lo cual me decidí por iniciar la tesis doctoral. Al Dr. Agustín Zapata por darme la oportunidad de tener mi primer contacto con la investigación. A David, Javi y Sarita, por enseñarme por primera vez cómo se trabaja en un laboratorio y a desarrollar una visión crítica. A ti David me gustaría especialmente darte las gracias por haberme transmitido los valores del esfuerzo, humildad y constancia en la ciencia, y por haberme guiado durante esos años con tus consejos y opiniones sinceras. Comenzaste como un jefe, pero terminaste siendo un amigo. Del mismo modo, también me gustaría dar las gracias a Fernando J Prados por contagiarme su amor por la reproducción asistida que me hizo especializarme en este campo de la medicina.

Fuera del laboratorio, gracias a Ezequiel, Álvaro, Sancha, Juan Carlos, Carlos y Paco por los buenos momentos y risas que hemos compartido en los últimos meses, y que me han ayudado a desconectar. De la misma forma, gracias a Alberto, Jose, Juan y Miriam por haber hecho que las experiencias tan inolvidables que vivimos durante el máster se continuaran durante los años siguientes, y os convirtierais en unos grandes pilares durante estos años. A mis amigos de Iviasa: Pablo, Miguel, Luis, Carlitos y Álex; gracias por estar siempre ahí durante tantos años y en todas las situaciones imaginables posibles.

Esta aventura no habría sido igual sin una segunda protagonista principal. Sin ella el cuento habría sido demasiado corto y sin final feliz. Esta tesis también es tuya. A Majo, por haber estado siempre a mi lado en todo momento, por haberme dado tu tiempo siempre que lo he necesitado, por haberme traído luz en los momentos de oscuridad, por haberme dado paz en los momentos de guerra, por haberme guiado cuando todas las luces se habían apagado, por haber tenido fe cuando nadie tenía esperanza. Simplemente gracias por todo este tiempo y por los proyectos venideros. No puedes conocer lo que traerá el futuro, pero sí puedes saber junto a quién quieres enfrentarlo. Mi elección serás siempre tú.

En último lugar, querría agradecer a mi familia su apoyo desmedido que ha hecho posible que hoy esté aquí, escribiendo los agradecimientos de esta tesis. A mis tías Fina y Segun, por darme su calor y amor año tras año. A mis padres, Fernando y Esperanza, por enseñarme los valores y principios de la constancia, el sacrificio y el trabajo que han hecho posible que no me rindiera ante las adversidades. Por inculcarme la educación, el respeto y la humildad como señas de identidad. Por haber sido mis mayores apoyos durante estos años, y en los proyectos que aún están por llegar. A mi hermano, Fernando, gracias por hacerme sentir que hay alguien con quien contar para enfrentarme a cualquier desafío que se presente, por darme fuerzas y valor ante los nuevos proyectos, y por acompañarme en todas mis aventuras. Con vuestra compañía cualquier cima es conquistable.

MUCHAS GRACIAS A TODOS POR ESTA HISTORIA

Contents

Abbreviations

A

AKT	Protein kinase B
ALK4	Activin A receptor type 1B
ALK5	Transforming growth factor-β receptor 1
ALK6	Bone morphogenetic protein receptor type 1B
AMH	Anti-Mullerian hormone
Apex1	Apurinic/apyrimidinic endo-deoxy-ribonuclease 1
ATM	Ataxia-telangiectasia mutated kinase or pathway
ATR	Ataxia telangiectasia and Rad3-related
A.U.	Arbitrary units

B

BAK	Bcl-2 homologous antagonist killer
BAX	Bcl-2-associated X
BCL2	B-cell lymphoma 2
BER	Base excision repair pathway
bFGF	Basic fibroblast growth factor
BLAST	Basic Local Alignment Search Tool
BMPs	Bone morphogenetic protein
BMP15	Bone morphogenetic protein 15
BMPR2	Bone morphogenetic protein receptor 2
BSA	Bovine Serum Albumin

C

C1P	Ceramide-1-phosphate
c-Abl	Abelson tyrosine kinase
cAMP	Cyclic adenosine monophosphate
cGMP	Cyclic guanosine monophosphate
CC3	Cleaved Caspase 3
CDC42	Cell division control 42
cDNA	Complementary DNA
CDK	Cip/Kip family of cyclin-dependent kinase
CHK1	Checkpoint kinase 1
CHK2	Checkpoint kinase 2
ChT	Chemotherapy group
ChT+LH-1x	Chemotherapy plus 1 IU of LH
ChT+LH-5x	Chemotherapy plus 5 IU of LH
COC	Cumulus-oocyte complexes
COS	Controlled ovarian stimulation
CT	Cycle threshold
Cx37	Connexin 37
Cx43	Connexin 43

D

DAPI	4,6-diamidino-2-phenylindole
DO	Denuded oocyte
DMSO	Dimethyl sulfoxide
DSB	Double strain breaks

E

E2	Estradiol
EGF	Epidermal growth factor
Ercc3	Excision repair cross-c omplementation group 3
ERK1/2	Extracellular Signal-Regulated Kinase 1 and 2
E-Cad	Epithelial cadherin

F

FBS	Fetal Bovine Serum
FOXL2	Forkhead Box L2
FOXO3	Forkhead box O3
FSH	Follicle stimulating hormone

G

G	Gauge
GC	Granulosa cells
G-CSF	Granulocyte-colony stimulating factor
GDF9	**G**rowth differentiation factor 9
GnRH	Gonadotrophin-releasing hormone
GnRHa	**G**onadotrophin-releasing hormone agonists
GNS	Goat normal serum
Gy	Gray (ionizing radiation units)

H

H2AX	H2A histone family member X
γH2AX	Phosphorylated-H2AX
hCG	**H**uman chorionic gonadotropin
H&E	Hematoxylin and eosin staining
HR	Homologous Recombination pathway
HRP	Horseradish peroxidase

I

IF	Intact follicle
IL	Interleukin
IU	International units

J

JNK	Jun N-terminal Kinase

K

KIT	Tyrosine protein kinase receptor
KITLG	KIT ligand, also known as stem cell factor (SCF)

L

LH	Luteinizing hormone.
LHX8	LIM homeobox 8
LIF	Leukemia inhibitory factor

M

MII	Metaphase II
MAPK	Mitogen-activated protein kinase
ERK	Extracellular signal-regulated kinase
MMR	Mismatch repair pathway
Msh6	MutS homolog 6
mTOR	Mammalian target of rapamycin

N

N-Cad	Neural cadherin
NER	Nucleotide excision repair pathway
NHEJ	Non-homologous end-joining pathway
NOBOX	Newborn ovary homeobox gene
NOXA	Phorbol-12-myristate-13-acetate-induced protein 1
N.S.	No significant

O

O/N	Overnight

P

pAKT	Phosphorylated protein kinase B
PARP	Poly ADP-ribose polymerase
PBS	Phosphate-buffered saline
PCR	Polymerase chain reaction
pERK1/2	Phosphorylated Extracellular Signal-Regulated Kinase 1/2
PFA	Paraformaldehyde
PGC	Primordial germ cells
PI3K	Phosphoinositide 3-kinase

PIP2	Phosphatidylinositol-4,5-bisphosphate
PIP3	Phosphatidylinositol-3,4,5-bisphosphate
PKA	Protein kinase A
PMAF	Percentage of morphologically abnormal follicles
PMSG	Pregnant Mare Serum Gonadotropin
POI	Premature ovarian insufficiency
Prkdc	Protein kinase DNA-activated catalytic subunit
PTEN	Tensin homolog deleted on chromosome 10
PUMA	Bcl-2-binding component 3
PVDF	Polyvinylidene difluoride

R

RAD001	Everolimus
Rad51	RAD51 recombinase
RIPA	Radioimmunoprecipitation Assay
Rn18S	18S ribosomal gene
RPM	Revolutions Per Minute
RT	Room temperature
RT-PCR	Reverse transcription polymerase chain reaction
RT-qPCR	Real-time quantitative polymerase chain reaction

S

S1P	Sphingosine-1-phosphate
SDS	Sodium dodecyl sulfate
SOHLH1	Spermatogenesis and oogenesis specific basic helix-loop-helix containing protein 1
SRY	Sex-determining region Y
SSB	Single strain breaks

T

TBST	Tris-buffered saline with 0.1% Tween 20
TGF-β	Transforming growth factor-β
TJP1	Tight junction protein 1
TNFα	Tumour necrosis factor α
TZP	Transzonal projections
TUNEL	Terminal deoxynucleotidyl transferase-mediated dUTP nick-end labeling

W

WB	Western blotting
Wpc	Weeks postconception (equivalent as weeks of gestation)

List of figures

List of tables

Resumen

Introducción

1. El aparato reproductor femenino: el ovario

El **ovario** es un órgano par con una doble función: la diferenciación de ovocitos maduros y la producción de hormonas esteroideas.

Desde el punto de vista **anatómico e histológico,** el ovario es una estructura conectada a la pared pélvica y al útero mediante ligamentos en el que se pueden distinguir 3 regiones: I) en la superficie se aprecia una capa externa de epitelio simple cuboidal llamada epitelio germinal seguida de una capa de tejido conectivo llamado túnica albugínea; II) una corteza compuesta por estroma (tejido conectivo, fibras de colágeno y otros componentes de la matriz extracelular) y numerosos folículos; y una médula en la parte más interna con un alto componente en material conectivo, elástico y vascular.

Los **folículos** constituyen la unidad funcional básica de los ovarios. Están compuestos por un componente germinal, el ovocito, rodeado por células somáticas llamadas GC (del inglés, *Granulosa Cells*), estableciendo una relación íntima entre ovocito y GC. Asociados a los folículos también se distinguen otros tipos celulares, como las células de la teca, y estructuras, como el antro o la zona pelúcida, importantes para el correcto crecimiento del folículo y el desarrollo del ovocito.

El **desarrollo embriológico de los folículos** comienza con la migración de las células primordiales germinales a las crestas genitales a las 5-6 semanas de gestación, donde parte de estas células se diferencian para generar ovogonias con una intensa actividad proliferativa. Las divisiones celulares ocurren en ausencia de citocinesis, originando estructuras celulares multinucleadas llamadas cistos, cuyas células entrarán en meiosis para originar los ovocitos. La meiosis de los ovocitos se detendrá en Profase I. Posteriormente, células somáticas de su

alrededor provocan la rotura e individualización de los ovocitos, los cuales quedarán rodeados por estas células somáticas para generar los folículos primordiales en un proceso en el que se produce la apoptosis de la mayoría de ovocitos. A partir de este punto, queda establecido el *pool* de folículos que contiene una mujer, también conocido como reserva ovárica, estimado en unos 300.000 – 500.0000 folículos primordiales antes del nacimiento. A partir de la pubertad, una cohorte de 1000 folículos se activarán e iniciarán un desarrollo cada mes, pero solo lo completará uno de ellos para ovular un ovocito competente que completará la primera división meiótica y se detendrá en metafase II hasta ser fecundado.

La **foliculogénesis** es el proceso por el cual un folículo primordial se activa y comienza su crecimiento, pasando por diversos estadios de maduración, hasta finalmente ovular un ovocito. Durante este proceso, el ovocito del folículo primordial activado empieza a crecer y la capa de células somáticas aplanadas que le rodean, conocidas como pregranulosa, se transforman en células cuboidales para alcanzar el estadio de folículo primario, el cual posteriormente se transforma en secundario cuando se forma una segunda capa de GC. En este momento las GC aumentan su actividad mitótica para formar sucesivas capas alrededor del ovocito en continuo crecimiento formando la fase de folículo preantral tardío. Rodeando las GC se diferencian unas células somáticas llamadas células de la teca, y los folículos siguen creciendo hasta que se forma una cavidad entre las capas de GC llamado antro, el cual está relleno de líquido folicular. Esta fase de desarrollo se llama folículo antral, y en él las GC reducen su proliferación a la par que aumenta su actividad secretora y el grado de vascularización del folículo. El antro crece progresivamente hasta que rodea casi por completo al ovocito, constituyendo el folículo preovulatorio o folículo de Graaf, que representa la última fase antes de que se produzca la ovulación del ovocito en los oviductos o trompas de Falopio.

La **activación folicular** es un proceso irreversible por el que una cohorte de folículos primordiales es reclutada para iniciar su desarrollo. Entre los mecanismos implicados destaca la importancia de la ruta de señalización PI3K-AKT, y su asociación con la ruta mTOR para mediar la activación de los folículos primordiales y regular la diferenciación de la pregranulosa en GC cuboidales, es decir, en la transición al estadio de folículo primario. Además de estas rutas, también intervienen toda una serie de factores de transcripción y moléculas accesorias. Además,

se ha observado la influencia del ambiente ovárico en la regulación de la activación folicular, como la hipoxia o el estrés mecánico. En el desarrollo de los folículos hasta el estadio preantral (incluido) intervienen numerosos factores de crecimiento, péptidos y moléculas esteroideas producidas por el ovocito y/o las GC para mediar el crecimiento del ovocito, y la proliferación y diferenciación de las GC. Aunque el desarrollo de los folículos preantrales es independiente de gonadotropinas, podría favorecer el crecimiento folicular en estas fases. En cambio, el desarrollo folicular a partir de los folículos preantrales tardíos ya es **dependiente de las gonadotropinas** FSH (del inglés, *Follicle Stimulating Hormone*) y LH (del inglés, *Luteinizing Hormone*).

Durante el proceso de foliculogénesis se establece un proceso de **comunicación entre el ovocito y las GC**. Este diálogo es bidireccional, de modo que las GC proporcionan al elemento germinal segundos mensajeros, amino ácidos, péptidos y moléculas para su crecimiento y metabolismo, mientras que el ovocito envía señales a las GC para regular su proliferación y diferenciación. Para ello, las GC emiten unas prolongaciones citoplasmáticas llamadas TZP (del inglés, *Transzonal Projections*) que contactan con la membrana del ovocito. En la zona de contacto ovocito-GC se establecen uniones adherentes (mediadas fundamentalmente por las E- y N-cadherinas), uniones estrechas (mediadas por la proteína TJP1, del inglés *Tight Junction Protein 1*), y uniones comunicantes (mediadas por las conexinas 37 y 43). Las señales enviadas por el ovocito a la GC, como la secreción de las proteínas GDF9 (del inglés, G*rowth Differentiation Factor 9*) y BMP15 (del inglés, B*one Morphogenetic Protein 15*), no dependen de las uniones comunicantes para llegar hasta las GC.

2. El cáncer y la fertilidad en la mujer

El cáncer ha sido reconocido como uno de los principales problemas de salud pública internacional que causa casi 10 millones de muertes al año, según datos de la Organización Mundial de la Salud. Se estima que 1 de cada 3 mujeres desarrollarán algún tipo de neoplasia invasiva durante sus vidas. Aproximadamente el 10% de los cánceres registrados en mujeres afectan a aquellas pacientes menores de 45 años y, por tanto, que se encuentran en la edad reproductiva. La mejora de las técnicas diagnósticas y terapéuticas ha permitido reducir

progresivamente la tasa de mortalidad debida al cáncer en las últimas décadas, así como la aparición de efectos secundarios derivados de los tratamientos oncológicos. No obstante, los tratamientos radioterapéuticos y quimioterapéuticos dañan comúnmente la función reproductiva. En el caso de la mujer, estos efectos causan frecuentemente la atrofia del ovario y el agotamiento de la reserva ovárica, derivando en muchos casos en la insuficiencia ovárica prematura (POI, del inglés, Premature Ovarian Insufficiency), e incluso en la pérdida completa de la fertilidad en los peores casos. Dado que la tasa de supervivencia al cáncer ha aumentado, también lo ha hecho el número de mujeres que experimentarán estos efectos secundarios sobre su fertilidad. Por ello, el campo de la preservación de la fertilidad cobra especial importancia para establecer un puente entre la oncología y la medicina reproductiva.

3. Gonadotoxicidad inducida por los tratamientos oncológicos

Los tratamientos oncológicos afectan negativamente a la función reproductiva de la mujer, dañando el ovario. Tradicionalmente se han utilizado los métodos quirúrgicos, radioterapéuticos y quimioterapéuticos para tratar el cáncer. Si bien es cierto que el impacto de las estrategias quirúrgicas en la fertilidad de la mujer depende de la gravedad de la neoplasia y la zona del cuerpo afectada, la radioterapia y quimioterapia sí alteran significativamente la función reproductora.

El daño causado por la **radioterapia** en el ovario depende fundamentalmente del campo corporal irradiado, la dosis utilizada y la edad de la paciente. Así, se ha visto que la radiación de la zona pélvica es la más sensible; el uso de radiaciones superiores a 2 Gray es suficiente para reducir la dotación folicular de la paciente; y el impacto es directamente proporcional a la edad de la mujer.

Por otra parte, la administración de **quimioterapia** causa la pérdida masiva de folículos en crecimiento y/o quiescentes que conlleva la alteración de la función ovárica, clínicamente evidenciado por la interrupción del ciclo menstrual durante varios meses en la mayoría de casos. Con el tiempo las pacientes recuperan la menstruación, pero el daño ovárico persiste. Esto hace que pasados unos años la paciente sufra POI. El impacto de la quimioterapia en la fertilidad

femenina depende de 3 factores principales: el tipo de agente quimioterapéutico usado, siendo los agentes alquilantes los que conllevan mayor riesgo de inducir fallo ovárico; la dosis utilizada; y la edad de la paciente en el momento de inicio del tratamiento.

Todos los tipos celulares que componen el ovario constituyen **dianas** que potencialmente pueden ser dañadas directa o indirectamente por la quimioterapia, incluyendo folículos quiescentes y en crecimiento y, dentro de ellos, tanto las GC como los ovocitos. Del mismo modo, el estroma ovárico también puede ser afectado por la quimioterapia. El **mecanismo molecular de la quimioterapia para dañar los ovarios** radica fundamentalmente en su habilidad para producir alteraciones en la estructura molecular del ADN incompatibles con la viabilidad celular, de modo que estas células afectadas si no son capaces de reparar estos daños en el ADN, activarán rutas encaminadas a la apoptosis. Además del daño en el ADN, también se ha visto que la quimioterapia promueve efectos oxidativos y pro-inflamatorios para inducir la muerte celular. Otros mecanismos diferentes a la apoptosis que parecen estar también implicados en la pérdida folicular es la activación de un número masivo de folículos quiescentes que no completarán su desarrollo y terminarán atresiándose; y, en menor medida y de forma menos conocida, la autofagia.

4. Preservación de la fertilidad en pacientes oncológicas jóvenes

En los últimos años se ha promovido el desarrollo de nuevas estrategias para minimizar los efectos gonadotóxicos de la quimioterapia, lo que ha hecho posible establecer un grupo de técnicas destinadas a preservar el potencial reproductivo de las mujeres jóvenes sometidas a estos tratamientos altamente gonadotóxicos. Según los expertos en reproducción, la mejor estrategia de preservación de fertilidad sería aquella que pudiera aplicarse en pacientes de todas las edades, que no implicara ningún riesgo para la salud de la paciente, ni interfiriera con la eficacia del tratamiento antineoplásico, ni retrasara la administración de la terapia oncológica, ni requiriera procedimientos invasivos. Sin embargo, ninguna opción actual cumple todas las características anteriores. La elección de una técnica sobre otra para la preservación de la fertilidad femenina atiende a una serie de factores:

- La edad de la paciente.
- La localización de la neoplasia, estadio y pronóstico.
- El tiempo disponible antes de iniciar el tratamiento oncológico.
- La reserva ovárica de la paciente.
- La disponibilidad de pareja masculina.
- Aspectos éticos y culturales en relación a la preservación y generación de gametos y embriones.

Entre las alternativas actuales, destaca la **criopreservación de embriones y ovocitos**, considerada la técnica de referencia para los procedimientos de preservación de la fertilidad, aunque no eviten el daño ovárico y la pérdida de la dotación folicular por el tratamiento oncológico. Esta estrategia implica la estimulación ovárica de la paciente, la recogida de los ovocitos madurados y su criopreservación, o fertilización *in vitro* y posterior criopreservación según la técnica a realizar. Aunque cada año nacen miles de niños con estas dos técnicas, hay una serie de aspectos a tener en cuenta antes de ser aconsejadas:

1. Se pueden recomendar solo en aquellas pacientes que pueden retrasar el inicio de su tratamiento oncológico al menos 10 días para realizar la estimulación ovárica.
2. Es necesario usar protocolos específicos de estimulación ovárica con inhibidores de la enzima aromatasa para aquellas pacientes con neoplasias hormono-dependientes.
3. La edad de la paciente, ya que el rendimiento de la estimulación ovárica en pacientes en fases de desarrollo anteriores a la pubertad es menor, así como la implicación de connotaciones éticas.

A diferencia de la criopreservación de embriones, la vitrificación de ovocitos se recomienda a pacientes adolescentes (postpuberales) y a mujeres que no tengan pareja sentimental masculina, o tengan objeciones éticas y culturales respecto a la criopreservación de embriones.

La **criopreservación de tejido ovárico** constituye la única opción para la preservación de la fertilidad en pacientes pediátricas (prepuberales), así como en pacientes adolescentes y adultas que no pueden retrasar el inicio de su tratamiento oncológico. Esta técnica consiste en la extracción de parte de la corteza ovárica, que se fragmenta y criopreserva para su posterior

trasplante una vez la paciente haya terminado la terapia antineoplásica. Sin embargo, existe la preocupación de que las células cancerosas, especialmente en los casos de leucemia, puedan haber migrado al tejido ovárico antes de su extracción, de modo que persistan en las muestras criopreservadas y sean reintroducidas con el trasplante. Además, la fertilidad de la paciente depende de la vida media del tejido trasplantado, que varía entre meses y pocos años, así como del número limitado de folículos primordiales presentes en los fragmentos trasplantados. Esto hace que sea de importancia capital el desarrollo de nuevas alternativas encaminadas a la prevención del daño ovárico inducido por el tratamiento oncológico, es decir, a la protección *in situ* de la reserva ovárica durante el tratamiento gonadotóxico.

Por ello, en los últimos años ha surgido una nueva estrategia llamada **terapia fertoprotectiva** dirigida a evitar el daño ovárico desencadenado por la quimioterapia. Esta estrategia consiste en la administración de un agente específico antes y durante el tratamiento oncológico, para inhibir específicamente el proceso molecular activado por el fármaco antineoplásico. El principal beneficio sobre las otras técnicas establecidas es su potencial aplicación a pacientes de todas las edades y tipos de cánceres, sin necesidad de estimulación ovárica que retrasase el inicio de la quimioterapia, y los procesos quirúrgicos que conllevan las otras alternativas. Por el contrario, presentan preocupaciones referentes a su posible interferencia con el mecanismo de acción del tratamiento oncológico, la escasa evidencia disponible de su eficacia y seguridad, y la posibilidad de mantener ovocitos dañados que puedan producir alteraciones embrionarias. Por ello, la mayoría de estos agentes fertoprotectores están limitados al campo de la investigación, salvo los **agonistas de la GnRH** (GnRHa, del inglés *Gonadotrophin-Releasing Hormone agonists*). Los GnRHa inducen una supresión temporal del eje hipotálamo-hipófisis-gonadal que inhibe la secreción de FSH y LH. Este efecto reduce significativamente la pérdida de folículos primordiales tras el tratamiento quimioterapéutico, aunque se desconoce con claridad el mecanismo molecular implicado. Actualmente hay un extenso número de estudios y publicaciones que afirman la eficacia de los GnRHa para la preservación de la fertilidad femenina, pero actualmente es considerada una técnica experimental. Por este motivo, puede ofrecerse como una opción complementaria a la criopreservación de ovocitos/embriones o tejido ovárico para la protección ovárica en pacientes oncológicas premenopáusicas, pero nunca sustituir a las técnicas ya establecidas de criopreservación.

Además de los GnRHa, muchos estudios en modelos animales han descrito la eficacia de **otros agentes fertoprotectores** para la protección *in situ* de la reserva ovárica. Algunos agentes actúan directamente sobre los folículos primordiales para inhibir las rutas moleculares implicadas en el daño en el ADN y la apoptosis para evitar la muerte celular de estos folículos, como por ejemplo los agentes S1P (del inglés, *sphingosine-1-phosphate*), C1P (del inglés, *ceramide-1-phosphate*), imatinib, inhibidores de las quinasas ATM (del inglés, *Ataxia-Telangiectasia Mutated*) y ATR (del inglés, *Ataxia Telangiectasia and Rad3-related*). Otro candidato a destacar como agente fertoprotector es la LH, quien ha demostrado en un estudio reciente ser capaz de generar *in vitro* señales antiapoptóticas en células somáticas del ovario para reducir los daños inducidos por el agente quimioterapéutico cisplatino. Concretamente, se vio que la LH redujo el daño en el ADN de los ovocitos expuestos a la quimioterapia, disminuyendo con ello la expresión de marcadores apoptóticos. Además, la administración *in vivo* de LH a ratones evitó significativamente la pérdida de folículos primordiales, permitiendo posteriormente la mejora de la tasa de embarazo y número de crías nacidas en los animales tratados con LH. A pesar de estos resultados prometedores, es necesario validar la eficacia de la LH como agente fertoprotector contra fármacos quimioterapéuticos más gonadotóxicos, puesto que el cisplatino se asocia con un riesgo moderado de inducir POI. Del mismo modo, los ovarios prepuberales en el ratón contienen mayoritariamente folículos primordiales, careciendo de otras poblaciones foliculares, lo que impide evaluar los efectos de la LH en estas poblaciones y cómo contribuye la sobreactivación en la pérdida folicular. El potencial de desarrollo de los ovocitos protegidos por la LH y sus mecanismos moleculares de acción también necesitan ser elucidados antes de ser reconocida la LH como agente fertoprotector.

Otros agentes fertoprotectores están dirigidos a inhibir las rutas de activación folicular, como la ruta PI3K-AKT, que son inducidas por la quimioterapia para prevenir el reclutamiento masivo de folículos quiescentes que inicien su desarrollo. Algunos de estos factores inhibidores son el inmunomodulador AS101, everolimus, rapamicina, hormona antimulleriana, melatonina y grelina.

Por otra parte, dado que la vasculatura ovárica y el estado de oxidación frecuentemente son comprometidos por la quimioterapia, varios agentes contrarrestan los efectos del tratamiento

oncológico sobre estos procesos, como el tamoxifeno, la crocetina, el resveratrol y el factor estimulante de colonias de granulocitos.

Finalmente, respecto el **futuro de las técnicas de la preservación de la fertilidad** no se puede obviar la existencia de otras técnicas experimentales que potencialmente podrían ser aplicadas para la preservación de la fertilidad en el futuro, pero que actualmente se encuentran en fases tempranas de su desarrollo como, por ejemplo, la maduración *in vitro* de los folículos, tanto primordiales como antrales, para la obtención de ovocitos MII que pudieran ser criopreservados. Esta opción sería una alternativa especialmente recomendada para aquellas pacientes jóvenes que no pudieran demorar el inicio de su tratamiento oncológico. Así mismo, la creación de un ovario artificial que permitiera realizar todo el proceso de desarrollo folicular para producir ovocitos fecundables sería todo un descubrimiento con una gran aplicabilidad en el campo de la preservación de la fertilidad.

Hipótesis

El tratamiento con LH podría ser utilizado como una estrategia para la protección *in situ* de la reserva ovárica en pacientes oncológicas que se someten a terapias altamente gonadotóxicas. La acción de la LH sobre el ovario se basaría en generar un ambiente propicio para contrarrestar los efectos nocivos de la quimioterapia basada en los agentes alquilantes para preservar el potencial reproductivo a largo plazo.

Objetivos

El **objetivo principal** del presente estudio es evaluar el tratamiento con LH como una nueva estrategia para proteger *in situ* la dotación folicular y preservar la esperanza reproductiva de ratonas adultas frente a los efectos deletéreos del tratamiento oncológico con agentes alquilantes.

Se pueden distinguir los siguientes objetivos secundarios:

- Determinar *in vivo* los efectos a corto plazo del tratamiento de LH en los folículos quiescentes expuestos a los agentes alquilantes.
- Investigar *in vivo* los mecanismos de acción de la LH para ejercer la protección ovárica frente a la quimioterapia.
- Evaluar la eficacia del tratamiento de LH para la preservación de la esperanza reproductiva a largo plazo.
- Analizar *in vivo* los efectos a corto plazo de la administración de LH en los folículos en desarrollo en el momento de exposición a la quimioterapia, mediante el uso de una cepa murina subfértil.

Material y métodos

Todos los experimentos de esta tesis han sido realizados en animales mediante procedimientos previamente aprobados por el Comité d'Experimentació i Benestar Animal de la Universitat de València (A1510573656187) y por la Dirección General de Agricultura, Ganadería y Pesca, Generalitat Valenciana (2018/VSC/PEA/0010 y 2019/VSC/PEA/0206).

1. Efectos de la LH en los folículos quiescentes expuestos a agentes alquilantes

Para analizar los efectos de la LH en los folículos primordiales, 31 ratonas CD-1 de 7 semanas de edad fueron distribuidas aleatoriamente en 3 grupos experimentales: control (n=9), quimioterapia (ChT, n=11) y quimioterapia con LH (ChT+LH-1x, n=11). A los animales del grupo control se les administró intraperitonealmente solución salina seguida de una segunda inyección de dimetil-sulfóxido (vehículo) 24 horas después. El grupo ChT recibió una primera inyección de salino seguido de la solución de quimioterapia (120 mg/kg de ciclofosfamida + 12 mg/kg busulfán

disueltos en dimetil-sulfóxido). El grupo ChT+LH-1x recibió 1 unidad internacional de LH (2.3ng/ml) seguida de 1 unidad internacional de LH junto con la quimioterapia a las 24 horas. Las ratonas fueron estabuladas durante 30 días y estimuladas ováricamente para asegurar la recogida de ovocitos y embriones procedentes de folículos primordiales en el momento de administración a la quimioterapia. Dos ratones por grupo fueron sacrificados 16 horas tras desencadenarles la ovulación para la recogida de ovocitos maduros, mientras que el resto de ratonas fueron mantenidas en estabulación y cruzadas con machos durante 40 horas para finalmente recoger los ovarios, ovocitos y embriones.

Para evaluar los efectos de la LH sobre la fertilidad a largo plazo, en el día 30 después de la administración de los tratamientos, 4 animales por grupo fueron cruzadas en 6 rondas sucesivas. Tras la última ronda de cruce, las ratonas fueron estimuladas ováricamente, cruzadas y finalmente sacrificadas para recoger los ovarios, ovocitos y embriones para evaluar la respuesta de los animales a la estimulación. Para este experimento a largo plazo, se incluyó un cuarto grupo experimental tratado con 5 unidades internacionales de LH (ChT+LH-5x, n=4) para analizar si el posible efecto de la LH es dosis dependiente.

Una vez recogidas todas las muestras, se procedió a su análisis para analizar los efectos de la LH contra la quimioterapia con agentes alquilantes:

- Análisis del estroma: se identificaron las áreas de estroma degenerado en los ovarios como la presencia de regiones acelulares y/o fibróticas en muestras teñidas con hematoxilina-eosina. Se estimó el índice de área degenerada relativizando la extensión del área afectada respecto el área total de tejido ovárico.
- Recuentos foliculares: se determinó el número de folículos en cada estadio de maduración en secciones ováricas seriadas teñidas con hematoxilina-eosina. Para evitar posibles errores en el recuento, sólo se contó aquellos folículos morfológicamente normales que presentaran un núcleo. También se determinó el número de folículos que presentaran alguna anormalidad morfológica (multinucleación, multivacuolización del ovoplasma, alteraciones en las capas de GC o degeneración folicular) para comprobar el efecto de la LH en el desarrollo folicular.

- Recuento y clasificación de ovocitos metafase II y embriones en base a criterios morfológicos.
- Análisis de la calidad de los ovocitos metafase II: se estudió la morfología, tamaño y disposición del huso meiótico, así como la organización de los cromosomas en la placa ecuatorial por microscopía confocal de fluorescencia.
- Efectos a largo plazo: se registró la tasa de gestación, número de crías por camada y total de crías nacidas a lo largo de 6 rondas de cruce consecutivas. También se evaluó la respuesta a la estimulación ovárica y viabilidad ovocitaria al registrar el número y calidad morfológica de ovocitos metafase II y embriones recuperados.

2. Efectos de la LH en la comunicación entre el ovocito y las GC

Debido a la relevancia del proceso de comunicación bidireccional entre el ovocito y GC para el correcto crecimiento folicular y desarrollo del ovocito, se evaluó este proceso mediante ensayos histológicos y moleculares en muestras ováricas obtenidas de ratonas control (n=3), ChT (n=5), y ChT+LH-1x (n=5) recogidas a los 30 días después de la administración de los tratamientos.

- Para los análisis moleculares se aislaron mecánicamente todos los folículos contenidos en cada ovario analizado. Se seleccionó solo aquellos folículos con un diámetro igual o superior a 100 µm por corresponder al estadio de desarrollo secundario o posterior, en los que el proceso de la comunicación ovocito-GC es más evidente. La mitad de los folículos fue almacenada, mientras que la otra mitad se decumuló para obtener ovocitos y GC. Posteriormente se analizaron en los folículos, ovocitos y GC obtenidos la expresión de moléculas relacionadas con uniones comunicantes (Cx37 y Cx43), uniones adherentes (E-Cad y N-Cad), uniones estrechas (TJP1) y factores secretados por los ovocitos (GDF9, BMP15 y sus receptores) mediante RT-qPCR y western blot.
- Se visualizó por microscopía confocal de fluorescencia las uniones comunicantes (Cx37 y Cx43), adherentes (E-Cad) y factores secretados por los ovocitos (GDF9 y BMP15), en secciones ováricas.

3. Mecanismos de acción de la LH

Con el fin de investigar la respuesta que se desencadena en el ovario tras la administración de LH para ejercer su protección, 16 ratonas CD-1 de 7 semanas de edad se distribuyeron en los 4 grupos experimentales: control, ChT, ChT+LH-1x y ChT+LH-5x. Los tratamientos se administraron como se ha descrito en la sección “Efectos de la LH en los folículos quiescentes expuestos a agentes alquilantes”. Las ratonas se sacrificaron a las 12 y 24 horas después de la administración de quimioterapia, recogiendo los ovarios para realizar los siguientes análisis funcionales:

- Daño en el ADN: se visualizaron las roturas en la doble cadena de ADN mediante inmunofluorescencia contra la histona H2AX fosforilada (γH2AX).
- Apoptosis: se determinó el porcentaje de folículos apoptóticos en secciones ováricas mediante ensayo TUNEL.
- Gonadotoxicidad: para comprobar si la LH era capaz de prevenir la toxicidad inducida por la quimioterapia en los ovarios, se midieron los niveles de expresión de las proteínas γH2AX, Cleaved Caspase 3 (CC3), B-cell lymphoma 2 (Bcl2), Extracellular Signal-Regulated Kinase 1 and 2 (ERK1/2), y ERK1/2 fosforilada (pERK1/2) en lisados ováricos por western blot.
- Reparación del ADN: para evaluar el papel de la LH en la activación de rutas de reparación del ADN se analizó por western blot la expresión de la quinasa ATM y recombinasa Rad51 implicadas en la ruta ATM, considerada la más importante para la reparación de las roturas dobles del ADN en los folículos primordiales. También se midieron los niveles de Protein Kinase B (AKT) y AKT fosforilada (pAKT) en lisados ováricos. Además, a nivel génico se investigó la expresión de otros factores involucrados en otras rutas de reparación del ADN: Msh6 (reparación por mal apareamiento), Apex 1 (reparación por escisión de bases), Prkdc (reparación por unión de extremos no homólogos), Ercc3 (reparación por escisión de nucleótidos), y Rad51.

4. Efectos de la LH en los folículos en crecimiento expuestos a agentes alquilantes

Para analizar si la LH protege a los folículos en desarrollo durante la exposición a la quimioterapia, se utilizó la cepa de ratón NOD-SCID, considerada menos fértil que la utilizada en los procedimientos anteriores, con el fin de representar un escenario reproductivo más adverso. Para ello, 16 ratonas NOD-SCID de 7 semanas de edad fueron distribuidas aleatoriamente en los grupos control (n = 5), ChT (n = 5) y ChT+LH-1x (n = 6). Los grupos control y ChT se trataron de igual manera a la expuesta en el apartado “Efectos de la LH en los folículos quiescentes expuestos a agentes alquilantes”. Las ratonas del grupo ChT+LH-1x tan solo recibieron 1 unidad internacional de LH junto con la quimioterapia para comprobar si una sola dosis de LH es suficiente para inducir la protección ovárica. Pasados 7 días desde la aplicación de los tratamientos, las ratonas recibieron un ciclo de estimulación ovárica controlada para asegurar que los ovocitos y embriones recogidos procedan de folículos en crecimiento en el momento de exposición a la quimioterapia. Dos ratonas por grupo fueron sacrificadas a las 16 horas de inducir la ovulación para recuperar ovocitos metafase II, mientras que el resto fueron cruzadas con machos durante 40 horas para recoger ovocitos, embriones y ovarios.

Las muestras biológicas recogidas se utilizaron para realizar los siguientes análisis funcionales:

- Evaluación del estroma: se determinó el índice de área estromal degenerada.
- Recuentos foliculares: se estudió el efecto de la LH en la reserva ovárica y poblaciones foliculares en crecimiento en secciones ováricas teñidas con hematoxilina-eosina. También se determinó el porcentaje de folículos morfológicamente anormales.
- Daño en el ADN y apoptosis: es estudió el papel de la LH para la prevención y reducción del daño en el ADN y la apoptosis de los ovocitos y GC mediante inmunofluorescencia de γH2AX y ensayo TUNEL, respectivamente.
- Recuento y clasificación de ovocitos metafase II y embriones en base a criterios morfológicos.
- Calidad de los ovocitos metafase II: se investigó mediante microscopía confocal de inmunofluorescencia el potencial meiótico como símbolo de calidad de los ovocitos

recogidos analizando la presencia o ausencia del huso meiótico, y características morfométricas del mismo. También se evaluó la disposición y alineamiento de los cromosomas en la placa metafásica.

Resultados

1. Efectos en los folículos quiescentes

La **evaluación macroscópica** de los ovarios reveló que tanto el grupo ChT como ChT+LH-1x sufrieron una reducción similar en la relación entre el peso ovárico y corporal comparado con el grupo control. No obstante, el tratamiento con LH evitó en un 10% la reducción del tamaño ovárico vista en el grupo ChT respecto los controles. El examen histológico demostró que la quimioterapia afecta negativamente al estroma incrementando significativamente el **índice de degeneración del estroma** ovárico 2.3 veces respecto el grupo control, mientras que la LH evita parte de este daño al verse un aumento de 1.6 veces.

Los **recuentos foliculares** mostraron que los ovarios del grupo ChT presentaban un 69.8% menos folículos que el grupo control, que afectó especialmente a las poblaciones de folículos primordiales, primarios y secundarios con una reducción del 76.4%, 68.0% y 67.8%, respectivamente. En cambio, la LH redujo parte de esta pérdida encontrando un 34.6% más folículos que el grupo ChT, con un incremento del 38.1%, 36.1% y 25.0% de folículos primordiales primarios y secundarios respecto el grupo ChT, respectivamente. Además, la LH restauró los valores controles en el porcentaje de folículos morfológicamente anormales, mejorando significativamente los niveles detectados en el grupo ChT. La población folicular más afectada por las alteraciones morfológicas en los 3 grupos experimentales fue el estadio secundario, representando más del 50% de los folículos anormales.

El tratamiento con LH permitió recuperar un 25% más **ovocitos metafase II** morfológicamente normales que el grupo ChT, evitando la reducción estadísticamente significativa respecto el grupo control. Del mismo modo, el análisis de la **calidad ovocitaria** por microscopía confocal mostró que los ovocitos del grupo tratado con LH presentaban un huso meiótico 31.1% más

grande que los del grupo ChT, restaurando los valores observados en el grupo control, así como también redujo el número de ovocitos con al menos un cromosoma mal alineado respecto la placa metafásica en comparación con el grupo ChT. Sin embargo, no se vio mejora en el número de **embriones** en estadio de 2 células.

El **estudio a largo plazo** demostró que el tratamiento con LH, y especialmente la dosis baja (1 unidad internacional), es capaz de revertir notablemente los efectos negativos de la quimioterapia en la tasa de gestación acumulada y tamaño de las camadas, lo que permitió aumentar en un 21% el número total de crías nacidas en el grupo ChT+LH-1x respecto el grupo ChT. Todas las crías nacidas presentaron valores similares de tamaño y peso en el momento del nacimiento para los tres grupos. Por otra parte, para justificar parte de estos resultados a largo plazo, se observó que los ovarios de las ratonas estimuladas después de la sexta ronda de cruce de los grupos tratados con LH, y en especial las del grupo ChT+LH-1x, fueron significativamente más grandes que los del grupo ChT. Además, se recuperó un mayor número de ovocitos metafase II y embriones con buena calidad morfológica procedentes de ratonas tratadas con LH respecto el grupo ChT, todas ellas estimuladas ováricamente tras la última ronda de cruces.

2. Efecto de la protección de la LH en el proceso de la comunicación entre ovocito y GC

Con el fin de entender mejor cómo la administración de LH puede mejorar la calidad de los ovocitos que proceden de folículos en el estadio primordial en el momento de la quimioterapia, se estudió la capacidad de estos folículos tratados con LH para establecer una correcta comunicación entre el ovocito y GC durante el desarrollo folicular, analizando para ello las uniones intercelulares y los factores de crecimiento secretados por los ovocitos.

El **aislamiento de los folículos** reveló que los ovarios contenidos en el grupo tratado con LH contenía un mayor número de folículos, reduciendo significativamente los efectos de la quimioterapia vistos en el grupo ChT.

El **estudio de expresión de las uniones intercelulares** mostró que a nivel génico la quimioterapia redujo la expresión de todos los genes analizados (Cx37, E-Cad, Cx43, N-Cad y TJP1) en folículos intactos, ovocitos aislados y GC, mientras que el grupo tratado con LH mostró valores de expresión similares a los detectados en el grupo control. Se obtuvieron similares resultados en el análisis de expresión proteica por western blot para los factores Cx37, E-Cad y Cx43. La **visualización de las uniones intercelulares** por microscopía confocal mostró que la administración de LH revertió significativamente los efectos de la quimioterapia en la expresión de las moléculas Cx37, E-Cad y Cx43 en los folículos a partir del estadio secundario, confirmando la capacidad de la LH para mantener la capacidad de los folículos primordiales protegidos en el momento de la exposición a la quimioterapia para establecer correctamente uniones intercelulares entre el ovocito y las GC durante el desarrollo folicular.

La evaluación de la **expresión de los factores de crecimiento intercambiados por los ovocitos y GC** mostró que la quimioterapia causó una reducción notable en 5 de los 6 genes analizados (GDF9, BMP15, BMPR2, ALK4, ALK5 y ALK6), mientras que la LH mantuvo valores similares al grupo control para la mayoría de ellos en las muestras de folículos, ovocitos y GC analizados. La preservación de la expresión de los factores GDF9 y BMP15 por la LH frente la quimioterapia fue posteriormente validada a nivel proteico por western blot, así como por su **visualización** mediante microscopía confocal.

3. Mecanismos de protección de la LH

Para dilucidar el mecanismo de acción de la LH para la protección ovárica, se evaluó en primer lugar el **daño en el ADN y apoptosis** en las primeras 12 horas tras la administración de los tratamientos, mostrando que ambos grupos de LH (ChT+LH-1x y ChT+LH-5x) redujeron significativamente el porcentaje de ovocitos con daño en el ADN y folículos apoptóticos detectados en el grupo ChT.

Del mismo modo, en el **ensayo de ovotoxicidad** se observó que el tratamiento con LH evitó los efectos de la quimioterapia en la expresión proteica de γH2AX, la relación entre la proteína anti-

apoptótica Bcl2 y la proteína pro-apoptótica CC3, y el ratio de fosforilación de ERK1/2, a las 12 y 24 horas de administración de los reactivos.

Dado que los mecanismos de reparación del ADN pueden reducir el daño celular y la apoptosis, se estudió el papel de la LH como inductor de la activación de estos procesos. Se detectó por western blot que la LH potenció a las 12 y 24 horas la expresión de proteínas implicadas directamente (ATM y Rad51) en el proceso de reparación del ADN llamado recombinación homóloga, y evitó la sobreactivación de otras que pueden regular negativamente el proceso (pAKT/AKT). Además, se vio que la dosis baja de LH potenció la expresión génica de moléculas implicadas en otras rutas de reparación del ADN por encima de la quimioterapia en las primeras 12 horas, conservando la sobreexpresión del gen Rad51 a las 24 horas.

4. Efectos de la LH en los folículos en crecimiento expuestos a los agentes alquilantes

El **examen macroscópico** mostró que la LH no fue capaz de revertir los efectos de la quimioterapia ni en la relación del peso ovárico respecto el peso corporal, ni en el tamaño de los ovarios. En cambio, la administración de LH redujo significativamente el **índice de degeneración del estroma** respecto el grupo ChT, pasando de un incremento de 3.5 veces para ChT a 1.9 veces para ChT+LH-1x respecto el grupo control.

La **dotación folicular** se vio significativamente disminuida en los grupos ChT y ChT+LH-1x respecto el grupo control, pero los ovarios del grupo tratado con LH contenían un 31.2% más folículos que el grupo ChT. Esta protección frente la quimioterapia benefició especialmente a la población de folículos primordiales y primarios, registrando un 83.2% y 48.4% más folículos, respectivamente, respecto el grupo ChT. Sin embargo, el porcentaje de folículos con alguna anomalía morfológica aumentó significativamente en los grupos ChT y ChT+LH-1x de forma similar respecto el grupo control.

La evaluación del **daño folicular** en las secciones ováricas reveló que la LH redujo el número de folículos cuyo ovocito era positivo para γH2AX y, por tanto, presentaba daño en el ADN, así

como el porcentaje de folículos con una alta tasa de apoptosis en las GC, medido por ensayo TUNEL.

Respecto el **número de ovocitos y embriones**, la quimioterapia redujo significativamente el número de ovocitos metafase II y embriones morfológicamente normales respecto el grupo control, mientras que la LH evitó parcialmente los efectos en los ovocitos, recuperando un 26.3% más que el grupo ChT.

Finalmente, el análisis de la **calidad de los ovocitos metafase II** recuperados demostró que el tratamiento con LH incrementó la probabilidad de formación del huso meiótico en los ovocitos respecto el grupo ChT. Además, aunque el huso meiótico de los ovocitos del grupo ChT+LH-1x fue significativamente más pequeño que el del grupo control, el área ocupada por el huso resultó ser 3 veces superior a la identificada en el grupo ChT. Del mismo modo, la LH redujo significativamente respecto el grupo ChT el número de ovocitos metafase II con al menos uno de los cromosomas desplazado respecto la placa ecuatorial, mostrando con ello una mejor calidad meiótica.

Discusión

Los tratamientos quimioterapéuticos basados en el uso de agentes alquilantes son ampliamente utilizados en las neoplasias ginecológicas y hematológicas, que representan el 48.4% y 7.7%, respectivamente, del total de nuevos casos de cáncer en mujeres menores de 45 años a nivel global. Los efectos secundarios que tienen estos agentes alquilantes sobre la fertilidad de la mujer es una de las principales preocupaciones de los profesionales en medicina reproductiva. Aunque en la actualidad se dispone de técnicas exitosas para la preservación de la fertilidad en pacientes oncológicas, todavía se necesitan nuevas alternativas para la protección *in situ* de la reserva ovárica. La prevención de la apoptosis inducida por el cisplatino en ovocitos de ratones prepúberes mediante la suplementación de LH postuló a la LH como un sólido candidato para la gonadoprotección contra la quimioterapia. Con este propósito, esta tesis ha evaluado el efecto del tratamiento de la LH sobre 1) los folículos quiescentes en ratones CD-1, y 2) los folículos en

crecimiento en ratones subfértiles NOD-SCID tras la quimioterapia con agentes alquilantes a una dosis equivalente a la utilizada en pacientes con cáncer.

En la primera aproximación experimental para evaluar los efectos de la LH en la población de folículos quiescentes en el momento de exposición a la quimioterapia, las muestras se recogieron 30 días después de la administración de los tratamientos debido a que es el tiempo que requiere un folículo primordial para activarse y completar su crecimiento hasta ovular un ovocito maduro. Nuestros resultados revelaron que la quimioterapia reduce significativamente el número de folículos contenidos en los ovarios, afectando a todos los estadios de desarrollo, lo cual derivó en una reducción significativa de los ovocitos metafase II recogidos tras la estimulación ovárica de las ratonas. En cambio, el tratamiento con LH mejoró notablemente tanto el número de folículos como el de ovocitos recogidos. Teniendo en cuenta que los folículos y ovocitos analizados procedían de folículos primordiales en el momento de administración de la quimioterapia, nuestros resultados sugieren que la LH protege a la reserva ovárica frente al tratamiento oncológico. Además, nuestros resultados también sugieren que hay una estrecha relación entre la pérdida de reserva ovárica y el daño folicular, ya que encontramos que los agentes alquilantes causaron un aumento significativo del porcentaje de folículos con ovocitos con el ADN dañado y de GC apoptóticas en las primeras horas tras su exposición, tal y como han descrito estudios previos. El hecho que los grupos tratados con LH evitaran significativamente el daño folicular, tanto en el ovocito como en las GC, indicaba que esta hormona puede tener un efecto positivo en la salud folicular, y esto podría explicar también la mejora de los recuentos foliculares y el número de ovocitos recogidos. Este efecto protector de la LH podría ser realizado mediante señales producidas por células ováricas somáticas que expresen su receptor, como sugieren diversos estudios, aunque se desconozca el mecanismo de acción.

Por ello, dado que el daño en el ADN y la apoptosis están íntimamente relacionados con los mecanismos de reparación del ADN, encontramos que la LH era capaz de aumentar la expresión de factores relacionados con varias rutas de reparación del ADN, especialmente la recombinación homóloga, la cual se considera el mecanismo más importante para la reparación del ADN en los folículos primordiales. Así mismo, nuestros resultados nuevamente mostraron

que la LH era capaz de reducir la expresión de marcadores del daño en el ADN y la apoptosis. Por tanto, estos hallazgos sugieren que la LH favorece la activación de mecanismos de reparación del ADN para preservar la integridad del material genético ovocitario y minimizar el daño ovárico causado por la quimioterapia.

El nicho ovárico juega un papel fundamental para la correcta fisiología del folículo (activación, desarrollo, crecimiento), de modo que la protección del estroma ovárico por la LH frente a la quimioterapia puede ser otro de los motivos para explicar la protección ejercida por la LH. Nuestros resultados también mostraron que la quimioterapia induce la aparición de anomalías morfológicas en los folículos, fundamentalmente registradas en la población de folículos secundarios, sugiriendo que podría alterar su potencial de desarrollo y calidad. En cambio, la LH evitó parte de estos efectos y, con ello, posiblemente su capacidad de desarrollo. Por ello, como el proceso de comunicación bidireccional que se produce entre el ovocito y las GC es de capital importancia para el correcto proceso de foliculogénesis, nos encontramos con que el tratamiento con LH evitó significativamente los efectos de la quimioterapia en la expresión de moléculas involucradas en el establecimiento de uniones intercelulares, fundamentalmente comunicantes y adherentes, entre el ovocito y las GC, así como de factores de crecimiento que son intercambiados entre el compartimento germinal y somático para el correcto desarrollo de ambos componentes foliculares. Además, estas alteraciones de la comunicación ovocito-GC inducidas por la quimioterapia se produjeron a partir del estadio secundario, sugiriendo una alteración en la transición entre el folículo primario a secundario que pueda afectar a su desarrollo.

La formación del huso meiótico y el correcto alineamiento cromosómico en la placa ecuatorial es un marcador de calidad ovocitaria. Nuestros resultados mostraron que los ovocitos procedentes de folículos primordiales tratados con LH presentan mejores características del huso meiótico y alineamiento cromosómico que los tratados solamente con quimioterapia. Estos hallazgos podrían ser debidos a la capacidad de la LH para disminuir el daño folicular y el mantenimiento del proceso de comunicación ovocito-GC que aseguren un correcto desarrollo del folículo para que termine ovulando un ovocito maduro de buena calidad.

Los efectos a corto plazo de la LH para proteger la reserva ovárica, y mejorar el número y calidad de los ovocitos resultantes pareció traducirse en una mejora a largo plazo de la fertilidad. Por

tanto, las ratonas tratadas con LH presentaron mayores tasas de embarazo y tamaño de camadas que condujeron a un mayor número total de crías que el grupo tratado solo con quimioterapia. Además, el tratamiento con LH no afectó a la salud de las crías resultantes, confirmando la seguridad de la técnica. La mejora a largo plazo se confirmó posteriormente al aumentar el número y calidad morfológica de ovocitos y embriones de las ratonas tratadas con LH. No obstante, hay que destacar que encontramos mejores resultados para las ratonas del grupo tratado con la dosis baja de LH, lo que sugiere que dosis elevadas de la hormona pueden tener un efecto adverso sobre la reproducción femenina a largo plazo, tal y como sucede con otros agentes. De hecho, niveles circulantes de LH suprafisiológicos permanentemente causan una pérdida significativa de la reserva ovárica. Por ello, a diferencia de las estrategias de preservación de la fertilidad basadas en la toma prolongada de GnRHa para la supresión del eje hipotálamo-hipofisario-gonadal, nosotros con esta tesis proponemos la administración de una dosis puntual de LH con la quimioterapia. No obstante, es necesario profundizar en la eficacia de la estrategia y determinación de la mejor dosis y tiempo de administración.

En el experimento para evaluar los efectos de la LH sobre los folículos que ya estaban en crecimiento en el momento de la exposición a la quimioterapia, utilizamos una cepa de ratones considerada subfértil para validar los efectos fertoprotectores de la LH. En primer lugar, encontramos que la LH protegió significativamente las poblaciones de folículos más indiferenciadas (primordiales y primarios), apoyando los resultados obtenidos en el primer modelo animal. Esta preservación de los folículos primordiales por parte de la LH podría deberse a un efecto inhibidor de la sobreactivación de los folículos quiescentes que normalmente desencadena la quimioterapia (efecto *Burnout*), o evitando el daño folicular que desemboque en su apoptosis. Para darse la primera opción, tendríamos que haber visto un aumento proporcional del número de folículos en crecimiento a la pérdida de folículos primordiales, pero nuestros resultados solo muestran una pérdida global de todas las poblaciones foliculares, indicando que la LH ejerce su efecto protector al generar señales anti-apoptóticas encaminadas a la supervivencia de los folículos dañados. De hecho, nuestros análisis mostraron un descenso de folículos con daño en el ADN ovocitario y apoptosis en las GC. La reducción del daño folicular contribuyó a ovular más ovocitos metafase II, y de mejor calidad medida por análisis del huso meiótico y alineamiento cromosómico. Por tanto, el tratamiento de LH protegería la reserva

ovárica y los folículos que ya estuvieran en crecimiento en el momento de administración de la quimioterapia para permitir recuperar ovocitos metafase II competentes.

Por todo ello, aunque la totalidad de los experimentos recogidos en esta tesis se realizaron en un modelo animal, abre la puerta a una nueva estrategia sin intervenciones quirúrgicas, protocolos de estimulación ovárica, y basada en la protección *in situ* de la reserva ovárica para la preservación de la fertilidad en pacientes jóvenes con cáncer

Conclusiones

1. El tratamiento con LH evita la alteración de la arquitectura ovárica inducida por la quimioterapia, que contribuye a disminuir el área de estroma con regiones acelulares y/o fibróticas.
2. La LH confiere protección de la reserva ovárica *in situ* que lleva a reducir la incidencia de folículos con anomalías morfológicas en el ovoplasma y en las GC a lo largo del crecimiento y desarrollo folicular.
3. La protección de los folículos primordiales por parte de la LH previene la alteración detectada tras la administración de quimioterapia sobre las uniones gap y las uniones adherentes en los compartimentos somático y germinal de los folículos a partir del estadio secundario, manteniendo estable la interacción entre ovocito y GC durante el crecimiento folicular.
4. La administración de LH contrarresta los efectos de la quimioterapia al preservar la expresión de los factores de crecimiento que se intercambian entre los ovocitos y las GC en los folículos en estadios avanzados del desarrollo folicular, lo que promueve la maduración de ambos compartimentos foliculares para obtener ovocitos metafase II competentes.
5. La protección folicular ejercida por la LH mejora el número, la calidad morfológica, la competencia meiótica y el alineamiento cromosómico de los ovocitos metafase II ovulados.

6. La administración de LH preserva el potencial y la esperanza reproductiva de las ratonas adultas sin afectar a la salud de la descendencia.
7. El papel de la LH está mediado, al menos en parte, por una potenciación de la respuesta al daño del ADN, que desencadena mecanismos de reparación del ADN, como la recombinación homóloga, así como genera señales anti-apoptóticas durante las primeras horas tras la exposición a la quimioterapia para mantener la viabilidad folicular.
8. Existe un rango óptimo de concentración de LH para lograr un equilibrio adecuado entre la prevención de la gonadotoxicidad aguda a corto plazo y la preservación de la fertilidad a largo plazo.
9. La LH ejerce efectos anti-apoptóticos sobre el ovocito y las GC proliferativas de los folículos que se encuentran en fase de crecimiento en el momento de la administración de la quimioterapia, lo que se traduce en una mejora de la cantidad y la calidad de los ovocitos metafase II resultantes.

Resum

Introducció

1. L'aparell reproductor femení: l'ovari

L'ovari és un òrgan parell amb una doble funció: la diferenciació d'ovòcits madurs i la producció d'hormones esteroidals.

Des del punt de vista **anatòmic i histològic**, l'ovari és una estructura connectada a la paret pelviana i a l'úter mitjançant lligaments en el qual es poden distingir 3 regions: I) en la superfície s'aprecia una capa externa d'epiteli simple cuboidal anomenada epiteli germinal seguida d'una capa de teixit connectiu anomenat túnica albugínea; II) una escorça composta per estroma (teixit connectiu, fibres de col·lagen i altres components de la matriu extracel·lular) i nombrosos fol·licles; i una medul·la en la part més interna amb un alt component en material connectiu, elàstic i vascular.

Els **fol·licles** constitueixen la unitat funcional bàsica dels ovaris. Estan compostos per un component germinal, l'ovòcit, envoltat per cèl·lules somàtiques anomenades GC (de l'anglès, *Granulosa Cells*), establint una relació íntima entre ovòcit i GC. Associats als fol·licles també es distingeixen altres tipus cel·lulars, com les cèl·lules de la teca, i estructures, com l'antre o la zona pel·lúcida, importants per al correcte creixement del fol·licle i el desenvolupament de l'ovòcit.

El **desenvolupament embriològic dels fol·licles** comença amb la migració de les cèl·lules primordials germinals a les crestes genitals a les 5-6 setmanes de gestació, on part d'aquestes cèl·lules es diferencien per a generar ovogònies amb una intensa activitat proliferativa. Les divisions cel·lulars ocorren en absència de citocinesi, originant estructures cel·lulars multinucleades anomenades cistos, les cèl·lules dels quals entraran en meiosis per a originar els ovòcits. La meiosi dels ovòcits es detindrà en Profase I. Posteriorment, cèl·lules somàtiques del seu voltant provoquen el trencament i individualització dels ovòcits, els quals quedaran envoltats

per aquestes cèl·lules somàtiques per a generar els fol·licles primordials en un procés en el qual es produeix l'apoptosi de la majoria d'ovòcits. A partir d'aquest punt, queda establert el pool de fol·licles, també conegut com a reserva ovàrica, que conté una dona estimat en uns 300.000 – 500.0000 fol·licles primordials abans del naixement. A partir de la pubertat, una cohort de 1000 fol·licles s'activarà i iniciarà un desenvolupament cada mes, però només el completarà un d'ells per a ovular un ovòcit competent que completarà la primera divisió meiòtica i es detindrà en metafase II fins a ser fecundat.

La **foliculogènesi** és el procés pel qual un fol·licle primordial s'activa i comença el seu creixement, passant per diversos estadis de maduració, fins finalment ovular un ovòcit. Durant aquest procés, l'ovòcit del fol·licle primordial activat comença a créixer i la capa de cèl·lules somàtiques aplanades que l'envolten, conegudes com a pregranulosa, es transformen en cèl·lules cuboidals per a aconseguir l'estadi de fol·licle primari, el qual posteriorment es transforma en secundari quan es forma una segona capa de GC. En aquest moment les GC augmenten la seua activitat mitòtica per a formar successives capes al voltant de l'ovòcit en continu creixement formant la fase de fol·licle preantral tardà. Envoltant les GC es diferencien unes cèl·lules somàtiques anomenades cèl·lules de la teca, i els fol·licles continuen creixent fins que es forma una cavitat entre les capes de GC anomenat antre, el qual està farcit de líquid fol·licular. Aquesta fase de desenvolupament es diu fol·licle antral, i en ell les GC redueixen la seua proliferació al mateix temps que augmenta la seua activitat secretora i el grau de vascularització del fol·licle. L'antre creix progressivament fins que envolta quasi per complet a l'ovòcit, constituint el fol·licle preovulatori o fol·licle de Graaf, que representa l'última fase abans que es produïsca l'ovulació de l'ovòcit en els oviductes o trompes de Fal·lopi.

L'**activació fol·licular** és un procés irreversible pel qual una cohort de fol·licles primordials és reclutada per a iniciar el seu desenvolupament. Entre els mecanismes implicats destaca la importància de la ruta de senyalització PI3K-AKT, i la seua associació amb la ruta mTOR per mediar l'activació dels fol·licles primordials i regular la diferenciació de la pregranulosa en les GC cuboidals, és a dir, en la transició a l'estadi de fol·licle primari. A més d'aquestes rutes, també intervenen tota una sèrie de factors de transcripció i molècules accessòries. També s'ha observat la influència de l'ambient ovàric en la regulació de l'activació fol·licular, com la hipòxia o l'estrès

mecànic. En el desenvolupament dels fol·licles fins a l'estadi preantral (inclòs) intervenen nombrosos factors de creixement, pèptids i molècules esteroidals produïdes per l'ovòcit i/o les GC per mediar el creixement de l'ovòcit, i la proliferació i diferenciació de les GC. Encara que el desenvolupament dels fol·licles preantrals és independent de gonadotropines, podria afavorir el creixement fol·licular en aquestes fases. En canvi, el desenvolupament fol·licular a partir dels fol·licles preantrals tardans ja és **dependent de les gonadotropines** FSH (de l'anglès, *Follicle Stimulating Hormone*) i LH (de l'anglés, *Luteinizing Hormone*).

Durant el procés de foliculogènesi s'estableix un procés de **comunicació entre l'ovòcit i les GC**. Aquest diàleg és bidireccional, de manera que les GC proporcionen a l'element germinal segons missatgers, aminoàcids, pèptids i molècules per al seu creixement i metabolisme, mentre que l'ovòcit envia senyals a les GC per a regular la seua proliferació i diferenciació. Per a això, les GC emeten unes prolongacions citoplasmàtiques anomenades TZP (de l'anglés, *Transzonal Projections*) que contacten amb la membrana de l'ovòcit. En la zona de contacte ovòcit-GC s'estableixen unions adherents (intervingudes fonamentalment per les E- i N-cadherines), unions estretes (intervingudes per la proteïna TJP1, de l'anglès *Tight Junction Protein 1*), i unions comunicants (intervingudes per les conexines 37 i 43). Els senyals enviats per l'ovòcit a la GC, com la secreció de les proteïnes GDF9 (de l'anglès, *Growth Differentiation Factor 9*) i BMP15 (de l'anglès, *Bone Morphogenetic Protein 15*), no depenen de les unions comunicants per a arribar fins a les GC.

2. El càncer i la fertilitat en la dona

El càncer ha sigut reconegut com un dels principals problemes de salut pública internacional que causa quasi 10 milions de morts a l'any, segons dades de l'Organització Mundial de la Salut. S'estima que 1 de cada 3 dones desenvoluparan algun tipus de neoplàsia invasiva durant les seues vides. Aproximadament el 10% dels càncers registrats en dones afecten aquelles pacients menors de 45 anys i, per tant, que es troben en l'edat reproductiva. La millora de les tècniques diagnòstiques i terapèutiques ha permès reduir progressivament la taxa de mortalitat deguda al càncer en les últimes dècades, així com l'aparició d'efectes secundaris derivats dels tractaments

oncològics. No obstant això, els tractaments radioterapèutics i quimioterapèutics danyen comunament la funció reproductiva. En el cas de la dona, aquests efectes causen sovint l'atròfia de l'ovari i l'esgotament de la reserva ovàrica, derivant en molts casos en la insuficiència ovàrica prematura (POI, de l'anglès, *Premature Ovarian Insufficiency*), i fins i tot a la pèrdua completa de la fertilitat en els pitjors casos. Atès que la taxa de supervivència al càncer ha augmentat, també l'ha fet el nombre de dones que experimentaran aquests efectes secundaris sobre la seua fertilitat. Per això, el camp de la preservació de la fertilitat cobra especial importància per a establir un pont entre l'oncologia i la medicina reproductiva.

3. Gonadotoxicitat induïda pels tractaments oncològics

Els tractaments oncològics afecten negativament la funció reproductiva de la dona, danyant l'ovari. Tradicionalment s'han utilitzat els mètodes quirúrgics, radioterapèutics i quimioterapèutics per a tractar el càncer. Si bé és cert que l'impacte de les estratègies quirúrgiques en la fertilitat de la dona depèn de la gravetat de la neoplàsia i la zona del cos afectada, la radioteràpia i quimioteràpia sí que alteren significativament la funció reproductora.

El mal causat per la r**adioteràpia** en l'ovari depèn fonamentalment del camp corporal irradiat, la dosi de radiació i l'edat de la pacient. Així, s'ha vist que la radiació de la zona pelviana és la més sensible; l'ús de radiacions superiors a 2 Gray és suficient per a reduir la dotació fol·licular de la pacient; i l'impacte és directament proporcional a l'edat de la dona.

D'altra banda, l'administració de **quimioteràpia** causa la pèrdua massiva de fol·licles en creixement i/o quiescents que comporta l'alteració de la funció ovàrica, clínicament evidenciat per la interrupció del cicle menstrual durant diversos mesos en la majoria de casos. Amb el temps les pacients recuperen la menstruació, però el mal ovàric persisteix. Això fa que passats uns anys la pacient patisca POI. L'impacte de la quimioteràpia en la fertilitat femenina depèn de 3 factors principals: el tipus d'agent quimioterapèutic usat, sent els agents alquilants els que comporten major risc d'induir fallada ovàrica; la dosi utilitzada; i l'edat de la pacient en el moment d'inici del tractament.

Tots els tipus cel·lulars que componen l'ovari constitueixen **dianes** que potencialment poden ser danyades directament o indirectament per la quimioteràpia, incloent fol·licles quiescents i en creixement i, dins d'ells, tant les GC com els ovòcits. De la mateixa manera, l'estroma ovàric també pot ser afectat per la quimioteràpia. El **mecanisme molecular de la quimioteràpia per a danyar els ovaris** radica fonamentalment en la seua habilitat per a produir alteracions en l'estructura molecular de l'ADN incompatibles amb la viabilitat cel·lular, de manera que aquestes cèl·lules afectades si no són capaces de reparar aquests danys en l'ADN, activaran rutes encaminades a l'apoptosi de la cèl·lula. A més del dany en l'ADN, també s'ha vist que la quimioteràpia promou efectes oxidatius i pro-inflamatoris per a induir la mort cel·lular. Altres mecanismes diferents a l'apoptosi que semblen estar també implicats en la pèrdua fol·licular és l'activació d'un nombre massiu de fol·licles quiescents que no completaran la seua maduració i acabaran endarrerint-se; i, en menor mesura i de forma menys coneguda, l'autofàgia.

4. Preservació de la fertilitat en pacients oncològiques joves

En els últims anys s'ha promogut el desenvolupament de noves estratègies per a minimitzar els efectes gonadotòxics de la quimioteràpia, la qual cosa ha fet possible establir un grup de tècniques destinades a preservar el potencial reproductiu de les dones joves sotmeses a aquests tractaments altament gonadotòxics. Segons els experts en reproducció, la millor estratègia de preservació de fertilitat seria aquella que poguera aplicar-se en pacients de totes les edats, que no implicara cap risc per a la salut de la pacient, ni interferira amb l'eficàcia del tractament antineoplàsic, ni retardara l'administració de la teràpia oncològica, ni requerira procediments invasius. No obstant això, cap opció actual compleix totes les característiques anteriors. L'elecció d'una tècnica sobre una altra per a la preservació de la fertilitat femenina atén una sèrie de factors:

- L'edat de la pacient.
- La localització de la neoplàsia, estadi i pronòstic.
- El temps disponible abans d'iniciar el tractament oncològic.
- La reserva ovàrica de la pacient.

- La disponibilitat de parella masculina.
- Aspectes ètics i culturals en relació a la preservació i generació de gàmetes i embrions.

Entre les alternatives actuals, destaca la criopreservació d'embrions i ovòcits, considerada la tècnica de referència per als procediments de preservació de la fertilitat, encara que no evita el mal ovàric i la pèrdua de la dotació fol·licular pel tractament oncològic. Aquesta estratègia implica l'estimulació ovàrica de la pacient, la recollida dels ovòcits madurats i la seua criopreservació, o fertilització *in vitro* i posterior criopreservació segons la tècnica a realitzar. Encara que cada any naixen milers de xiquets amb aquestes dues tècniques, hi ha una sèrie d'aspectes a tindre en compte abans de ser aconsellades:

1. Es poden recomanar només en aquelles pacients que poden retardar l'inici del seu tractament oncològic almenys 10 dies per a realitzar l'estimulació ovàrica.
2. És necessari usar protocols específics d'estimulació ovàrica amb inhibidors de l'enzim aromatasa per a aquelles pacients amb neoplàsies hormono-dependents.
3. L'edat de la pacient, ja que el rendiment de l'estimulació ovàrica en pacients en fases de desenvolupament anteriors a la pubertat és menor, així com la implicació de connotacions ètiques.

A diferència de la criopreservació d'embrions, la vitrificació d'ovòcits es recomana a pacients adolescents (postpuberals) i a dones que no tinguen parella sentimental masculina, o tinguen objeccions ètiques i culturals respecte la criopreservació d'embrions.

La **criopreservació de teixit ovàric** constitueix l'única opció per a la preservació de la fertilitat en pacients pediàtriques (prepuberals), així com en pacients adolescents i adultes que no poden retardar l'inici del seu tractament oncològic. Aquesta tècnica consisteix en l'extracció de part de l'escorça ovàrica, que es fragmenta i criopreserva per al seu posterior trasplantament una vegada la pacient haja acabat la teràpia antineoplàsica. No obstant això, existeix la preocupació que les cèl·lules canceroses, especialment en els casos de leucèmia, puguen haver migrat al teixit ovàric abans de la seua extracció, de manera que persistisquen en les mostres criopreservades i siguen reintroduïdes amb el trasplantament. A més, la fertilitat de la pacient depèn de la vida mitjana del teixit trasplantat, que varia entre mesos i pocs anys, així com del nombre limitat de fol·licles

primordials presents en els fragments trasplantats. Això fa que siga d'importància cabdal el desenvolupament de noves alternatives encaminades a la prevenció del mal ovàric induït pel tractament oncològic, és a dir, a la protecció *in situ* de la reserva ovàrica durant el tractament gonadotòxic.

Per això, en els últims anys ha sorgit una nova estratègia anomenada **teràpia fertoprotectiva** dirigida a evitar el mal ovàric desencadenat per la quimioteràpia. Aquesta estratègia consisteix en l'administració d'un agent específic abans i durant el tractament oncològic, per a inhibir específicament el procés molecular activat pel fàrmac antineoplàsic. El principal benefici sobre les altres tècniques establides és la seua potencial aplicació a pacients de totes les edats i tipus de càncers, sense necessitat d'estimulació ovàrica que retardara l'inici de la quimioteràpia, i els processos quirúrgics que comporten les altres alternatives. Per contra, presenten preocupacions referents a la seua possible interferència amb el mecanisme d'acció del tractament oncològic, l'escassa evidència disponible de la seua eficàcia i seguretat, i la possibilitat de mantindre ovòcits danyats que puguen produir alteracions embrionàries. Per això, la majoria d'aquests agents fertoprotectors estan limitats al camp de la investigació, excepte els **agonistes de la GnRH** (GnRHa, de l'anglès *Gonadotrophin-relising Hormone agonists*). Els GnRHa indueixen una supressió temporal de l'eix hipotàlem-hipòfisi-ovari que inhibeix la secreció de FSH i LH. Aquest efecte redueix significativament la pèrdua de fol·licles primordials després del tractament quimioterapèutic, encara que es desconeix amb claredat el mecanisme molecular implicat. Actualment hi ha un extens nombre d'estudis i publicacions que afirmen l'eficàcia dels GnRHa per a la preservació de la fertilitat femenina, però actualment és considerada una tècnica experimental. Per això, pot oferir-se com una opció complementària a la criopreservació d'ovòcits/embrions o teixit ovàric per a la protecció ovàrica en pacients oncològiques premenopàusiques, però mai substituir a les tècniques ja establides de criopreservació.

A més dels GnRHa, molts estudis en models animals han descrit l'eficàcia d'altres agents fertoprotectors per a la protecció *in situ* de la reserva ovàrica. Alguns agents actuen directament sobre els fol·licles primordials per a inhibir les rutes moleculars implicades en el mal en l'ADN i l'apoptosi per a evitar la mort cel·lular d'aquests fol·licles, com per exemple els agents S1P (de l'anglès, *sphingosine-1-phosphate*), C1P (de l'anglès, *ceramide-1-phosphate*), imatinib,

inhibidors de les quinases ATM (de l'anglès, *Atàxia-Telangièctasi Mutated*) i ATR (de l'anglès, *Atàxia Telangièctasi and Rad3-related*). Un altre candidat a destacar com a agent fertoprotector és la LH, qui ha demostrat en un estudi recent ser capaç de generar *in vitro* senyals antiapoptòtiques en cèl·lules somàtiques de l'ovari per a reduir els danys induïts per l'agent quimioterapèutic cisplatí. Concretament, es va veure que la LH va reduir el mal en l'ADN dels ovòcits exposats a la quimioteràpia, disminuint amb això l'expressió de marcadors apoptòtics. A més, l'administració *in vivo* de LH a ratolins femella va evitar significativament la pèrdua de fol·licles primordials, permetent posteriorment la millora de la taxa d'embaràs i nombre de cries nascudes en els animals tractats amb LH. Malgrat aquests resultats prometedors, és necessari validar l'eficàcia de la LH com a agent fertoprotector contra fàrmacs quimioterapèutics més gonadotòxics, ja que el cisplatí s'associa amb un risc moderat d'induir POI. De la mateixa manera, els ovaris prepuberals en el ratolí contenen majoritàriament fol·licles primordials, mancant d'altres poblacions fol·liculars, la qual cosa impedeix avaluar els efectes de la LH en aquestes poblacions i com contribueix la sobreactivació en la pèrdua fol·licular. El potencial de desenvolupament dels ovòcits protegits per la LH i els seus mecanismes moleculars d'acció també necessiten ser elucidats abans de ser reconeguda la*LH com a agent fertoprotector.

Altres agents fertoprotectores estan dirigits a inhibir les rutes d'activació fol·licular, com la ruta PI3K-AKT, que són induïdes per la quimioteràpia per a previndre el reclutament massiu de fol·licles quiescents que inicien el seu desenvolupament. Alguns d'aquests factors inhibidors són l'immunomodulador AS101, everolimus, rapamicina, hormona antimulleriana, melatonina i grelina.

D'altra banda, atès que la vasculatura ovàrica i l'estat d'oxidació sovint són compromesos per la quimioteràpia, diversos agents contraresten els efectes del tractament oncològic sobre aquests processos, com el tamoxifen, la crocetina, el resveratrol i el factor estimulant de colònies de granulòcits.

Finalment, respecte el **futur de les tècniques de la preservació de la fertilitat** no es pot obviar l'existència d'altres tècniques experimentals que potencialment podrien ser aplicades per a la preservació de la fertilitat en el futur, però que actualment es troben en fases primerenques del seu desenvolupament com, per exemple, la maduració *in vitro* dels fol·licles, tant primordials com

antrals, per a l'obtenció d'ovòcits MII que pogueren ser criopreservats. Aquesta opció seria una alternativa especialment recomanada per a aquelles pacients joves que no pogueren demorar l'inici del seu tractament oncològic. Així mateix, la creació d'un ovari artificial que permetera realitzar tot el procés de desenvolupament fol·licular per a produir ovòcits fecundables seria tot un descobriment amb una gran aplicabilitat en el camp de la preservació de la fertilitat.

Hipòtesi

El tractament amb LH podria ser utilitzat com una estratègia per a la protecció *in situ* de la reserva ovàrica en pacients oncològiques que se sotmeten a teràpies altament gonadotòxiques. L'acció de la LH sobre l'ovari es basaria a generar un ambient propici per a contrarestar els efectes nocius de la quimioteràpia basada en els agents alquilants per a preservar el potencial reproductiu a llarg termini.

Objectius

L'**objectiu principal** del present estudi és avaluar el tractament amb LH com una nova estratègia per a protegir *in situ* la dotació fol·licular i preservar l'esperança reproductiva de ratolins femella adults enfront dels efectes deleteris del tractament oncològic amb agents alquilants.

Es poden distingir els següents objectius secundaris:

- Determinar *in vivo* els efectes a curt termini del tractament de LH en els fol·licles quiescents exposats als agents alquilants.
- Investigar *in vivo* els mecanismes d'acció de la LH per a exercir la protecció ovàrica front la quimioteràpia.
- Avaluar l'eficàcia del tractament de LH per a la preservació de l'esperança reproductiva a llarg termini.

- Analitzar *in vivo* els efectes a curt termini de l'administració de LH en els fol·licles en desenvolupament en el moment d'exposició a la quimioteràpia, mitjançant l'ús d'un cep murí subfèrtil.

Materials i mètodes

Tots els experiments d'aquesta tesi han sigut realitzats en animals mitjançant procediments prèviament aprovats pel Comité d'Experimentació i Benestar Animal de la Universitat de València (A1510573656187) i per la Direcció General d'Agricultura, Ramaderia i Pesca, Generalitat Valenciana (2018/VSC/PEA/0010 i 2019/VSC/PEA/0206).

1. Efectes de la LH en els fol·licles quiescents exposats a agents alquilants

Per a analitzar els efectes de la LH en els fol·licles primordials, 31 ratolins femella CD-1 de 7 setmanes d'edat van ser distribuïdes aleatòriament en 3 grups experimentals: control (n=9), quimioteràpia (ChT, n=11) i quimioteràpia amb LH (ChT+LH-1x, n=11). Als animals del grup control se'ls va administrar intraperitonealment solució salina seguida d'una segona injecció de dimetilsulfòxid (vehicle) 24 hores després. El grup ChT va rebre una primera injecció de salí seguit de la solució de quimioteràpia (120 mg/kg de ciclofosfamida + 12 mg/kg busulfà dissolts en dimetilsulfòxid). El grup ChT+LH-1x va rebre 1 unitat internacional de LH (2.3 ng/ml) seguida d'1 unitat internacional de LH juntament amb la quimioteràpia a les 24 hores. Els ratolins femella van ser estabulats durant 30 dies i estimulats ovàricament per a assegurar la recollida d'ovòcits i embrions procedents de fol·licles primordials en el moment d'administració a la quimioteràpia. Dos ratolins femella per grup van ser sacrificats 16 hores després de desencadenar-los l'ovulació per a la recollida d'ovòcits madurs, mentre que la resta de ratolins femella es van mantindre en estabulació i van ser creuades amb mascles durant 40 hores per a finalment recollir els ovaris, ovòcits i embrions.

Per a avaluar els efectes de la LH sobre la fertilitat a llarg termini, en el dia 30 després de l'administració dels tractaments, 4 animals per grup van ser creuats en 6 rondes successives.

Després de l'última ronda d'encreuament, els ratolins femella van ser estimulats ovàricament, es van creuar i finalment van ser sacrificats per a recollir els ovaris, ovòcits i embrions per a avaluar la resposta dels animals a l'estimulació. Per a aquest experiment a llarg termini, es va incloure un quart grup experimental tractat amb 5 unitats internacionals de LH (ChT+LH-5x, n=4) per a analitzar si el possible efecte de la LH és dosi dependent.

Una vegada recollides totes les mostres, es va procedir a la seua anàlisi per a analitzar els efectes de la LH contra la quimioteràpia amb agents alquilants:

- Anàlisi de l'estroma: es van identificar les àrees d'estroma degenerat en els ovaris com la presència de regions acel·lulars i/o fibròtiques en mostres tenyides amb hematoxilina-eosina. Es va estimar l'índex d'àrea degenerada relativitzant l'extensió de l'àrea afectada respecte l'àrea total de teixit ovàric.
- Recomptes fol·liculars: es va determinar el nombre de fol·licles en cada estadi de maduració en seccions ovàriques seriades tenyides amb hematoxilina-eosina. Per a evitar possibles errors en el recompte, només es va comptar aquells fol·licles morfològicament normals que presentaren un nucli. També es va determinar el nombre de fol·licles que presentaren alguna anormalitat morfològica (multinucleació, multivacuolització del ooplasma, alteracions en les capes de GC o degeneració fol·licular) per a comprovar l'efecte de la LH en el desenvolupament fol·licular.
- Recompte i classificació d'ovòcits metafase II i embrions sobre la base de criteris morfològics.
- Anàlisi de la qualitat dels ovòcits metafase II: es va estudiar la morfologia, grandària i disposició del fus meiòtic, així com l'organització dels cromosomes en la placa equatorial per microscòpia confocal de fluorescència.
- Efectes a llarg termini: es va registrar la taxa de gestació, nombre de cries per ventrada i total de cries nascudes al llarg de 6 rondes d'encreuament consecutives. També es va avaluar la resposta a l'estimulació ovàrica i viabilitat ovocitària en registrar el nombre i qualitat morfològica d'ovòcits metafase II i embrions recuperats.

2. Efectes de la LH en la comunicació entre l'ovòcit i les CG

A causa de la rellevància del procés de comunicació bidireccional entre l'ovòcit i GC per al correcte creixement fol·licular i desenvolupament de l'ovòcit, es va avaluar aquest procés mitjançant assajos histològics i moleculars en mostres ovàriques obtingudes de ratolins femella control (n=3), ChT (n=5), i ChT+LH-1x (n=5) recollides als 30 dies després de l'administració dels tractaments.

- Per a les anàlisis moleculars es van aïllar mecànicament tots els fol·licles continguts en cada ovari analitzat. Es va seleccionar només aquells fol·licles amb un diàmetre igual o superior a 100 µm per correspondre a l'estadi de desenvolupament secundari o posterior, en els quals el procés de la comunicació ovòcit-GC és més evident. La meitat dels fol·licles va ser emmagatzemada, mentre que l'altra meitat es va decumular per obtindre ovòcits i GC. Posteriorment es van analitzar en els fol·licles, ovòcits i GC obtinguts l'expressió de molècules relacionades amb unions comunicants (Cx37 i Cx43), unions adherents (E-Cad i N-Cad), unions estretes (TJP1) i factors secretats pels ovòcits (GDF9, BMP15 i els seus receptors) mitjançant RT-qPCR i western blot.
- Es va visualitzar per microscòpia confocal de fluorescència les unions comunicants (Cx37 i Cx43), adherents (E-Cad) i factors secretats pels ovòcits (GDF9 i BMP15), en seccions ovàriques.

3. Mecanismes d'acció de la LH

Amb la finalitat d'investigar la resposta que es desencadena en l'ovari després de l'administració de LH per a exercir la seua protecció, 16 ratolins femella CD-1 de 7 setmanes d'edat es van distribuir en els 4 grups experimentals: control, ChT, ChT+LH-1x i ChT+LH-5x. Els tractaments es van administrar com s'ha descrit en la secció “Efectes de la LH en els fol·licles quiescents exposats a agents alquilants”. Els ratolins femella es van sacrificar a les 12 i 24 hores després de l'administració de quimioteràpia, recollint els ovaris per a realitzar les següents anàlisis funcionals:

- Dany en l'ADN: es van visualitzar els trencaments en la doble cadena d'ADN mitjançant immunofluorescència contra la histona H2AX fosforilada (γH2AX).
- Apoptosi: es va determinar el percentatge de fol·licles apoptòtics en seccions ovàriques mitjançant l'assaig TUNEL.
- Gonadotoxicitat: per a comprovar si la LH era capaç de previndre la toxicitat induïda per la quimioteràpia en els ovaris, es van mesurar els nivells d'expressió de les proteïnes γH2AX, Cleaved Caspase 3 (CC3), B-cell lymphoma 2 (Bcl2), Extracellular Signal-Regulated Kinase 1 and 2 (ERK1/2), i ERK1/2 fosforilada (pERK1/2) en lisats ovàrics per western blot.
- Reparació de l'ADN: per a avaluar el paper de la LH en l'activació de rutes de reparació de l'ADN es va analitzar per western blot l'expressió de la cinasa ATM i recombinasa Rad51 implicades en la ruta ATM, considerada la més important per a la reparació dels trencaments dobles de l'ADN en els fol·licles primordials. També es van mesurar els nivells de Protein Kinase B (AKT) i AKT fosforilada (pAKT) en lisats ovàrics. A més, a nivell gènic es va investigar l'expressió d'altres factors involucrats en altres rutes de reparació de l'ADN: Msh6 (reparació per mal aparellament), Apex 1 (reparació per escissió de bases), Prkdc (reparació per unió d'extrems no homòlegs), Ercc3 (reparació per escissió de nucleòtids), i Rad51.

4. Efectes de la LH en els fol·licles en creixement exposats a agents alquilants

Per a analitzar si la LH protegeix els fol·licles en desenvolupament durant l'exposició a la quimioteràpia, es va utilitzar el cep de ratolí NOD-SCID, considerada menys fèrtil que l'utilitzat en els procediments anteriors, amb la finalitat de representar un escenari reproductiu més advers. Per a això, 16 ratolins femella NOD-SCID de 7 setmanes d'edat van ser distribuïdes aleatòriament als grups control (n = 5), ChT (n = 5) i ChT+LH-1x (n = 6). Els grups control i ChT es van tractar d'igual manera a l'exposada en l'apartat "Efectes de la LH en els fol·licles quiescents exposats a agents alquilants". Els ratolins femella del grup ChT+LH-1x tan sols van rebre 1 unitat internacional de LH juntament amb la quimioteràpia per a comprovar si una sola dosi de LH és

suficient per a induir la protecció ovàrica. Passats 7 dies des de l'aplicació dels tractaments, els ratolins femella van rebre un cicle d'estimulació ovàrica controlada per a assegurar que els ovòcits i embrions recollits procedisquen de fol·licles en creixement en el moment d'exposició a la quimioteràpia. Dos ratolins femella per grup van ser sacrificats a les 16 hores d'induir l'ovulació per a recuperar ovòcits metafase II, mentre que la resta van ser creuats amb mascles durant 40 hores per a recollir ovòcits, embrions i ovaris.

Les mostres biològiques recollides es van utilitzar per a realitzar les següents anàlisis funcionals:

- Avaluació de l'estroma: es va determinar l'índex d'àrea estromal degenerada.
- Recomptes fol·liculars: es va estudiar l'efecte de la LH en la reserva ovàrica i poblacions fol·liculars en creixement en seccions ovàriques tenyides amb hematoxilina-eosina. També es va determinar el percentatge de fol·licles morfològicament anormals.
- Dany en l'ADN i apoptosi: és va estudiar el paper de la LH per a la prevenció i reducció del dany en l'ADN i l'apoptosi dels ovòcits i GC mitjançant immunofluorescència de γH2AX i l'assaig TUNEL, respectivament.
- Recompte i classificació d'ovòcits metafase II i embrions sobre la base de criteris morfològics.
- Qualitat dels ovòcits metafase II: es va investigar mitjançant microscòpia confocal d'immunofluorescència el potencial meiòtic com a símbol de qualitat dels ovòcits recollits analitzant la presència o absència del fus meiòtic, i característiques morfomètriques d'aquest. També es va avaluar la disposició i alineament dels cromosomes en la placa metafàsica.

Resultats

1. Efectes en els fol·licles quiescents

L'**avaluació macroscòpica** dels ovaris va revelar que tant el grup ChT com ChT+LH-1x van patir una reducció similar en la relació entre el pes ovàric i corporal comparat amb el grup control. No obstant això, el tractament amb LH va evitar en un 10% la reducció de la grandària ovàrica vista

en el grup ChT respecte els controls. L'examen histològic va demostrar que la quimioteràpia afecta negativament a l'estroma incrementant significativament l'**índex de degeneració de l'estroma** ovàric 2.3 vegades respecte el grup control, mentre que la LH evita part d'aquest dany en veure's un augment d'1.6 vegades.

Els **recomptes fol·liculars** van mostrar que els ovaris del grup ChT presentaven un 69.8% menys fol·licles que el grup control, que va afectar especialment les poblacions de fol·licles primordials, primaris i secundaris amb una reducció del 76.4%, 68.0% i 67.8%, respectivament. En canvi, la LH va reduir part d'aquesta pèrdua trobant un 34.6% més fol·licles que el grup ChT, amb un increment del 38.1%, 36.1% i 25.0% de fol·licles primordials, primaris i secundaris respecte el grup ChT, respectivament. A més, la LH va restaurar els valors control en el percentatge de fol·licles morfològicament anormals, millorant significativament els nivells detectats en el grup ChT. La població fol·licular més afectada per les alteracions morfològiques en els 3 grups experimentals va ser l'estadi secundari, representant més del 50% dels fol·licles anormals.

El tractament amb LH va permetre recuperar un 25% més **ovòcits metafase II** morfològicament normals que el grup ChT, evitant la reducció estadísticament significativa respecte el grup control. De la mateixa manera, l'anàlisi de la **qualitat ovocitaria** per microscòpia confocal va mostrar que els ovòcits del grup tractat amb LH presentaven un fus meiòtic 31.1% més gran que els del grup ChT, restaurant els valors observats en el grup control, així com també va reduir el nombre d'ovòcits amb almenys un cromosoma mal alineat respecte la placa metafàsica en comparació amb el grup ChT. No obstant això, no es va veure millora per al nombre d'**embrions** en estadi de 2 cèl·lules.

L**'estudi a llarg termini** va demostrar que el tractament amb LH, i especialment la dosi baixa (1 unitat internacional), és capaç de revertir notablement els efectes negatius de la quimioteràpia en la taxa de gestació acumulada i grandària de les ventrades, la qual cosa va permetre augmentar en un 21% el nombre total de cries nascudes en el grup ChT+LH-1x respecte el grup ChT. Totes les cries nascudes van presentar valors similars de grandària i pes en el moment del naixement per als tres grups. D'altra banda, per a justificar part d'aquests resultats a llarg termini, es va observar que els ovaris dels ratolins femella estimulats després de la sisena ronda

d'encreuament dels grups tractats amb LH, i especialment les del grup ChT+LH-1x, van ser significativament més grans que els del grup ChT. A més, es va recuperar un major nombre d'ovòcits metafase II i embrions amb bona qualitat morfològica procedents de ratolins femella tractats amb LH respecte el grup ChT, totes elles estimulades ovàricament després de l'última ronda de creuaments.

2. Efecte de la protecció de la LH en el procés de la comunicació entre ovòcit i GC

Amb la finalitat d'entendre millor com l'administració de LH pot millorar la qualitat dels ovòcits que procedeixen de fol·licles en l'estadi primordial en el moment de la quimioteràpia, es va estudiar la capacitat d'aquests fol·licles tractats amb LH per a establir una correcta comunicació entre l'ovòcit i GC durant el desenvolupament fol·licular, analitzant per a això les unions intercel·lulars i els factors de creixement secretats pels ovòcits.

L'**aïllament dels fol·licles** va revelar que els ovaris continguts en el grup tractat amb LH contenia un major nombre de fol·licles, reduint significativament els efectes de la quimioteràpia vistos en el grup ChT.

L'**estudi d'expressió de les unions intercel·lulars** va mostrar que a nivell gènic la quimioteràpia va reduir l'expressió de tots els gens analitzats (Cx37, E-Cad, Cx43, N-Cad i TJP1) en fol·licles intactes, ovòcits aïllats i GC, mentre que el grup tractat amb LH va mostrar valors d'expressió similars als detectats en el grup control. Es van obtindre resultats similars en l'anàlisi d'expressió proteica per western blot per als factors Cx37, E-Cad i Cx43. La **visualització de les unions intercel·lulars** per microscòpia confocal va mostrar que l'administració de LH va revertir significativament els efectes de la quimioteràpia en l'expressió de les molècules Cx37, E-Cad i Cx43 en els fol·licles a partir de l'estadi secundari, confirmant la capacitat de la LH per a mantindre la capacitat dels fol·licles primordials protegits en el moment de l'exposició a la quimioteràpia per a establir correctament unions intercel·lulars entre l'ovòcit i les GC durant el desenvolupament fol·licular.

L'**avaluació de l'expressió dels factors de creixement intercanviats pels ovòcits i GC** va mostrar que la quimioteràpia va causar una reducció notable en 5 dels 6 gens analitzats (GDF9, BMP15, BMPR2, ALK4, ALK5 i ALK6), mentre que la LH va mantindre valors similars al grup control per a la majoria d'ells en les mostres de fol·licles, ovòcits i GC analitzats. La preservació de l'expressió dels factors GDF9 i BMP15 per la LH front la quimioteràpia va ser posteriorment validada a nivell proteic per western blot, així com per la seua **visualització** mitjançant microscòpia confocal.

3. Mecanismes de protecció de la LH

Per dilucidar el mecanisme d'acció de la LH per a la protecció ovàrica, es va avaluar en primer lloc el **dany en l'ADN i apoptosi** en les primeres 12 hores després de l'administració dels tractaments, mostrant que tots dos grups de LH (ChT+LH-1x i ChT+LH-5x) van reduir significativament el percentatge d'ovòcits amb dany en l'ADN i fol·licles apoptòtics detectats en el grup ChT.

De la mateixa manera, en l'**assaig d'ovotoxicitat** es va observar que el tractament amb LH va evitar els efectes de la quimioteràpia en l'expressió proteica de γH2AX, la relació entre la proteïna anti-apoptòtica Bcl2 i la proteïna pro-apoptòtica CC3, i el ràtio de fosforilació d'ERK1/2, a les 12 i 24 hores d'administració dels reactius.

Atès que els mecanismes de reparació de l'ADN poden reduir el mal cel·lular i l'apoptosi, es va estudiar el paper de la LH com a inductor de l'activació d'aquests processos. Es va detectar per western blot que la LH va potenciar a les 12 i 24 hores l'expressió de proteïnes implicades directament (ATM i Rad51) en el procés de reparació de l'ADN anomenat recombinació homòloga, i va evitar la sobreactivació d'unes altres que poden regular negativament el procés (pAKT/AKT). A més, es va veure que la dosi baixa de LH va potenciar l'expressió gènica de molècules implicades en altres rutes de reparació de l'ADN per damunt de la quimioteràpia en les primeres 12 hores, conservant la sobreexpressió del gen Rad51 a les 24 hores.

4. Efectes de la LH en els fol·licles en creixement exposats als agents alquilants

L'**examen macroscòpic** va mostrar que la LH no va ser capaç de revertir els efectes de la quimioteràpia ni en la relació del pes ovàric respecte el pes corporal, ni en la grandària dels ovaris. En canvi, l'administració de LH va reduir significativament l'**índex de degeneració de l'estroma** respecte el grup ChT, passant d'un increment de 3.5 vegades per a ChT a 1.9 vegades per a ChT+LH-1x respecte el grup control.

La **dotació fol·licular** es va veure significativament disminuïda en els grups ChT i ChT+LH-1x respecte el grup control, però els ovaris del grup tractat amb LH contenien un 31.2% més fol·licles que el grup ChT. Aquesta protecció front la quimioteràpia va beneficiar especialment a la població de fol·licles primordials i primaris, registrant un 83.2% i 48.4% més fol·licles, respectivament, respecte el grup ChT. No obstant això, el percentatge de fol·licles amb alguna anomalia morfològica va augmentar significativament en els grups ChT i ChT+LH-1x de manera similar respecte el grup control.

L'avaluació del **dany fol·licular** en les seccions ovàriques va revelar que la LH va reduir el nombre de fol·licles l'ovòcit dels quals era positiu per a γH2AX i, per tant, presentava dany en l'ADN, així com el percentatge de fol·licles amb una alta taxa d'apoptosi en les GC, mesurat per l'assaig TUNEL.

Respecte el **nombre d'ovòcits i embrions**, la quimioteràpia va reduir significativament el nombre d'ovòcits metafase II i embrions morfològicament normals respecte el grup control, mentre que la LH va evitar parcialment els efectes en els ovòcits, recuperant un 26.3% més que el grup ChT.

Finalment, l'anàlisi de la **qualitat dels ovòcits metafase II** recuperats va demostrar que el tractament amb LH va incrementar la probabilitat de formació del fus meiòtic en els ovòcits respecte el grup ChT. A més, encara que el fus meiòtic dels ovòcits del grup ChT+LH-1x va ser significativament més xicotet que el del grup control, l'àrea ocupada pel fus va resultar ser 3 vegades superior a la identificada en el grup ChT. De la mateixa manera, la LH va reduir

significativament respecte el grup ChT el nombre d'ovòcits metafase II amb almenys un dels cromosomes desplaçat respecte la placa equatorial, mostrant amb això una millor qualitat meiòtica.

Discussió

Els tractaments quimioterapèutics basats en l'ús d'agents alquilants són àmpliament utilitzats en les neoplàsies ginecològiques i hematològiques, que representen el 48.4% i 7.7%, respectivament, del total de nous casos de càncer en dones menors de 45 anys a nivell global. Els efectes secundaris que tenen aquests agents alquilants sobre la fertilitat de la dona és una de les principals preocupacions dels professionals en medicina reproductiva. Encara que en l'actualitat es disposa de tècniques reeixides per a la preservació de la fertilitat en pacients oncològiques, encara es necessiten noves alternatives per a la protecció *in situ* de la reserva ovàrica. La prevenció de l'apoptosi induïda pel cisplatí en ovòcits de ratolins prepúbers mitjançant la suplementació de LH va postular a la LH com un sòlid candidat per a la gonadoprotecció contra la quimioteràpia. Amb aquest propòsit, aquesta tesi ha avaluat l'efecte del tractament de la LH sobre 1) els fol·licles quiescents en ratolins femella CD-1, i 2) els fol·licles en creixement en ratolins femella subfèrtils NOD-SCID després de la quimioteràpia amb agents alquilants a una dosi equivalent a la utilitzada en pacients amb càncer.

En la primera aproximació experimental per a avaluar els efectes de la LH en la població de fol·licles quiescents en el moment d'exposició a la quimioteràpia, les mostres es van recollir 30 dies després de l'administració dels tractaments pel fet que és el temps que requereix un fol·licle primordial per a activar-se i completar el seu creixement fins a ovular un ovòcit madur. Els nostres resultats van revelar que la quimioteràpia redueix significativament el nombre de fol·licles continguts en els ovaris, afectant a tots els estadis de desenvolupament, la qual cosa va derivar en una reducció significativa dels ovòcits metafase II recollits després de l'estimulació ovàrica dels ratolins femella. En canvi, el tractament amb LH va millorar notablement tant el nombre de fol·licles com el d'ovòcits recollits. Tenint en compte que els fol·licles i ovòcits analitzats procedien de fol·licles primordials en el moment d'administració de la quimioteràpia, els nostres resultats

suggereixen que la LH protegeix la reserva ovàrica front el tractament oncològic. A més, els nostres resultats també suggereixen que hi ha una estreta relació entre la pèrdua de reserva ovàrica i el dany fol·licular, ja que trobem que els agents alquilants van causar un augment significatiu del percentatge de fol·licles amb ovòcits amb l'ADN danyat i de GC apoptòtiques en les primeres hores després de la seua exposició, tal com han descrit estudis previs. El fet que els grups tractats amb LH evitaren significativament el dany fol·licular, tant en l'ovòcit com en les GC, indicava que aquesta hormona pot tindre un efecte positiu en la salut fol·licular, i això podria explicar també la millora dels recomptes fol·liculars i el nombre d'ovòcits recollits. Aquest efecte protector de la LH podria ser realitzat mitjançant senyals produïts per cèl·lules ovàriques somàtiques que expressen el seu receptor, com suggereixen diversos estudis, encara que es desconega el mecanisme d'acció.

Per això, atès que el dany en l'ADN i l'apoptosi estan íntimament relacionats amb els mecanismes de reparació de l'ADN, vam trobar que la LH era capaç d'augmentar l'expressió de factors relacionats amb diverses rutes de reparació de l'ADN, especialment la recombinació homòloga, la qual es considera el mecanisme més important per a la reparació de l'ADN en els fol·licles primordials. Així mateix, els nostres resultats novament van mostrar que la LH era capaç de reduir l'expressió de marcadors del dany en l'ADN i l'apoptosi. Per tant, aquests descobriments suggereixen que la LH afavoreix l'activació de mecanismes de reparació de l'ADN per a preservar la integritat del material genètic ovocitari i minimitzar el dany ovàric causat per la quimioteràpia.

El nínxol ovàric juga un paper fonamental per a la correcta fisiologia del fol·licle (activació, desenvolupament, creixement), de manera que la protecció de l'estroma ovàric per la LH enfront de la quimioteràpia pot ser un altre dels motius per a explicar la protecció exercida per la LH. Els nostres resultats també van mostrar que la quimioteràpia indueix l'aparició d'anomalies morfològiques en els fol·licles, fonamentalment registrades en la població de fol·licles secundaris, suggerint que podria alterar el seu potencial de desenvolupament i qualitat. En canvi, la LH va evitar part d'aquests efectes i, amb això, possiblement la seua capacitat de desenvolupament. Per això, com el procés de comunicació bidireccional que es produeix entre l'ovòcit i les GC és de cabdal importància per al correcte procés de foliculogènesi, vam trobar que el tractament amb LH va evitar significativament els efectes de la quimioteràpia en l'expressió de molècules

involucrades en l'establiment d'unions intercel·lulars, fonamentalment comunicants i adherents, entre l'ovòcit i les GC, així com de factors de creixement que són intercanviats entre el compartiment germinal i somàtic per al correcte desenvolupament de tots dos components fol·liculars. A més, aquestes alteracions de la comunicació ovòcit-GC induïdes per la quimioteràpia es van produir a partir de l'estadi secundari, suggerint una alteració en la transició entre el fol·licle primari a secundari que puga afectar el seu desenvolupament.

La formació del fus meiòtic i el correcte alineament cromosòmic en la placa equatorial és un marcador de qualitat ovocitària. Els nostres resultats van mostrar que els ovòcits procedents de fol·licles primordials tractats amb LH presenten millors característiques del fus meiòtic i alineament cromosòmic que els tractats solament amb quimioteràpia. Aquests descobriments podrien ser deguts a la capacitat de la LH per a disminuir el dany fol·licular i el manteniment del procés de comunicació ovòcit-GC que asseguren un correcte desenvolupament del fol·licle perquè acabe ovulant un ovòcit madur de bona qualitat.

Els efectes a curt termini de la LH per protegir la reserva ovàrica, i millorar el nombre i qualitat dels ovòcits resultants va semblar traduir-se en una millora a llarg termini de la fertilitat. Per tant, els ratolins femella tractats amb LH van presentar majors taxes d'embaràs i grandària de ventrades que van conduir a un major nombre total de cries que el grup tractat sol amb quimioteràpia. A més, el tractament amb LH no va afectar la salut de les cries resultants, confirmant la seguretat de la tècnica. La millora a llarg termini es va confirmar posteriorment en augmentar el nombre i qualitat morfològica d'ovòcits i embrions dels ratolins femella tractats amb LH. No obstant això, cal destacar que vam trobar millors resultats per als ratolins femella del grup tractat amb la dosi baixa de LH, la qual cosa suggereix que dosis elevades de l'hormona poden tindre un efecte advers sobre la reproducció femenina a llarg termini, tal com succeeix amb altres agents. De fet, nivells circulants de LH suprafisiològics permanentment causen una pèrdua significativa de la reserva ovàrica. Per això, a diferència de les estratègies de preservació de la fertilitat basades en la presa prolongada de GnRHa per a la supressió de l'eixhipotàlem-hipòfisi-ovari, nosaltres amb aquesta tesi proposem l'administració d'una dosi puntual de LH amb la quimioteràpia. No obstant això, és necessari aprofundir en l'eficàcia de l'estratègia i determinació de la millor dosi i temps d'administració.

En l'experiment per a avaluar els efectes de la LH sobre els fol·licles que ja estaven en creixement en el moment de l'exposició a la quimioteràpia, vam utilitzar un cep de ratolins considerat subfèrtil per a validar els efectes fertoprotectors de la LH. En primer lloc, vam trobar que la LH va protegir significativament les poblacions de fol·licles més indiferenciades (primordials i primaris), donant suport als resultats obtinguts en el primer model animal. Aquesta preservació dels fol·licles primordials per part de la LH podria deure's a un efecte inhibidor de la sobreactivació dels fol·licles quiescents que normalment desencadena la quimioteràpia (efecte *Burnout*), o evitant el dany fol·licular que desemboque en la seua apoptosi. Per a donar-se la primera opció, hauríem d'haver vist un augment proporcional del nombre de fol·licles en creixement a la pèrdua de fol·licles primordials, però els nostres resultats només mostren una pèrdua global de totes les poblacions fol·liculars, indicant que la LH exerceix el seu efecte protector en generar senyals anti-apoptòtiques encaminades a la supervivència dels fol·licles danyats. De fet, les nostres anàlisis van mostrar un descens de fol·licles amb dany en l'ADN ovocitari i apoptosi en les CG. La reducció del dany fol·licular va contribuir a ovular més ovòcits metafase II, i de millor qualitat mesurada per anàlisi del fus meiòtic i alineament cromosòmic. Per tant, el tractament de LH protegiria la reserva ovàrica i els fol·licles que ja estigueren en creixement en el moment d'administració de la quimioteràpia per a permetre recuperar ovòcits metafase II competents.

Per tot això, encara que la totalitat dels experiments recollits en aquesta tesi es van realitzar en un model animal, obri la porta a una nova estratègia sense intervencions quirúrgiques, protocols d'estimulació ovàrica, i basada en la protecció *in situ* de la reserva ovàrica per a la preservació de la fertilitat en pacients joves amb càncer.

Conclusions

1. El tractament amb LH evita l'alteració de l'arquitectura ovàrica induïda per la quimioteràpia, que contribueix a disminuir l'àrea d'estroma amb regions acel·lulars i/o fibròtiques.

2. La LH confereix protecció de la reserva ovàrica *in situ* que porta a reduir la incidència de fol·licles amb anomalies morfològiques en el ooplasma i en les GC al llarg del creixement i desenvolupament fol·licular.
3. La protecció dels fol·licles primordials per part de la LH prevé l'alteració detectada després de l'administració de quimioteràpia sobre les unions gap i les unions adherents en els compartiments somàtic i germinal dels fol·licles a partir de l'estadi secundari, mantenint estable la interacció entre ovòcit i GC durant el creixement fol·licular.
4. L'administració de LH contraresta els efectes de la quimioteràpia en preservar l'expressió dels factors de creixement que s'intercanvien entre els ovòcits i les GC en els fol·licles en estadis avançats del desenvolupament fol·licular, la qual cosa promou la maduració de tots dos compartiments fol·liculars per obtindre ovòcits metafase II competents.
5. La protecció fol·licular exercida per la LH millora el nombre, la qualitat morfològica, la competència meiòtica i l'alineament cromosòmic dels ovòcits metafase II ovulats.
6. L'administració de LH preserva el potencial i l'esperança reproductiva dels ratolins femella adults sense afectar la salut de la descendència.
7. El paper de la LH està mediat, almenys en part, per una potenciació de la resposta al dany de l'ADN, que desencadena mecanismes de reparació de l'ADN, com la recombinació homòloga, així com genera senyals anti-apoptòtiques durant les primeres hores després de l'exposició a la quimioteràpia per mantindre la viabilitat fol·licular.
8. Existeix un rang òptim de concentració de LH per aconseguir un equilibri adequat entre la prevenció de la gonadotoxicitat aguda a curt termini i la preservació de la fertilitat a llarg termini.
9. La LH exerceix efectes anti-apoptòtics sobre l'ovòcit i les GC proliferatives dels fol·licles que es troben en fase de creixement en el moment de l'administració de la quimioteràpia, la qual cosa es tradueix en una millora de la quantitat i la qualitat dels ovòcits metafase II resultants.

Introduction

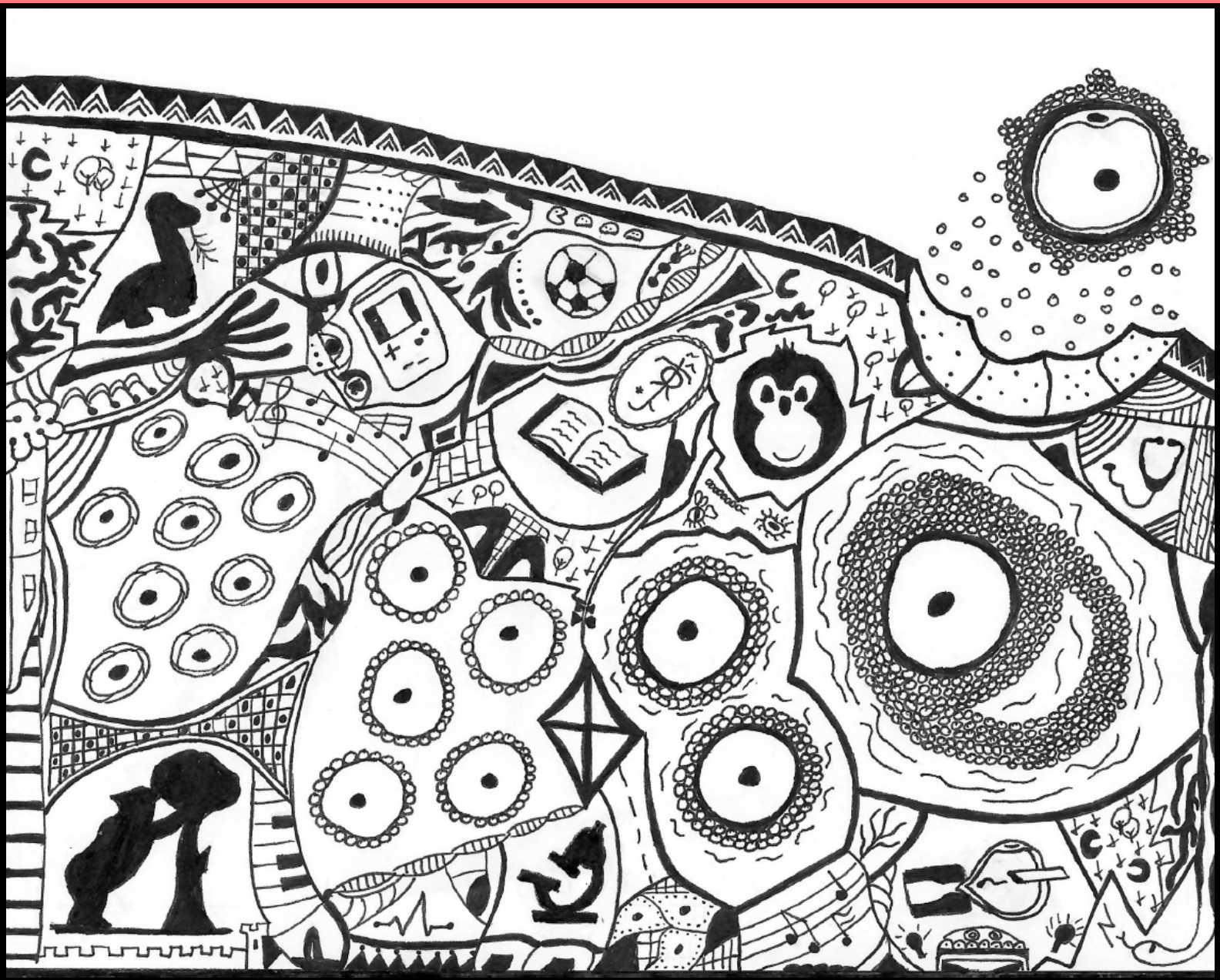

1. Female reproductive system: the ovary

The ovary is a bilateral paired multicompartmental organ with a complex embryonic development derived from mesoderm and mesonephric ridges (1). The function of the female gonad is the differentiation of mature oocytes with full competence to be fertilized and maintain subsequent embryo development. In addition, ovarian function is also associated with the production of steroid hormones (oestrogen and progesterone), required for the development of female secondary sexual characteristics and the creation of a suitable environment within the reproductive tract for fertilization and pregnancy, in response to pituitary gonadotropins (follicle stimulating hormone (FSH), and luteinizing hormone (LH)).

1.1. Ovarian anatomy and histology

Ovaries are small almond-shaped structures connected to the pelvic sidewall by the suspensory ligament, to the uterus by the ovarian ligament, and to the posterior surface of the broad ligament of the uterus by the mesovarium, which attaches to the hilum of the ovary (*rete ovarii*) enclosing its neurovascular structures.

The ovary is characterized by three different histological layers or components (Fig. 1):

- Surface: the outer layer is formed by a simple cuboidal epithelium, known as the germinal epithelium, followed by an avascular and dense irregular connective tissue capsule named tunica albuginea.
- Cortex: intermediate zone comprised of connective tissue with fibroblast-like cells, collagen fibers and other extracellular matrix components generating the ovarian stroma, as well as numerous follicles consisting of one oocyte surrounded by a single or multiple layers of somatic cells.
- Medulla: high vascular inner zone of the ovary with connective tissue, elastic fibers, blood and lymph vessels, and nerve fibers.

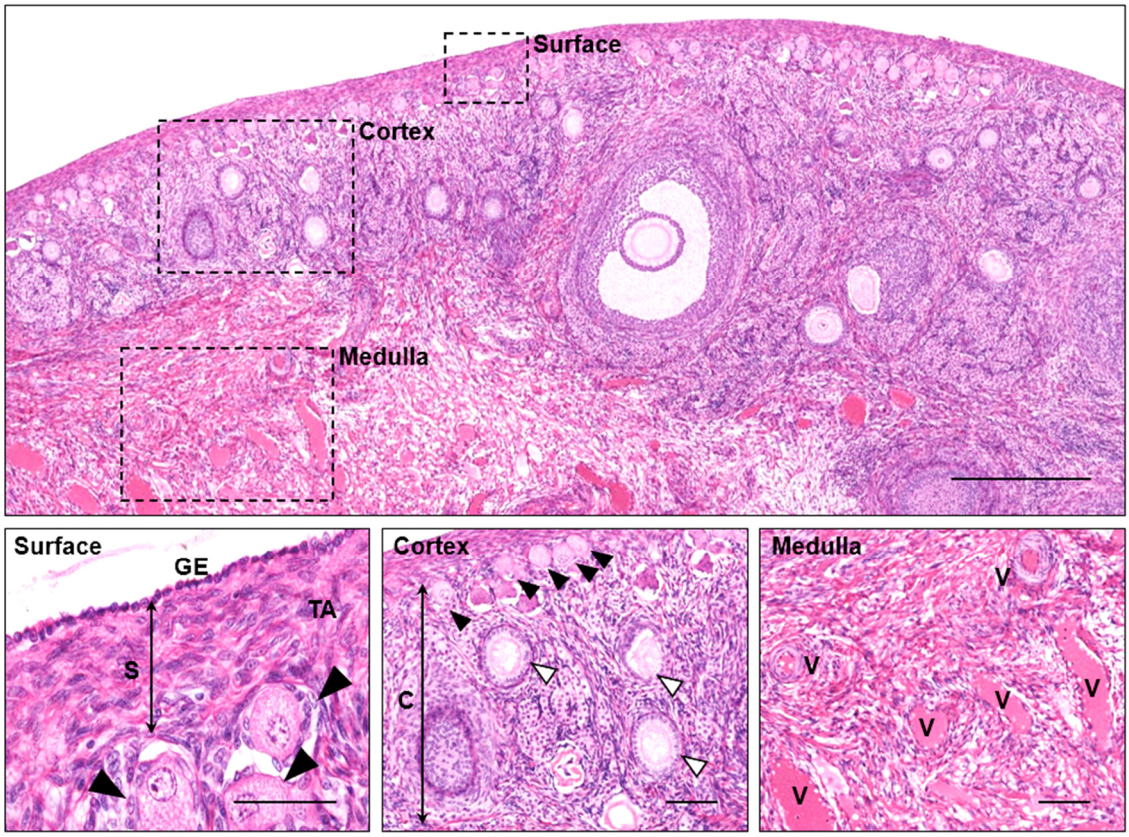

Figure 1. Histology of ovary. *Ovarian section stained with hematoxylin and eosin (H&E) reflecting the three histological features of the female gonad and high magnification images of each one: ovarian surface (S) as the outer region comprised with the germinal epithelium (GE) and the tunica albuginea (TA); the ovarian cortex (C) where numerous follicles in quiescent (black arrowhead) and growing (white arrowhead) developmental stages can be found; and the medulla as the innermost ovarian region showing a complex neurovascular network with sinusoid blood and lymph vessels (V). Upper scale bar: 500 µm; bottom scale bars: 100 µm. Images adapted from histologyguide.com.*

1.2. The ovarian follicle: structure and formation

Follicles are considered the basic functional units of the ovaries and represent a dual cell compartment with germ and somatic cell components. As a result, each follicle encloses a single female gamete, the oocyte, surrounded by one or more layers of somatic cells called granulosa cells (GC). The GC act as the nurse cells of oocytes supplying molecules for bioenergetic metabolism, growth, and maturation. Both oocyte and GC are physically connected via adherens and gap junctions allowing the exchange and transport of molecules among cells. Once the oocyte is surrounded by two layers of GC, an additional somatic cell layer, the theca, is formed just outside the basement membrane of GC and supplies them with steroid hormones. In late follicle stages, a fluid-filled cavity, hereafter antrum, can be found and granulosa and theca layers

are further classified into cumulus and mural cells, as well into theca interna and theca externa, respectively. In addition, there is a glycoprotein membrane covering the oocyte with a critical role in fertilization, known as zona pellucida. Likewise, follicles are embedded in the ovarian stroma and separated from the stromal cells by the basal lamina (Fig. 2).

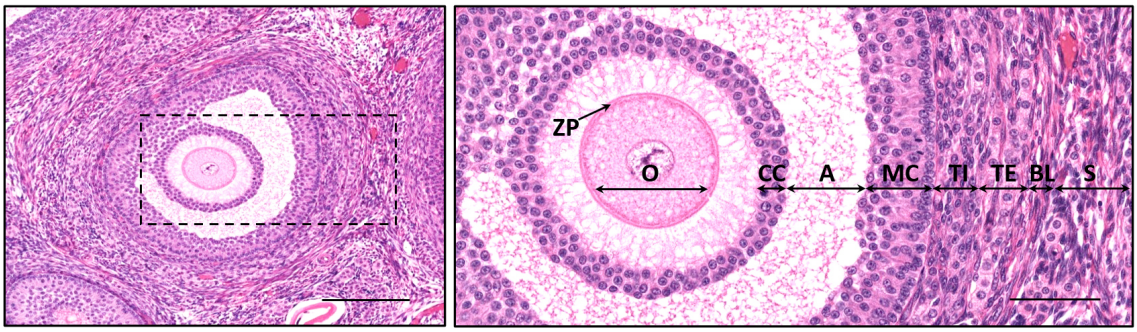

Figure 2. Follicle structure. *Ovarian section stained with H&E showing on the left side a growing follicle at a late developmental stage embedded within the ovarian stroma. The right-side image depicts a high magnification of the follicular components. A: antrum; BL: basal lamina; CC: cumulus granulosa cells; MC: mural granulosa cells; O: oocyte; S: stroma; TE: theca externa; TI: theca interna; ZP: zona pellucida. Left scale bar: 200 µm; right scale bar: 80 µm. Images adapted from histologyguide.com.*

Important landmarks of ovarian follicle development are greatly similar in mammals, albeit the timing varies through species (Fig. 3). Oocytes are originated from the primordial germ cells (PGC) during embryo development. First, a limited number of PGC derives from the epiblast adjacent to the extra-embryonic ectoderm (2), and differentiates as the embryonic precursor of gametes allowing the onset of germ cell competence and pluripotency retention in a coordinated process depending on a large group of transcription factors and genes (3-7). Conditioned PGC migrate to the genital ridge following an extracellular matrix gradient and in response to secreted chemoattractants, presumably by ligand for the tyrosine protein kinase receptor (KITLG), to colonize the gonadal ridges at 5 – 6 weeks postconception (wpc) (8). Once in the urogenital ridge, female sex determination occurs at 6 – 7 wpc by which the bipotential gonad will form an ovary. This process occurs when PGC lacks the Y chromosome gene (sex-determining region Y (SRY)) and activates a group of genes implicated in female sex determination, conditioning the PGC fate. After this point, PGC, known as oogonia, undergo highly mitotic proliferation until they number 5-6 million. This proliferation occurs rapidly and with incomplete cytokinesis resulting in special clusters called germline cysts or nests, where the daughter cells remain connected by intercellular

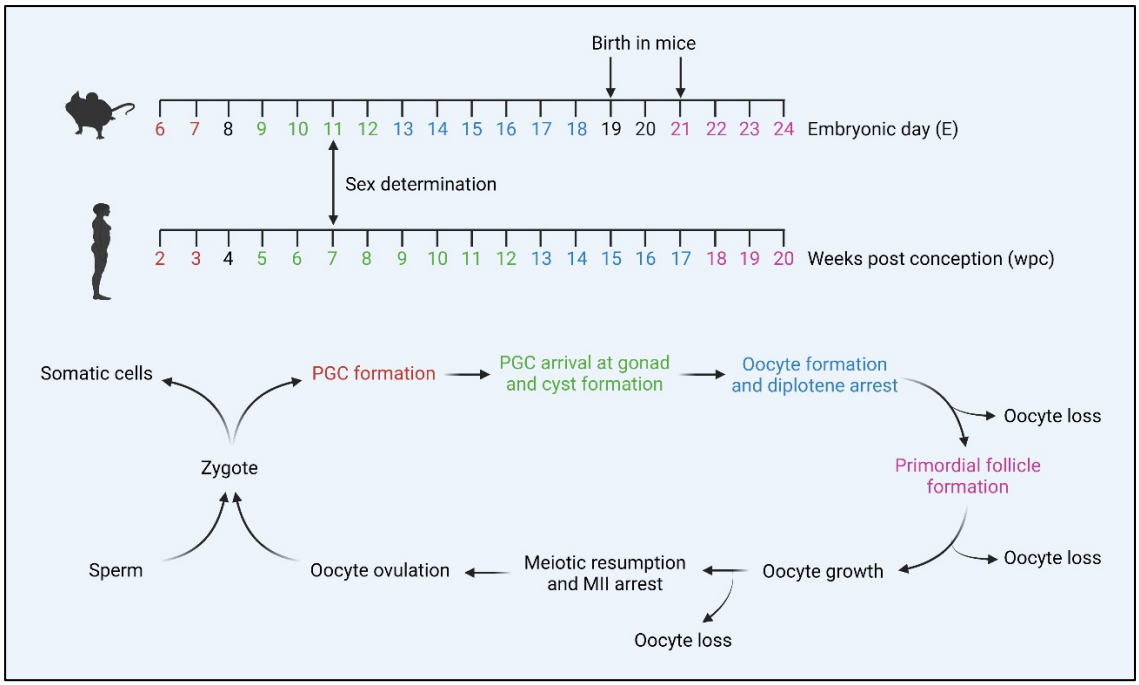

Figure 3. Schematic diagram of the reproductive life cycle in mammalian females. *Mouse and human timelines for major processes involved in the formation of primordial follicles during fetal development are depicted. Although main events involved in ovarian development and oogenesis are common between mice and humans, the timing is greatly compressed in the mouse. A spermatozoon fertilizes an ovulated oocyte to form a zygote, which undergoes continuous embryonic developmental stages. During the first weeks of gestation in humans, PGC specify from the epiblast adjacent to the extra-embryonic ectoderm and migrate to colonize the gonadal ridge at 5 – 6 wpc. In XX-specimens, PGC proliferate by continuous mitosis rounds with incomplete cytokinesis leaving germ syncytial structures called germline cysts or nests at 8 – 12 wpc. Germ cells enter in meiosis and keep arrested in the diplotene step of meiotic prophase I from 13 wpc to form oocytes. Subsequently, germline cysts break down and primordial follicles are assembled at 18 – 20 wpc, followed by a massive cell death of oocytes. Each month, a cohort of follicles is recruited to develop, degenerating most of them during the growth. LH secretion will induce the meiotic resumption of remaining oocytes up to the metaphase II (MII), where oocytes will be arrested, followed by the oocyte ovulation into the oviducts. The second meiotic division of oocyte will conclude at the fertilization point to repeat the cycle. Image adapted from Edson et al., (9) and created with biorender.com.*

bridges at 8 – 12 wpc (10, 11). The vast majority of these cells act as nurse cells supplying molecules and growth factors to the other germ cells from which the oocytes will develop (12). Therefore, the mitotic activity of oogonia will determine the size of the oocyte pool. Simultaneously, germline cysts are surrounded by somatic cells. After several mitosis rounds, germ cells enter in meiosis allowing oocyte formation by a process known as oogenesis. The premeiotic step of germ cells corresponding to the cell cycle S-phase, by which sister chromatids are synthesized, represents the end of the oogonial stage and the beginning of the oocytes (13).

After chromosomal crossover between maternal and paternal chromatids, performed during the pachytene stage of meiotic prophase I, oocytes undergo a meiotic arrest at the diplotene stage of prophase I. Subsequently, somatic cells invade the cell clusters inducing their breakdown and enclosing the cells to assemble the primordial follicles, which represent the earliest developmental stage of ovarian follicles (14, 15). Most oocytes undergo apoptosis during this follicle formation, which takes place during the second half of gestation in humans. From this point, the endowment of primordial follicles, termed ovarian reserve, in mammals is fully established, and each human ovary contains a non-renewable pool of 300,000 – 500,000 primordial follicles at birth. At puberty, continuous oocyte loss occurs over the course of follicle development at a rate of approximately 1,000 follicles per month by apoptotic cell death and atresia until the menopause onset. Oocytes destined to ovulate (one per month) will resume the meiosis to complete the first meiotic division achieving the haploid genetic stage. However, oocytes undergo a second meiotic arrest at the metaphase II (MII) up to the fertilization time, when the second meiosis will end (Fig. 3). It is known that women only ovulate a total number of 300 – 400 oocytes along with their reproductive age (15 - 49 years). In other words, most oocytes degenerate from the embryonic to the adult phase, being only 1% selected to ovulate and originate a fertilizable oocyte (13).

1.3. Folliculogenesis

After formation, follicles are able to grow and maturate along different developmental stages up to finally ovulate a fertilizable oocyte in a coordinated process called folliculogenesis or follicle development. However, primordial follicles in mammals can undergo one out of four following fates (16-18):

- To remain in a dormant or quiescent stage during the entire reproductive life.
- To be selected to initiate the follicle growth to the endpoint of ovulation.
- To be selected to initiate the follicle growth and undergo atresia.
- To die in the quiescent stage by attrition.

The destiny of each primordial follicle is controlled by a complex procedure that involves multiple paracrine and autocrine factors highly synchronized. Despite several investigations have focused on follicle development, the regulatory mechanisms to determine follicular fate are not fully elucidated.

Although folliculogenesis is quite similar among mammals, the timing greatly varies among species and individual age. It is accepted that the entire transition from the primordial follicle to an ovulating oocyte takes around one month in rodents and three to six months in humans (19-22). However, recent studies have demonstrated the presence of two classes of primordial follicles within mammal ovaries that differ in the life stage to activate, and the time to develop. Thus, the first wave is activated after being formed at birth, needing one month for mouse developmental time, while the second wave is activated gradually in the adult phase and needs two months to ovulate (23, 24).

When a dormant primordial follicle is activated, the diplotene arrested oocyte grows and the surrounded flattened GC differentiate into cuboidal shape cells achieving the primary stage. From this point, GC become high proliferative, generating a second granulosa layer to reach the secondary phase, and subsequent late preantral stage when the oocyte is surrounded by multi-layered GC. Theca cells originate from progenitor cells within the ovary and differentiate as the outermost layer of follicles since the secondary phase (25). Afterwards, fluid-filled vesicles appear among GC layers that finally coalesce into a single antrum, achieving the antral follicle. In this late developmental phase, GC decline their proliferative activity and vascular network develops within the mature theca cells. Eventually, the antrum expands covering the oocyte to represent the last stage of follicular growth known as preovulatory or Graafian follicle. Finally, the oocyte is ovulated into oviducts (Fig. 4). The preantral phases of folliculogenesis are mediated by local growth factors throughout autocrine and paracrine signals, while the last follicular stages are gonadotropin-dependent (9, 26).

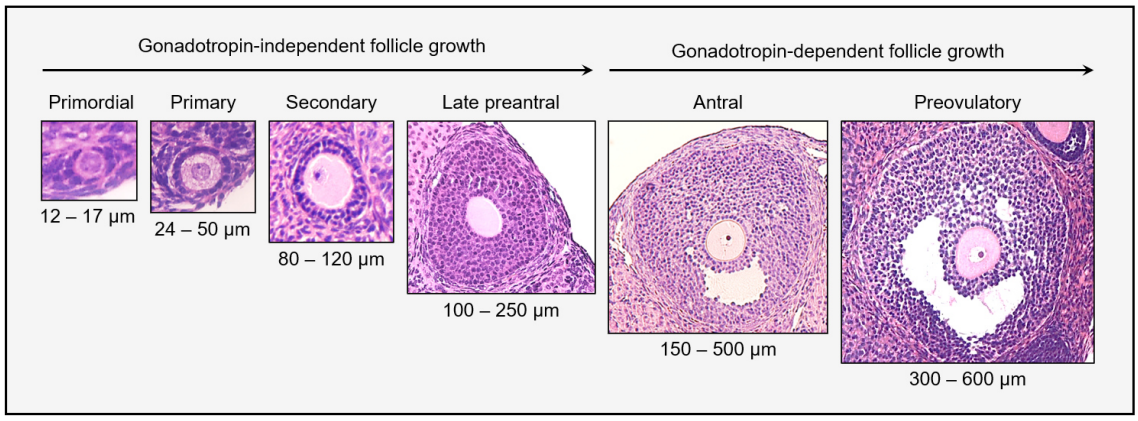

Figure 4. Classification of follicle stages during folliculogenesis. *H&E-stained sections showing representative images of the major stages of mammal follicles. Follicle diameter ranges are indicated at the bottom of each developmental stage. Follicle growth occurs independently of gonadotropins during the preantral stages. Oocytes and GC contained in antral and preovulatory follicles are highly dependent on FSH and LH gonadotropins to proliferate and maturate.*

1.3.1. Follicle activation and preantral follicle growth

Activation of primordial follicles represents an irreversible process by which a cohort of dormant follicles is recruited into the growing pool until the endpoint of either ovulation or atresia. The transition from the primordial to the primary stage is characterized by the growth of oocyte and the differentiation of flattened pregranulosa cells into proliferative cuboidal GC. Several key factors and pathways have been identified to mediate the primordial transition to the primary stage, albeit whether the oocyte or the pregranulosa orchestrates the follicle activation remains unclear (22, 27-29). The phosphoinositide 3-kinase (PI3K) signaling pathway is formed by kinases, phosphatases, and transcription factors regulating cell proliferation, metabolism, migration, and survival (30-32), and has been proposed as the core regulator pathway of the primordial follicle activation (33). PI3K phosphorylates phosphatidylinositol-4,5-bisphosphate (PIP2) to produce phosphatidylinositol-3,4,5-bisphosphate (PIP3) at the intercellular membrane, whose accumulation into the oocyte stimulates the phosphorylation of serine/threonine protein kinase B (AKT) and induces the nuclear extrusion of forkhead box O3 (FOXO3) into the oocyte cytoplasm, hereafter ooplasm, allowing the primordial follicle activation in mammals (34, 35). PI3K pathway is regulated by molecules, such as tensin homolog deleted on chromosome 10 (PTEN), cell division control 42 (CDC42) (36), and $p27^{kip1}$ (15, 37) mediating PIP3 and FOXO3 activity to control primordial follicle activation (15, 36-38). The PI3K-AKT pathway is also associated with

the mammalian target of rapamycin (mTOR) signal to mediate the activation of primordial follicles, maintain the follicle pool size, and regulate the pregranulosa differentiation in cuboidal GC (28, 39, 40). Furthermore, multiple transcription factors and molecules regulate the primordial follicle recruitment to create a balance between the activation and the maintenance of the follicle pool (Table I). The dormant state of primordial follicles is also influenced by environmental conditions within the ovary, like hypoxia and mechanical stress (41, 42), which would explain the primordial follicle restriction to the avascular and collagen enriched ovarian cortex (43, 44) (Fig. 5).

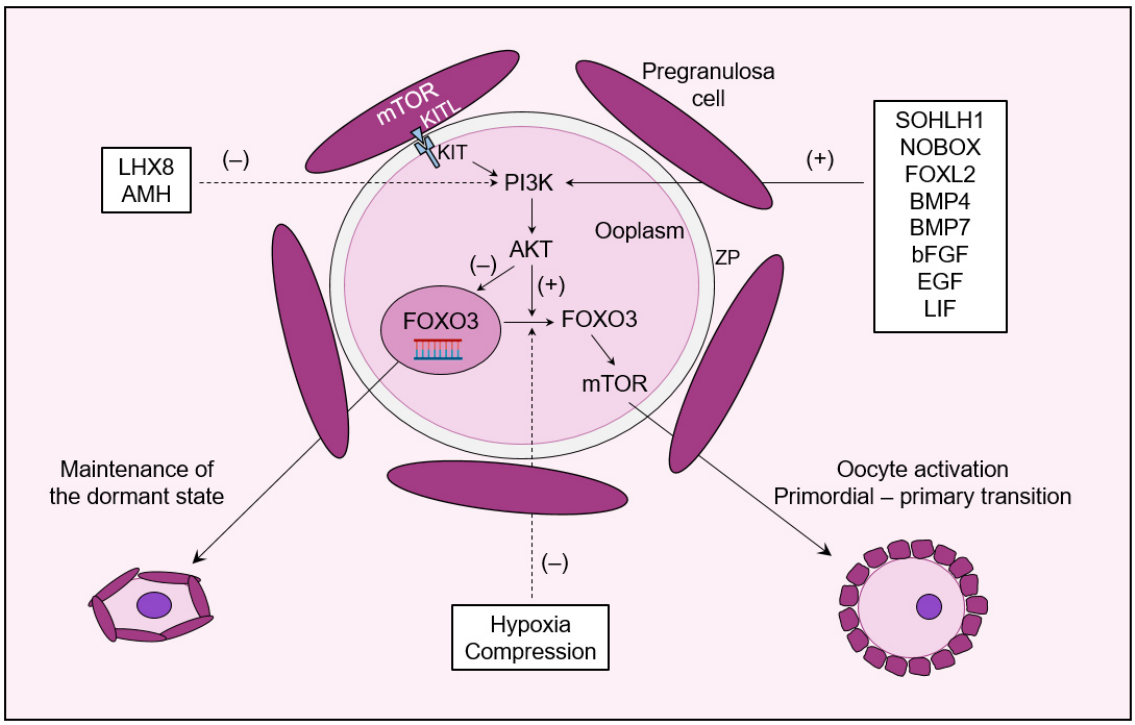

Figure 5. Factors and signaling cascade regulating the primordial follicle activation. *The awakening of quiescent oocytes to initiate follicle growth is mainly dependent on the PI3K-AKT pathway. On the one side, the activation of PI3K and AKT leads to the nuclear export of FOXO3 into the ooplasm, where activates the mTOR pathway and triggers the primordial – primary follicle transition. Follicle activation can also be performed by mTOR pathway in pregranulosa cells via KITL – KIT signaling system. Factors such as SOHLH1, NOBOX, FOXL2, BMP4, BMP7, bFGF, EGF and LIF promote follicle activation, while LHX8 and AMH act as inhibitory molecules. On the other side, the nuclear localization of FOXO3 induces the dormant follicle stage. Environmental conditions surrounding the primordial follicles, like hypoxia and mechanical stress induced by collagen fibers and extracellular matrix, repress FOXO3 into a nuclear localization inhibiting the primordial follicle activation. ZP: zona pellucida.*

Table I. Transcription and paracrine factors influencing the activation of primordial follicles and primordial-primary transition.

Factor (abbreviature)	Species	Role	References
Tyrosine protein kinase receptor (KIT) and its ligand (KITL)	Mouse and rat	This signaling system acts as a bridge between oocytes and GC to mediate follicle activation, oocyte growth, and GC proliferation via PI3K-AKT-mTOR system	(28, 45, 46)
Spermatogenesis and oogenesis specific basic helix-loop-helix containing protein 1 (SOHLH1)	Mouse	Oocyte-specific gene whose deletion alters the expression of germ cell markers in primary follicles and subsequent development by downregulating KIT/KITL and PI3K/AKT signaling systems	(47, 48)
Newborn ovary homeobox gene (NOBOX)	Mouse	NOBOX is expressed by oocytes and controls the follicle activation by modulating the mRNA transcription encoding for FOXO3	(49)
LIM homeobox 8 (LHX8)	Mouse	Oocyte-specific transcription factor that inhibits PI3K pathway. LHX8 lack causes a massive follicle activation and impairs the primordial-primary follicle transition	(50, 51)
Forkhead Box L2 (FOXL2)	Mouse	Transcriptional factor preferentially expressed by pregranulosa cells whose deletion leads to fail pregranulosa differentiation into cuboidal GC	(52)
Bone morphogenetic proteins (BMPs)	Rat	Growth factors of the largest transforming growth factor-β (TGF-β) family. Among BMPs, several studies indicate BMP4 and BMP7 as positive regulators of primordial-primary follicle transition	(53, 54)
Anti-Mullerian hormone (AMH)	Human and mouse	Glycoprotein of the TGF-β family secreted by GC of growing follicles that serves as an inhibitory factor of follicle activation to maintain follicle pool	(55-57)
Basic fibroblast growth factor (bFGF)	Human	bFGF is mainly expressed by oocytes and mediates primordial follicle activation via KITL interaction	(58)
Epidermal growth factor (EGF)	Rat	EGF upregulates the upstream proto-oncogene c-src that interacts with PI3K pathway to control follicle activation	(59)
Leukemia inhibitory factor (LIF)	Mouse and rat	Cytokine of the interleukin-6 family that promotes the primordial to primary transition, but impairs the growth of later follicle stages	(60, 61)

Afterwards, primary follicles develop into secondary and subsequent preantral stages in a process characterized by the robust oocyte growth, the active GC proliferation, and the acquisition of theca cells (9, 62, 63). During this preantral follicle growth, at least three oocytes-secreted paracrine factors are capable of promoting the proliferation and differentiation of neighboring GC: growth differentiation factor 9 (GDF9), bone morphogenetic protein 15 (BMP15) and R-spondin 2 (64-66). Likewise, a large group of peptides, neurotrophins and steroid molecules is produced by somatic cells to modulate the preantral folliculogenesis (67-69). Although preantral follicle growth is gonadotropin-independent, FSH receptors can be found in GC of late preantral follicles, suggesting that FSH plays a physiological, but non-essential, role in preantral growth (70).

1.3.2. Gonadotropin-dependent follicle growth

Follicle development beyond the late preantral stage is under gonadotropin control. FSH and LH gonadotropins are produced in response to the pulsatile secretion of gonadotrophin-releasing hormone (GnRH), which is itself mediated by the hypothalamus. Acquisition of FSH receptors by GC of late preantral follicles highlights the FSH dependence during the preantral-antral follicle transition and points out this gonadotropin as the responsible for the initiation of antral and preovulatory development (71). FSH declines GC apoptosis and promotes the proliferation and differentiation via cyclic adenosine monophosphate/protein kinase A (cAMP/PKA) pathway, mitogen-activated protein kinase extracellular signal-regulated kinase (MAPK/ERK) pathway, and PI3K/AKT pathway (72). Moreover, GC of antral follicles secrete estradiol (E2) to promote further follicle growth and the expression of LH receptors (73). In humans, a group of 5-15 follicles achieves the antral stage, but only a single dominant follicle is selected to complete the development influenced by the FSH-E2-inhibin axis (74, 75). During this dominant follicle selection, the expression of FSH receptors is strongly suppressed, accompanied by a high increase of LH receptors (76). Subsequently, LH surge influenced by E2 levels triggers the final maturation of the dominant follicle and its ovulation that releases a fertilizable oocyte arrested in MII into the oviducts (9).

1.3.3. Oocyte – somatic cell communication

Oocytes and their neighboring GC establish a reciprocal communication over the course of folliculogenesis essential to produce a healthy egg. By this bidirectional cross-talk, oocytes are supplied by GC with second messengers, amino acids, peptides, and molecules to support the oocyte metabolic activity and growth, while the oocyte sends signals to the somatic cells that regulate their differentiation, proliferation and help create a suitable microenvironment that ensures the oocyte maturation (77). Oocytes and GC are physically interconnected throughout thin cytoplasmic projections, called transzonal projections (TZP), that extend from GC to the oocyte membrane and carry out two major functions. On the one hand, TZP preserve the granulosa-oocyte complex integrity maintaining the adhesion between both compartments. This task is performed, at least in part, by adherens and tight junctions, where epithelial and neural cadherins (E-Cad and N-Cad, respectively), and tight junction protein 1 (TJP1) play key roles (78). On the other hand, TZP tips harbor gap junctions, which consist of intercellular channels composed of transmembrane proteins, termed connexins, that allow the rapid exchange of molecules up to 1 kDa in size between the coupled cells (79). Connexin 37 and 43 (Cx37 and Cx43, respectively) are the most abundant in mammals and indispensable for follicular development and oocyte growth (80). Moreover, gap junctions allow the oocyte to regulate its pH (81), as well as control the meiotic status of developing oocytes by mediating the transfer of cyclic adenosine monophosphate (cAMP) and cyclic guanosine monophosphate (cGMP) from GC into the oocytes to maintain the meiotic arresting, up to the LH surge, and the subsequent meiotic resumption (82-84). However, signals sent by oocytes to the surrounding GC are not depending on gap junctions. Oocyte-derived factors, like GDF9 and BMP15, are secreted as homo- or hetero-dimers that bind to receptor dimers expressed on GC membrane that are composed of BMP receptor 2 (BMPR2) and activin A receptor type 1B (ALK4), BMPR2 – ALK4, or by BMPR2 and TGF-β receptor 1 (ALK5), BMPR2 – ALK5, to trigger SMAD2/3 signal after GDF9 binding, while BMP15 binds to BMP receptor type 1B (ALK6), BMPR2 – ALK6, to trigger SMAD1/5/8 activation (65, 77). These oocyte-secreted factors play a synergistic role in promoting follicle development, influencing oocyte-GC interactions, somatic cell differentiation and proliferation, cumulus expansion, and oocyte competence (64, 85-87) (Fig. 6).

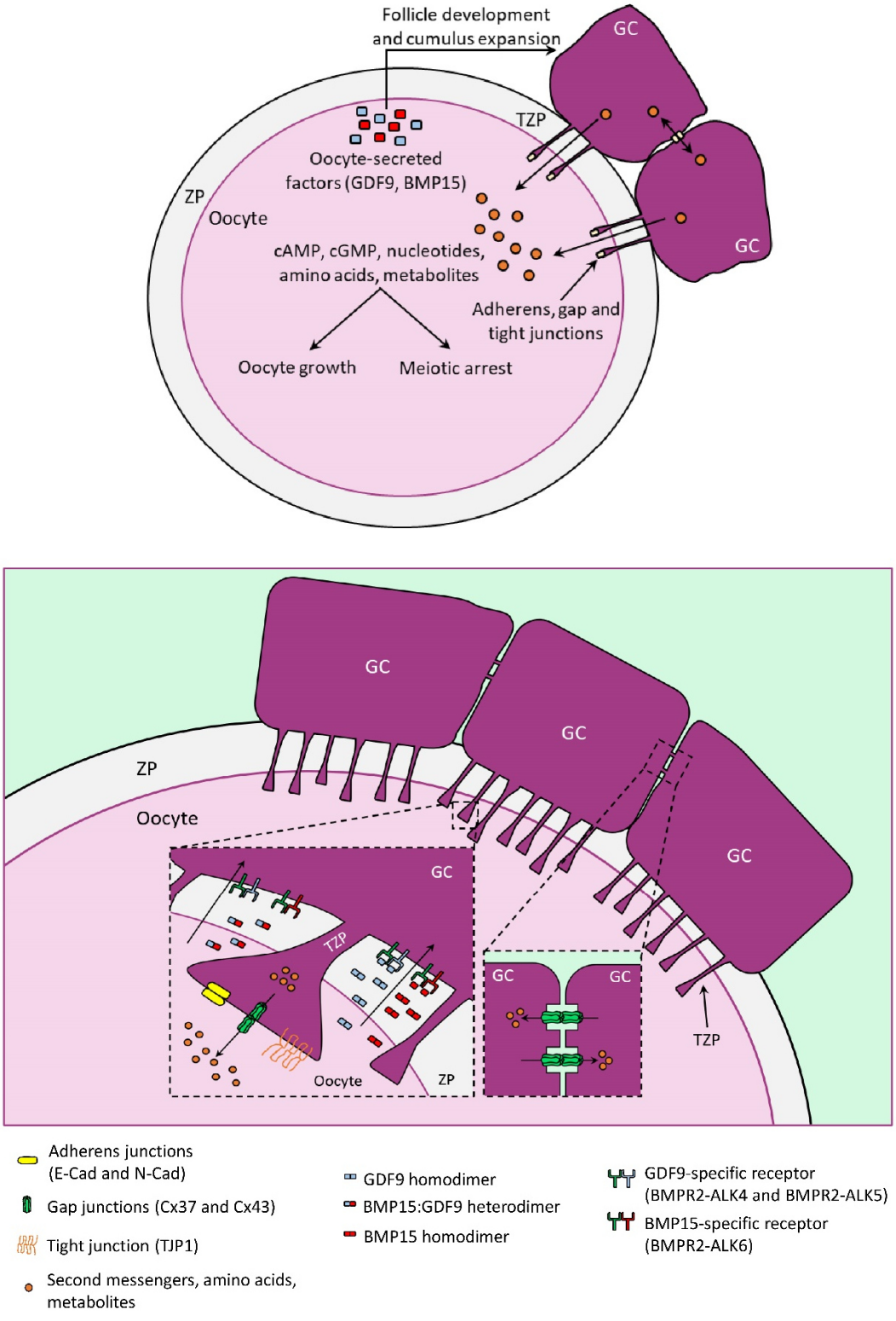

Figure 6. Bidirectional oocyte-GC communication regulates follicle development. *Transzonal projections (TZP) span zona pellucida (ZP) to couple granulosa cells (GC) and oocyte. These physical interactions are mediated by adherens and tight junctions, while gap junctions mediate the transference of second messengers, nucleotides, amino acids, and other metabolites mandatory for oocyte growth and maturation. GC are also interconnected between them to exchange molecules via gap junctions. Oocytes from growing follicles not only receive signals from surrounding GC, but also send autocrine and paracrine signals via secretion of factors involved in different aspects of oocyte and somatic cells physiology to promote folliculogenesis.*

2. Cancer and fertility in women

Cancer, malignant tumors or neoplasms involve a large group of diseases that begins when cells harbored in any organ or tissue become uncontrollably proliferative. When these abnormal cells acquire the capacity to migrate to adjacent organs, a process known as metastasis occurs, being the leading cause of death from neoplasms. Cancer has been recognized as a major worldwide public health issue with more than 19 million new cancer cases per year, and has been identified as the first or second leading cause of death globally, according to the World Health Organization, with almost 10 million deaths annually (88, 89). More than 1,806,590 new cancer cases were expected to be diagnosed only in the United States during 2020, of which 912,930 and 16,850 affected to women and children (age birth to 19 years), respectively (90). The American Cancer

Society estimates that 1 in 3 women will develop any invasive neoplasm along their lifetimes (91). Although most cancer cases are detected in aged people, approximately 10% affected to women younger than 45 years old who are in childbearing age until the menopause onset at 50-52 years old in developed countries (92), being breast cancer the most common form (Fig. 7A). The cancer death rate is progressively declined resulting in an overall 2% annual reduction and 30% drop since 1991, which represents almost 3 million fewer estimated cancer deaths only in the United States (90) (Fig. 7B). This improvement is driven at least in part by the novel techniques for early diagnosis and therapies, whereby the 5-year relative survival rate has risen to 75% in women <45 years old, and up to 85% for some pediatric cancers (93, 94).

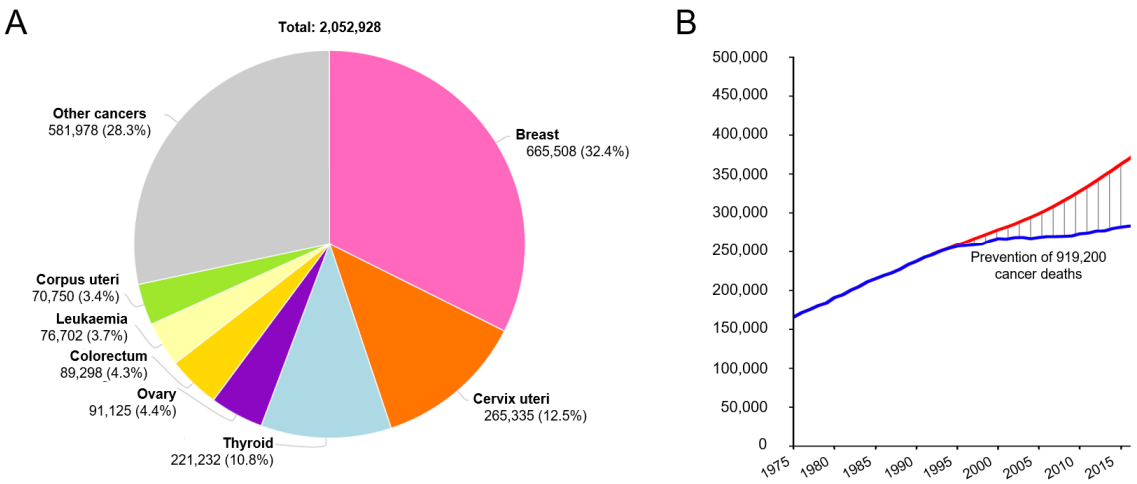

Figure 7. Epidemiology of cancer. *(A) Worldwide estimated cancer incidence according to its site in 2020 for women <49 years old. Breast cancer represents the most common female malignancy during the childbearing age. (B) Total number of cancer deaths for women between*

1991 and 2015 in the United States. Blue line reflects the real number of deaths derived from cancer patients, while the red line shows the estimated number of cancer deaths based on the trend registered before 1991. Progress in diagnosis and therapy technologies have led to decrease cancer deaths. Data and images adapted from Ferlay et al., and Siegel et al., (90, 95).

As the result of progress in current precise medicine, cancer survivors' quality of life has been improved in the last years because of a significant reduction of side effects derived from cancer treatments. However, a recent study reported that most pediatric cancer survivors would suffer at least one side effect induced by the antineoplastic agents (96). These aggressive treatments commonly affect reproductive function, leading to long-term fertility issues. It is well-accepted that radiotherapy and chemotherapy trigger deleterious and irreversible consequences on gametes, embryos, and ovarian function (97, 98). The main gonadotoxic effect in women is ovarian atrophy and follicle depletion, by which the oocyte pool dramatically declines, giving rise to premature ovarian insufficiency (POI) and the loss of fertility in worst cases. Notably, the oncologic treatment causes an overall 38% reduction in the likelihood of achieving a pregnancy (99) (Fig. 8). Given the increased survival rates, there will be a growing number of female patients who will experience the undesired gonadotoxicity associated with oncologic treatments. Besides, the uncertain fertility status of cancer survivors disturbs their future quality of life, affecting psychological and social aspects (100). Hence, fertility preservation has emerged to serve as a bridge between oncology and reproductive medicine for patients receiving treatments that might affect their future reproductive outcomes.

3. Gonadotoxicity induced by oncologic treatments

Cancer diseases are traditionally treated by surgery, radiotherapy, and chemotherapy procedures. The impact of the first one on female fertility is limited by the neoplasm gravity and the body site affected. On the other side, several studies have demonstrated that both high-dose radiotherapy and chemotherapy induce no effects on the ovary, altering the gonad physiology. Thus, patients undergoing gonadotoxic treatments will suffer any fertility issues ranging from temporary, partial, POI, and infertility in the worst cases (101-103). POI condition implicates the

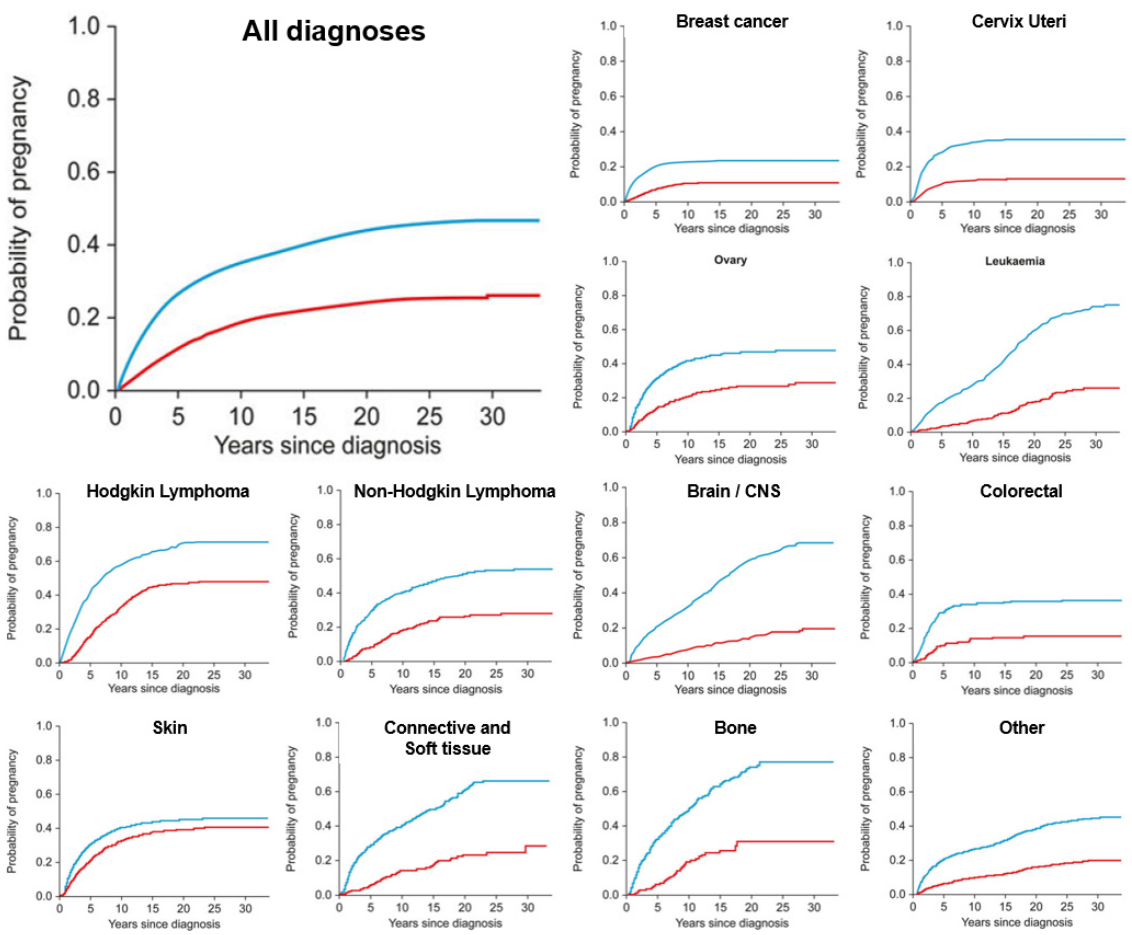

Figure 8. The impact of cancer on the subsequent chance of pregnancy. *Cumulative likelihood of first pregnancy up to 30 years after cancer diagnosis and gonadotoxic treatment. Lines represent the oncologic patients according to cancer site (red) and control group comprised of the healthy general population (blue). Image adapted from Anderson et al., (99).*

early dysfunction of both reproductive and endocrine functions of the female gonad by a massive depletion of ovarian reserve, similarly to menopause. Therefore, POI worsens the quality of life in women and is associated with significant health alterations such as osteoporosis (104), heart diseases (105), and psychological disorders (106, 107).

3.1. Ovarian damage by radiotherapy

Gonadotoxicity induced by ionizing radiation is mainly influenced by three aspects: irradiation field, dosage, and the patient's age (108). The pelvic region constitutes the most sensitive localization to develop ovarian failure in women after radiotherapy. It is described that ionizing radiation strongly damages the ovarian reserve, being a 2 Gray (Gy) dose sufficient to cause a 2-

fold reduction of the follicle pool (109). Patient's age also influences the reproductive status after radiotherapy, thereby the exposure of the abdominal region to 20-30 Gy leads to develop POI in 97% of women >40 years old, while only was detected in 72% of pediatric and adolescent patients (110). Moreover, the dose of ionizing radiation to induce ovarian failure declines up to 10 Gy when patients are also exposed to additional high-gonadotoxic agents like co-adjuvant chemotherapy in adult women, albeit the probability reduces up to 50-80% in pediatric patients (111), highlighting the relevance of female age to develop ovarian failure following radiotherapy.

3.2. Ovarian damage by chemotherapy

Chemotherapy is not only used in the treatment of cancer patients, but also is recommended for a wide range of non-malignant diseases, such as auto-immune illnesses, as well as prior to stem cell transplant for hematological conditions, like sickle cell anemia. The effects of chemotherapy on reproductive lifespan are important for both pediatric cancers and adult women affected up to the age of menopause. An increase in infertility rate and early menopause onset is usually described in cancer survivors treated with high doses of chemotherapy agents (112). Chemotherapy impact on future female fertility is highly dependent on the remaining follicle endowment after oncologic treatment (113). From a clinical point of view, chemotherapy induces short- and long-term effects to compromise reproductive function:

- The first impact occurs during the chemotherapy administration, when the oncologic treatment causes a massive death of the growing follicle pool, which disturbs the menstrual cycle leading to amenorrhea in most patients. Once chemotherapy is already administered, remaining primordial follicles initiate their development to take the place of damaged follicles, restoring ovarian function and menses resumption (114). This chemotherapy-induced effect is demonstrated by a prospective study whereby albeit 84% of patients of childbearing age treated with doxorubicin and cyclophosphamide chemotherapy suffered amenorrhea, monthly bleeding and ovarian function were recovered after 9 months in almost half patients (115). It is important to note that although patients may still menstruate, ovarian damage can persist, and finally it will be showed as infertility when attempting conception (116). Thus, menses resumption after chemotherapy may underestimate the extent of gonadotoxicity.

- As a result of a huge depletion of ovarian reserve, ovarian failure is manifested a few years or several decades after chemotherapy depending on follicle depletion severity (114). A study reported a significant increase in ovarian failure rate in childhood cancer survivors compared to healthy women that progressively increased with the time after chemotherapy administration (117).

The magnitude of ovarian damage and diminished fertility potential in cancer survivors treated with chemotherapy relies on three risk elements: type of chemotherapeutic agent used, drug regimen, and the patient's age (108, 117):

- Type of chemotherapy: alkylating agents, platinum-based compounds, antibiotics, antimetabolites, plant alkaloids, and taxanes are the six major kinds of chemotherapeutic drugs. The extent of ovarian damage varies according to the type of chemotherapy being administered (Table II). Alkylating agents, like cyclophosphamide and busulfan, represent the highest risk to induce POI. In fact, administration of alkylating chemotherapy raises 9-folds the likelihood of suffering premature menopause (118). In addition, the rate of ovarian failure increases up to 42% in women of reproductive age after exposure to alkylating agents, while the rate rises to 14% using non-alkylating chemotherapy (119).
- Dose: there is a direct relationship between the cumulative dose of the drug administered and the extent of ovarian damage. Thus, high chemotherapy dosages may lead to ovarian failure and infertility.
- Patient's age during chemotherapy administration: age is considered a crucial factor to determine how resilient the ovary will be to treatment. Several studies have demonstrated that women with older age at cancer diagnosis and chemotherapy exposure are more likely than young patients to suffer POI or early menopause (112, 115, 120). This age effect is mainly owing to the opposite correlation between age and ovarian reserve. Therefore, chemotherapy-induced follicle depletion will be more marked in those older women with an already diminished follicle endowment by aging than in young patients with a large follicle pool (121) (Fig. 9).

Although the precise mechanisms of chemotherapy to induce ovarian damage remain unclear, deleterious effects on several ovarian components have been identified, including oocytes, GC, stroma, and vasculature.

Table II. Chemotherapeutic agents used in the treatment of gynecologic cancers, their mechanisms of action, and the associated risk of POI.

Class of chemotherapy	Chemotherapeutic agent	Mechanism of action	Targeting cell cycle	Risk of infertility
Alkylating agents	Cyclophosphamide, melphalan, busulfan, chlorambucil	Induction of DNA cross-link with DNA, abnormal base pairing, and DNA double-strand breaks that disturb DNA synthesis, transcription and replication leading to prevention of cell division and apoptosis	Non-specific	High
Platinum-based compounds	Cisplatin, carboplatin	Inhibition of DNA synthesis, repair, and function via intra- and inter-strand DNA cross-link formation by covalent binding with purine bases	Non-specific	Medium
Antitumor antibiotics – Anthracyclines	Doxorubicin, epirubicin	Inhibition of DNA synthesis and function by interfering RNA polymerase movement along DNA, inactivating DNA topoisomerase II, generating toxic oxygen-free radicals, thereby inducing DNA double-strand breaks and apoptosis	Non-specific	Medium
Antitumor antibiotics – Others	Dactinomycin	Inhibition of mRNA transcription by binding to the transcription initiation complex	Non-specific	Medium
	Bleomycin	Single and double strand break formation via free oxygen radicals	G2-M phases	Low
Plant alkaloids – mitotic inhibitors	Vincristine, vinblastine	Inhibition of tubulin polymerization and microtubule assembly during cell division. This arrests mitosis metaphase and leads to cell death	M phase	Low
Plant alkaloids – Topoisomerase inhibitors	Etoposide	Inhibition of DNA replication via blocking topoisomerase II activity, and suppression of microtubule aggregation required for spindle assembly	G1-S phase	Low
Antimetabolites	5-Fluorouracil, Methotrexate	Inhibition of enzymes required for cell metabolism and molecule synthesis, such as nucleotides and proteins, leading to cell death	S phase	Low
Taxanes	Paclitaxel, docetaxel	Inhibition of cell division by disturbing tubulin polymerization into microtubules, spindle assembly and causing metaphase arrest	M phase	Low

Table modified from Taylan et al., (122)

3.2.1. Potential ovarian targets of chemotherapy

Ovary harbors seven different cell types (oocytes, GC, stromal cells, smooth muscle cells, endothelial cells, natural killer T cells, and macrophages) according to single-cell transcriptome analysis, which may be potentially damaged by chemotherapeutic agents (123, 124). To date, the knowledge regarding the effects of chemotherapy on human ovarian tissue derives from studies performed *in vitro* under controlled conditions. Most information about mechanisms and target cells of chemotherapy comes from animal studies, where a single chemotherapeutic drug is used to examine its specific effects on female gonads. At any point in female reproductive life, there are follicles at various developmental stages within ovaries, yet it is not fully elucidated whether a specific stage is more susceptible to cytotoxicity than others. The primordial follicle population has been shown to be diminished in size following a wide range of chemotherapeutic agents, such as cyclophosphamide (125, 126), cisplatin (127-129), and doxorubicin (130, 131). Direct damage of gonadotoxic treatment on follicles at the earliest developmental stage following their loss has been reported (132-134). However, studies assessing chemotherapy effects on ovarian reserve often report that primordial follicle depletion is, at least in part, an indirect consequence of gonadotoxic treatment. Later developmental stages are also susceptible to be damaged by chemotherapy with a deterioration in follicle quality and atresia following treatment (135). The serum concentration of inhibin-α and AMH strongly declines after chemotherapy administration corresponding to loss of late follicle stages (136, 137). Thus, damage of growing follicles disturbs the secretion of primordial follicle activation inhibitors leading to induce an accelerated initiation of primordial follicles development to replace the affected growing population by a biological process known as the burnout effect (102). Altogether, both primordial and growing stages have been shown vulnerable to chemotherapy-induced damage.

Antineoplastic drugs are specifically designed to act upon cells with high mitotic activity to prevent their proliferation beyond their boundaries. At first glance, this fact becomes GC more likely to be damaged than oocytes, since somatic cells enclosed oocytes are high proliferative during folliculogenesis to produce a multi-layered follicle, while oocytes are non-dividing cells due to their meiotic arrest from their formation. Moreover, it is important to note the potential role of oocyte-GC communication on this issue, thereby any harm to GC that compromises their viability can negatively affect oocytes inducing their death. Given the non-proliferative status of oocytes during

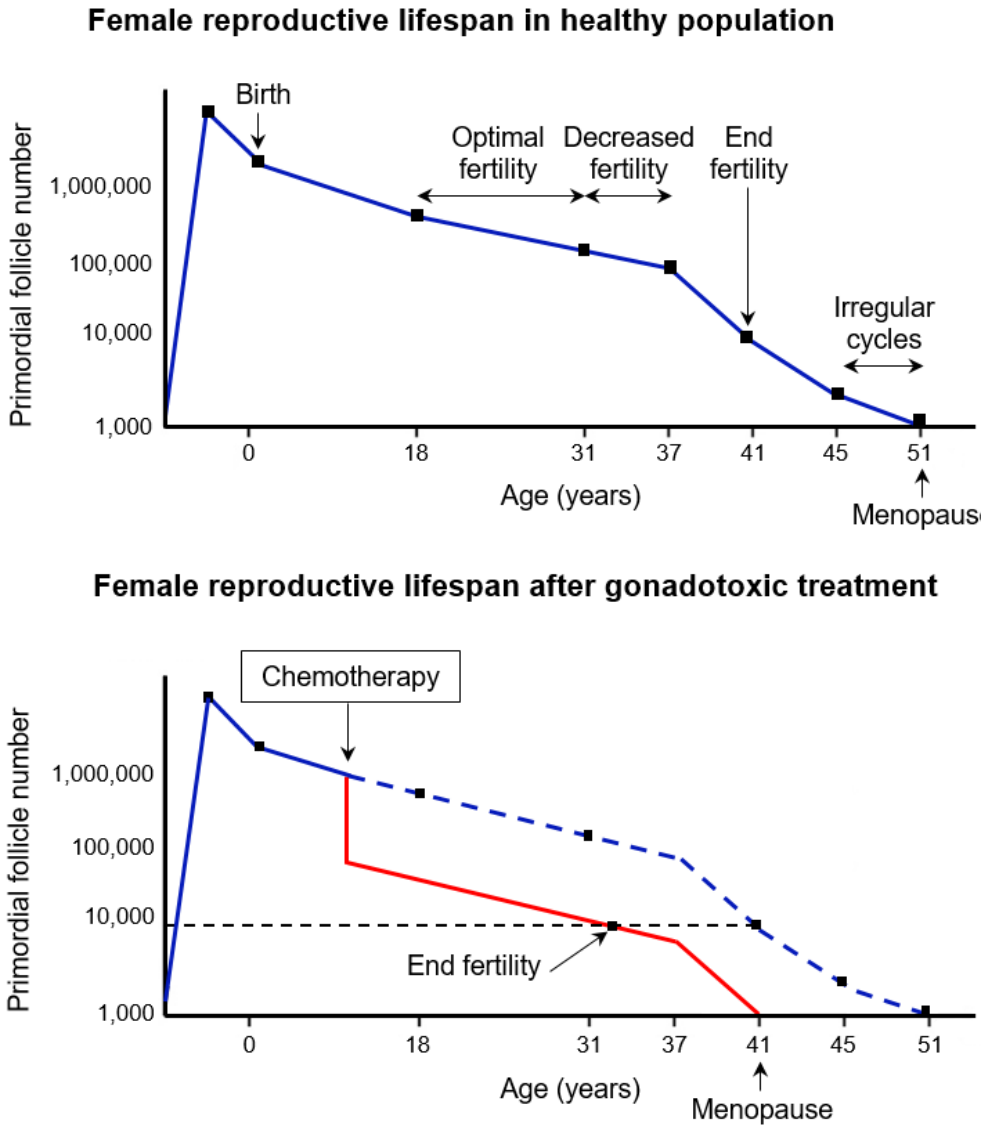

Figure 9. Impact of age and chemotherapy on ovarian reserve. *The upper panel represents the physiologic reduction of ovarian reserve with age. The lower graph illustrates the consequences of gonadotoxic treatment with chemotherapy (red) on the female reproductive lifespan compared with the physiological scenario (blue). Chemotherapy administration accelerates the age-related decline in ovarian reserve; thereby, subsequent end of fertility and menopause onset will occur earlier. Image adapted from Filippi et al., (138).*

follicle development, chemotherapy-induced damage can be latent up to meiotic resumption at fertilization, when oocyte alteration would manifest, producing embryo abnormalities and fetus malformations (139, 140).

However, DNA damage and apoptosis are frequently detected on oocytes and GC of primordial and growing follicles following antineoplastic treatment, which indicates that both cells are vulnerable to chemotherapy during follicle development (141-144). Interestingly, the extent of chemotherapy impact on oocytes is not only limited to the exposed subject's gametes since

transgenerational effects have been described in sons and daughters of chemotherapy-exposed women to chemotherapy (145), with epigenetic alterations detected in offspring's oocytes (146).

Likewise, ovarian stroma can also be altered via oxidative stress (147) or vascular toxicity (143, 148, 149), leading to a reduction of fertile lifespan (150). Stromal damage indirectly compromises oocyte and GC viability (131), as well as modifies the circulating hormone profile by reducing E2 levels (151). Moreover, gonadal blood flow is diminished, accompanied by thickening and hyalinization of blood vessels after chemotherapy administration (148, 149, 152).

A diagram of all ovarian targets at risk by chemotherapeutic agents is depicted on Fig. 10.

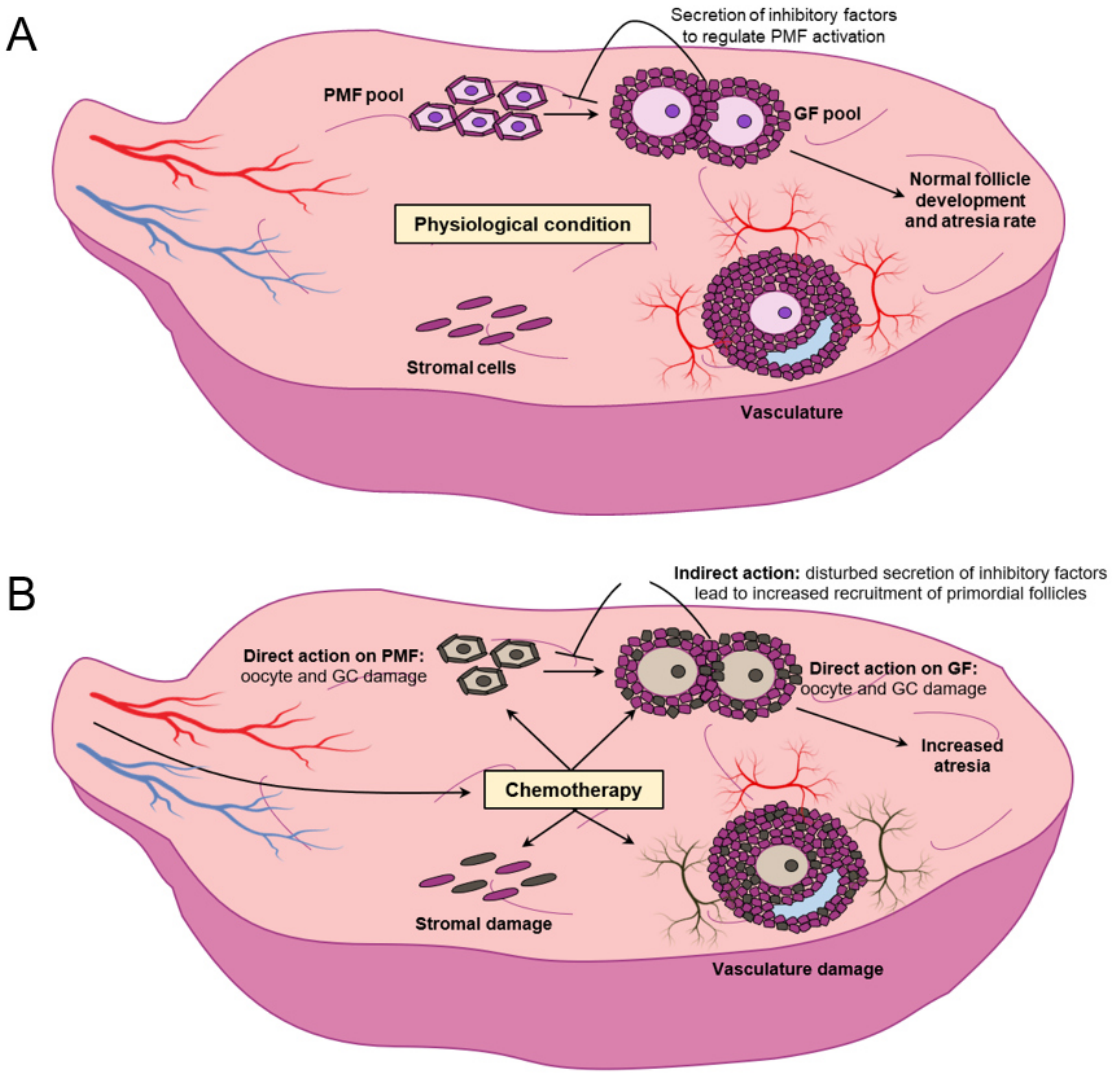

Figure 10. Summary of potential targets to be damaged by chemotherapy administration in ovaries. *Comparison between a (A) physiological condition and an (B) altered stage after chemotherapy reflects the deleterious impact of antineoplastic drugs on the female gonad by inducing primordial follicle (PMF) loss through direct actions on oocytes and granulosa (GC), accelerated PMF activation, cell death on oocytes and GC of growing follicles (GF) that increase follicular atresia, as well as stromal and vascular network damage.*

3.2.2. Molecular mechanisms of chemotherapy to damage ovaries

Antineoplastic activity of chemotherapeutic drugs, at least the most common to treat premenopausal cancers (cyclophosphamide, cisplatin, and doxorubicin), mainly derives from its ability to trigger cell death via apoptosis on the target cells, and secondary on the ovarian cells. Although specific pathways mediating chemotherapy-induced cytotoxicity may vary widely depending on the agent, according to Table II, DNA is the primary biological target of most chemotherapeutic drugs. Thus, chemotherapy commonly interferes with the DNA of ovarian cells, especially oocytes, compromising DNA integrity and function by forming inter- and intra- strand DNA adducts, as well as altering molecules and enzymes associated with DNA replication, synthesis, and transcription (153). This DNA damage frequently results in single- or double-strain breaks (SSB and DSB, respectively), which are immediately recognized after formation by specific proteins that transduce the signal downstream. Subsequently, several tyrosine kinases, including Abelson tyrosine kinase (c-Abl), ataxia-telangiectasia mutated (ATM), ataxia telangiectasia, and Rad3-related (ATR), AKT, MAPK, ERK or Jun N-terminal Kinase (JNK) are activated to modulate numerous pathways. The extent of DNA damage and the signal cascade will determine the subsequent cell fate. Thus, damaged cells activate cell cycle checkpoints termed Checkpoint kinase 1 and 2 (CHK1 and CHK2, respectively), resulting in cell cycle arrest that allows cells to initially attempt to repair the DNA insult promoting DNA repair pathways to maintain cell survival (154, 155). Simultaneously, a large group of biological events occurs, like the phosphorylation of H2A histone family member X (H2AX), next to the injury site to increase the damage signal and to allow the recruitment of more molecules to repair the DNA insult. SSB and DSB can be repaired through ATR- and ATM-mediated pathways, respectively, being DSB the most detrimental type of damage after cyclophosphamide, cisplatin, and doxorubicin administration on oocytes. Homologous recombination (HR) and non-homologous end joining (NHEJ) represent the two primary DNA repair mechanisms of DSBs induced via ATM pathway (156). Upregulation of repairing genes and mechanisms following chemotherapy administration have been identified (157, 158). On the other side, cells in which the DNA damage cannot be repaired become senescence or trigger cell death via apoptosis. In the latter scenario, activated proteins, such as cleaved poly ADP-ribose polymerase (PARP), ATM, ATR, and c-Abl kinases transduce the apoptotic signal downstream inducing the transcription of the tumor suppressor p53 and its

isoform Tap63α. Traditionally, activated Tap63α has been considered as indispensable for apoptosis in oocytes of primordial follicles, yet recent studies have suggested the predominant activity of phosphorylated-p53 driving the oocyte apoptosis following cyclophosphamide treatment (129, 159, 160). Thus, the accumulation of activated forms for p53 and Tap63α in the oocyte nucleus increases the expression of pro-apoptotic factors of the Bcl-2 family called Bcl-2-binding component 3 (PUMA) and phorbol-12-myristate-13-acetate-induced protein 1 (NOXA), firstly, followed by Bcl-2-associated X protein (BAX) and Bcl-2 homologous antagonist killer (BAK). These proteins subsequently influence caspase activation, especially caspases-2, -3, and -12 on oocytes (143, 161), as the final downstream effector of apoptotic pathway, leading to the death of those oocytes that are irreparably injured following chemotherapy treatment (Fig. 11).

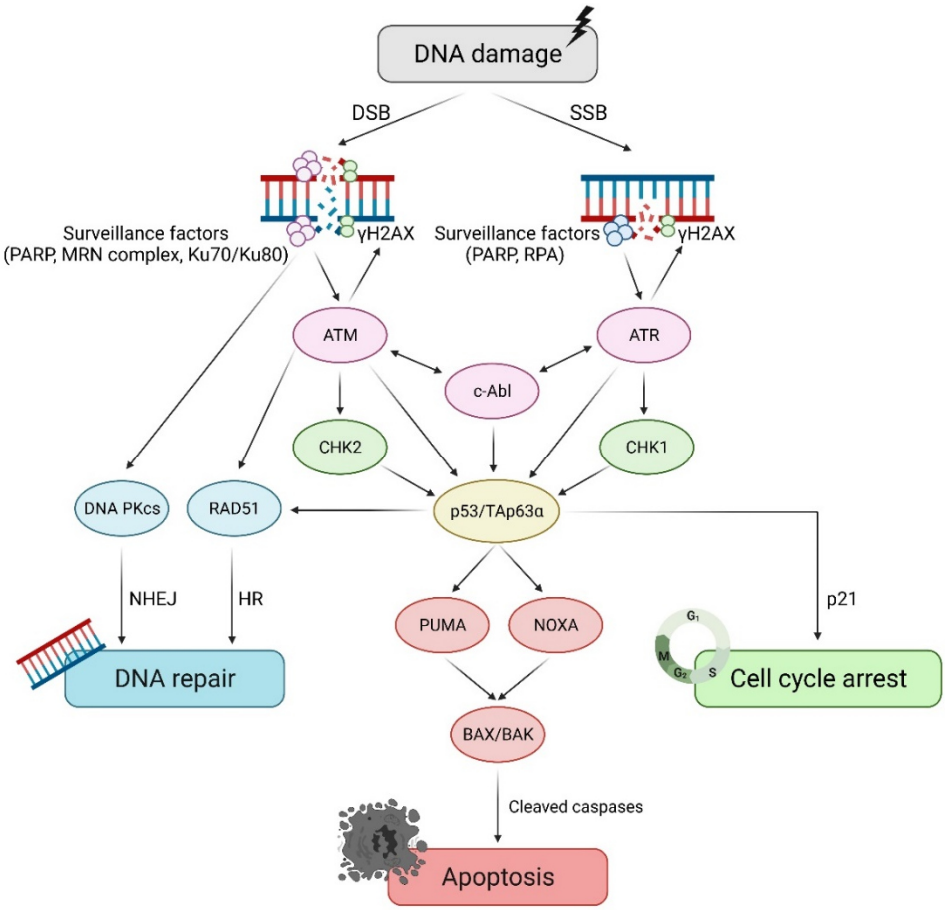

Figure 11. Molecular pathways activated in response to chemotherapy-induced DNA damage in oocytes. *Chemotherapeutic drugs induce DNA SSB and DSB on ovarian cells, specifically on oocytes. DNA damage is recognized by several surveillance factors which transduce the signal downstream, activating tyrosine kinases such as ATM, ATR and c-Abl. Kinases increase the recruitment of molecules and biological events near the injury site, like the phosphorylation of H2AX. Simultaneously, the cell cycle of damaged cells is arrested for allowing the repair of DNA insult by proteins involved in the cell cycle checkpoint (CHK1, CHK2). Moderate or low activation of damage signal promotes DNA repair via Rad51 and DNA PKcs through*

homologous recombination (HR) and non-homologous end joining (NHEJ), respectively, for DNA DSB. By contrast, elevated damage signals trigger senescence via cell cycle arrest pathways or apoptosis, and subsequent cell death, via p53 and Tap63α. These latter proteins constitute the major modulators of apoptosis, inducing the transcription of pro-apoptotic family members, PUMA and NOXA, which then bind to BAX and BAK to transduce apoptotic signal downstream. Finally, caspases are activated becoming cleaved caspases, which induce cell death on DNA unrepaired oocytes. Image created with biorender.com.

Other molecular pathways have also been associated, besides DNA damage, to mediate chemotherapy-induced gonadotoxicity and follicle loss. Chemotherapy is also associated with oxidative and inflammatory events within the ovary. Chemotherapeutic drugs are able to interfere with the electron transport chain through their direct interaction that compromises the mitochondrial activity by inducing a reduction in mitochondrial membrane potential and accumulation of cytochrome c in the cytoplasm, as well as reactive oxygen species and superoxides (161-163). Likewise, an inflammatory response occurs in the ovary following cyclophosphamide and busulfan administration inducing the increase of the pro-inflammatory cytokines tumor necrosis factor α (TNFα), interleukin (IL) 6 and 8 (IL-6 and IL-8, respectively) levels, accompanied by the anti-inflammatory cytokine IL-10 concentration decline. Altogether leads to enhance oxidative stress levels (164) that subsequently activate the caspase family of proteins and finally result in apoptosis and cell death.

In addition, cyclophosphamide, cisplatin, and doxorubicin agents are able to up-regulate the PI3K-AKT-mTOR signaling pathway resulting in the nuclear export of FOXO3, which in turn suppresses its inhibitory function leading to primordial follicle overactivation and subsequent atresia (102, 165-167). In addition, macroautophagy, also known as autophagy, is a lysosomal degradative process implicated in cellular homeostasis and mainly regulated through PI3K-AKT pathway. Recently, autophagy has been described as a cell survival mechanism of germ cells with an essential role in follicle pool maintenance (168). Cyclophosphamide administration modifies the levels of proteins associated with the autophagy process within the ovary, indicating that chemotherapeutic agents can inhibit autophagy leading to subsequent follicle loss via non-apoptotic mechanisms (169).

Table III gathers specific molecular pathways activated on the ovary following chemotherapy administration for the most common agents used to treat premenopausal women with cancer.

Table III. Molecular pathways mediating chemotherapy-induced ovarian damage.

Molecular marker	Agent	Species	Biological process triggered	Cell damaged	Reference
ATM-CHK2	Cy, Cs, Dx	Mouse	DNA damage and cell cycle arrest	Oocyte, GC	(155, 159, 160)
ATR-CHK1-CK1	Cs	Mouse	DNA damage and cell cycle arrest	Oocyte, GC	(159, 170, 171)
Cleaved PARP	Cy, Cs, Dx	Mouse	Apoptosis	Oocyte, GC, SC, WO	(160, 166, 172)
γH2AX	Cy, Cs, Dx	Mouse, rat, marmoset monkey	DNA damage and apoptosis	Oocyte, GC, WO	(128, 131-134, 142, 143, 157, 160, 167, 173)
Glutathione	Cs	Mouse, Rat	Oxidative stress	Oocyte, GC, WO	(174, 175)
Inflammatory cytokines	Bu, Cy	Mouse	Inflammation	Serum	(164)
MAPK-ERK	Cs	Mouse	Accelerated PMF activation	WO	(132, 166, 176)
p53 and TAp63α	Cy, Cs	Mouse	Apoptosis	Oocyte, WO	(128, 155, 159, 160)
PI3K-Akt-mTOR	Cy, Cs, Dx	Mouse	Accelerated PMF activation	Oocyte, GC, WO	(37, 102, 165-167, 177)
Pro-apoptotic factors (PUMA, NOXA, BAX, BAK, cleaved caspases)	Bu, Cy, Cs, Dx	Mouse	Apoptosis	Oocyte, GC, SC, WO	(132, 160, 163, 170, 171, 178, 179)
Rad51 and PKcs	Cy	Rat	DNA repair	Oocyte, GC, WO	(157, 180)
Reactive oxygen species	Cs, Dx	Mouse	Oxidative stress	Oocyte, GC	(161, 163, 175)
Mitochondrial activity	Cy, Cs, Dx	Mouse, rat	Oxidative stress	Oocyte, GC, WO	(161-163, 174, 175)
Autophagosome factors (LC3, p62)	Cy	Mouse	Inhibition of autophagy	WO	(169)

Bu: busulfan; Cy: cyclophosphamide; Cs: cisplatin; Dx: doxorubicin; PMF: primordial follicle; GC: granulosa cells; SC: stromal cells; WO: whole ovarian lysate.

4. Fertility preservation in premenopausal women with cancer

The development of novel alternatives to minimize the gonadotoxic effects of chemotherapy on female fertility has been promoted in the last years. These research efforts have led to establish a group of strategies destined to preserve the reproductive potential of young women undergoing high gonadotoxic treatments, like chemotherapy. Thus, the fertility preservation field is considered among oncologists and professionals in reproductive medicine an essential pillar of cancer treatment (181).

Since the American Society of Clinical Oncology published on 2006 the first guideline for oncologic patient management and fertility preservation, several updates and reproductive institutions have published new guidelines emphasizing the relevance of gonadotoxicity induced by the oncologic treatments, as well as the best clinical practice in female fertility preservation based on the current evidence available (182, 183). Moreover, a list of medical criteria, such as Bologna and Edinburgh, can also be found to facilitate the selection of patients whom fertility preservation technics may be recommended (184, 185). Notwithstanding, there are many clinicians with a great unknowledge about fertility preservation counseling that compromises the suitable communication between oncologists and young cancer patients to preserve their fertility. Indeed, several studies have reported only a few number of young women that preserved their fertility before chemotherapy exposure, at least in part, due to a lack of receiving fertility counseling through oncologist specialists (186-189). Thus, a multidisciplinary team specialized in fertility preservation is mandatory to assist young cancer patients properly.

According to reproductive experts, the ultimate strategy for fertility preservation would be that which can be performed regardless of the patient's age and menstrual phase, which does not carry any health risks, nor interfere with the efficacy of antineoplastic treatment, nor delay administration of oncologic therapy, and nor require invasive procedures. Nevertheless, no current technique accomplishes all the above criteria. There are several key points to take in mind before selecting a fertility preservation technique:

- Patient's age: they should be recommended in patients under 40 years old, especially in those patients who do not have children, since chemotherapy may drastically decrease reproductive potential in older patients with an already reduced ovarian reserve.

- Cancer site, stage, and prognosis: a patient with ovarian cancer, in advanced stage, or poor prognosis would not be a good candidate to undergo a fertility preservation procedure.
- Time available before initiating gonadotoxic treatment: this factor will determine the strategy to be applied due to there are options that require a few weeks to be performed.
- Ovarian reserve: those patients with an already diminished ovarian reserve will have fewer chances of preserving their fertility.
- Availability of a male partner.
- Ethical and cultural aspects related to germ cell and embryo preservation.

A detailed comparison among the most used techniques for fertility preservation in cancer women is summarized in Table IV.

4.1. Embryo and oocyte cryopreservation

Embryo cryopreservation is an effective technique available for many years. It was recognized for decades as the only non-experimental method for fertility preservation by the American Society for Reproductive Medicine since the first pregnancy from a cryopreserved embryo in 1983 (190). Likewise, oocyte cryopreservation was also declared a clinical technique in 2013, being both methods the current gold standard procedures for fertility preservation (182, 183).

Embryo and oocyte cryopreservation requires controlled ovarian stimulation cycles to produce multiple follicles in a process that typically entails 10-12 days. The patient's age, ovarian reserve levels, and tumor sensitivity to hormones will determine the exact protocol to be recommended (181). Growing follicles are monitored periodically with transvaginal ultrasonography and serum hormone testing. Once follicles achieve the suitable size, a trigger shot is administered to induce the final maturation of oocytes, which are then retrieved by ultrasonography-guided transvaginal 34-36 hours after. Therefore, the entire process takes 12-14 days. Subsequently, rescued oocytes can be cryopreserved, or *in vitro* fertilized through sperm from a male partner or donor, followed by cryopreservation of resulting embryos for future use. Cryopreservation is usually performed by vitrification, an ultraquick cooling method that prevents intracellular crystal formation

Table IV. Most commonly used fertility preservation options for reproductive age women with cancer.

	Oocyte cryopreservation	Embryo cryopreservation	Ovarian tissue cryopreservation	Ovarian suppression
Definition	Hormonal stimulation, oocyte retrieval and freezing for subsequent fertilization and transfer	Hormonal stimulation, oocyte retrieval, fertilization, embryo culture and freezing for subsequent transfer	Laparoscopic surgery, medulla removal, ovarian cortex tissue freezing and subsequent transplantation after chemotherapy	Monthly injection of a GnRH agonist to suppress ovulation and menstruation
Status	Non-experimental	Non-experimental	Non-experimental	Experimental
Application timing	Before first oncologic treatment	Before first oncologic treatment	Preferably, before first oncologic treatment	Preferably, at least 1 week before first oncologic treatment and continue until completion
Delay for oncologic treatment initiation	Approximately 2 weeks	Approximately 2 weeks	Does not delay oncologic therapy	7-10 days until suppression reached
Success rate	PR: 34-52% LBR: 24-42% Highly age-dependent	PR: 37-55% LBR: 25-47% Highly age-dependent	PR: 29-50% LBR: 23-41% Restored ovarian activity: >95% Age-dependent (<35 years)	PR is generally improved after chemotherapy completion Approximately 15% of follicle endowment protected POI is frequently delayed
Special indications	Most popular option for adolescent and single adult women, or those opposed to embryo freezing	Only chance for post-pubertal patients Requires a male partner or sperm donor	Feasible in pediatric patients Invasive surgical procedure Risk of cancer cells reintroduction Moderate lifespan of grafts	May be combined with any of the established options Potential side effects

LBR: live birth rate; POI: premature ovarian insufficiency; PR: pregnancy rate. Table modified from Warner et al., (191).

since it increases the survival rates of oocytes and embryos compared to slow freezing methods (192). Once the patient is recovered from cancer, oocytes are thawed and fertilized *in vitro*, or cryopreserved embryos are thawed and finally transferred into the patient's uterus.

Thousands of children are born each year by this technique. Pregnancy and live birth rates range 4-12% and 36-61% per cryopreserved oocyte and embryo transfer, respectively, being akin to rates obtained from fresh cycles with non-cryopreserved oocytes and embryos (193-196). Therefore, a cohort of approximately 10 cryopreserved oocytes is required to guarantee a live birth, which can be compromised in those patients with an already diminished ovarian reserve before gonadotoxic treatment, in aged women, and in cancer patients who only have a limit of cycle attempts before antineoplastic treatment (191, 197) (Fig. 12).

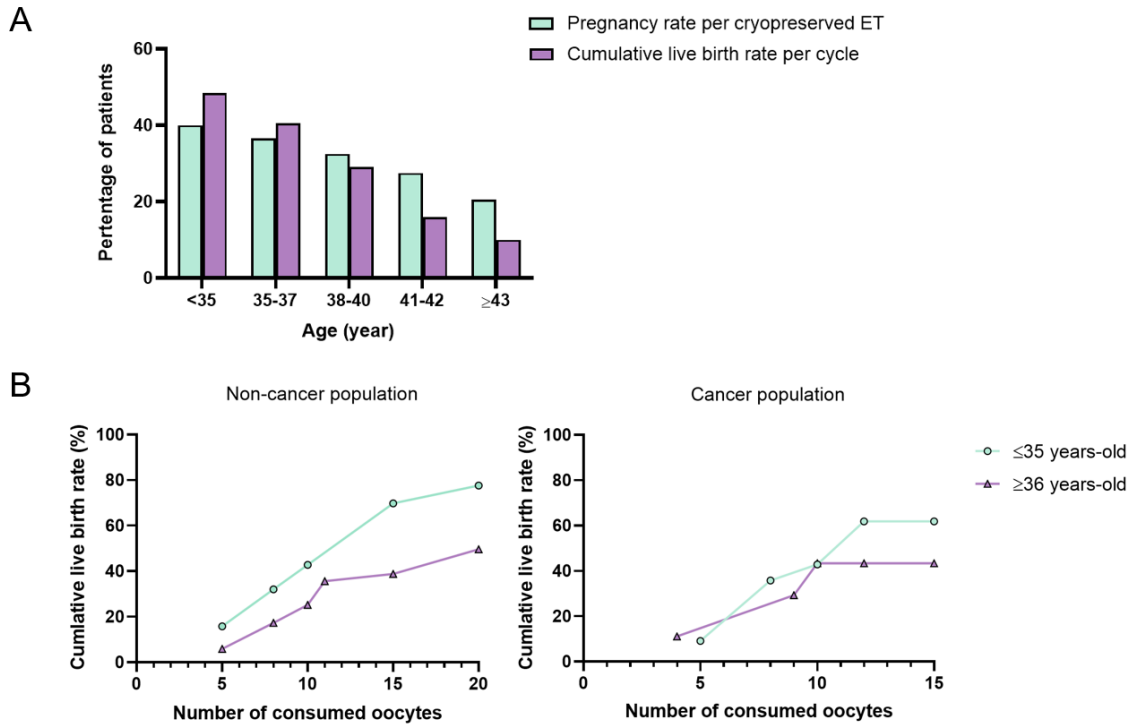

Figure 12. Reproductive outcomes for embryo and oocyte cryopreservation cycles, by patient's age. *(A) Success rates for cryopreserved embryo transfer (ET) from one single ovarian stimulation cycle according to age. (B) Effect of patient's age on the cumulative live birth rate of at least one baby according to the number of oocytes consumed at vitrification in non-cancer and oncologic female populations. Both graphs show a significant decline in reproductive outcomes with age by using cryopreserved embryos and oocytes from cancer and non-cancer patients. Images adapted from Warner et al., and Cobo et al., (191, 197).*

Before counseling embryo and oocyte cryopreservation to women with cancer, there are some key points to bear in mind. First, this technique only should be recommended for those patients who can delay the antineoplastic treatment for at least 10 days to perform the ovarian stimulation and oocyte retrieval, even if random-start protocols are used. Second, specific ovarian stimulation protocols with aromatase inhibitors are required depending on the hormone sensitivity of the cancer. Finally, the patient must be postpubertal since the efficiency of ovarian stimulation in the prepubertal period is limited and ethically unacceptable. Unlike embryo cryopreservation, oocyte vitrification is a recommended alternative for adolescent patients, as well as for adult women who do not have a male partner, who desire reproductive autonomy and who have embryo freezing objections for religious or ethical reasons. Nevertheless, both embryo and oocyte cryopreservation does not prevent ovarian damage and follicle endowment loss following gonadotoxic treatment. Thus, the patient's chance to get pregnant is limited to the number of retrieved oocytes after stimulation cycles.

4.2. Ovarian tissue cryopreservation

Ovarian tissue cryopreservation is no longer considered as an experimental technique for female fertility preservation by the American Society of Reproductive Medicine (182) and by the European Society of Human Reproduction and Embryology (183). This approach represents the only option for pediatric patients, as well as for those adolescent and adult women where cancer treatment cannot be delayed (198).

The procedure entails the retrieval of ovarian tissue through laparoscopic surgery followed by the isolation of the ovarian cortex tissue by medulla removal. The resulting ovarian cortex is subsequently cut into small fragments, which are then cryopreserved by slow-freezing or vitrification methods. After oncologic therapy completion, the ovarian fragments are thawed and orthotopically or heterotopically transplanted back into the patient.

Reproductive outcomes derived from this technique are highly encouraging, showing an exponential increase since the first pregnancy from this procedure in 2004. The endocrine function of the ovary is restored in over 95% of cases after tissue transplantation in the pelvic cavity (orthotopic transplant). Several reports have indicated pregnancy and live birth rates

oscillating 29-50% and 23-41%, respectively, which result in the birth of more than 130 children worldwide until 2017, albeit that figure has probably reached more than 200 by now (198-200).

Ovarian tissue cryopreservation involves minimum teratogenic risks with similar fetal malformation rates than patients who have not undergone this procedure (201, 202). However, as the lifespan of grafted tissue varies between months and a few years, the transplant is recommended to be performed when patients will be ready to carry out their motherhood project. There is also a concern by which cancer cells may reside in the cryopreserved ovarian tissue and may be reintroduced, especially in leukemia, neuroblastoma, and Burkitt lymphoma cases, albeit tissue is tested by histological and molecule analysis for such malignant cells before transplantation (198). In addition, the patient's fertility depends on the graft lifespan and the limited number of primordial follicles contained in the fragments transplanted. Hence, it is of paramount importance to develop novel alternatives focused on the *in situ* protection of ovarian reserve during gonadotoxic treatment.

4.3. Fertoprotective therapy

A large group of agents with a gonadoprotective effect against chemotherapy has been identified in the last 10 years. In this regard, a novel strategy named fertoprotective therapy has arisen to prevent chemotherapy-induced damage in ovaries. This fertility preservation method comprises the administration of a specific agent before and during chemotherapy treatment in order to *in situ* protect the follicular pool by preventing follicle depletion. Therefore, each agent is designed to prevent a specific gonadotoxic effect of chemotherapeutic drugs, mainly modulating apoptosis or follicle activation pathways.

Unlike the above fertility preservation options, the major benefit of this alternative is that it can be applied to patients of all ages and diagnoses, preserving their ovarian reserve. Furthermore, it allows the avoidance of the ovarian stimulation cycle and surgery involved in cryopreservation alternatives. However, there are some concerns about fertoprotective agents regarding their interference with the mechanism of action of chemotherapeutic drugs, the limited evidence available to validate their efficacy and safety, and the chance of preserving damaged oocytes that

may lead to produce embryo alterations. Hence, most fertoprotective agents are restricted to the research field except for GnRH agonists (GnRHa).

4.3.1. GnRHa for fertility preservation in women receiving chemotherapy

Adjuvant administration of GnRHa before and during chemotherapy treatment desensitizes and decreases the number of pituitary GnRH receptors inducing a temporary suppression of the pituitary–gonadal axis that subsequently results in repression of FSH and LH secretion. Animal studies have reported a significant reduction of primordial follicle loss following adjuvant GnRHa administration with chemotherapy (203). As early follicle stages are gonadotropin-independent, it is not biologically plausible that release suppression by GnRHa would have a direct protective effect on primordial follicles. Thus, the precise molecular mechanism by which GnRHa prevents follicle loss is unclear. Some biological effects have been proposed:

- Ovarian blood flow is correlated with circulating gonadotropin levels, being decreased following pituitary desensitization with GnRHa (204, 205). Hence, GnRHa might reduce the exposure of follicles to chemotherapy to protect the follicle pool (152).
- GnRHa would enhance the expression of anti-apoptotic molecules within the ovary (206).
- GnRHa might regulate factors mediating primordial follicle activation (207).

Although the utility of GnRHa for fertility preservation in premenopausal women receiving chemotherapy is currently debated, so far more than 50 publications including 14 randomized controlled trials, 25 non-randomized controlled trials, and 20 meta-analyses, as well as five international expert consensus meetings have reported a reduction of POI rate in cancer survivors underwent GnRHa during chemotherapy treatment (208). Moreover, long-term follow-up (>5 years) of GnRHa treated patients has reported an increase in the pregnancy rate and delayed ovarian failure with similar survival rates, indicating that GnRHa administration does not appear to reduce the chemotherapy effectiveness (209-211). Thus, although GnRHa should not be considered as an equivalent alternative for fertility preservation comparing with the already established cryopreservation techniques, GnRHa administration can be offered as a complementary option for ovarian protection in premenopausal cancer patients receiving chemotherapy to increase the chances of natural conception (182, 183).

4.3.2. Other molecules as experimental fertoprotective agents

Additional agents have been reported to prevent the chemotherapy-induced follicle loss by protecting *in situ* the ovarian reserve. At present, most scientific evidence to analyze the effectiveness of each candidate derives from animal studies.

Some agents act directly on immature oocytes disturbing DNA alteration and apoptosis to avoid cell death and atresia. Bioactive sphingolipids such as sphingosine-1-phosphate (S1P) and ceramide-1-phosphate (C1P) are inhibitors of the ceramide-induced death pathway and vascular regulators, which administration decreases the apoptosis of primordial follicles and improves the stromal vasculature following cyclophosphamide and doxorubicin treatment in animal and human ovaries (178, 179, 212). The use of tyrosine kinase inhibitors involved in the transduction of DNA damage and apoptotic signals downstream is also appealing. Imatinib, a competitive c-Abl kinase inhibitor, prevents the TAp63α accumulation in cisplatin-treated mice resulting in a reduction of follicle loss and improvement of long-term reproductive outcomes (128-130), albeit some studies have contested these results because its participation in other regulatory processes in the ovary (213, 214). Pharmacological inhibition of ATM and ATR kinases, as well as the downstream factors CHK2/CHK1, have been shown to be effective at rescuing oocytes from TAp63-mediated apoptosis following cyclophosphamide, cisplatin and doxorubicin chemotherapies (134, 155, 159). Moreover, a gonadotropin involved in ovulation and maintenance of the corpus luteum, the LH, has recently been proposed as an encouraging candidate to protect the follicle pool from cisplatin (132). In this study, *in vitro* LH exposure of mouse prepubertal ovarian fragments, mainly containing primordial follicles, generated anti-apoptotic signals from a subset of ovarian somatic cells expressing the LH receptor (LHR). Such signals ameliorated DNA damage induced by cisplatin in oocytes and thus prevented cell death. Further, *in vivo* administration of LH to mice during chemotherapy prevented a reduction in primordial follicles, resulting in a slight improvement in the subsequent number of pregnancies and pups. Despite the fact that these results are encouraging, further research is required because cisplatin only associates with a moderate risk of inducing POI (108), and prepubertal ovaries lack late preantral and antral follicles, precluding evaluation of how over-activation contributes to follicular exhaustion. Furthermore, the developmental potential of LH-preserved oocytes and the underlying protective mechanisms remain unclear.

On another note, there are fertoprotective agents focused on PI3K-AKT pathway regulation to minimize the accelerated primordial follicle recruitment following chemotherapy administration. The immunomodulator AS101 is a non-toxic tellurium-based compound that reduces AKT and rpS6 activation after cyclophosphamide administration. *In vivo* treatment of mice with AS101 attenuates cyclophosphamide-induced loss of primordial follicles and improves long-term reproductive outcomes without interfering with anti-tumoral activity (102). Bearing in mind that mTOR is involved in follicle activation mediating PI3K-AKT pathway, the use of mTOR inhibitors, such as everolimus (RAD001) and rapamycin, can be a potential option to preserve the ovarian reserve from chemotherapy by inhibiting the accelerated activation of primordial follicles (165, 177). Furthermore, given the inhibiting role of AMH to limit the activation of primordial follicles, this hormone has been recently proposed by three studies as an effective treatment to limit the ovarian reserve depletion induced by cyclophosphamide, doxorubicin, and carboplatin, without affecting the therapeutic effects of chemotherapy (169, 215, 216). Likewise, melatonin and ghrelin administrations maintain primordial follicles in a dormant state during cisplatin treatment by suppressing PTEN and FOXO3 phosphorylation (37, 176).

Ovarian vasculature and oxidation status are commonly compromised following chemotherapy. Therefore, specific agents to counteract these biological processes, like tamoxifen, crocetin, resveratrol, and granulocyte-colony stimulating factor (G-CSF), have shown their protective effects on the ovarian reserve from chemotherapy via indirect actions (217-220).

Altogether, although evidence of each candidate is limited and based on animal studies, the observed improvement of ovarian protection and fertility from chemotherapy should not be denied. Hence, further research is needed to validate their effectiveness and safety as novel options to prevent ovarian damage, preserving *in situ* the ovarian reserve.

Table V summarizes the main fertoprotective agents to *in situ* protect the follicle pool to date, as well as their chemotherapeutic drug specificity and mechanism of action.

Table V. Agents used to protect *in situ* the follicle pool by preventing chemotherapy-induced ovarian damage.

Group	Mechanism of action	Fertoprotective agent	Drug	Species	Reference
Antioxidants	Reduction of free radical damage	Bilberry	Cs	R	(221)
		Mesna	Cs	R	(174)
		Mirtazapine	Cs	R	(222)
		Resveratrol	Cs	R	(219)
		Sildenafil citrate	Cs	R	(223)
Natural compounds	Inhibition of accelerated primordial follicle activation and ovarian oxidation	Crocetin	Cy	M	(217)
		Curcumin and capsaicin	Cy	R	(224)
Ceramide pathway inhibitors	Reduction of DNA damage and apoptosis on PMFs, and vascular injury	C1P	Cy	M	(178)
		S1P	Bu, Cy, Dx	H, M, R	(179, 212, 225)
Stem cell factors	Reduction of DNA damage, and vascular injury	G-CSF	Bu, Cy, Cs	M, R	(220, 226)
Drug delivery	Reduction of oocyte susceptibility to chemotherapy	MDR1	Cy	M	(227, 228)
Estrogen receptor modulator	Reduction of apoptosis and inflammation	Tamoxifen	Cy, Dx	R	(218, 229)
Gonadotropin	Reduction of DNA damage and apoptosis on PMFs	LH	Cs	M	(132)
Immunomodulators	Inhibition of accelerated primordial follicle activation and mitochondrial activity	AS101	Cy	M	(102, 217)
Iron chelating drugs	Reduction of metal ions complexed with anthracycline decreasing DNA damage, apoptosis, and superoxide radical formation	Dexrazoxane	Dx	M, MM	(173, 230)

Bu: busulfan; Cp: carboplatin; Cs: cisplatin; Cy: cyclophosphamide; Dx: doxorubicin; H: human; M: mouse; MDR1: multidrug resistance mutation 1; MM: marmoset monkey; PMF: primordial follicle; R: rat.

Table V. Continued

Hormones	Inhibition of accelerated primordial follicle activation	AMH	Cy, Cp, Dx	M	(169, 215, 216)
		Ghrelin	Cs	M	(37)
		Melatonin	Cs	M	(37, 176)
Kinase inhibitors	Reduction of DNA damage and apoptosis on PMFs	ATM inhibitors (ETP-46464, KU55399)	Cs, Dx	M	(155, 159)
		ATR inhibitors (AZD6738, NVP-BEZ235, ETP-46464,)	Cs	M	(134, 159)
		c-Abl inhibitor (Imatinib)	Cs, Dx	M	(128-130, 155, 159, 214)
		CHK1/2 inhibitors (BML277, CHK2II, LY2603618, PF670462)	Cy, Cs, Dx	M	(134, 155, 159, 231)
mTOR inhibitors	Inhibition of accelerated primordial follicle activation	Everolimus	Cy, Cs	M	(165, 232)
		Rapamycin	Cy	M	(177)
Proteosome inhibitors	Reduction of DNA damage and apoptosis on preantral follicles	Bortezomib	Dx	M	(233)

Bu: busulfan; Cp: carboplatin; Cs: cisplatin; Cy: cyclophosphamide; Dx: doxorubicin; H: human; M: mouse; MDR1: multidrug resistance mutation 1; MM: marmoset monkey; PMF: primordial follicle; R: rat.

4.4. Future techniques for fertility preservation

There are several new developing approaches that may be available in the future for the fertility preservation of female oncologic patients. One alternative to obtain mature oocytes would be the *in vitro* growth and maturation of follicles. Early antral follicles can be matured *in vitro* for 24 hours following their cryopreservation, being a potential option for those cancer patients who cannot delay the start of chemotherapy or who cannot be stimulated. However, few centers worldwide currently offer this approach due to its complexity and poor reproductive outcomes (234). In addition, *in vitro* growth of early developmental stages is an encouraging option by which primordial and preantral follicles can be harvested to produce mature and fertilizable MII oocytes by using a multistep culture system that provides all the nutrients, as well as emulates the physiological conditions (235). The *in vitro* growth of immature oocytes combined with the ovarian tissue cryopreservation would maximize the future reproductive potential of cancer patients. This approach has gained interest among clinicians specialized in fertility preservation due to several reports have supported its feasibility leading to live births (236-239). Nevertheless, more clinical evidence is required, and long-term follow-up of children conceived by this experimental approach is needed.

The development of an artificial ovary is another research approach to obtain mature oocytes for fertility preservation. Isolated primordial follicles would be transferred onto a scaffold which is subsequently transplanted into the patient to replace the native organ. This artificial ovary would allow the entire folliculogenesis process leading to produce fertilizable oocytes. Although many advances have been made in animal models, further research is still required to validate its potential to be performed in the clinical practice (240).

Hypothesis

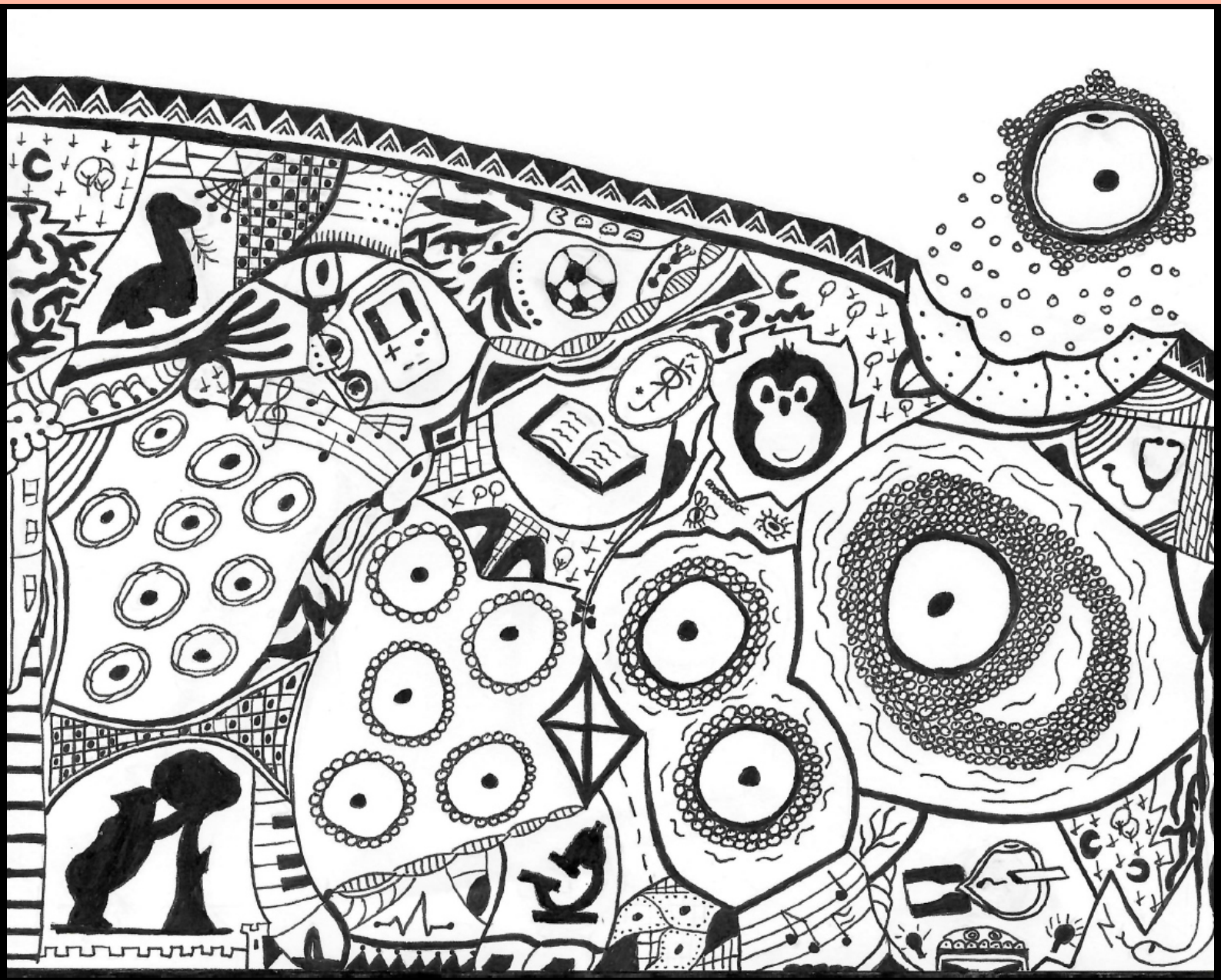

Hormone-based treatments could be used for ovarian protection during chemotherapy. LH administration has been shown as a novel fertoprotective agent in prepubertal mice treated with cisplatin, which is associated with a moderate risk of inducing POI. LH-based treatment could be used for the *in situ* protection of the ovarian reserve in cancer patients undergoing antineoplastic regimens with highly gonadotoxicity agents. LH effects could generate a suitable environment within the ovary during chemotherapy exposure with alkylating agents to preserve the reproductive potential at the long-term.

Objectives

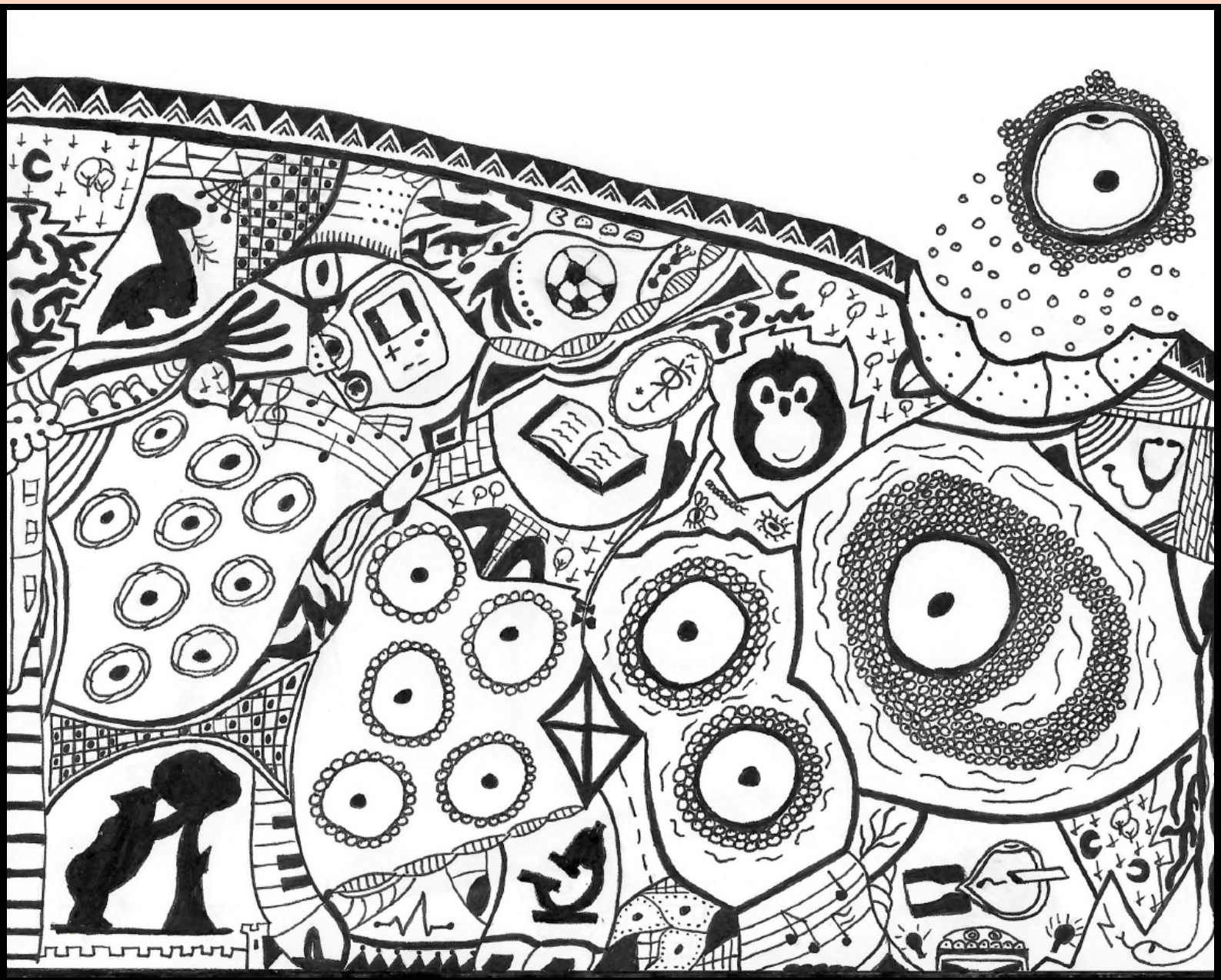

1. Main objective

The main objective of the present study is to evaluate LH treatment as a novel approach to protect *in situ* the follicle pool and to preserve the reproductive lifespan against the gonadotoxic effects of oncologic treatment with alkylating drugs in adult mouse ovaries.

2. Specific objectives

- To determine *in vivo* the short-term effects of LH treatment on the quiescent follicles exposed to alkylating agents.
- To investigate *in vivo* the underlying mechanisms of LH to confer ovarian protection against chemotherapy.
- To assess the effectiveness of LH treatment for the preservation of long-term reproductive lifespan.
- To test *in vivo* the short-term effects of LH administration on the growing follicles at the time of chemotherapy exposure by using a natural subfertile mouse strain.

Materials and methods

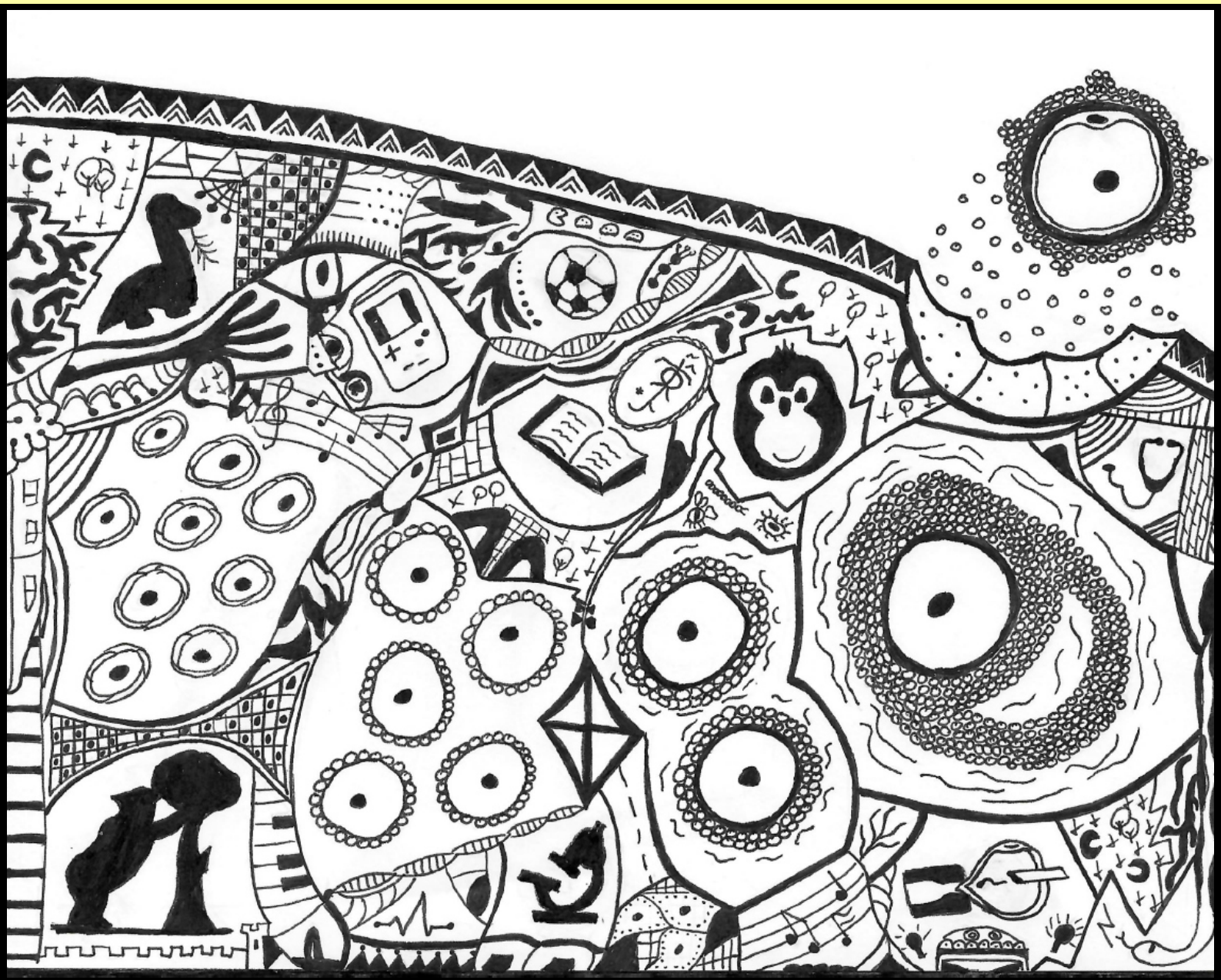

LH protection against chemotherapy with the most gonadotoxic alkylating agents was investigated on adult ovaries containing all follicular populations. A broad specter of effects on both quiescent and growing follicles during chemotherapy administration was assessed in specific experiments. Likewise, some of the mechanisms underlying gonadoprotection were *in vivo* elucidated in a mouse model to explain how LH treatment would preserve female fertility.

Animal procedures were performed in the animal facilities of the *Unitat Central d'Investigació de Medicina* of the *Facultat de Medicina i Odontologia* at the *Universitat de València*, according to the current normative. Animal research procedures were approved by the *Comité d'Experimentació i Benestar Animal* of the *Universitat de València* (A1510573656187) and by the Directorate General of Agriculture, Livestock and Fisheries, Generalitat Valenciana (2018/VSC/PEA/0010 and 2019/VSC/PEA/0206).

CD-1 (strain code 022; Crl:CD1, ICR) and NOD/SCID mice (strain code 394; NOD.CB17-Prkdcscid/NCrCrl), both from Charles River Laboratories (Saint-Germain-Nuelles, France) were maintained free access to standard diet and water *ad libitum*, and housed in controlled temperature (22 ± 2°C) and humidity (55 ± 10%) standard conditions in an environmentally controlled room with 12:12 hour light-dark cycle.

1. LH effects on quiescent follicles exposed to alkylating agents

1.1. Study design

In a first step, LH effects were evaluated on follicles at the dormant primordial stage during chemotherapy exposure (Fig. 13). With this aim, thirty-one 7-week-old CD-1 female mice were randomly allocated to control (n = 9), chemotherapy (ChT, n = 11) and chemotherapy with LH (ChT+LH-1x, n = 11) experimental groups. Control mice were intraperitoneally injected with saline followed by a second injection of dimethyl sulfoxide (DMSO, chemotherapy vehicle) 24 hours later. The ChT group received saline followed by alkylating agents (cyclophosphamide and busulfan), while ChT+LH-1x animals were injected with 1 international unit (IU) of LH (2.3 ng/mL, Luveris, Merck Serono, Darmstadt, Germany) followed by a second LH dose simultaneously with chemotherapy 24 hours later. This regimen should activate LH-associated protective mechanisms and pathways before chemotherapy-induced insult. Mice were maintained for 30 days and then

underwent controlled ovarian stimulation (COS) to ensure that retrieved oocytes and embryos derived from follicles damaged at the primordial stage. Two mice from each group were euthanized 16 hours after human chorionic gonadotropin (hCG) administration to collect mature oocytes, while the remaining were housed with males immediately after hCG injection and euthanized 40 h later to collect ovaries, oocytes, and early cleavage-stage embryos. To assess the long-term effects of LH, on day 30 after treatments 4 mice/group were housed with fertile males for 6 months to allow continuous breeding. Thirty days after the sixth delivery attempt, mice underwent COS, mated with males and finally euthanized collecting ovaries, oocytes and embryos to evaluate the response to ovarian stimulation. For long-term assessment, an additional group treated with a high-dose, i.e., 5 IU, of LH (11.5 ng/mL) was included (ChT+LH-5x, n = 4).

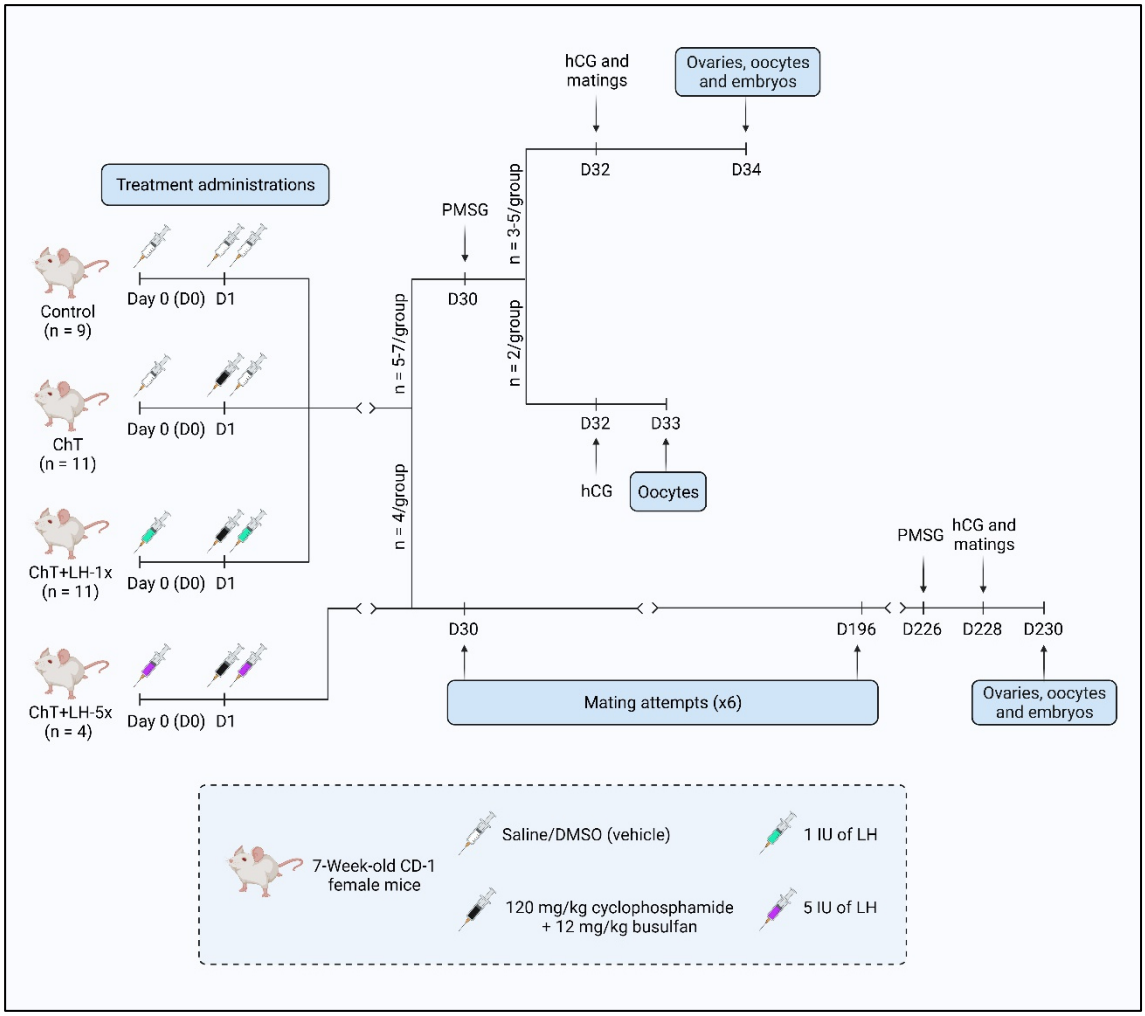

Figure 13. Study design to evaluate the LH effects on quiescent follicles exposed to alkylating agents in CD-1 adult mice. *Thirty days after treatment administrations, 5-7 females from control, ChT and ChT+LH-1x groups received a controlled ovarian stimulation cycle with pregnant mare serum gonadotropin (PMSG) and hCG. Two mice/group were sacrificed 16 hours after hCG injection for oocyte retrieval (on day 33), while 3-5 mice/group were mated for two days*

to collect ovaries, oocytes, and embryos on day 34. Simultaneously, 4 mice/group, including ChT+LH-5x group, underwent six mating attempts to evaluate LH effects on reproductive potential at long-term. Thirty days after the last breeding round, mice were stimulated and mated to collect ovaries, oocytes, and embryos on day 230. Image created with biorender.com.

1.2. Chemotherapy preparation and administration

Alkylating agents were selected to simulate a POI condition due to their high-toxicity risk (108) and chemotherapy was prepared as previously described (150) with minor modifications. Briefly, 48 mg of cyclophosphamide (Sigma-Aldrich, St. Louis, Missouri, MO, USA) and 4,8 mg of busulfan (Sigma-Aldrich, USA) were dissolved in 2 mL of DMSO (Sigma-Aldrich, USA) and filtered through a 0.45 µm pore size filters (VWR International Eurolab, S.L., Barcelona, Spain). To ensure sterile conditions, all reagents were handled in a laminar hood.

To adjust the chemotherapy dose to 120 and 12 mg/kg of cyclophosphamide and busulfan, respectively, bodyweight data of female mice were registered. For a standard weight of 25 g in 7-week-old female mice, 100 µL of chemotherapy was intraperitoneally administered by using 1 mL syringes (VWR International Eurolab, S.L., Spain) and a 25-gauge (G) needle (Braun Vetcare, S.A., Barcelona, Spain). This chemotherapy dose causes irreversible effects on ovarian function and fertility, allowing survival (150).

1.3. Controlled ovarian stimulation and matings

Female mice underwent a COS cycle with 10 IU of Pregnant Mare Serum Gonadotropin (PMSG) and 10 IU of hCG 30 days after chemotherapy administration. Stock reagents of PMSG (Folligon, MSD Animal Health, Kenilworth, NJ, USA) and hCG (Ovitrelle, Merck Serono, Germany) were diluted under sterility conditions to a final concentration of 100 IU/mL each with 0.9 % chloride sodium solution (Braun Vetcare, S.A., Spain), and filtered with 0.45 µm pore size filter (VWR International Eurolab, S.L., Spain). By 1 mL syringes (VWR International Eurolab, S.L., Spain) and 25 G needles (Braun Vetcare, S.A., Spain), 100 µL of PMSG solution were intraperitoneally administered to female mice on day 30 after treatments to promote follicular development, followed by 100 µL of hCG 48 hours after to induce ovulation.

Subsequently, thirteen female mice (n = 3 from control, and n = 5 from ChT and ChT+LH-1x groups) were mated with 10-week-old CD-1 fertile males (Charles River Laboratories, France) in a 2:1 ratio for 40 hours until the euthanasia and sample collection point.

1.4. Euthanasia and sample collection

Sixteen hours after hCG injection, 2 mice / group were euthanized to collect mature MII oocytes, while the remaining mice were housed with males for 40 additional hours up to euthanasia for ovarian, oocyte and embryo collection. Body and ovarian weight from each female mouse was registered at sacrifice. Cervical dislocation following cardiac rhythm absence exploration was the method carried out for euthanasia. The entire reproductive tract was removed and transferred to a small petri dish containing flushing medium (Origio, Måløv, Denmark) previously warmed at 37°C. Oviducts were then carefully isolated by separating firstly from the distal part of uterine horns and secondary from ovaries through the infundibulum (Fig. 14). Isolated ovaries and oviducts containing oocytes and embryos were transferred to new dishes for further processing. All microdissections were performed by using sterilized blades and a binocular loupe (SZX2, Olympus, Tokyo, Japan).

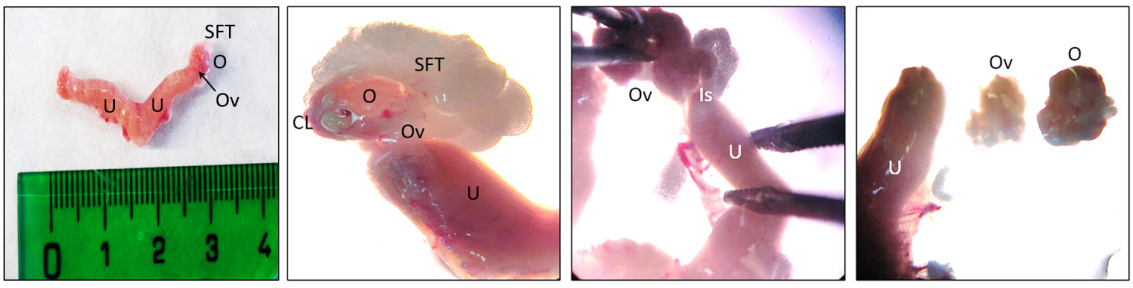

Figure 14. Reproductive tract processing for ovary and oviduct isolation. *Macroscopic and microscopic identification of tissue components in mouse reproductive apparatus mechanically processed to isolate ovarian and oviduct samples. CL: corpus luteum; Is: isthmus; O: ovary; Ov: oviduct; SFT: supporting fat tissue; U: uterine horn.*

Subsequently, supporting fat tissue was removed from the isolated ovaries with a blade and ovarian weight was recorded using a precision scale. Ovarian weight was normalized with bodyweight on euthanasia day to discard the impact of body mass on ovarian weight results. One ovary per mouse was frozen in liquid nitrogen and stored at -80°C, while the remaining ovaries

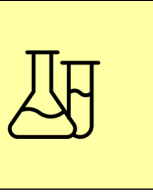

were fixed on buffered pH 6.9 formaldehyde solution 4% overnight (O/N) at room temperature (RT) for histological analysis.

1.5. Histological analysis

Fixed ovaries were transferred to 70% ethanol for at least 24 hours at 4°C. Subsequently, ovarian samples were dehydrated in an increasing graded series of ethanol (70%, 80%, 96% and 100%) and xylol washes, and paraffin embedding following Table VI.

Table VI. Fixed-tissue processing for dehydration and paraffin embedding.

Reagent	Time (minutes)	Temperature (°C)
Ethanol – 70%	30	RT
Ethanol – 80%	30	RT
Ethanol – 96%	30	RT
Ethanol – 100% – I	30	RT
Ethanol – 100% – II	30	RT
Xylol – I	15	RT
Xylol – II	15	RT
Xylol – III	15	RT
Paraffin – I	60	60
Paraffin – II	60	60

For further histological analysis, paraffin-embedded ovaries were cut into 4-µm thick sections with HM 310 microtome (Microm, Bicester, UK), mounted onto Superfrost Plus slides (ThermoFisher, Waltham, MA, USA) and stored for at least 24 hours at 37°C. Given that primordial follicles in mice measure around 20 µm (241-243), every fifth section was selected and stained with hematoxylin and eosin (H&E) for further follicle count and stromal evaluation. For this purpose, ovarian sections were placed for 1 hour at 60°C for deparaffinization, followed by a rehydration process with xylol, decreasing graded series of ethanol (100%, 96%, 80% and 70%), and distilled water washes (Table VII). Further to this, sections were firstly incubated with Harris hematoxylin

for 1 - 2 minutes, rinsed twice with distilled water, and secondary incubated with eosin for 30 seconds as counterstaining. After twice washes in distilled water, stained sections were air-dried and mounted with Eukitt Quick-hardening mounting medium (Sigma-Aldrich, USA).

Table VII. Paraffin-embedded tissue processing for deparaffinization and rehydration.

Reagent	Time (minutes)	Temperature (°C)
Xylol – I	5	RT
Xylol – II	5	RT
Xylol – III	5	RT
Ethanol – 100% – I	5	RT
Ethanol – 100% – II	5	RT
Ethanol – 96%	5	RT
Ethanol – 80%	5	RT
Ethanol – 70%	5	RT
Distilled water – I	5	RT
Distilled water – I	5	RT

1.5.1. Stromal evaluation

To analyze ovarian stroma, degenerated areas identified as the presence of fibrotic non-cellular or tissue absent regions embedded in the ovarian stroma were assessed in 5 representative H&E-stained sections per ovary. The ovarian surface in each section was captured by a bright-field microscope attached to a digital camera (Leica DM4000B and DFC450C, Leica Microsystems GmbH, Wetzlar, Germany). Degenerated area index was then established as the disrupted area / total tissue area of each sample using ImageJ software (National Institutes of Health, Bethesda, MD, USA). For each treatment group (ChT and ChT+LH-1x), mean stromal degeneration index was calculated, normalized to the index of the control group, and expressed as fold-change.

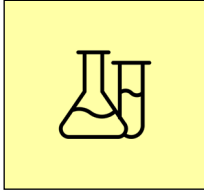

1.5.2. Follicle count

To determine the effects of LH treatment on the follicle pool against alkylating agents, follicle count was performed by three independent observers in every fifth 4-µm H&E-stained section by bright-field microscope (Leica DM4000B, Leica Microsystems GmbH, Germany). Developmental stages (Fig. 4) were classified according to standard criteria (244). Briefly:

- Primordial follicle: oocyte surrounded by a single layer of few flattened cells (known as pre-granulosa cells).
- Primary follicle: oocyte surrounded by a single layer of cuboidal GC.
- Secondary follicle: oocyte showing at least two-three complete layers of cuboidal GC with no visible antrum.
- Late preantral: oocyte with four or more complete layers of cuboidal GC with no visible antrum.
- Antral: follicle containing an initial or well-defined antrum cavity.
- Preovulatory: large antral follicle where oocyte is surrounded by cumulus cells.

To avoid double-counting, only morphologically normal follicles with a visible nucleus were counted. In addition, follicles showing morphological abnormalities were also counted to assess LH effects on the follicular morphology during their development. Those follicles showing any of the following features were considered as morphologically abnormal (Fig. 15):

- Type I: multinucleate oocyte in the same follicle.
- Type II: multiple vesicles on ooplasm.
- Type III: disrupted granulosa layers.
- Type IV: complete degenerated follicles.

Afterward, the percentage of morphologically abnormal follicles (PMAF) was calculated according to the following formula:

$$PMAF = \frac{Number\ of\ abnormal\ follicles\ per\ ovary}{Number\ of\ normal\ and\ abnormal\ follicles\ per\ ovary} \times 100$$

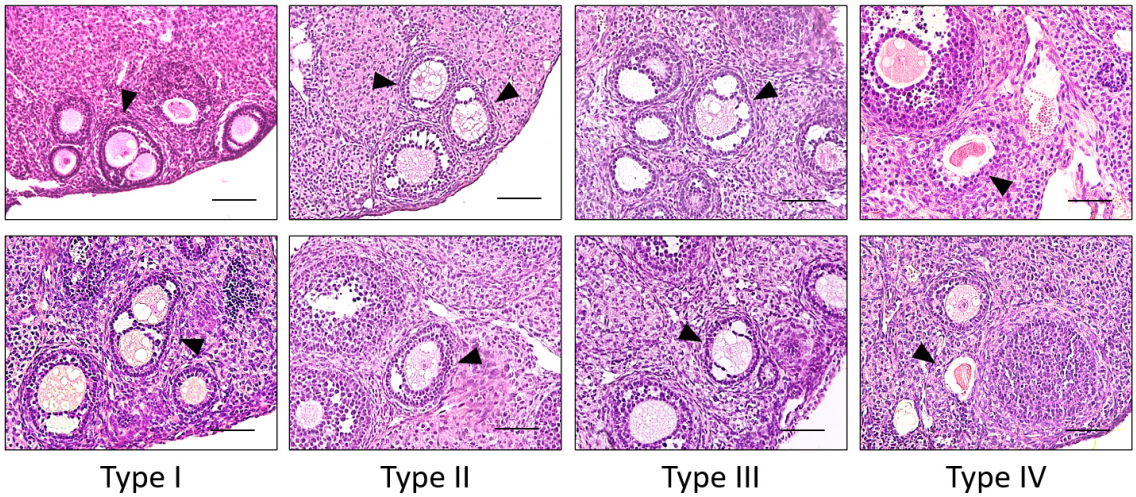

Figure 15. Morphological abnormalities visualized in follicles. *The main abnormalities detected in H&E-stained sections were: polynuclear follicles (Type I), multi-vacuolized ooplasm (Type II), loss of granulosa cell layer attachment (Type III), and total degeneration (Type IV). Black arrows indicate follicular alterations. Scale bars: 100 µm.*

1.6. Retrieval of MII oocytes and embryos

To release MII oocytes and embryos from isolated oviducts, a 30 G needle (Braun Vetcare, S.A., Spain) was inserted into the infundibulum, and a new warmed flushing medium (Origio, Denmark) was flushed throughout the oviduct following uterine sense (Fig. 16A). To determine an oocyte's maturation stage, cumulus-oocyte complexes (COC) were denudated by pipetting COC with 140 µm Flexipet pipettes adjusted to Flexipet handle (Cook Medical, Bloomington, Indiana, IN, USA) in warmed flushing medium (Origio, Denmark) supplemented with 300 µg/mL hyaluronidase (Sigma-Aldrich, USA) for 30-60 seconds. Oocytes and embryos were classified according to morphological criteria under SZX2 binocular loupe (Olympus, Japan). On the one hand, those oocytes with a single corpuscular body, non-granulated ooplasm, homogeneous zona pellucida, and non-large perivitelline space were considered morphologically normal MII oocytes (Fig. 16B). On the other hand, embryos showing two non-fragmented and symmetric blastomeres were classified as morphological normal 2-cell embryos (Fig. 16C).

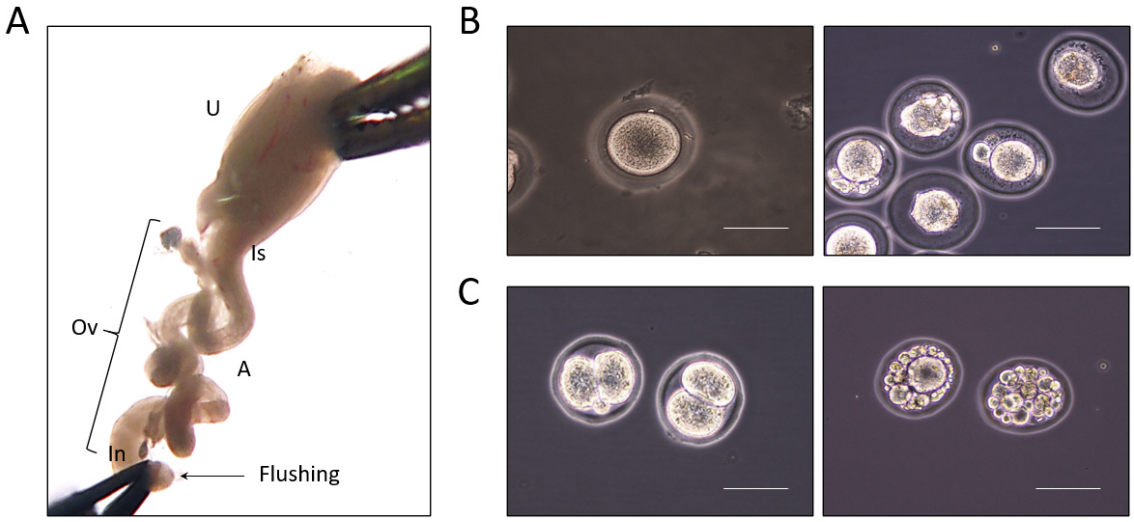

Figure 16. Germ cells retrieval and morphological classification. *(A) Distal part of uterine horn and oviduct containing oocytes and embryos visualized under bright-field binocular loupe. Oocytes and embryos were released by flushing medium with a needle inserted in the infundibulum (arrow). A: ampulla; In: infundibulum; Is: isthmus; Ov: oviduct; U: uterine horn. (B) Representative images of morphologically normal (left) and abnormal (right) MII oocytes retrieved from oviducts. The following oocyte abnormalities were depicted in the right image: large perivitelline space, fragmented and large corpuscular body, and granulated ooplasm. (C) Morphologically normal (left) and abnormal (right) 2-cell embryos. Blastomere multi-fragmentation was reflected in the abnormal embryos. Scale bars: 100 µm.*

1.7. Meiotic spindle staining and chromosome assessment

To evaluate oocyte quality, meiotic spindle and chromosome alignment were analyzed in MII oocytes obtained 16 hours after hCG administration (n = 9 MII oocytes in control, and n = 12 MII oocytes in ChT and ChT+LH-1x groups). Thus, MII oocytes were immersed in microtubule stabilizing fixative solution with PHEM 1x buffer (60 mM PIPES, 25mM HEPES, 10 mM EGTA, 2 mM $MgCl_2$, distilled water, pH 6.9), supplemented with 50% deuterium oxide, 0.01% Triton X-100, 0.01% Aprotinin, 1 mM dithiothreitol, 1 µM paclitaxel, and 4% paraformaldehyde (PFA) (all from Sigma-Aldrich, USA) for 25 minutes at 37°C. Fixed oocytes were washed twice with phosphate-buffered saline (PBS) and stored in the dark at 4°C in a blocking solution containing PBS supplemented with 2% fetal bovine serum (FBS), 1% bovine serum albumin (BSA), 0.2% non-fat powdered milk, 0.1 M glycine, 0.2% sodium azide, and 0.01% Triton X-100 (Sigma-Aldrich, USA) until staining. For microtubule and centromere staining, oocytes were incubated with anti µ-Tubulin-FITC (1:50 dilution; F2168 – Sigma-Aldrich, USA) and anti-CREST (1:20 dilution; 15-234 – Antibodies Incorporated, Davis, CA, USA) primary antibodies O/N at 4°C inside a dark

humidified chamber. Following several washes in blocking solution, oocytes were incubated with an Alexa Fluor 594 secondary antibody (1:1000 dilution; A-11014 – Invitrogen, Carlsbad, CA, USA) for 1 hour at RT. Chromosomes were labeled using 20 µg/mL Hoechst fluorescent staining (H33342 – Sigma-Aldrich, USA) for 20 minutes at RT. Finally, oocytes were transferred to µ-slide 8-well glass bottom chambers (Ibidi, Gräfelfing, Germany) and high-resolution images were captured at 405 nm (for Hoechst), 488 nm (for tubulin), and 594 nm (for CREST) with Leica TCS SP8 confocal microscope (Leica Microsystems GmbH, Wetzlar, Germany) and LAS X image software (Leica Microsystems GmbH, Germany). Oocyte handle was performed with 170 µm Flexipet pipettes adjusted to Flexipet handle (Cook Medical, USA). For spindle examination, we firstly determined the spindle organization by detecting the following configurations:

- Optimal: spindle showing barrel-shape with the central area wider than the extremes, two well-defined poles and high microtubules density (Fig. 17A).
- Suboptimal: spindle describes extended shapes with equivalent width between central and extremes regions. Suboptimal spindle has less microtubule density than the optimal organization (Fig. 17B).
- Disorganized: spindle shows a non-defined structure, with a single or at least 3 poles, and numerous microtubules in the cytoplasm (Fig. 17C).

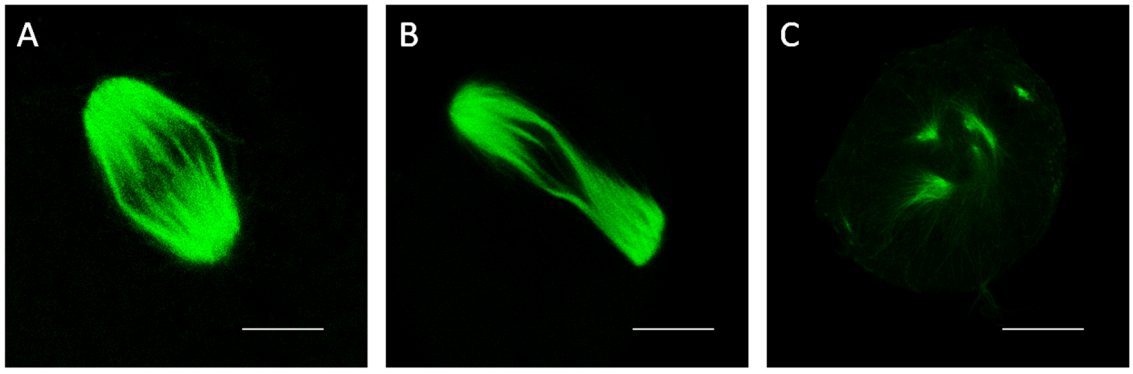

Figure 17. Meiotic spindle organization. *Immunofluorescence staining of µ-Tubulin (green) showing meiotic spindles with (A) barrel-shape classified as optimal organization, (B) elongated shape identified as sub-optimal configuration, and (C) disorganized multipolar spindle. Scale bars: 10 µm.*

Secondary, spindle area and chromosome alignment were determined on the images obtained with the highest intensity projection over the Z-axis for each oocyte by using ImageJ software (National Institutes of Health, USA). Those oocytes without visible meiotic spindle or with a

disorganized configuration were associated with a null area. For chromosome alignment, the oocytes with at least one chromosome diverged by ≥2 µm from the equatorial plate were considered as misaligned (Fig. 18), as described Coticchio *et al.,* (245).

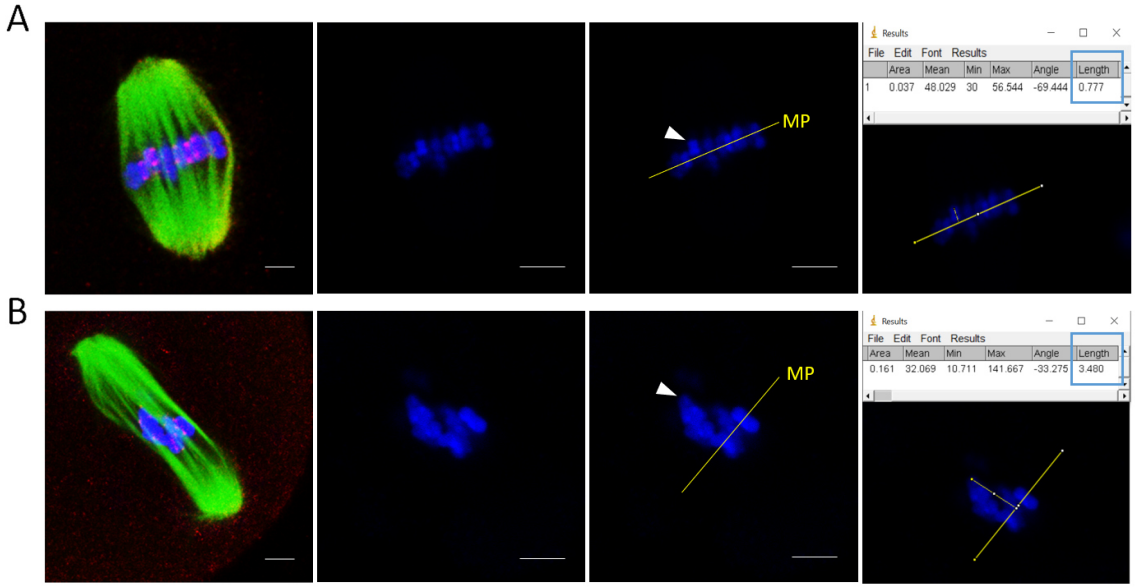

Figure 18. Assessment of chromosome alignment in MII oocytes. *Confocal images of immunofluorescence staining showing meiotic spindle (green), chromosomes (blue), and centromeres (red) in (A) aligned and (B) misaligned MII oocytes. Metaphase plate (MP) was outlined enclosing mostly of chromosomes and perpendicular to meiotic spindle. Chromosome alignment was determined quantifying the distance of the farthest chromosome (white arrowhead) from the metaphase plate by ImageJ software. Any chromosome distanced ≥2 µm from the metaphase plate was considered misaligned. Scale bars: 5 µm.*

1.8. Long-term effects on fertility

To estimate the effects of LH treatment on the reproductive potential and lifespan preservation against chemotherapy, a breeding trial and subsequent assessment of ovarian stimulation response were performed in all experimental groups, including the ChT+LH-5x mice.

1.8.1. Breeding trial

Thirty days after treatments, 4 mice/group were mated with fertile males for 6 months to allow continuous breeding. For each mating round, females were housed with 10-week-old CD-1 fertile males (Charles River Laboratories, France) in 2:1 proportion (female:male) for 7 days, followed by female individualization up to delivery. Pregnancy rate (number of pregnant mice / number of mice in the corresponding group and breeding round), number of delivered pups per mouse, as

well as pups' weight and size at 1-2 postnatal days were registered for each mating attempt. A total of 6 consecutive breeding rounds were performed for each experimental group, with 7 days between delivery and the new mating attempt.

1.8.2. Assessment of ovarian stimulation response

Thirty days after the sixth delivery, mice underwent COS and mating to collect ovaries, oocytes and embryos as described in sections 1.4. and 1.6. With this approach, we aimed to evaluate the long-term response of LH-treated mice to ovarian stimulation, as well as the MII-oocyte and cleavage-stage embryo morphological quality to better understand the results of breeding trials.

1.9. Statistical analysis

SPSS v.22.0 (IBM, Chicago, IL, USA) and R statistical programming language (R Core Team, Vienna, Austria) were used to perform the statistical analysis. Data are presented as mean and standard deviation (Mean ± SD). The sample size was estimated with pwr package (R Core Team, Austria). Two-by-two comparisons between experimental groups were performed with the non-parametric Mann-Whitney test. For spindle assessment data, multiple comparisons between groups were performed using the Turkey all-pair comparisons method (multcomp R package) with the R statistical programming language. The spindle area was analyzed by linear regression and the remaining variables by logistic regression. A p-value <0.05 was considered statistically significant. Graphics were generated by using GraphPad Prism 8.3.0 (GraphPad Software, San Diego, CA, USA).

2. The effect of LH-mediated gonadoprotection in oocyte – GC communication

Given the relevance of a suitable bidirectional communication between the oocyte and the surrounding GC for follicle development and oocyte competence (246), cell junctions established, and oocyte-secreted factors exchanged between oocytes and GC were evaluated in follicles

exposed to chemotherapy at the primordial developmental stage (section 1.1.) by molecular and immunofluorescence analysis. Key factors in gap (Cx37 and Cx43), adherens (E-Cad and N-Cad) and tight (TJP1) junctions, as well as oocyte-secreted paracrine factors (GDF9 and BMP15) and their specific receptor components (BMPR2, ALK4, ALK5 and ALK6) were specifically assessed in follicles, oocytes and GC.

2.1. Molecular analysis of oocyte – GC communication

Follicular cell junctions and oocyte-secreted factors were analyzed at the gene and protein levels on isolated follicles at secondary and later developmental stages.

2.1.1. Follicle isolation

Follicles were mechanically isolated from frozen-thawed ovaries (n = 3 from control, and n = 5 from ChT and ChT+LH-1x groups) collected 30 days after chemotherapy or/with LH treatments and stored at -80°C in section 1. Isolation was carried out by puncture with 30 G needles (Braun Vetcare, S.A., Spain) on a plastic dish containing Leibovitz's L-15 medium (Gibco, Fisher Scientific, Hampton, NH, USA) under SZX2 binocular loupe (Olympus, Japan). Minced tissue was carefully revised to detect any isolated follicle using Leica DMI 3000B inverted bright floor microscope attached to Leica DFC450C digital camera (Leica Microsystems GmbH, Germany). The number of isolated follicles was normalized with the ovarian weight to express the isolation yield. Every isolated follicle was classified by using LAS v4.13 software (Leica Microsystems GmbH, Germany) attending to its diameter size (Fig. 19A) in follicles <100 µm, that correspond to primordial and primary developmental stages, and follicles ≥100 µm, that represent the secondary, late preantral, antral and preovulatory subpopulations (Fig. 4). Those follicles measuring ≥100 µm were selected and placed on a plastic dish containing PBS with calcium and magnesium (Gibco, Fisher Scientific, USA) drops. Half of ≥100 µm follicles were kept intact, hereafter complete follicles (FOL), while the remaining were decumulated by using a decreasing diameter series of Flexipet pipettes (170, 140, 80 µm) adjusted to Flexipet handle (all from Cook Medical, USA) to obtain denuded oocytes (OO) and GC released (Fig. 19B). Subsequently, CF,

DO and GC were placed on separated microtubes and centrifuged for 10 minutes at 2500 RPM at 4°C. Finally, the supernatant was carefully discarded and the pellet containing the samples was stored at -80°C until further analysis.

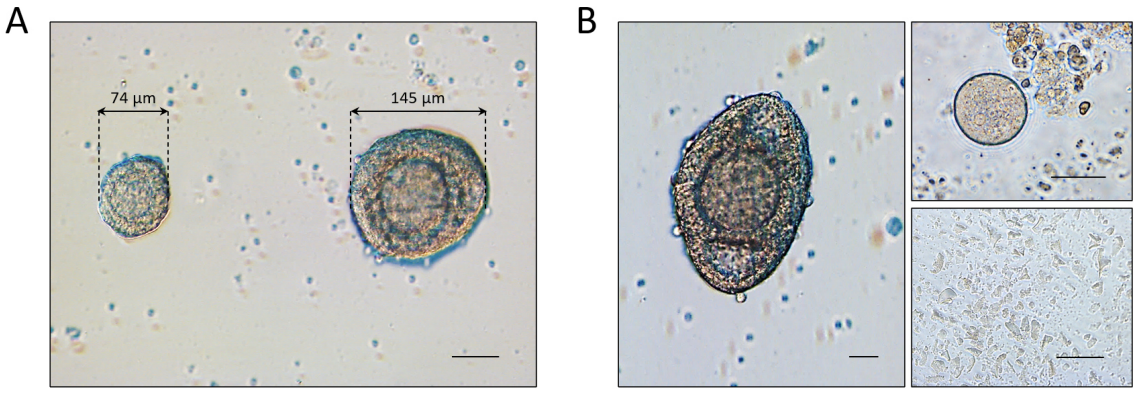

Figure 19. Follicle isolation from ovaries collected 30 days after chemotherapy administration. *(A) Isolated follicles with a diameter <100 µm (left) and ≥100 µm that represent the primary and secondary developmental stages, respectively. (B) Representative FOL measuring ≥100 µm corresponding to antral stage (left) before decumulation, as well as the OO (upper right) and part of the GC released (bottom right) as the result of denudation procedure. Scale bars: 50 µm.*

2.1.2. Gene expression

Oocyte – GC communication was analyzed at the gene level by real-time quantitative polymerase chain reaction (RT-qPCR) in FOL (at least n = 47/group), OO (at least n = 38/group) and GC (from at least n = 41 follicles ≥100 µm /group) from ovaries collected 30 days after chemotherapy administration. Interactions between oocytes and GC were evaluated by analyzing gene expression of cell junctions (Cx37, Cx43, E-Cad, N-Cad and TJP1), and oocyte-secreted factors (GDF9 and BMP15), including their specific receptor components (BMPR2, ALK4, ALK5 and ALK6).

Total RNA from the isolated FOL, OO and GC was extracted using Quick-RNA micropep kit (Zymo Research, Irvine, CA, USA) following the manufacturer's instructions. Briefly, samples were lysed adding 100 µL of RNA buffer lysis followed by 100 µL of absolute ethanol for molecular biology (Sigma-Aldrich, USA). Cell lysates were transferred to Zymo-Spin IC column in a collection tube and centrifuged 30 seconds at 13000 revolutions per minute (RPM). After several buffered washes and centrifugations, RNA was eluted in 11 µL of DNase/RNase-free water and

concentration was measured by NanoDrop One/OneC Spectrophotometer (Thermo Scientific, USA). Finally, RNA samples were immediately used to carry out reverse transcription polymerase chain reaction (RT-PCR).

Thus, complementary DNA (cDNA) was synthesized with the High-Capacity cDNA reverse transcription kit (Applied Biosystems, USA), according to manufacturer's instructions. For each reaction, 2 µg of RNA per sample was mixed with 2 µL of 10x RT Buffer, 0.8 µL of 25x dNTP Mix (100 mM), 2 µL of 10x RT Random Primers, 1 µL of MultiScribe Reverse Transcriptase (50 U/µL), and DNase/RNase-free water up to a final volume of 20 µL. Subsequently, RT-PCR was performed in T3000 thermocycler (Biometra GmbH, Göttingen, Germany) following the reaction settings described in Table VIII. Finally, cDNA content was quantified by NanoDrop One/OneC Spectrophotometer (Thermo Scientific, USA) and diluted with DNase/RNase -free water up to a final concentration of 100 ng cDNA/µL.

Table VIII. Thermocycler program to synthesize cDNA from RNA samples by RT-PCR.

Stage	Time (minutes)	Temperature (°C)
1	10	25
2	120	37
3	5	85
4	∞	4

RT-qPCR analysis was performed with specific primers for genes encoding for key factors involved in oocyte – GC communication and designed by Basic Local Alignment Search Tool (BLAST) and purchased from Invitrogen, USA. The sequence of primers used was detailed in Appendix I. Every polymerase chain reaction (PCR) was performed from 1 µL containing 100 ng cDNA sample, 0.5 µL of 10 µM forward specific primer, 0.5 µL of 10 µM reverse specific primer, 5 µL of PoweUp Sybr Green (ThermoFisher, USA) and 3 µL RNase-free water in a final volume of 10 µL. All PCR reactions were run in triplicate at MicroAmp Optical 384 well plates (Applied Biosystems, Foster City, CA, USA) using ViiA 7 Real-Time PCR System (Applied Biosystems, USA). The RT-qPCR protocol with melt curve stage was performed as described in Table IX. The

relative gene expression was calculated by the cycle threshold (CT) method (247) using 18S ribosomal (Rn18s) as a housekeeping gene.

Table IX. Thermocycler program to perform RT-qPCR reactions.

Stage	Time (minutes)	Temperature (°C)	Number of cycles	Temperature variation (°C/second)
Hold	10:00	95	1	1.6
PCR	00:15	95	45	1.6
	01:00	60	45	1.6
Melt curve	00:15	95	1	1.6
	01:00	60	1	1.6
	00:15	95	1	0.05

2.1.3. Protein extraction

All samples from a same experimental group were pooled and total protein content was extracted from isolated FOL (at least n = 103/group), OO (at least n = 100/group) and GC (from at least n = 108 follicles ≥100 µm /group) using radioimmunoprecipitation assay (RIPA) buffer (50 mM Tris-HCl, 150 mM NaCl, 4% Nonidet P-40, 0.5% sodium deoxycholate, 0.1% sodium dodecyl sulfate (SDS), pH 7.4) containing phosphatase (PhospSTOP EASYpack, Roche Diagnostics, Switzerland) and protease (cOmplete tablets EDTA-free EASY-pack, Roche Diagnostics, Switzerland) inhibitors. Samples were incubated for 30 minutes on ice and centrifuged for 20 minutes at 13000 revolutions per minute (RPM) at 4°C. The supernatant containing the protein fraction was collected and transferred to new microtubes. Protein content was determined by a colorimetric assay based on the Bradford method using Protein Assay Dye Reagent Concentrate (Bio-Rad, Hercules, CA, USA) following the manufacturer's instructions. Colorimetric absorbances were measured at 595 nm wavelength by SpectraMax 190 Microplate Reader (Molecular Devices, San José, CA, USA). Protein samples were stored at -80°C for western blotting (WB).

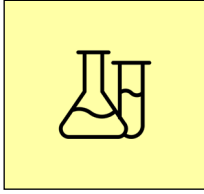

2.1.4. Western blotting

Protein samples were denatured in the presence of Laemmli Sample Buffer (Bio-Rad, USA) for 5 minutes at 95°C. Subsequently, 15 µg of protein from each sample were loaded into 1.5 mm wells and separated by electrophoresis on 10% SDS-polyacrylamide gels. Kaleidoscope prestained protein standard (Bio-Rad, USA) was also added to determine the molecular weights of sample bands. Electrophoresis was performed by incubating gels into running buffer containing 25 mM Tris, 190 mM glycine and 0.1% SDS (Bio-Rad, USA) for 60 - 75 minutes at 30 mA per gel with constant voltage. Separated proteins were transferred from gels to polyvinylidene difluoride (PVDF) membranes (Bio-Rad, USA) for 180 minutes at 240 mA using a transfer buffer containing 25 mM Tris, 190 mM glycine, 20% methanol (Bio-Rad, USA). Blots were incubated with blocking solution containing 5% BSA (Sigma-Aldrich) or non-fat powdered milk (depending on primary antibody) dissolved in Tris-buffered saline with 0.1% Tween 20 (TBST) for 1 hour at RT, and then exposed to primary antibodies O/N on an orbital shaker at 4°C. Primary antibodies were diluted in 3% BSA or non-fat powdered milk with TBST as follows: Cx37 (1:500 dilution; 40-4300 – Invitrogen, USA), Cx43 (1:5000 dilution; C6219 – Sigma-Aldrich, USA), E-Cad (1:1000 dilution; 3195 – Cell Signaling, USA), GDF9 (1:1000 dilution; ab93892 – Abcam, UK), BMP15 (1:1000 dilution; PA5-95615 – Invitrogen, USA), and β-Actin (1:2000 dilution; sc47778) – both from Santa Cruz Biotechnology, Dallas, TX, USA. After incubation, blots were washed three times in TBST, and incubated with appropriate Horseradish peroxidase (HRP)-conjugated secondary antibodies (sc-516102 and sc-2004; 1:2000 dilution; Santa Cruz Biotechnology, USA) for 1 h at RT on a shaker. After three washes in TBST, membranes were incubated with a chemiluminescence detection reagent (Super Signal West Femto Maximum Sensitivity Substrate, ThermoFisher, USA) and protein bands visualized by chemiluminescence imaging using Amersham Imager 680 (GE HealthCare Life Sciences, Marlborough, MA, USA). Integrated light intensity of each band was determined by ImageJ software (National Institutes of Health, USA). Signal intensities were normalized to the intensity of the housekeeping protein β-Actin.

2.2. Immunofluorescence

Oocyte – GC communication was evaluated on paraffin-embedded sections from ovaries collected on section 1., at 30 days after treatments. A total of 8 ovarian sections per ovarian sample were deparaffined and rehydrated as described in section 1.5. and Table VI. Subsequently, tissue antigens were unmasked to enable a suitable binding between antibody and target protein by a step named antigen retrieval. Thus, samples were incubated with Envision FLEX Target retrieval solution High pH (Dako Denmark A/S, Glostrup, Germany) in a pressure cooker for 3 minutes at 125°C and 1.5 atm. After two washes in PBS - 0.01% Triton X-100, tissue endogen avidin was blocked by using Avidin/Biotin blocking kit (Vector Laboratories, Burlingame, CA, USA) following the manufacturer's instructions. Afterwards, blocking step was performed by incubating sections with 3% BSA (Sigma-Aldrich, USA) and 2% Goat Normal Serum (GNS, Vector Laboratories, USA) in PBS - 0.01% Triton X-100 for 1 hour at RT. Afterwards, samples were incubated O/N at 4°C with the following primary antibodies described in section 2.1.4., which were prepared at the following dilutions: Cx37 (1:50 dilution), Cx43 (1:200 dilution), E-Cad (1:200 dilution), Gdf9 (1:100 dilution), Bmp15 (1:100 dilution). Then, sections were incubated with anti-mouse or anti-rabbit biotinylated IgG secondary antibodies (1:500 dilution; BA-9200 and BA-1000 – Vector Laboratories, USA) for 1 hour at RT, followed by 1 hour incubation at RT with streptavidin-conjugated Alexa Fluor 488 or 594 (1:500 dilution; S32354 and S32356, respectively, – Invitrogen, USA) for fluorescence labeling. Slides were mounted and nucleus were stained using Vectashield Vibrance antifade mounting medium with 4,6-diamidino-2-phenylindole (DAPI) (Vector Laboratories, USA). Leica TCS SP8 and LAS X software (Leica Microsystems GmbH, Germany) was used for confocal microscopy and image collection was performed with 1.3 numerical aperture x40 oil immersion objective at 405 nm (for DAPI), and 488 or 594 nm (for target proteins). For each follicle, high-resolution image was captured at the Z-axis point where the highest fluorescence intensity was detected. Relative intensity quantification of targeted proteins was determined by using ImageJ software (National Institutes of Health, USA) in all follicles visualized. For each treatment group (ChT and ChT+LH-1x), mean relative intensities were normalized to the control levels and expressed as fold-changes.

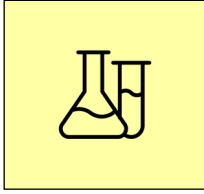

2.3. Statistical analysis

Statistical data analysis was performed by SPSS v.22.0 (IBM, USA) software, while the sample size was calculated with R statistical programming language with pwr package (R Core Team, Austria), and graphics were generated using GraphPad Prism 8.3.0 (GraphPad Software, USA). Data are expressed as mean and standard deviation (Mean ± SD). Any statistically significant difference between the experimental groups was identified through the non-parametric Mann-Whitney test for unpaired samples. A p-value <0.05 was considered statistically significant.

3. The protective mechanisms of LH

Early ovarian response to LH was evaluated by assessing the immediate effects of LH on ovaries and follicles to better understand how LH treatment primed gonadoprotection against alkylating agents.

3.1. Study design

Sixteen 7-week-old CD-1 female mice were randomly allocated to the four experimental groups: control, ChT, ChT+LH-1x and ChT+LH-5x. Treatments were administered to each experimental group as described in section 1.1. Mice were euthanized 12 and 24 hours after treatments to evaluate ovarian samples for DNA damage, apoptosis and DNA repair signaling (Fig. 20).

Protective early responses to LH were assessed in a complementary experiment. Sixteen 7-week-old CD-1 female mice were treated with LH and alkylators as described above. Mice were euthanized 12 and 24 h after treatment and ovarian samples were collected for apoptosis, DNA damage, and DNA repair signaling analysis.

3.2. Reagent administration

To induce POI condition, alkylating chemotherapy was prepared according to section 1.2., and administered to female mice allocated in ChT and both ChT+LH groups at 120 mg/kg of cyclophosphamide and 12 mg/kg of busulfan (both from Sigma-Aldrich, USA) doses. Control mice

only received DMSO (Sigma-Aldrich, USA) as vehicle. For LH treatment, the ChT+LH-1x and ChT+LH-5x animals received 1 or 5 IU LH (Luveris, Merck Serono, Germany) dose, respectively, before chemotherapy, then a second LH injection was administered with chemotherapy 24 hours later. All reagents were intraperitoneally administered by using 25 G needles (Braun Vetcare, S.A., Spain) attached to 1 mL syringes (VWR International Eurolab, S.L., Spain).

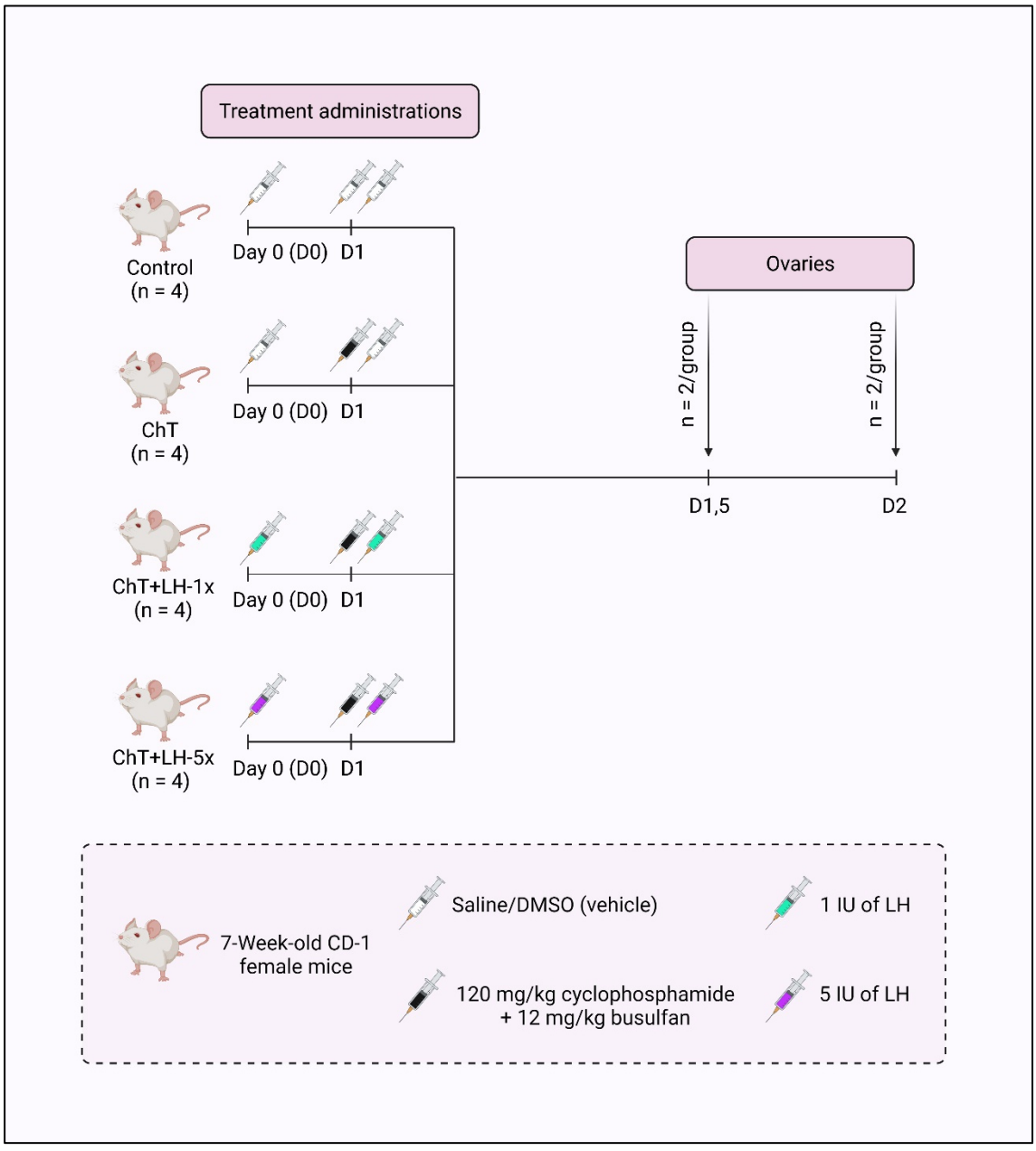

Figure 20. Study design to evaluate the early ovarian response to LH. *Ovaries from control, ChT, ChT+LH-1x and ChT+LH-5x groups were collected at 12 and 24 hours after chemotherapy and/or the second LH administration. Image created with biorender.com.*

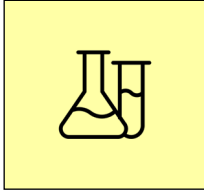

3.3. Euthanasia, and sample collection

Mice were euthanized by cervical dislocation at 12 (n = 2 mice/group) and 24 (n = 2 mice/group) hours after chemotherapy administration and ovaries were collected following the protocol described in section 1.4. Afterwards, ovarian samples were weighed and cut by half using a blade for each group and time-point. Four half-ovaries were fixed with PFA 4% O/N at RT, paraffin-embedded and serially sectioned at 4 µm on HM 310 microtome (Microm, UK), as described in section 1.5. for follicular damage assessment. The remaining ovarian fragments were pooled, submerged in liquid nitrogen, and stored at -80°C for further protein and gene expression analysis.

3.4. Follicular damage assessment

DNA damage and apoptosis in follicular cells were evaluated by immunofluorescence staining for γH2AX and TUNEL assay, respectively.

3.4.1. DNA DSBs

The functional activity of alkylating agents to induce DNA monoadducts and interstrand cross-links usually results in DNA DSBs that can be detected by the specific marker phosphorylated H2AX histone (γH2AX) (158, 248). With this purpose, a total of 8 ovarian sections per ovarian sample were deparaffined and rehydrated as described in section 1.5. and Table VI. γH2AX immunofluorescence staining was performed according to section 2.2. with minor modifications. For antigen retrieval, sections were incubated with 10 mM citrate buffer – 0.05% Tween 20 pH 6 for 20 minutes at 95°C. After cooling at RT for 20 minutes, samples were rinsed in tap water and washed twice in distilled water for 5 minutes. A subsequent permeabilization step, by incubating sections with PBS – 1% Triton X-100 for 10 minutes at RT, was needed due to γH2AX is a nuclear marker. After blocking step, samples were incubated O/N at 4°C with a monoclonal rabbit anti-γH2AX antibody (1:400 dilution; 9718 – Cell Signaling, Danvers, MA, USA) followed by 1 hour incubation at RT with a biotinylated goat anti-rabbit IgG secondary antibody (1:500 dilution; BA-1000 – Vector Laboratories, USA). Fluorescence staining was performed using streptavidin-conjugated Alexa Fluor 594 (1:1000 dilution; S32356 – Invitrogen, USA) for 45 minutes at RT.

Samples were mounted with Fluoroshield mounting medium with DAPI (Abcam, Cambridge, UK). A minimum of 150 follicles with visible oocyte nucleus per group were examined and high-magnification images were obtained using a fluorescence microscope with an attached digital camera (Leica DM4000B and DFC450C, Leica Microsystems GmbH, Germany). Oocytes containing positive γH2AX-labeled foci were considered damaged, and the DNA damage index for each sample was calculated as following:

$$DNA\ damage\ index = \frac{Number\ of\ \gamma\mathrm{H2AX} - positive\ oocytes}{Total\ number\ of\ oocytes} \times 100$$

3.4.2. Apoptosis

Apoptosis was assessed in follicular cells by terminal deoxynucleotidyl transferase-mediated dUTP nick-end labeling (TUNEL) immunofluorescence staining with TMR red *in situ* cell death detection kit (Roche Diagnostics, Basel, Switzerland). This technique detects fragmented DNA generated as the result of apoptosis, allowing the distinction from necrosis. For each ovarian sample, 8 paraffin-embedded sections were deparaffined and rehydrated as described in section 1.5. and Table VI. Antigen retrieval was performed by incubating sections with 10 mM citrate buffer – 0.05% Tween 20 pH 6 for 5 minutes at 850 W microwave. Cooled samples were rinsed in tap water followed by two washes with distilled water. Subsequently, TUNEL reaction solution was prepared for labeling step by mixing label and enzymatic solutions according to the manufacturer's instructions. Sections were incubated with TUNEL reaction solution for 1 hour at 37ºC inside a dark humidified chamber. Afterwards, sections were washed three times with PBS and slides mounted with Fluoroshield mounting medium with DAPI (Abcam, UK).

Positive and negative controls were also included to ensure specific tissue signal. For positive control, an ovarian section was incubated after antigen retrieval with 2000 U/mL of DNAsa I in 50 mM Tris-HCl, 1 mg/mL BSA pH 7.5 for 10 minutes at RT to induce DNA fragmentation. By contrast, an additional ovarian section was incubated only with label solution (non-enzymatic solution) after antigen retrieval to serve as a negative control with intact DNA.

TUNEL-positive (red) and DAPI-positive (blue) labeling was quantified from a minimum of 150 follicles per group by Image ProPlus 6.0 software (Media Cybernetics Inc., Rockville, MD, USA).

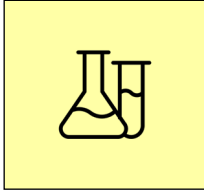

The percentage of follicular apoptotic cells was estimated by dividing the TUNEL-positive area (apoptotic cells) by the DAPI-positive area (nucleus) for each follicle. Those follicles showing ≥ 20% TUNEL-positive cells were considered as apoptotic follicles.

3.5. Ovotoxicity evaluation

To investigate whether LH treatment was able to prevent the chemotherapy-induced toxicity in ovaries, the protein expression of γH2AX, B-cell lymphoma 2 (BCL2), cleaved caspase 3 (CC3), extracellular signal-regulated kinase 1/2 (ERK1/2), and phosphorylated ERK1/2 (pERK1/2) was assessed by WB in ovarian pools collected at 12 and 24 hours after chemotherapy exposure. Thus, total protein content was extracted from frozen ovarian pools (n = 2 pools from 2 ovarian fragments each per group) according to section 2.1.3. Subsequently, protein expression levels were measured by WB following the steps detailed in section 2.1.4., with minor modifications. Briefly, 30 µg of protein from each sample was loaded into 10 - 12% SDS-polyacrylamide gels (depending on the molecular weight of the target protein). The primary antibodies used were prepared at the following dilutions: γH2AX antibody (1:1000 dilution; 9718), CC3 (1:1000 dilution; 9661), ERK1/2 (1:1000 dilution; 4695), pERK1/2 (1:1000 dilution; 4370) – all three from Cell Signaling, USA – Bcl2 (1:200 dilution; sc7382), and β-Actin (1:2000 dilution; sc47778) to normalize the targeted proteins. Band intensities were quantified by ImageJ software (National Institutes of Health, USA).

3.6. DNA repair analysis

LH role by triggering DNA repair pathways to protect ovaries against alkylating chemotherapy was evaluated at protein and gene expression levels by WB and RT-qPCR analysis, respectively, in ovaries collected at 12 and 24 hours after chemotherapy exposure.

3.6.1. Protein expression

HR, the specific DNA repair system for DNA DSBs in primordial follicles, was analyzed by assessing protein expression for the upstream ATM kinase and Rad51 recombinase, as well as AKT and phosphorylated AKT (pAKT), in protein samples extracted from ovarian lysates in section 2.1.3. section. Subsequently, 30 µg of protein from each sample were denatured and WB was performed as described in 2.1.4. section. Given the high molecular weight of ATM, protein samples were separated on 8 - 10% SDS-polyacrylamide gels. After blocking, blots were incubated with the following primary antibodies: ATM (1:2000 dilution; ab78), Rad51 (1:5000 dilution; ab133534) – both from Abcam, UK – Akt (1:500 dilution; 4691), pAkt (1:1000 dilution; 4060) – both from Cell Signaling, USA – or β-Actin (1:2000 dilution; sc47778 – Santa Cruz Biotechnology, USA). After protein band visualization, signal intensities were quantified by ImageJ software (National Institutes of Health, USA) and normalized to β-Actin values.

3.6.2. Gene expression

DNA repair analysis at the gene level was performed by RT-qPCR in ovaries collected at 12 and 24 hours after chemotherapy administration. The following key factors in DNA repair pathways were evaluated: Msh6 for mismatch repair (MMR) pathway, Apex1 for base excision repair (BER) pathway, Prkdc for non-homologous end joining (NHEJ) pathway, Ercc3 for nucleotide excision repair (NER) pathway, Rad51 for HR pathway.

For this purpose, total RNA was obtained from ovarian fragments stored at -80°C using the RNeasy micro kit (Qiagen, Hilden, Germany), according to the manufacturer's instructions. Briefly, ovarian fragments were mechanically disrupted and homogenized by 350 µL of lysis buffer and a rotor-stator homogenizer (Bel-Art, USA). Subsequently, cell lysates were gently mixed with 350 µL of 70% ethanol for molecular biology (Sigma-Aldrich, USA), transferred to RNeasy Mini Spin columns and centrifuged 30 seconds at 13000 RPM. Columns containing RNA in membranes underwent subsequent buffered washes and centrifugations to elute non-specific unbounded elements. RNA was finally eluted to microtubes by adding 30 µL of RNAse-free water directly to the spin column membrane and centrifuging for 1 minute at 13000 RPM. RNA content

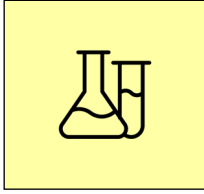

was quantified at 260 nm wavelength using NanoDrop One/OneC Spectrophotometer (Thermo Scientific, USA). RNA samples were stored at -80°C for further analysis.

cDNA was synthesized using the PrimeScript RT reagent kit (Takara Bio Inc., Kusatsu, Japan) following the manufacturer´s instructions. Briefly, 500 ng of RNA per sample was mixed with 2 µL of 5x PrimeScript Buffer, 0.5 µL PrimeScript RT Enzyme Mix I, 0.5 µL Oligo dT Primer (50 µM) and RNase-free water up to a final volume of 7 µL. RT-PCR was performed in T3000 thermocycler (Biometra GmbH, Göttingen, Germany) following the reaction program described in Table X. The cDNA content was subsequently measured using NanoDrop One/OneC Spectrophotometer (Thermo Scientific, USA) and diluted with RNase-free water up to a final concentration of 100 ng cDNA/µL.

RT-qPCR was carried out according to the protocol detailed in section 2.1.2. and Table VII. The list of primers (Invitrogen, USA) used for DNA repair associated genes and their specific sequences was detailed in Appendix II. The relative gene expression was calculated by the CT method applying the Rn18s housekeeping gene as normalization factor.

Table X. Run method set up to synthesize cDNA from RNA samples by RT-PCR.

Stage	Time (minutes)	Temperature (°C)
Reverse transcription	15:00	37
Inactivation of reverse transcriptase with heat treatment	00:05	85
To avoid cDNA degradation	∞	4

3.7. Statistical analysis

Statistical analysis, sample size estimation, and graph generation were carried out according to section 2.4. Data are expressed as mean and standard deviation (Mean ± SD).

4. LH effects on growing follicles exposed to alkylating agents

4.1. Study design

To test whether LH protects follicles at growing stages during chemotherapy exposure, NOD/SCID female mice were used (Fig. 21). This strain is considered as less fertile than the CD-1 mice (249) and represents a worst-case ovarian scenario. Sixteen 7-week-old NOD-SCID female mice were randomly allocated to control (n = 5), ChT (n = 5) and ChT+LH-1x (n = 6) groups. Treatments were administered for each experimental group as described in section 1.1. Seven days after treatments, mice underwent COS to ensure that any collected oocytes and embryos were derived from growing-stage follicles exposed to chemotherapy. Two mice per group were euthanized 16 hours after hCG injection to collect oocytes from the oviducts for spindle and chromosome analysis. The remaining mice (control = 3, ChT = 3, ChT+LH-1x = 4) were mated with fertile males immediately after hCG injection and euthanized 40 hours later (day 11 after treatments) to collect ovaries, MII-ovulated oocytes, and early cleavage-stage embryos from oviducts.

4.2. Reagent administration and matings

Alkylating chemotherapy with cyclophosphamide and busulfan agents was prepared according to the protocol described in section 1.2. Hence, female mice from ChT and ChT+LH-1x groups received an injection of 100 µL of chemotherapy solution, ChT+LH-1x mice simultaneously received 100 µL of LH solution containing 1 IU of LH (2.3 ng/ml, Luveris, Merck Serono, Germany). Mice from control group only received vehicle (DMSO). One week after, each mouse underwent COS consisting of the administration of 10 IU of PMSG (Folligon, MSD Animal Health, USA) followed by 10 IU of hCG (Ovitrelle, Merck Serono, Germany) 48 hours later, according to section 1.3. All reagents were intraperitoneally administered by using 25 G needles (Braun Vetcare, S.A., Spain) attached to 1 mL syringes (VWR International Eurolab, S.L., Spain).

Ten female mice (n = 3 from control and ChT groups, and n = 4 from ChT+LH-1x group) were mated immediately after hCG injection with 10-week-old C57BL/6 males in a 2:1 ratio for 40 hours until the euthanasia and sample collection point.

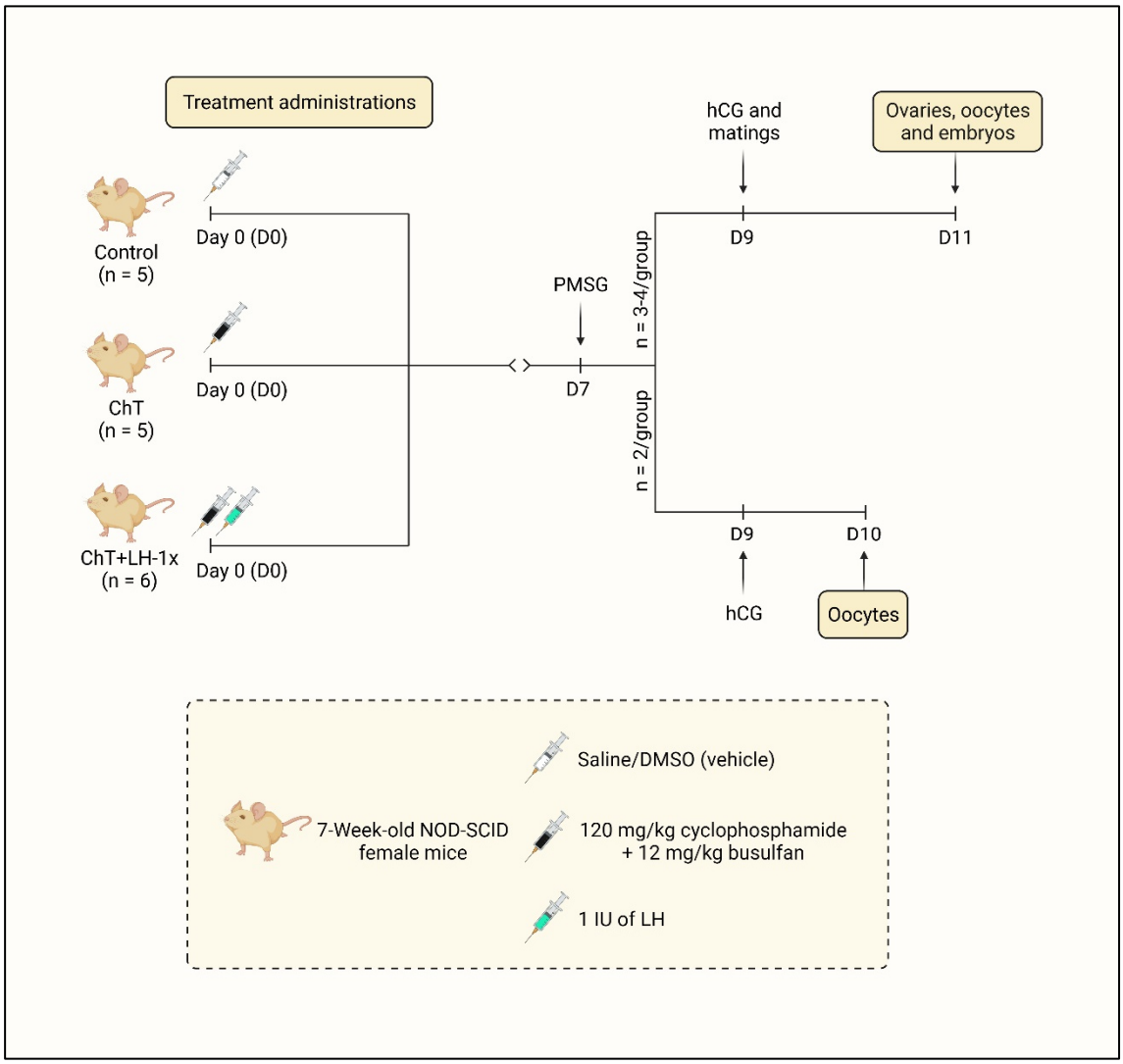

Figure 21. Study design to assess the LH effects on growing follicles exposed to alkylating agents in NOD/SCID adult mice. *One week after treatments, females underwent a controlled ovarian stimulation cycle with PMSG and hCG. MII oocytes were retrieved from 2 mice/group 16 hours after hCG (day 10), while remaining mice (3-4 mice/group) were mated after hCG injection for two days to collect ovaries, oocytes, and embryos on day 11. Image created with biorender.com.*

4.3. Euthanasia and sample collection

Euthanasia, sample collection and processing were performed according to section 1.4. Subsequently, fixed ovaries were paraffin-embedded and serially sectioned at 4 µm as described in sections 1.4 and 1.5. for further assessment of stromal degeneration, follicle count and follicular damage. Isolated oviducts containing oocytes and embryos were transferred to a small petri dish containing flushing medium onto a warming plate at 37°C for oocyte and embryo retrieval.

4.4. Histological analysis

To evaluate if LH treatment prevented chemotherapy-induced stromal alteration and follicular depletion, every fifth 4 µm ovarian section was stained with H&E according to section 1.5. and analyzed for stromal degeneration and follicle count.

4.4.1. Stromal evaluation

Given the relevance of ovarian stroma in the follicular development, stromal degeneration commonly induced by alkylating agents was measured in 5 representative H&E-stained sections of each ovary. Degeneration was identified as fibrotic regions with non-cellular or tissue absent areas in the stroma. The stromal architecture was assessed by quantifying the degenerated area index following the steps described in section 1.5.1.

4.4.2. Follicle count

Follicle endowment was assessed on every fifth 4 µm ovarian section stained with H&E for each sample. All morphologically normal follicles counted for every ovarian sample were classified according to their developmental stage in primordial, primary, secondary, late preantral, antral and/or preovulatory subpopulations (Fig. 4), as described in section 1.5.2. Likewise, PMAF was the result of the division between the number of follicles showing any morphological abnormality (type I, II, III, or IV; Fig. 15) and the total number of follicles counted per ovary.

4.5. Follicular damage assessment

Cell damage was examined in follicles by immunofluorescence staining of paraffin-embedded ovaries for DNA damage and apoptosis evaluation.

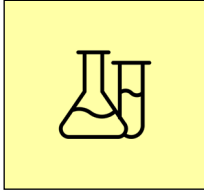

4.5.1. DNA damage

DNA DSBs in oocytes were detected by γH2AX staining, the specific marker of DSBs, following the protocol detailed in section 2.1.4.1. Eight 4 µm paraffin-embedded sections per ovarian sample were selected to perform the immunofluorescence staining, deparaffined and processed according to section 1.5. All follicles contained in stained sections were examined and high-magnification images were obtained using a Leica DM4000B fluorescence microscope with DFC450C attached digital camera (Leica Microsystems GmbH, Germany). Oocytes containing positive γH2AX-labeled foci were considered damaged, and the DNA damage index for each sample was calculated by dividing the number of γH2AX-positive oocytes by the total number of oocytes.

4.5.2. Apoptosis

Follicular apoptosis was determined in ovarian samples by TUNEL assay with TMR red *in situ* cell death detection kit (Roche Diagnostics, Switzerland). Eight sections per sample were deparaffined and processed as described in section 1.5., and TUNEL assay was performed following the protocol detailed in section 2.1.4.2. Positive and negative controls were also included to ensure DNA fragmentation specific signal. TUNEL and DAPI labeling from all follicles contained in the analyzed sections was quantified by Image ProPlus 6.0 software (Media Cybernetics Inc., USA). The percentage of follicular apoptotic cells was estimated by dividing the TUNEL-positive area (apoptotic cells) by the DAPI-positive area (nucleus) for each follicle. Follicles were considered apoptotic when showing ≥ 20% TUNEL-positive granulosa cells.

4.6. Retrieval of MII oocytes and embryos

Germ cell collection and processing were performed as it was detailed in section 1.6. Flushing medium (Origio, Denmark) containing 300 µg/mL hyaluronidase (Sigma-Aldrich, USA) and 140 µm Flexipet pipettes adjusted to Flexipet handle (Cook Medical, USA) were used for COC decumulation. The maturation stage and morphological quality of denuded oocytes and 2-cell

embryos were classified under SZX2 binocular loupe (Olympus, Japan) following criteria described in section 1.6. and showed in Fig. 16B-C.

4.7. Meiotic spindle staining and chromosome assessment

MII oocytes (n = 8 from control, n = 7 in ChT, and n = 13 in ChT+LH-1x groups) obtained 16 hours after hCG administration from NOD/SCID mice were processed and stained according to section 1.7. For each stained MII oocyte, high-resolution images were captured at 405 nm (for Hoechst), 488 nm (for tubulin), and 594 nm (for CREST) with Leica TCS SP8 confocal microscope and LAS X image software (Leica Microsystems GmbH, Germany). Oocytes were handled with 170 µm Flexipet pipettes adjusted to Flexipet handle (Cook Medical, USA). Meiotic spindle organization was categorized as optimal, suboptimal and disorganized, as showed Fig. 17. Total spindle areas and chromosome alignments were analyzed on the images obtained with the highest intensity projection over the Z-axis for each oocyte using ImageJ software (National Institutes of Health). Those oocytes with absent spindle or disorganized configuration were associated with null area. Oocytes were classified as misaligned when at least one chromosome diverged by ≥2 µm from the equatorial plate, as described in section 1.7. and Fig. 18.

4.8. Statistical analysis

Statistics were performed using SPSS v.22.0 (IBM, Chicago, IL, USA) and R statistical programming language (R Core Team, Vienna, Austria). Data are presented as mean and standard deviation (Mean ± SD). The sample size was estimated with pwr package (R Core Team, Austria). Two-by-two comparisons between experimental groups were performed with the non-parametric Mann-Whitney test for histological analysis, follicular damage and the number of oocytes and embryos. Multiple comparisons between groups were performed using the Turkey all-pair comparisons method (multcomp R package) by linear and logistic regression with the R statistical programming language for spindle assessment data. The spindle dichotomic variable (presence / absence) was determined by Bayesian analysis using a logistic regression and a normal non-informative prior (0 ± 3 as mean ± SD). Bayesian analysis was used instead of

frequentist statistics for the spindle variable “presence / absence” because we found a perfect separation scenario between experimental groups, which occurs when one of the explanatory variables of our model (in this case, the experimental groups) perfectly or almost perfectly separates 0 and 1 values of the response variable (spindle absence = 0; spindle presence = 1). Hence, in biological scenarios where a group has only the presence or absence for the variable of interest, the frequentist approach should be avoided due to its mathematical base, being Bayesian analysis more suitable for these cases. To test the quality of the Bayesian model, a posterior predictive check was performed by introducing spindle presence / absence data in the model generated for 1000 simulations with the R statistical programming language. A p-value <0.05 was considered statistically significant. Graphics were generated by using GraphPad Prism 8.3.0 (GraphPad Software, San Diego, CA, USA).

Results

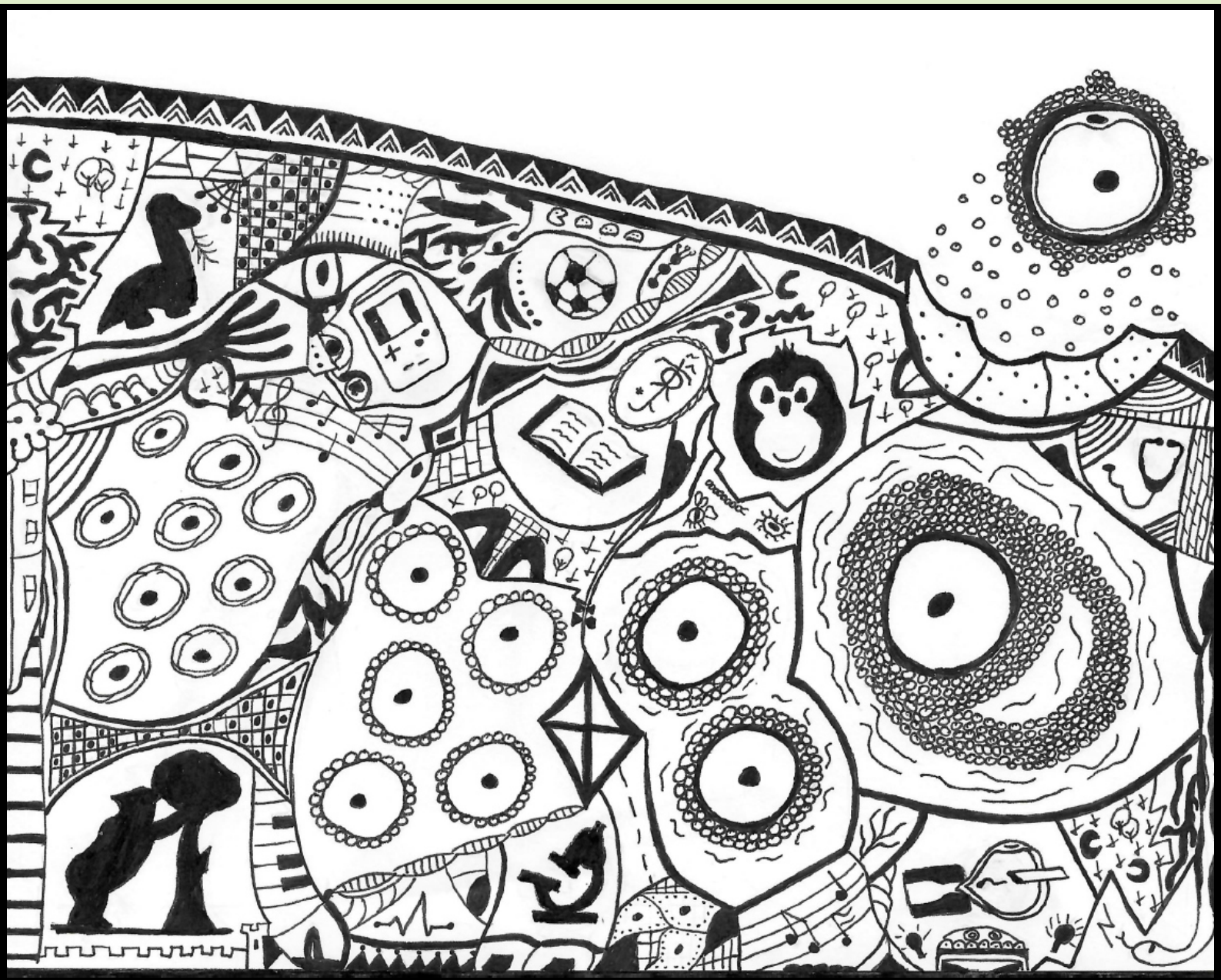

1. Effects on quiescent follicles

1.1. Macroscopic and histological examination of the ovaries

In a first step to evaluate the effects of treatments, ovarian samples were macroscopically assessed showing a reduction in the ovarian / body weight ratio induced by chemotherapy in both ChT and ChT+LH-1x ovaries compared to controls, being similar between both groups (Fig. 22A). The ovarian size was calculated on H&E-stained sections, where ChT ovaries showed a 30% decrease compared to control group (p = 0.036; Fig. 22B-C), while this reduction was partially avoided in LH-treated samples compared to controls (p = n.s.) being 10% lower than the observed in the ChT group.

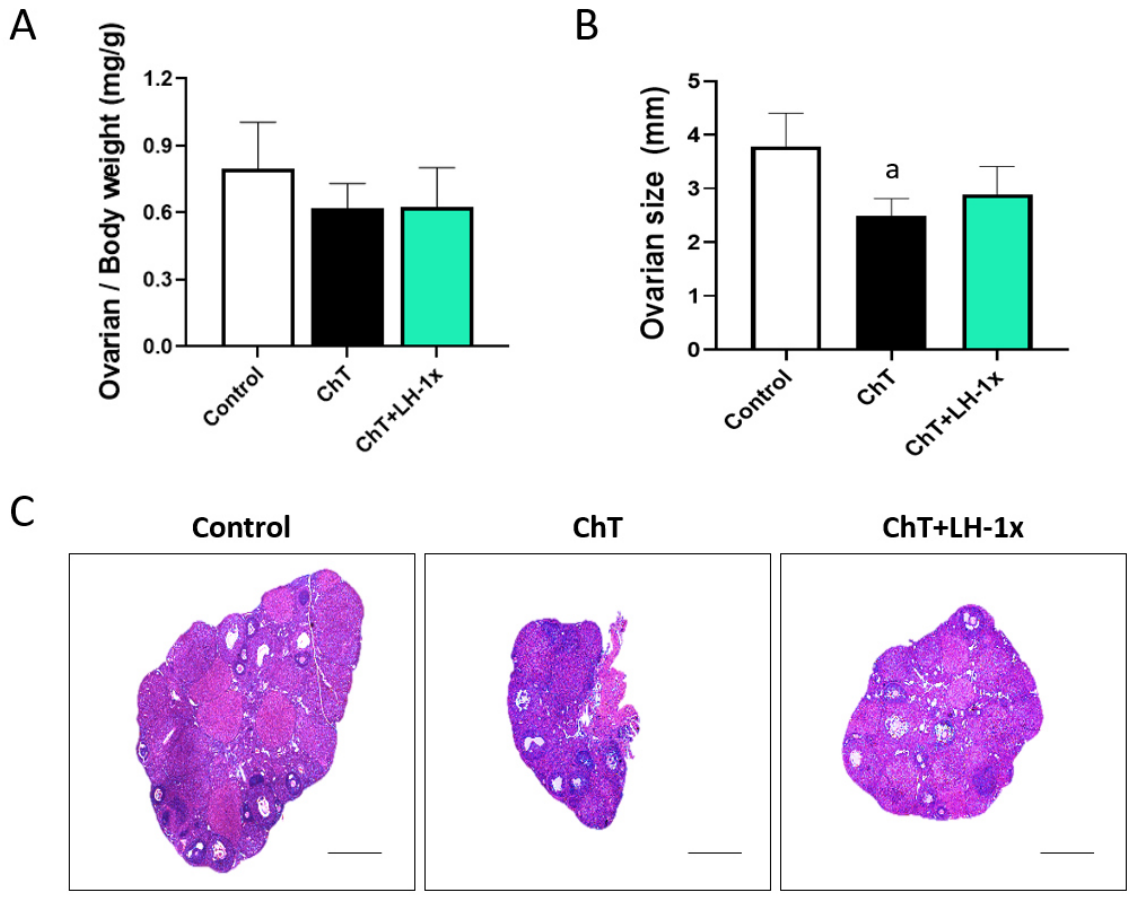

Figure 22. Macroscopic evaluation of ovaries. *Alkylating agents were administered with or without LH and ovaries were analyzed 30 days after. (A) Ovarian weight normalized with bodyweight registered on euthanasia day. Both groups receiving chemotherapy showed a similar reduction in the ovarian / body weight ratio. (B) Ovarian size and (C) representative images of the middle section of ovaries stained with H&E (2.5x magnification; scale bars: 800 µm). The middle section was established considering the total number of sections for each ovary. LH blunted the significant reduction in ovarian size induced by chemotherapy. Bar charts show means and SD*

for each experimental group (n = 3 mice for control group while n = 5 mice for ChT and ChT+LH-1x groups). [a]p-value < 0.05 vs. control group.

Given the role of ovarian stroma to maintain the gonad functionality, we analyzed its status. A disruption of the stromal structure was detected in ChT-group sections (Fig. 23), being fibrotic and non-cellular areas localized in the center of stroma the most common alterations found (Fig. 23A). The mean stromal degeneration index of the ChT group was 2.3-fold higher than that of the control group (p = 0.025; Fig. 23B). LH treatment blunted this effect, as showed by the well-preserved morphology and the slight 1.6-fold increase in the stromal degeneration index of ChT+LH-1x treated samples when compared to controls (p = n.s.). Despite this improvement, there was not a statistically significant difference between ChT and ChT+LH-1x groups.

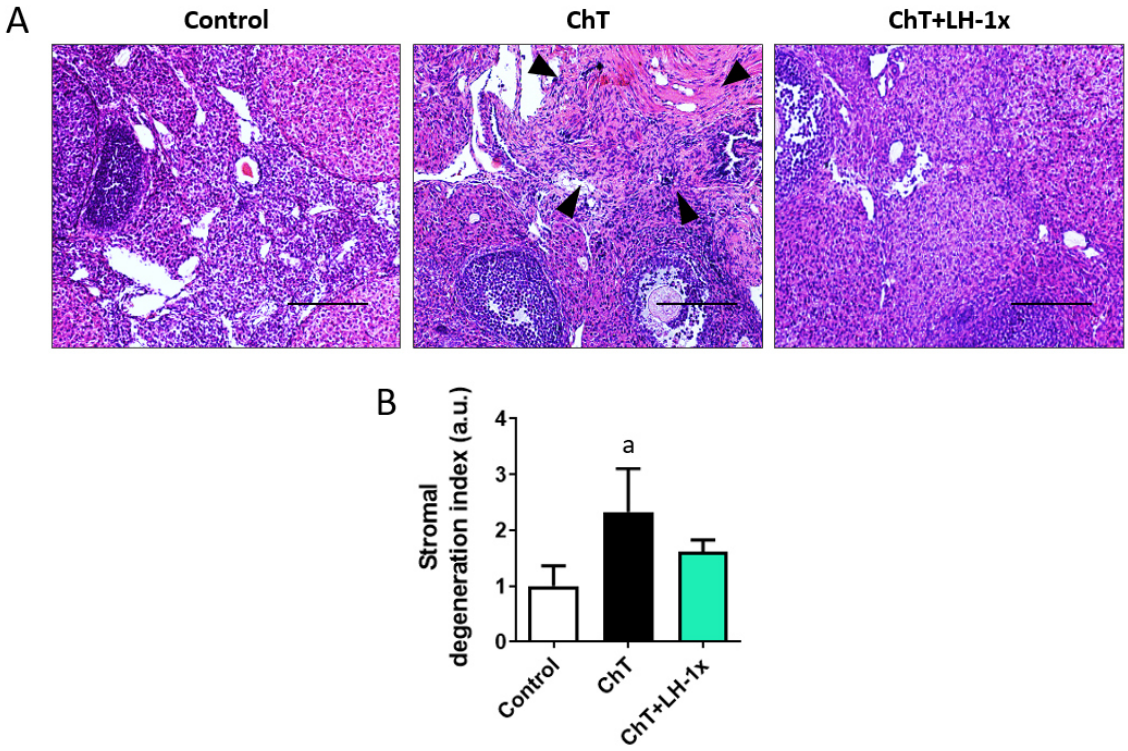

Figure 23. Stromal architecture and quantitative assessment of degeneration. *(A) Representative images of ovarian stromal architecture stained with H&E (10x magnification; scale bars: 200 µm) showing non-cellular regions and fibrotic areas (black arrowheads). (B) Quantification of stromal degeneration, where data were normalized with control values. LH treatment decreased the stromal disruption and fibrosis observed in ChT samples leading to recovered control-like levels on the stromal degeneration index. Bar chart shows means and SD for each experimental group (n = 3 mice for control group while n = 5 mice for ChT and ChT+LH-1x groups). [a]p-value < 0.05 vs. control group.*

1.2. Follicular endowment and follicular status

Follicle stockpiles were assessed to investigate whether LH could preserve follicles against alkylating agents. Ovaries from the ChT group exhibited 69.8 % fewer follicles than controls (p = 0.025; Fig. 24A). This depletion particularly affected to the primordial, primary, and secondary populations with a 76.4 % (p = 0.024), 68.0 % (p = 0.025) and 67.8 % (p = 0.034), decrease compared to control samples, respectively (Fig. 24B). LH-treated samples had 53.8 % fewer follicles than controls, but this difference was not statistically significant. LH treatment ameliorated follicle loss found in ChT ovaries by 34.6 % with a noteworthy increase in the number of primordial (38.1 %), primary (36.1 %), antral (25.0 %), and preovulatory (52.4 %) follicle numbers, although these differences were not statistically significant due to high variability between samples.

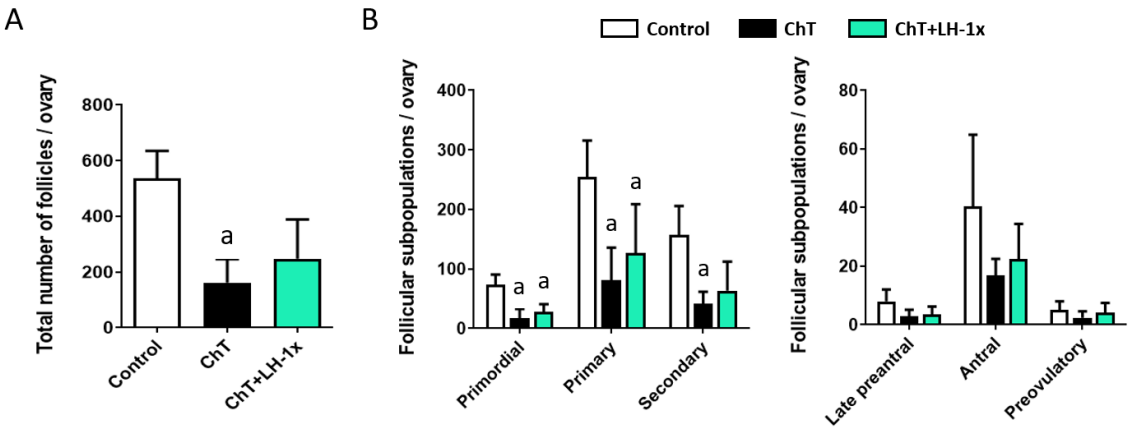

Figure 24. Follicle pool and populations derived from follicles at the primordial stage during chemotherapy administration. *(A) Total number of follicles and (B) follicular populations per ovary assessed in hematoxylin and eosin-stained sections. LH treatment diminished the follicle depletion detected in ChT ovaries by increasing the number of follicles from each developmental stage. Bar charts show means and SD for each experimental group (n = 3 mice for control group while n = 5 mice for ChT and ChT+LH-1x groups).* [a]*p-value < 0.05 vs. control group.*

Chemotherapy administration induced morphological abnormalities on follicles and, as such, the ChT ovaries had more morphologically abnormal follicles than the control group (p = 0.049; Fig. 25A). This effect was reverted by LH, finding similar numbers of abnormal follicles as the control group, and significantly fewer than the ChT group (p = 0.047). Although all abnormalities described in Fig. 15 were detected, ooplasm vacuolization (Fig. 25B) and disruption of granulosa cell layers (Fig. 25C) were the most common alterations found in ChT sections. Interestingly, these morphological abnormalities predominantly affected to the growing populations, finding that

more than 50% of abnormal follicles detected in each experimental group belonged to the secondary stage (Fig. 25D).

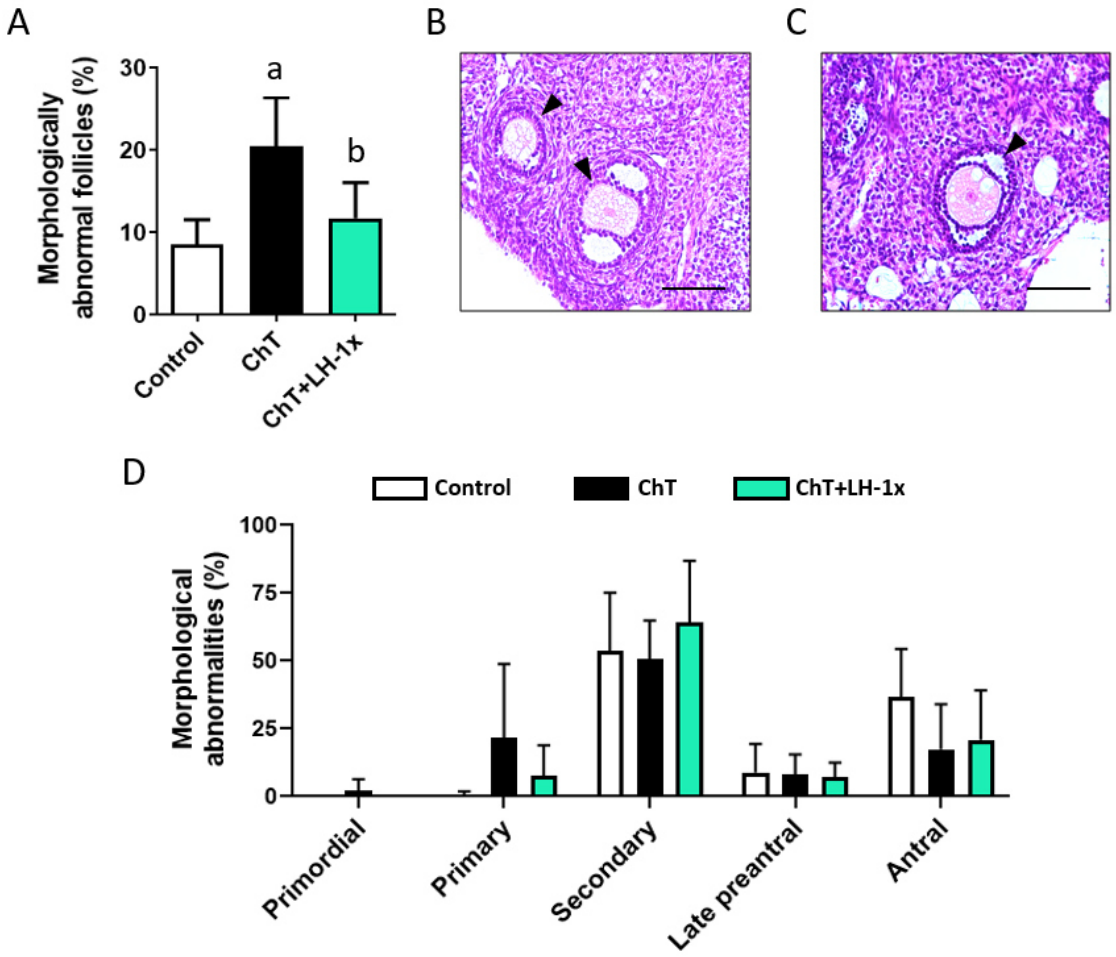

Figure 25. Morphological abnormalities in follicles. *(A) Rate of morphologically abnormal follicles increased 30 days after chemotherapy, but LH treatment prevented this effect with statistically significant differences. Pictures showing secondary follicles with morphological abnormalities consisting of (B) the ooplasm vacuolization and (C) the disruption of granulosa cell layers stained with hematoxylin and eosin (20x magnification; scale bars: 100 µm). (D) Distribution of morphologically abnormal follicles according to their developmental stage. Bar chart shows means and SD for each experimental group (n = 3 mice for control group while n = 5 mice for ChT and ChT+LH-1x groups). [a]p-value < 0.05 vs. control group; [b]p-value < 0.05 vs. ChT group.*

1.3. Ovulation and early embryo cleavage

Fewer morphologically normal MII oocytes and 2-cell embryos were collected after COS from ChT animals compared to controls (p = 0.044 and 0.032, respectively; Fig. 26A-B). In the ChT+LH-1x group, the number of MII oocytes rescued from LH-treated mice was statistically akin to that of control mice (p = n.s.), being 25.0 % higher than that from ChT mice. Despite this

improvement, a significant reduction in the number of morphologically normal embryos at the early cleavage stage was found compared to control mice (p = 0.034).

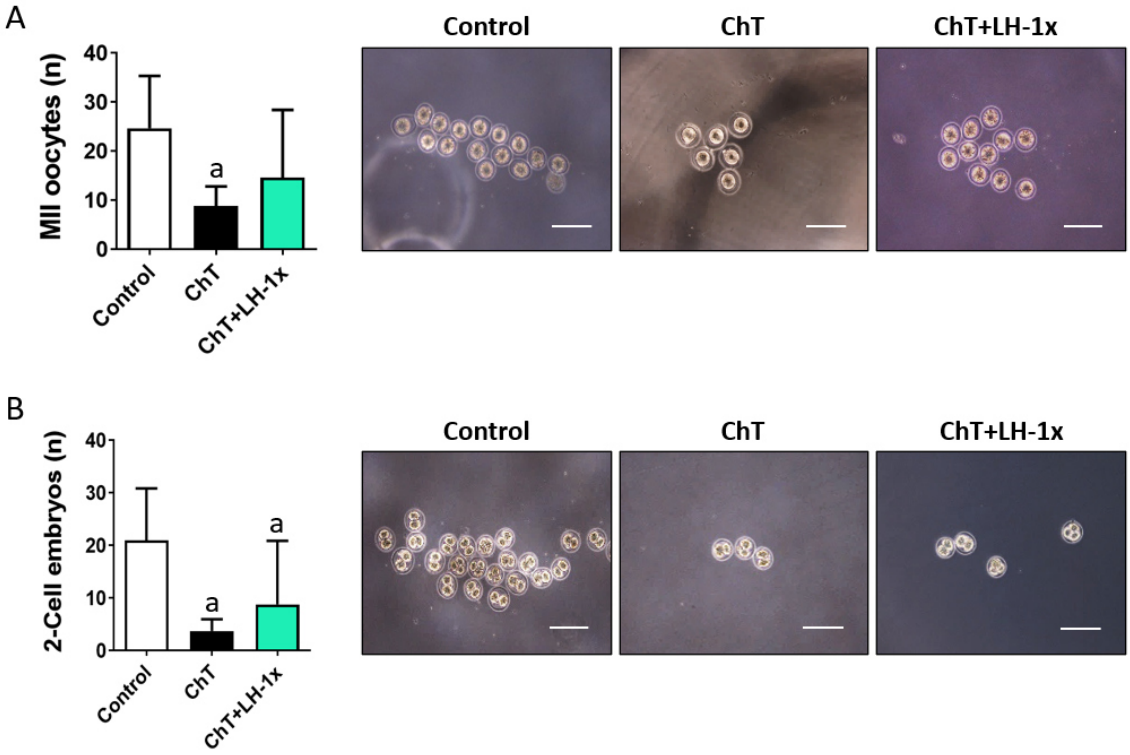

Figure 26. Number of MII oocytes and embryos. *(A) Total number of morphologically normal MII oocytes with representative images (10x magnification; scale bars: 200 µm), and (B) 2-cell embryos with representative images (10x magnification; scale bars: 200 µm) rescued from ovarian stimulated mice 30 days after treatments. LH-treated mice ovulated larger MII oocyte cohorts than ChT group, while no differences between both groups were observed for the number of early cleavage embryos. Bar charts show means and SD for each experimental group (n = 3 mice for control group while n = 5 mice for ChT and ChT+LH-1x groups). [a]p-value < 0.05 vs. control group.*

1.4. Oocyte quality

Further evaluation of oocyte protection by LH was performed to determine the quality of ovulated oocytes. Thus, meiotic spindle and chromosome disposition were measured by using immunofluorescence in MII oocytes derived from follicles in the primordial stage at the time of chemotherapy administration (Fig. 27A). The meiotic spindle was visualized in the 33 MII oocytes analyzed from all experimental groups suggesting that chemotherapy did not affect to spindle assembly of these oocytes. However, the mean spindle area of oocytes from the ChT group was 35.3 % lesser than the mean control area (p = 0.019; Fig. 27B). This effect was blunted by LH,

being the mean spindle area of the LH-treated oocytes akin to that of controls, and 31.1 % higher than that of the ChT group (p = 0.035).

Furthermore, our findings showed that ChT group had more misaligned MII oocytes than the control group (p = 0.019; Fig. 27C), while LH treatment recovered the chromosome misalignment. In fact, the number of misaligned MII oocytes was similar in the ChT+LH-1x and control groups.

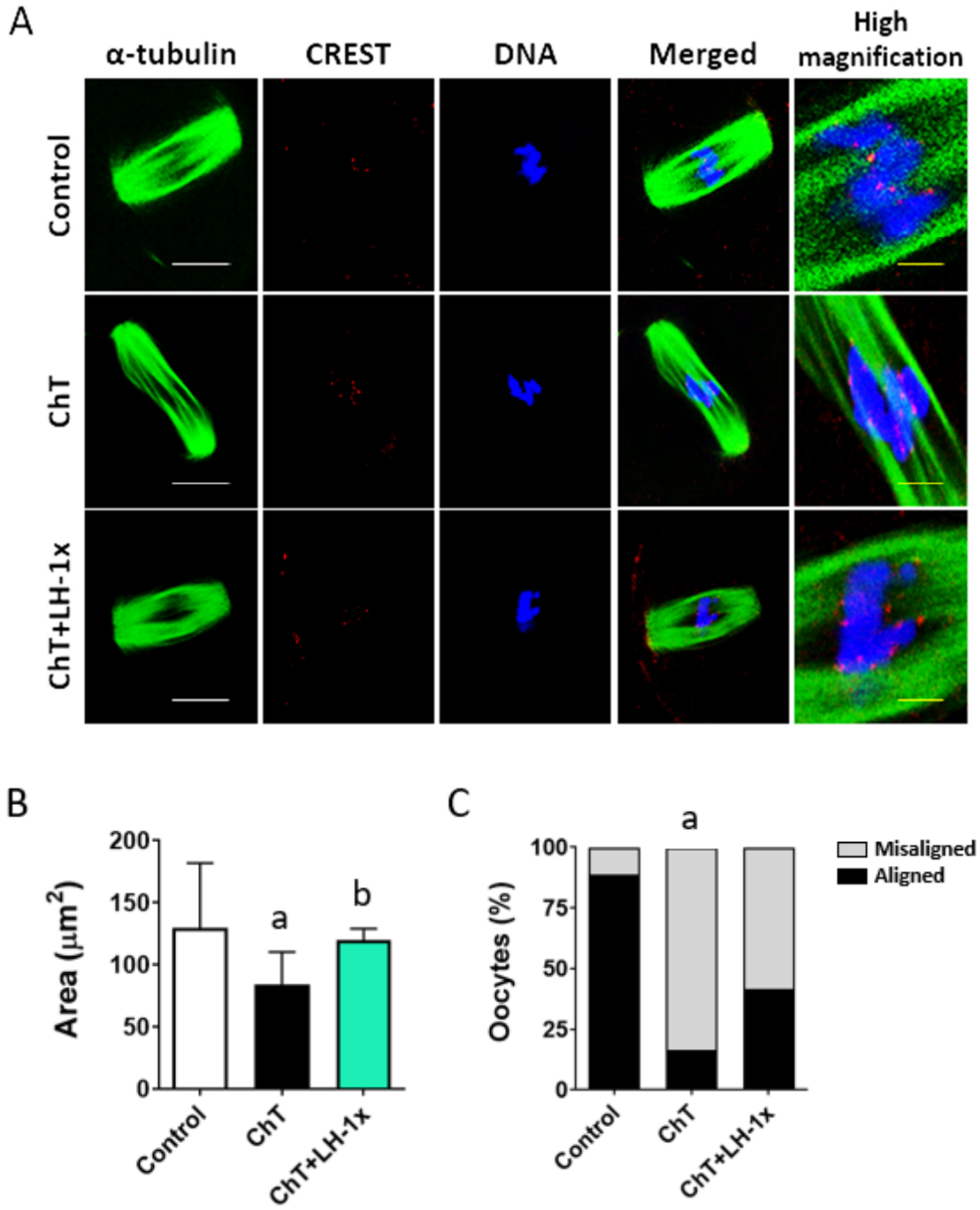

Figure 27. Meiotic spindle assessment of MII oocytes. *(A) Confocal images of meiotic spindles from MII oocytes collected 16 hours after hCG injection in animals previously treated with or without alkylating agents and LH. Immunofluorescence staining of α-tubulin (green) to represent*

microtubules, chromosomes (blue) and CREST as centromere protein (red) to evaluate chromosome alignment and microtubule-chromosome attachment. The right column shows a high magnification (120x magnification) of merged optical sections focused on the metaphase plate. White scale bars: 10 µm. Yellow scale bars: 2.5 µm. (B) Quantification of spindle areas. LH treatment reversed the chemotherapy-induced reduction in spindle size up to levels similar to control group. (C) Chromosomal alignment rate with reference to the metaphase plate. The LH-treated group had a lower percentage of misaligned chromosomes than the ChT group. Bar charts show means and, where indicated, SD for each experimental group (n = 9 MII oocytes in control, and n = 12 MII oocytes in ChT and ChT+LH-1x groups were analyzed from 2 mice / group). [a]p-value < 0.05 vs. control group; [b]p-value < 0.05 vs. ChT group.

1.5. Breeding trials

To assess whether LH could ameliorate the reproductive lifespan of mice exposed to alkylating agents, we monitored the breeding performance during six mating attempts. We also included an additional experimental group (ChT+LH-5x) to find out if LH protection was dose-dependent. Pregnancy rates and litter sizes progressively diminished as maternal age increased in all experimental groups. This decline was accelerated in the ChT group, with a reduced cumulative pregnancy rate and mean litter size per delivery (Fig. 28A-C). These issues resulted in a 45.8 % reduction in the number of live births relative to controls (Fig. 28D). In contrast, both LH-treated groups had better reproductive outcomes than the ChT group. In particular, low-dose LH resulted in 21 % more healthy pups than the ChT group.

In addition, we analyzed if treatments caused any alteration in offspring. Nevertheless, we did not observe statistically significant differences between groups for the litter´s weight (Control: 1.9 ± 0.1 g, ChT: 1.8 ± 0.1 g, ChT+LH-1x: 1.9 ± 0.2 g, ChT+LH-5x: 2.0 ± 0.1 g; p = n.s.) and length (Control: 4.7 ± 0.1 cm, ChT: 4.6 ± 0.1 cm, ChT+LH-1x: 4.8 ± 0.2 cm, ChT+LH-5x: 4.8 ± 0.1 cm; p = n.s.; Fig. 28D).

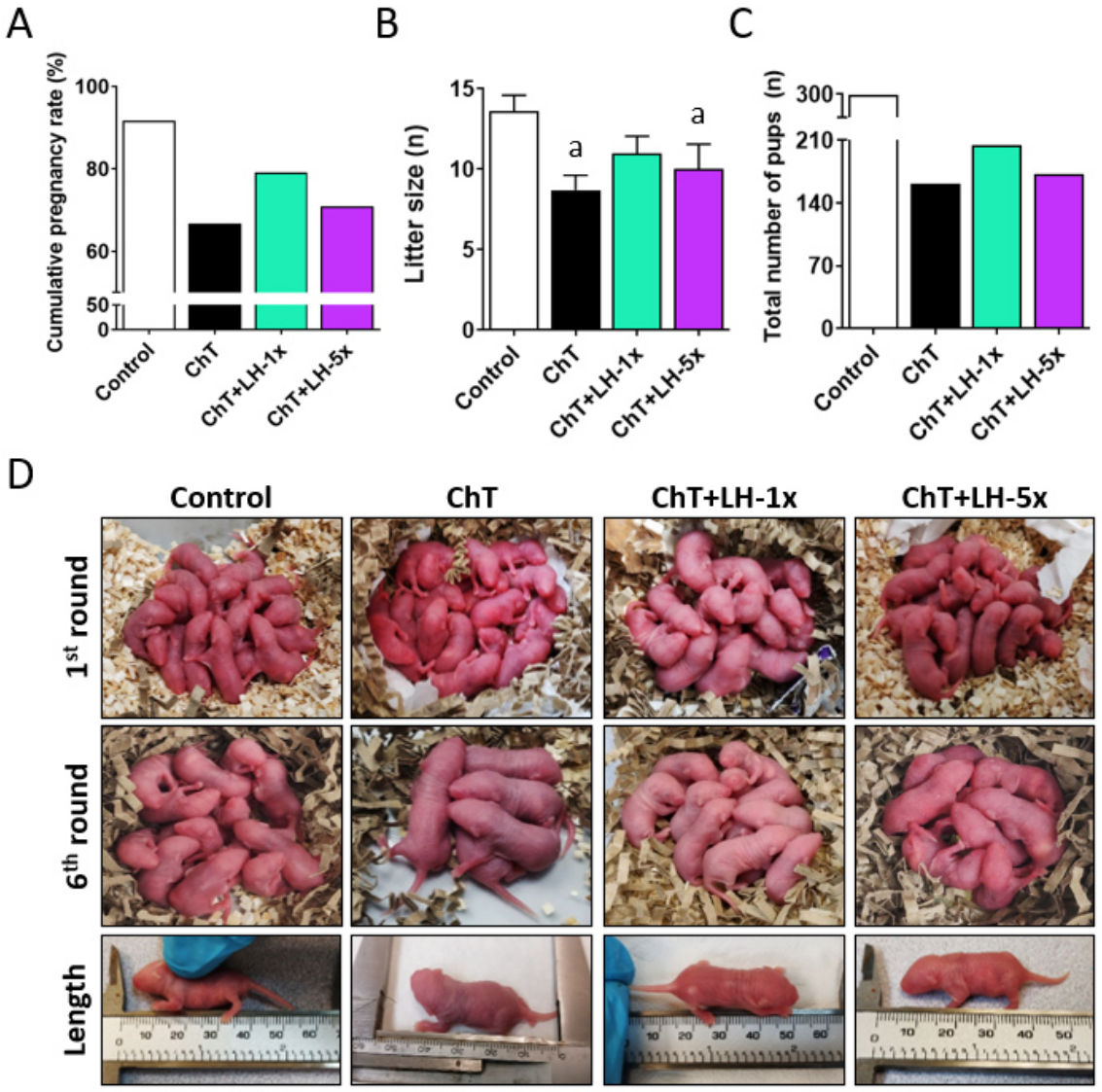

Figure 28. Breeding outcomes and reproductive lifespan assessment. *(A) Cumulative pregnancy rate after six consecutive mating attempts. ChT reduced the pregnancy rate and LH treatment reversed this, with the 1x dose being the most effective. (B) Mean litter size during the six breeding rounds. ChT reduced the litter size and LH-1x reversed this effect. (C) Total number of pups born for each experimental group. LH-1x ameliorated the chemotherapy-induced reduction in the total number of healthy pups delivered. (D) Representative images showing the first and the sixth litter, and the pups' length. LH-1x group showed an improvement in the reproductive outcomes compared to the ChT group by preventing the reduction in the litter size between the first and the last labor. Pups' length was similar between all experimental groups. Bar charts show means and, where indicated, SD for each experimental group (n = 4 mice / group).* ^{a}*p-value < 0.05 vs. control group.*

On the other side, ovaries stimulated 30 days after the sixth breeding round revealed a reduction in the ovarian / body weight ratio (p = 0.029; Fig. 29A) and ovarian size of ChT mice compared to controls (Fig. 29B), whereas LH treatment partially diminished these detriments, especially by the lower dose.

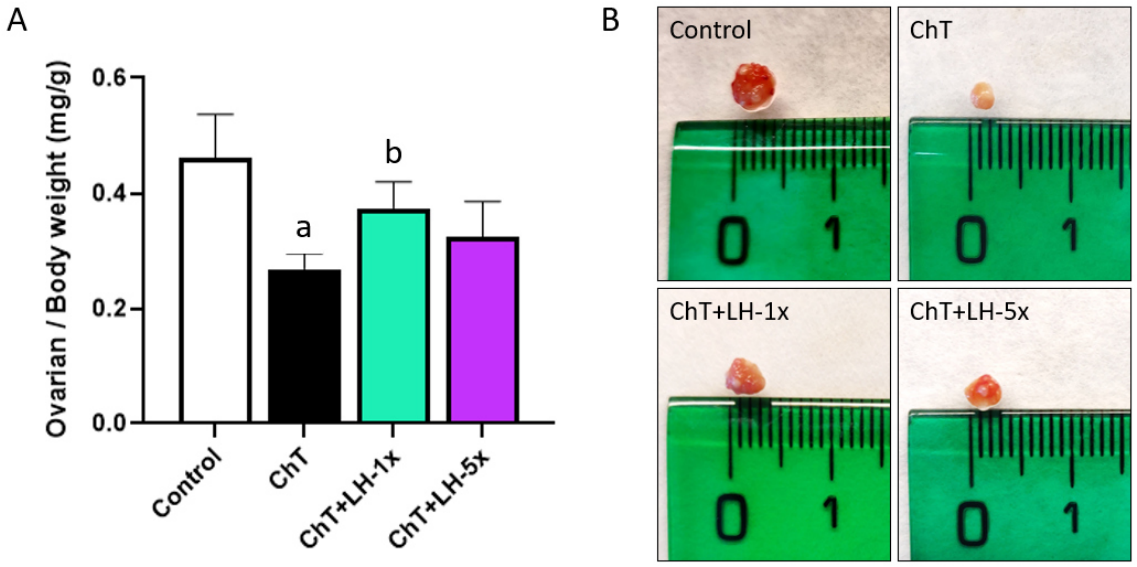

Figure 29. Macroscopic properties of ovaries after six breeding rounds. *(A) Ovarian weight normalized with the bodyweight at euthanasia day and (B) macroscopic images of ovaries collected from stimulated mice after the sixth breeding round. Both LH treatments reversed the chemotherapy effects on the ovarian / body weight and size. Note that the lower LH dose especially preserves the ovarian macroscopic properties. Bar chart shows means and SD for each experimental group (n = 4 mice / group).* [a]*p-value < 0.05 vs. control group;* [b]*p-value < 0.05 vs. ChT group.*

Moreover, animals from ChT group reduced the total number of MII oocytes and 2-cell embryos compared to control mice, suggesting a notable exhaustion of recruitable follicles (Table XI). Most MII oocytes (95.8 ± 7.2 %) and 2-cell embryos (87.5 ± 17.7 %) from ChT group showed morphological abnormalities like cytoplasm vacuolization, large perivitelline space and blastomere fragmentation. By contrast, despite a reduction in the number of oocytes and embryos detected in LH-treated groups compared to control mice (Table XI), the chemotherapy-induced decline in morphological quality was ameliorated in both LH groups, especially in the lower dose. LH-1x and -5x treatments partially recovered control-like values for the percentage of total abnormal ovulated MII oocytes (Control: 48.6 ± 16.5 %, ChT+LH-1x: 47.1 ± 15.3 %, ChT+LH-5x: 67.9 ± 27.3 %) and 2-cell embryos (Control: 36.5 ± 10.4 %, ChT+LH-1x: 33.3 ± 11.5 %, ChT+LH-5x: 41.7 ± 14.4 %).

Table XI. Number of morphologically normal and abnormal MII oocytes, and early cleavage stage embryos collected from stimulated mice after six consecutive breeding rounds.

Group (n = 4)	MII oocytes (n)			2-cell embryos (n)		
	Morphol. Normal	Morphol. Abnormal	Total	Morphol. Normal	Morphol. Abnormal	Total
Control	2.5 ± 2.1	3.3 ± 1.5	11.3 ± 3.9	3.5 ± 1.3	2.0 ± 0.8	5.5 ± 1.9
ChT	0	2.5 ± 1.7	4.0 ± 3.4[a]	0.3 ± 0.5[a]	1.3 ± 1.5	1.5 ± 1.9
ChT+LH-1x	1.3 ± 1.5	2.3 ± 2.6	7.3 ± 4.9	2.5 ± 1.7	1.3 ± 1.0	3.8 ± 2.5
ChT+LH-5x	0.5 ± 0.6	2.3 ± 1.0	5.3 ± 2.2	1.5 ± 1.3	1.0 ± 0.8	2.5 ± 1.9

Data expressed as Mean ± SD. Total number of 2-cell embryos was included in the total number of MII oocytes. [a]p-value <0.05 ChT group compared with control group. Morphol.: morphologically.

2. The effect of LH-mediated gonadoprotection in oocyte – GC communication

To understand how LH protection could improve the quality of MII oocytes derived from follicles exposed to chemotherapy at the primordial stage, we investigated whether LH might preserve the ability of these follicles to establish a proper bidirectional communication between the somatic and germ compartments during their growth. Therefore, cell junctions and oocyte-secreted growth factors were assessed at gene and protein levels in follicles measuring ≥100 µm that correspond to the secondary, late preantral, antral and preovulatory populations. Subsequently, communication was also visualized by immunofluorescence staining.

2.1. Follicle isolation yield

Chemotherapy administration induced a 2.1-fold reduction in the total number of isolated follicles ($p = 0.036$; Fig. 30A), affecting similarly to follicles measuring <100 µm (Control: 13.1 ± 3.2 follicles, ChT: 4.6 ± 1.7 follicles; $p = 0.036$) and ≥100 µm ($p = 0.036$; Fig. 30B-C). LH-treated ovaries showed similar values to control group for the total number of isolated follicles, preventing the chemotherapy-induced effects ($p = 0.032$). Although this LH improvement was observed in isolated follicles with both diameters, the smallest were significantly preserved (ChT+LH-1x: 8.6 ± 1.1 follicles; $p = 0.016$). These results suggest LH-treated ovaries contain a larger follicle pool than ChT group, with a relevant presence of the most undifferentiated developmental stages.

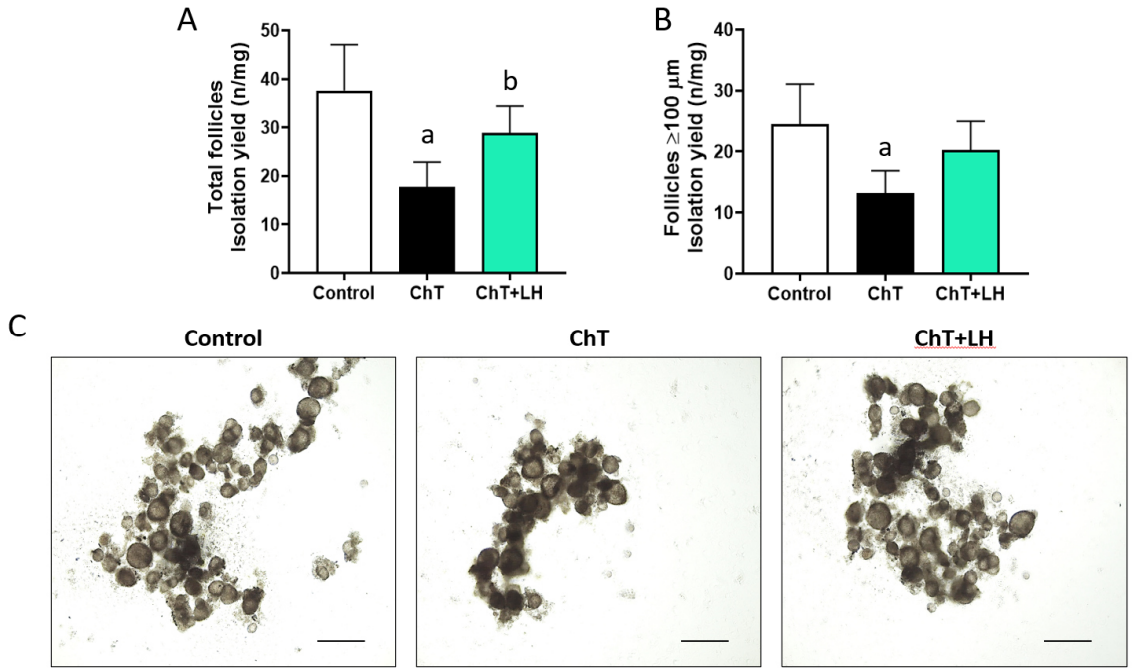

Figure 30. Follicle isolation from ovaries collected 30 days after treatments. *Isolation yield for (A) the total number of isolated follicles, (B) the follicles measuring ≥100 µm to represent the secondary, late preantral and antral stages. (C) Representative images of follicles with a diameter ≥100 µm isolated from each experimental group (5x magnification; scale bars: 500 µm). LH treatment reversed preserved the follicular pool depleted by chemotherapy. Bar charts show means and SD for each experimental group (n = 3 mice for control group while n = 5 mice for ChT and ChT+LH-1x groups). [a]p-value < 0.05 vs. control group; [b]p-value < 0.05 vs. ChT group.*

2.2. Expression of cell junctions between oocytes and GC

The expression of genes encoding for key factors in oocytes – GC junctions was assessed by RT-qPCR in FOL. Results showed an overall downregulation pattern in ChT samples for all genes (Fig. 31A), which indicated that chemotherapy administration might reduce the follicular ability to establish gap, adherens and tight junctions. This alteration was reverted on LH-treated samples by maintaining the expression of all analyzed genes similar to controls.

Given that these factors play essential roles in oocytes – GC or GC – GC interactions, OO and GC were also analyzed. A global downregulation similar to FOL samples was observed, where the expression of all genes was reduced in OO (Fig. 31B) and GC (Fig. 31C) of ChT group. LH treatment reverted the chemotherapy effects increasing the expression of all genes up to control-like values for most of them. Expression of *E-Cad* was not detected in GC of any experimental group.

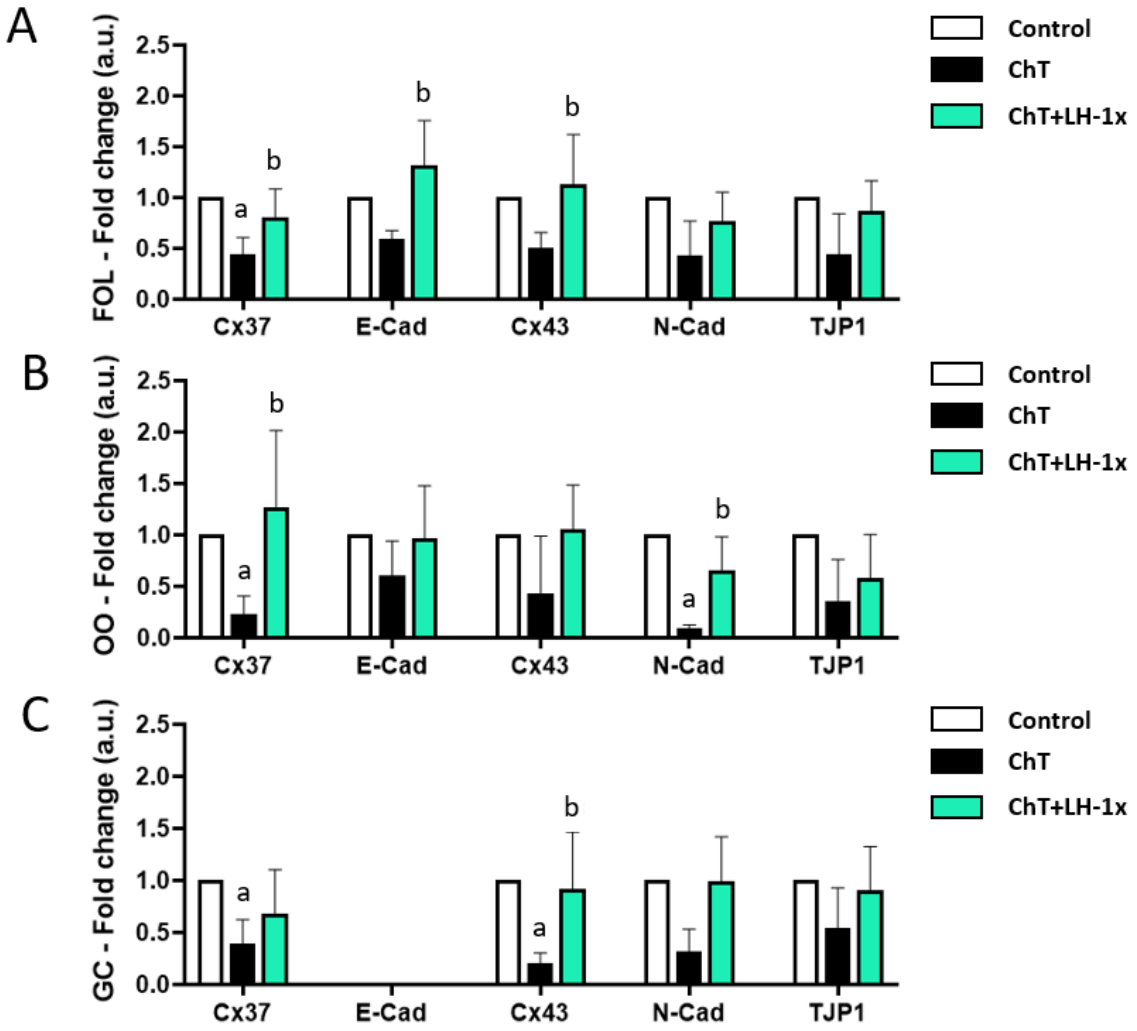

Figure 31. Assessment of GAP and tight junctions established between oocytes and GC, and between GC at the gene level. *Analysis of mRNA transcription levels for Cx37, E-Cad, Cx43, N-Cad and TJP1 in (A) FOL isolated from ovaries collected 30 days after treatments, in (B) OO and in (C) GC obtained from isolated follicles measuring ≥ 100 µm. LH treatment restored the chemotherapy-induced downregulation in FOL, OO and GC up to control-like values for all assessed genes. Expression values were normalized to those of the control group and were expressed as fold change. Bar charts show means and SD for each experimental group. Samples from n = 3 mice for control group and n = 5 mice for ChT and ChT+LH-1x groups were analyzed.* [a]*p-value < 0.05 vs. control group;* [b]*p-value < 0.05 vs. ChT group.*

Subsequently, these findings were validated by assessing the protein expression of differentially expressed factors by WB. This analysis confirmed a noteworthy reduction of Cx37, E-Cad and Cx43 levels on isolated FOL in ChT group, while LH administration blunted this effect (Fig. 32A). Given that these factors are predominantly expressed by one specific follicular compartment (oocytes or GC), Cx37 and E-Cad were further analyzed in OO (Fig. 32B), and Cx43 in GC (Fig.

32C). We found that LH counteracted the chemotherapy-induced decrease in protein expression, restoring the values up to control-like levels.

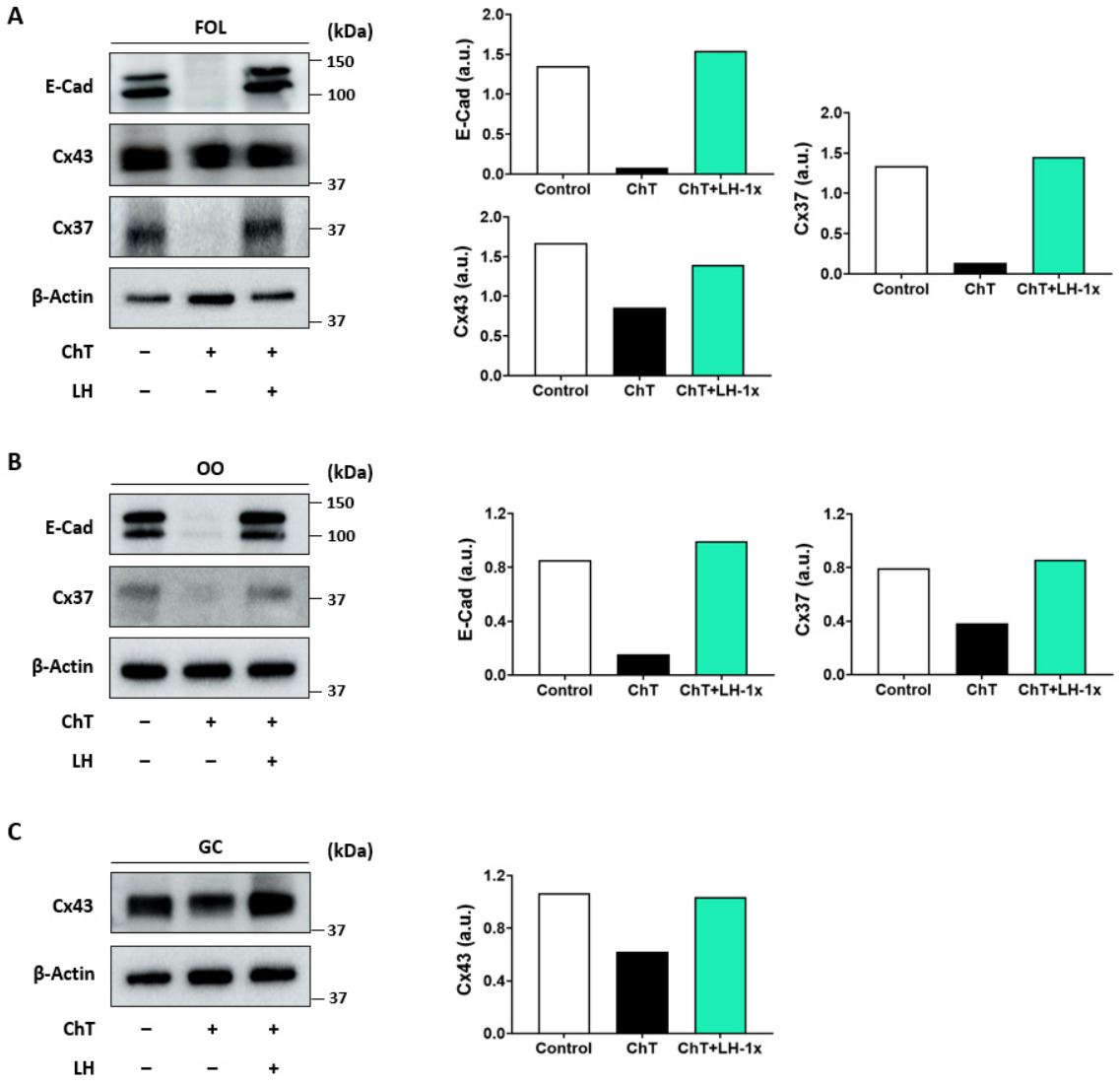

Figure 32. Protein expression of factors related to cell junctions. *Representative WB and densitometry analysis showing the levels of Cx37, E-Cad and Cx43 in (A) FOL, (B) OO, and (C) GC retrieved from follicles with a diameter ≥100 µm. Chemotherapy caused a significant reduction of protein levels and LH treatment reversed this effect up to values similar to controls. Pooled samples from n = 3 mice for control group and n = 5 mice for ChT and ChT+LH-1x groups were analyzed.*

2.3. Immunolocalization of cell junctions in follicles

Oocyte – GC interactions were visualized by fluorescence staining for Cx37, E-Cad and Cx43. Cx37 expression was observed in GC and oocytes of each follicular stage with a stronger signal in the germ compartment, where Cx37 was detected in the ooplasm and nucleus (Fig. 33A-B).

However, Cx37 expression in follicles was reduced in the ChT group compared to controls (p = 0.036; Fig. 33C). This alteration particularly appeared in the primary-secondary transition, with control-like intensity in the primary population, but reduced values beyond the secondary stage (Fig. 33D). On the other side, follicles in ChT+LH-1x group showed a fluorescence intensity similar to control samples in all follicular populations, thereby enhancing the Cx37 signal compared to ChT group with statistically significant differences from secondary to antral stages.

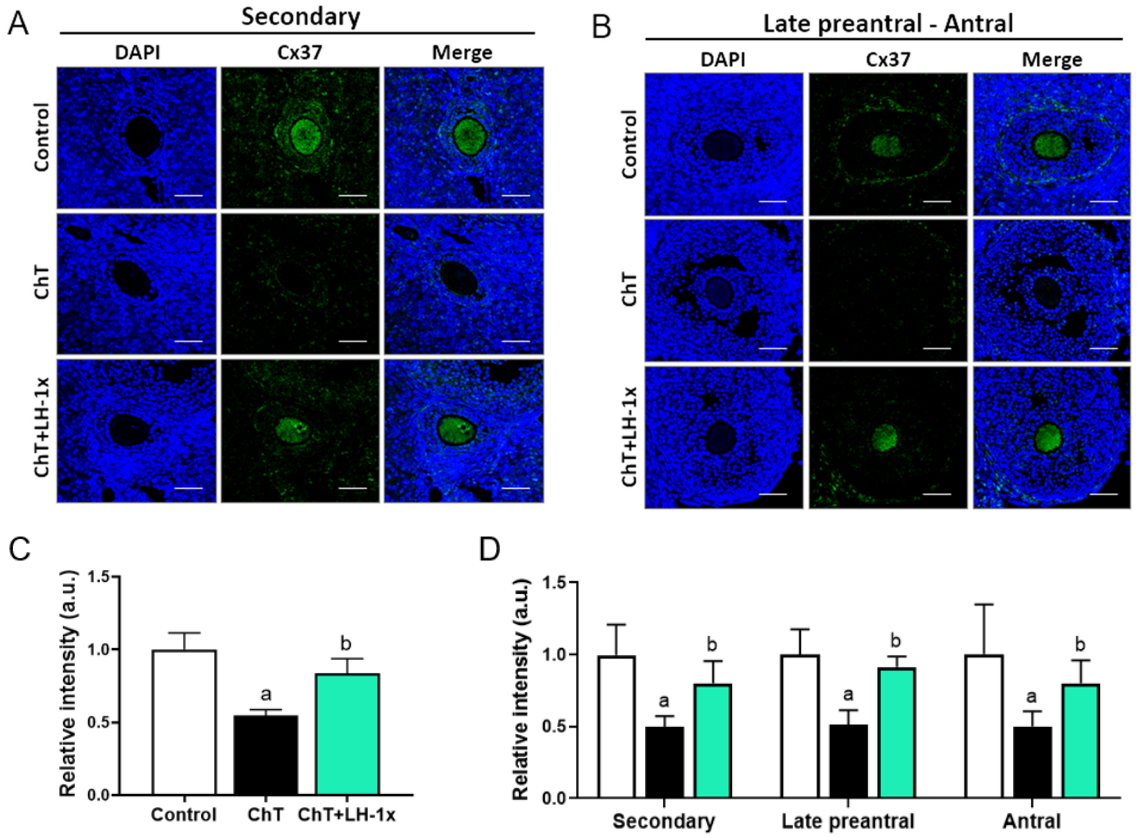

Figure 33. Immunofluorescence staining of connexin 37 (Cx37) involved in cell junctions. *Representative confocal images showing blue signal for nucleus (DAPI) and green signal for Cx37 in (A) secondary, and (B) late preantral and/or antral follicles. Scale bars: 50 µm. (C) Quantitative analysis of fluorescence intensity for Cx37 protein in all follicles analyzed and in (D) secondary to antral developmental stages. LH treatment prevented the significant chemotherapy-induced reduction of Cx37 signal beyond the secondary stage. Bar charts show means and SD for each experimental group. Samples from n = 3 mice for control group and n = 5 mice for ChT and ChT+LH-1x groups were analyzed. [a]p-value < 0.05 vs. control group; [b]p-value < 0.05 vs. ChT group.*

E-Cad expression was only detected in oocytes, where this factor was restricted to the outermost cell boundaries in all follicle populations. The intensity of E-Cad was similar among developmental stages (Fig. 34A-B). However, ChT-follicles showed a 2-fold reduction of fluorescence (p = 0.035;

Fig. 34C) that affected to growing populations excluding the primary stage (Fig. 34D). By contrast, LH-treated follicles exhibited a pattern expression for E-Cad similar to controls, thereby increasing the signal found in ChT group from the secondary stage.

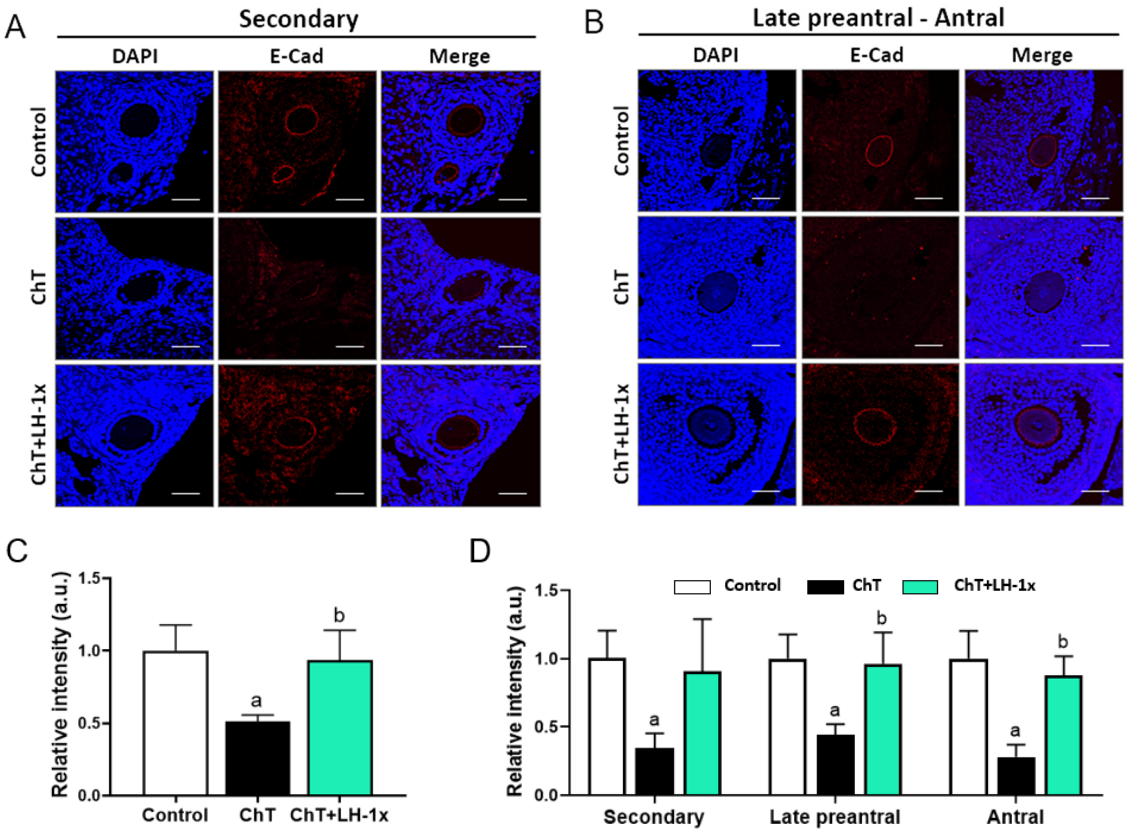

Figure 34. Immunofluorescence staining of epithelial cadherin (E-Cad) involved in cell junctions. *Representative confocal images showing blue signal for nucleus (DAPI) and red signal for E-Cad in (A) secondary, and (B) late preantral and/or antral follicles. Scale bars: 50 µm. (C) Quantitative analysis of fluorescence intensity for E-Cad protein in all follicles analyzed and in (D) each developmental stage. LH treatment prevented the significant chemotherapy-induced reduction of E-Cad signal beyond the secondary stage. Bar charts show means and SD for each experimental group. Samples from n = 3 mice for control group and n = 5 mice for ChT and ChT+LH-1x groups were analyzed. [a]p-value < 0.05 vs. control group; [b]p-value < 0.05 vs. ChT group.*

In addition, although Cx43 expression was visualized in the stroma, this factor was predominantly detected in GC, where it seemed to be differentially expressed depending on the developmental stage. So that primary follicles showed a weak fluorescence restricted to few GC, while secondary follicles contained a strong Cx43-signal by many GC (Fig. 35A), and late preantral to antral follicles exhibited the strongest intensity that was expressed by most GC (Fig. 35B). It is important to note that Cx43 was also found with a strong signal on the outermost edge of ooplasm from late

preantral population. Regarding treatment effects, we noticed a reduction of Cx43 signal on ChT-follicles (p = 0.036; Fig. 35C), which significantly affected to secondary – antral follicles (Fig. 35D). On the other side, LH treatment preserved Cx43-fluorescence values akin to controls among all follicles, showing a notable improvement of Cx43 expression compared to ChT group beyond the secondary stage.

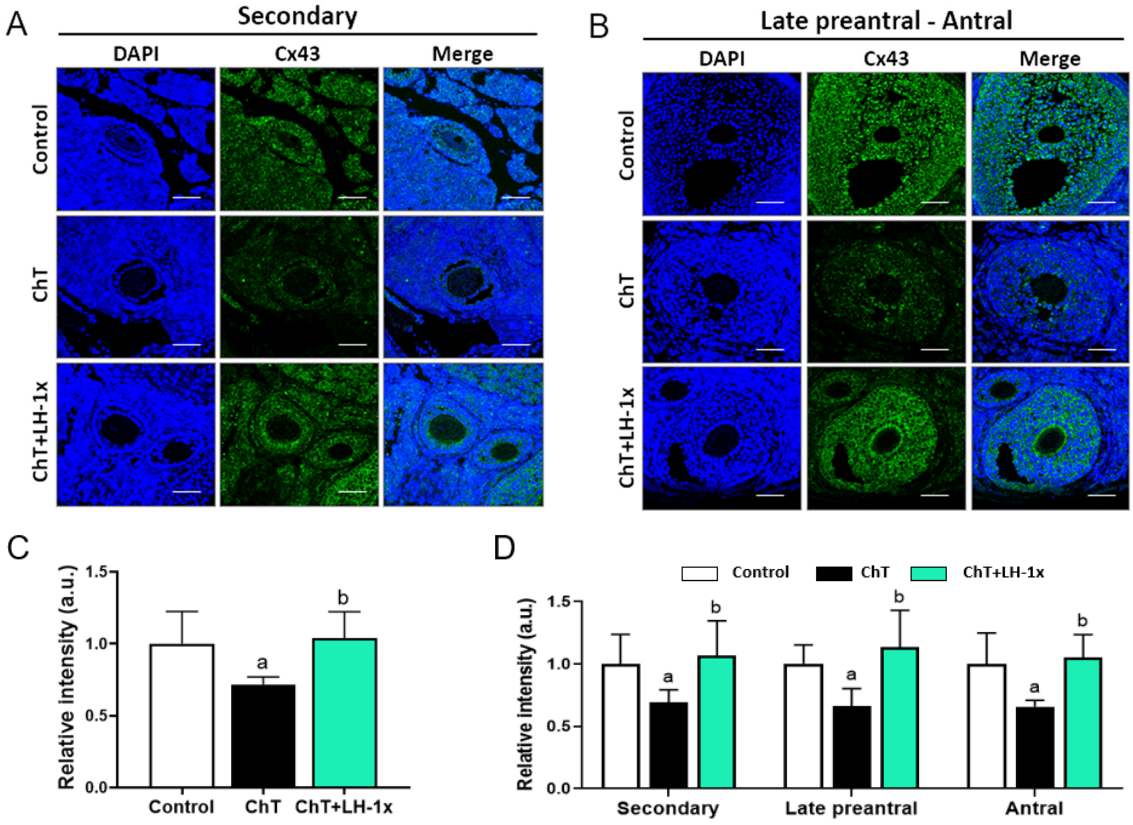

Figure 35. Immunofluorescence staining of connexin 43 (Cx43) involved in cell junctions. *Representative confocal images showing blue signal for nucleus (DAPI) and green signal for Cx43 in (A) secondary, and (B) late preantral and/or antral follicles. Scale bars: 50 µm. (C) Quantitative analysis of fluorescence intensity for Cx43 protein in all follicles analyzed and (D) each developmental stage. LH treatment prevented the significant chemotherapy-induced reduction of Cx43 signal beyond the secondary stage. Bar charts show means and SD for each experimental group. Samples from n = 3 mice for control group and n = 5 mice for ChT and ChT+LH-1x groups were analyzed. [a]p-value < 0.05 vs. control group; [b]p-value < 0.05 vs. ChT group.*

2.4. Expression of oocyte-secreted factors exchanged between oocytes and GC

Once we found an enhancement of cell interactions between oocytes and GC due to LH, we further investigated the oocyte – GC communication by analyzing the expression of genes encoding for two growth factors (*GDF9* and *BMP15*) exchanged between oocytes and GC along folliculogenesis, and their specific receptors (*BMPR2, ALK4, ALK5,* and *ALK6*), in FOL. We found

that LH prevented the gene downregulation detected in the ChT group for five out of six genes, restoring expression levels similar to controls (Fig. 36A). This LH improvement significantly benefitted to *GDF9* (p = 0.008) and *ALK5* (p = 0.016) genes. Subsequently, analysis of OO and GC revealed that, likewise on FOL assessment, chemotherapy caused an overall gene downregulation of analyzed factors (Fig. 36B-C), which similarly affected to both follicular compartments. By contrast, LH-treated samples showed an expression pattern akin to controls, with a significant increase compared to ChT group for *GDF9* (p = 0.008) and *ALK5* (p = 0.029) in OO, and for *GDF9* (p = 0.016), *BMP15* (p = 0.016), *BMPR2* (p = 0.008) and *ALK5* (p = 0.029) in GC.

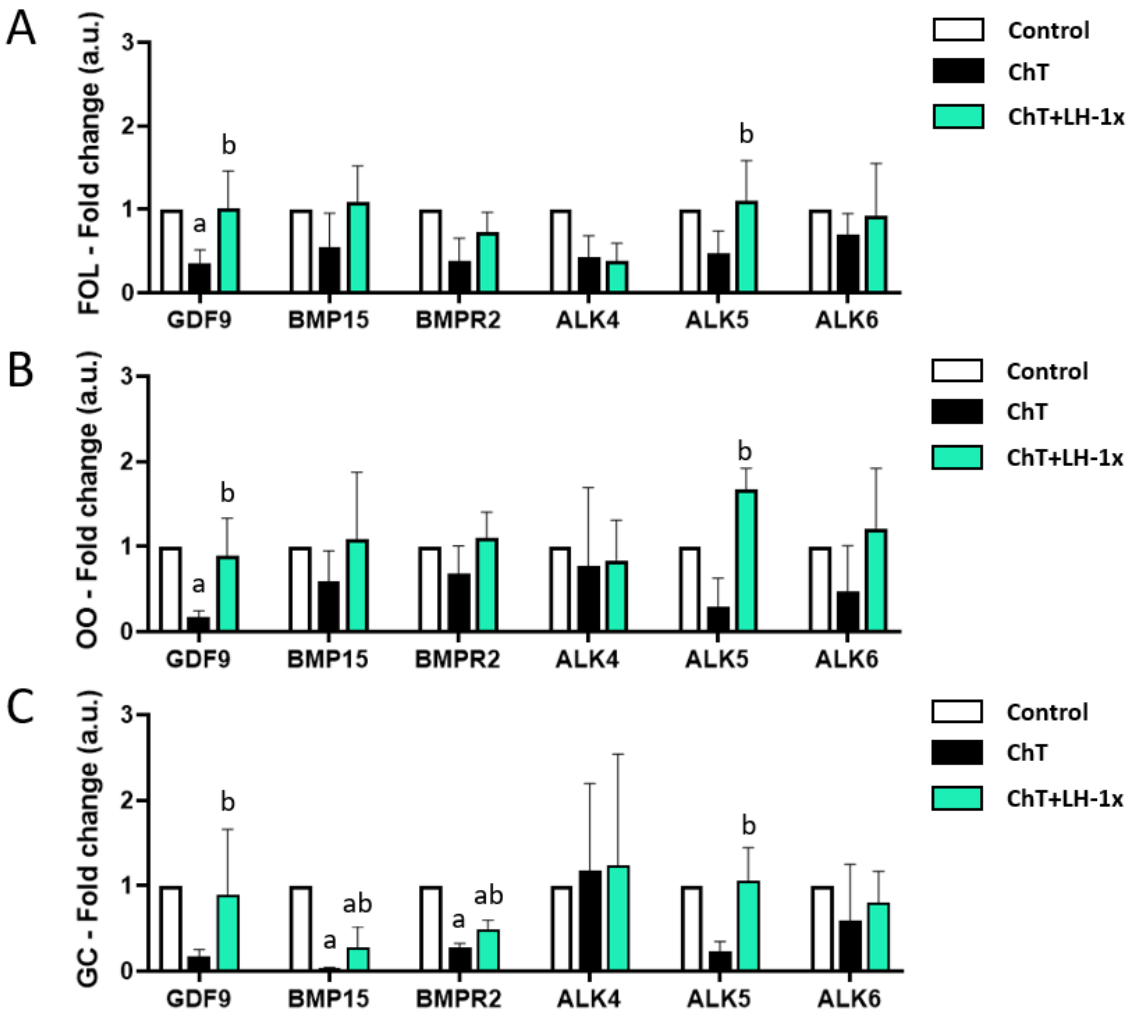

Figure 36. Analysis of oocyte-secreted factors exchanged between oocytes and GC during folliculogenesis at the gene level. *The expression of mRNA transcription levels for GDF9, BMP15, BMPR2, ALK4, ALK5 and ALK6 was evaluated in (A) FOL isolated from ovaries collected 30 days after treatments, in (B) OO and in (C) GC obtained from isolated follicles measuring ≥ 100 µm. The chemotherapy group showed an overall downregulation pattern in FOL, OO and GC compared to the control group, while LH treatment preserved the gene expression levels akin to control group for most of the analyzed genes. Expression values were normalized to those of the*

control group and were expressed as fold change. Bar charts show means and SD for each experimental group. Samples from n = 3 mice for control group and n = 5 mice for ChT and ChT+LH-1x groups were analyzed. [a]p-value < 0.05 vs. control group; [b]p-value < 0.05 vs. ChT group.

These GDF9 and BMP15 expression changes were subsequently validated at the protein level. A 4-fold and 3-fold reductions for GDF9 and BMP15, respectively, were observed in ChT FOL, while LH treatment restored control-like values (Fig. 37A). When both molecules were assessed on OO, a similar pattern to FOL was observed. Thereby, LH reverted the chemotherapy-induced reduction of GDF9 and BMP15 (Fig. 37B).

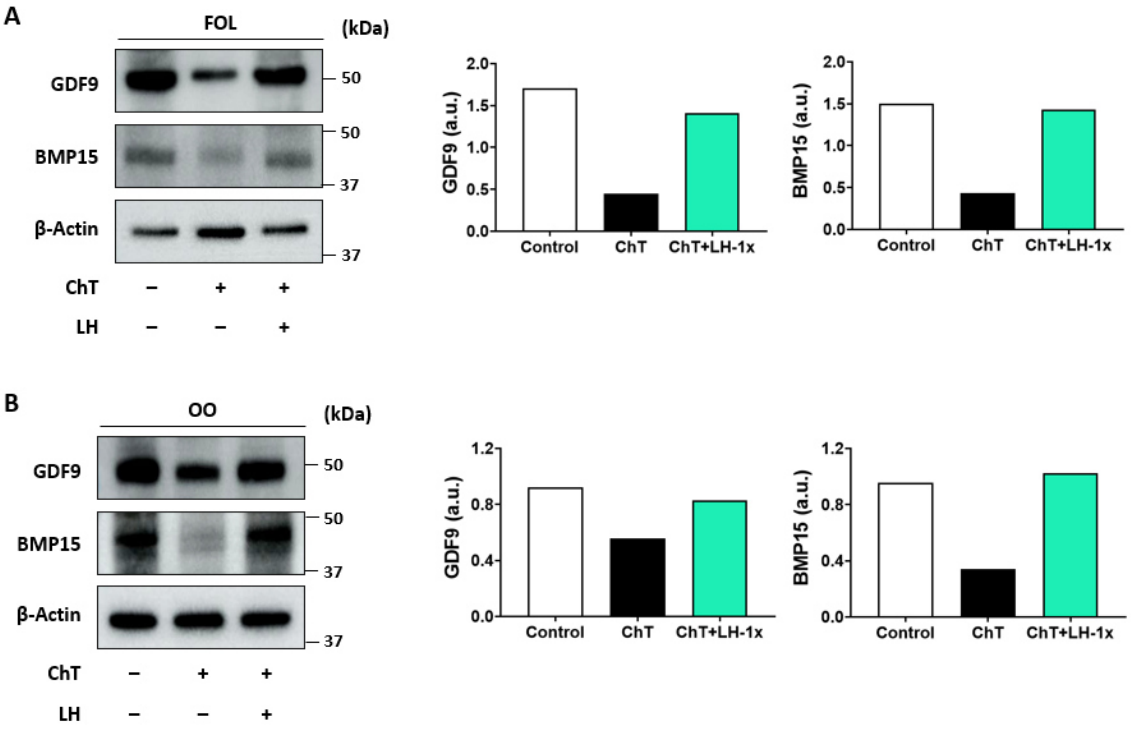

Figure 37. Protein expression of oocyte-secreted factors. *(A) Representative WB and densitometry analysis showing the levels of GDF9 and BMP15 in (A) FOL and (B) OO retrieved from follicles measuring ≥100 µm. LH prevented the chemotherapy-induced reduction in the levels of both proteins and restored the expression of both molecules until similar levels observed in controls. Pooled samples from n = 3 mice for control group and n = 5 mice for ChT and ChT+LH-1x groups were analyzed.*

2.5. Immunolocalization of oocyte-secreted factors in follicles

The oocyte-secreted factors, GDF9 and BMP15, were visualized in all follicle populations following a similar expression pattern due to specific signal was mainly detected on the ooplasm,

albeit some GC also expressed both molecules (Fig. 38A-B). No differences were found among follicular stages when signal intensity was quantified.

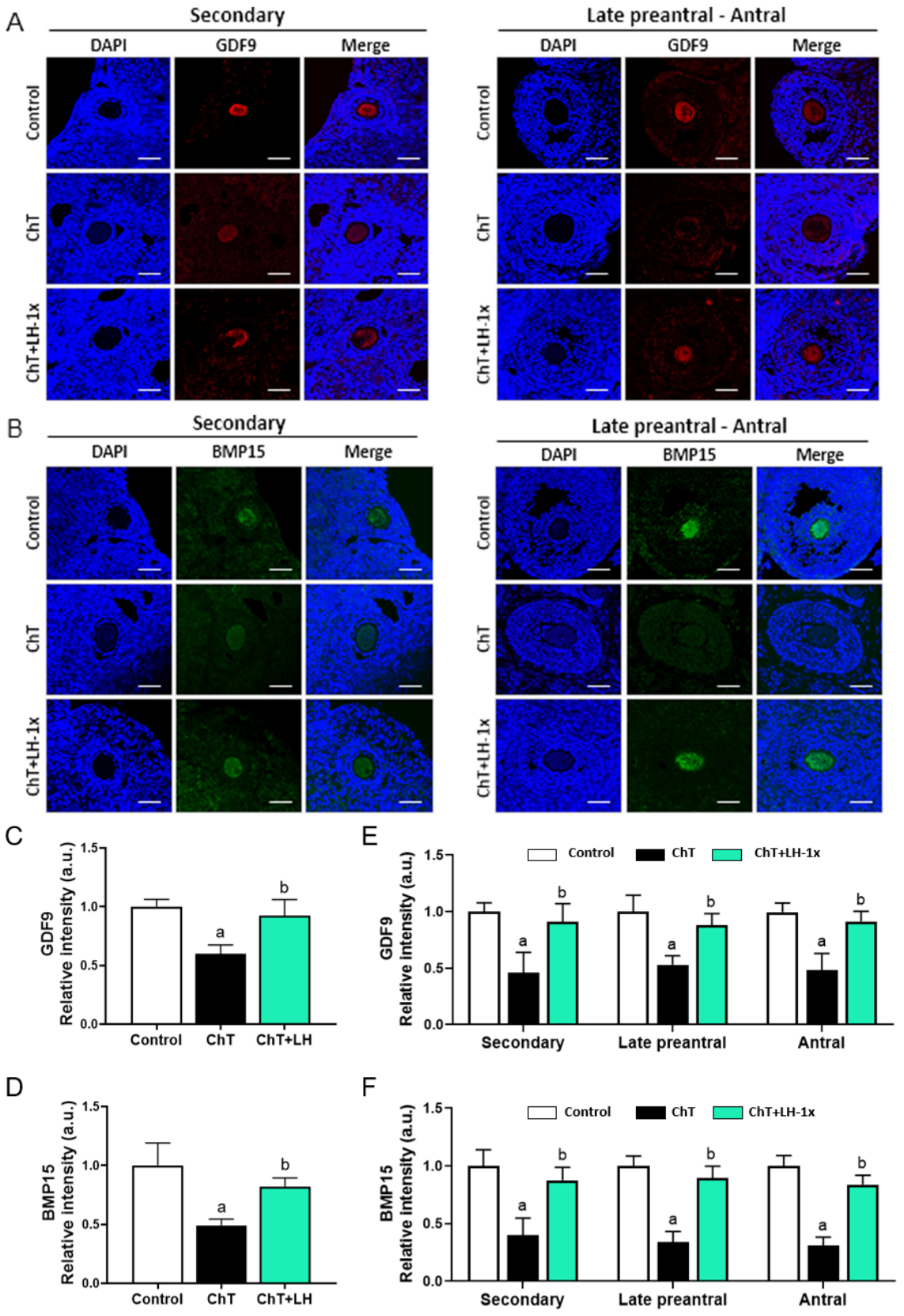

Figure 38. Immunofluorescence staining of growth differentiation factor-9 (GDF9) and bone morphogenetic protein 15 (BMP15) as oocyte-secreted factors. *Representative*

confocal images showing blue signal for nucleus (DAPI) and (A) red signal for GDF9 (B) or green signal for BMP15 in secondary, and late preantral and/or antral follicles. Scale bars: 50 μm. Quantitative analysis of fluorescence intensity for (C) GDF9 and (D) BMP15 proteins in all follicles analyzed, as well as in each developmental stage for (E) GDF9 and (F) BMP15 factors. LH treatment prevented the significant chemotherapy-induced reduction of fluorescence for both oocyte-secreted factors from the secondary stage, achieving values similar to controls. Bar charts show means and SD for each experimental group. Samples from n = 3 mice for control group and n = 5 mice for ChT and ChT+LH-1x groups were analyzed. [a]p-value < 0.05 vs. control group; [b]p-value < 0.05 vs. ChT group.

However, a 1.7-fold (p = 0.036) and more than 2-fold (p = 0.018) reductions were observed in the ChT samples for GDF9 and BMP15, respectively (Fig. 38C-D). These alterations for both factors were similarly detected from the secondary population in ChT group (Fig. 38E-F). On the other side, LH-treated follicles showed a fluorescence intensity for GDF9 and BMP15 akin to control group in all follicle populations that avoided the chemotherapy-induced effects (p = 0.008 and p = 0.008, respectively). Indeed, a significant increase in GDF9 and BMP15 signal intensities was found in ChT+LH-1x group compared to ChT for all growing populations, excluding the primary.

3. The protective mechanisms of LH

Once the efficacy of LH treatment to preserve the female fertility of mice against alkylating chemotherapy was established, we investigated the early ovarian response to LH by assessing damage and repairing systems 12 and 24 hours after chemotherapy and LH administrations.

3.1. DNA damage and apoptosis

Twelve hours after chemotherapy treatment, DSBs were identified by γH2AX staining in oocytes at all follicular stages. All experimental groups receiving chemotherapy showed significantly higher percentages of oocytes with γH2AX foci than controls (p = 0.034 in all cases; Fig. 39A-B), but both the high and low dose LH-treatments had significantly lower γH2AX-positive oocytes compared to ChT samples (p = 0.021 and p = 0.020, respectively). Growing follicles were the most affected population showing the highest percentage of γH2AX-positive oocytes after chemotherapy (Control: 22.4 ± 1.8 %, ChT: 69.4 ± 13.6 %, p = 0.034). Yet, both LH dosages significantly reduced the chemotherapy-induced DNA damage (ChT+LH-1x: 45.7 ± 4.8 %, ChT+LH-5x: 39.4 ± 5.7 %; p = 0.021 in both cases).

In addition, the percentage of apoptotic follicles 12 hours after chemotherapy administration by TUNEL assay showed an acute increase in the rate of apoptosis in the ChT (p = 0.034) and ChT+LH-1x (p = 0.034) samples compared to controls (Fig. 39C-D). However, ChT+LH-5x group showed similar levels of apoptosis as controls. LH treatment protected ovaries from ChT-induced apoptosis in a dose-dependent manner, as showed by the 1.6- and 6.7-fold reduction of apoptotic follicles in the ChT+LH-1x (p = 0.043) and ChT+LH-5x (p = 0.020) groups, respectively, when compared to ChT group. Growing follicles were the most susceptible population to apoptosis, but both the high and low doses of LH protected them from damage (Control: 2.0 ± 1.7 %, ChT: 10.3 ± 1.6 %, ChT+LH-1x: 5.6 ± 2.1 %, ChT+LH-5x: 1.5 ± 1.7 %), resulting in a significantly lower TUNEL signal in GC than that of the ChT group p = 0.020 and 0.021, respectively). TUNEL signal was not detected in oocytes from any experimental group.

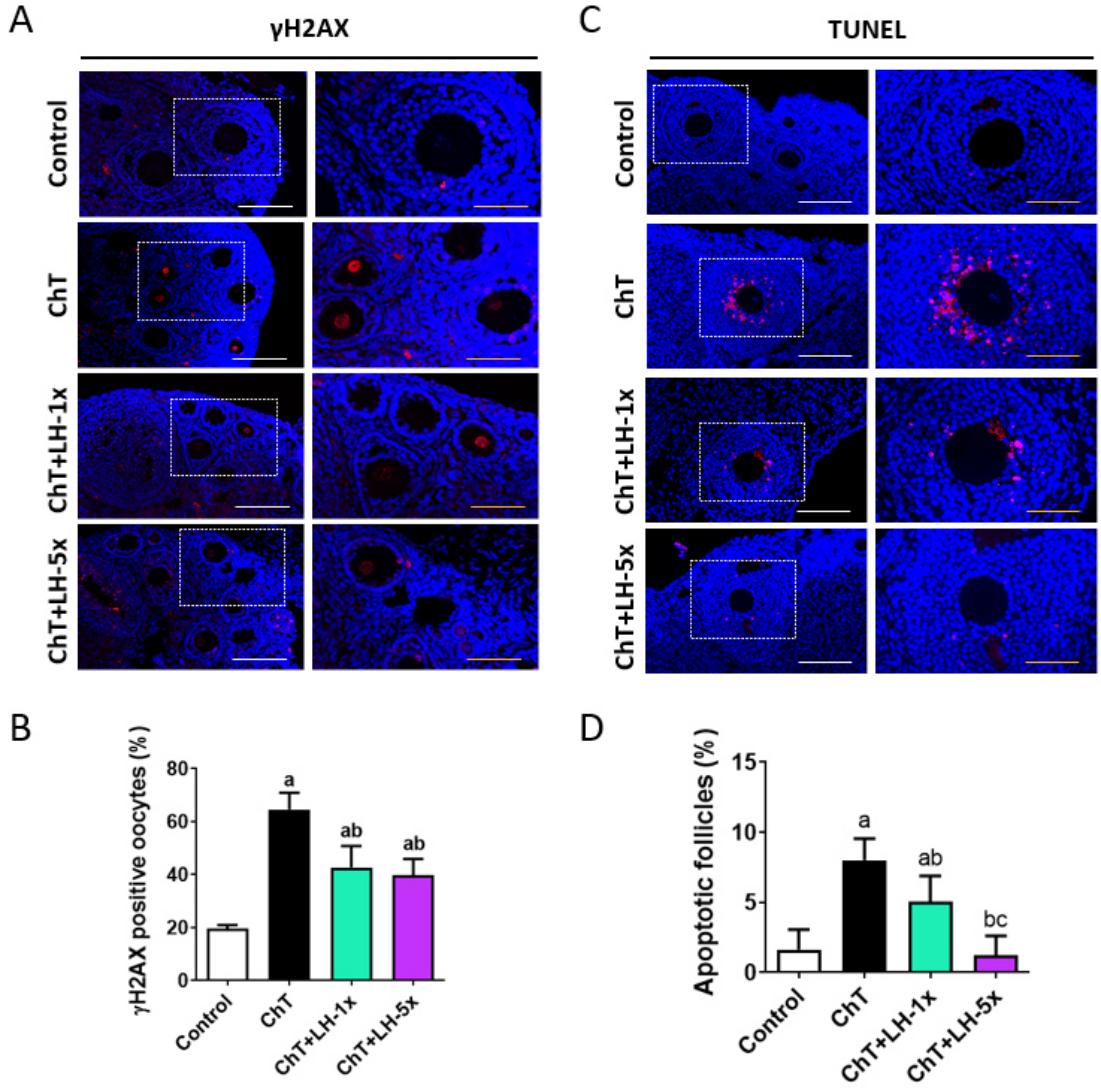

Figure 39. Follicular damage and apoptosis measured 12 hours after chemotherapy administration. *(A) Representative images showing immunofluorescence staining of γH2AX*

(red) to represent the nucleus with DSBs counterstained with DAPI (blue) in ovarian sections. Pictures on the left column were captured with 20x magnification (white scale bars: 100 μm) while those on the right with 40x magnification (yellow scale bars: 50 μm). (B) Percentage of follicles with DNA damaged oocytes (positive γH2AX signal). Both LH treatments decreased the percentage of follicles with DSBs with statistically significant differences compared to ChT samples. (C) TUNEL assay showing apoptotic cells (red) and nucleus (blue) in ovarian sections. Magnifications and scale bars are as described in A. (D) Percentage of apoptotic follicles (positive TUNEL signal). LH prevented the chemotherapy-induced apoptosis in follicles with statistically significant differences. The high-LH dose resulted the most effective. Bar charts show means and SD for each experimental group (n = 3 mice for control group while n = 4 mice for ChT, ChT+LH-1x and ChT+LH-5x groups). [a]p-value < 0.05 vs. control group; [b]p-value < 0.05 vs. ChT group; [c]p-value < 0.05 vs. ChT+LH-1x group.

3.2. Ovotoxicity

Ovarian damage was also assessed by determining γH2AX, Bcl2, CC3, pERK1/2 and ERK1/2 protein expression by WB. Indeed, a 2- and 1.5-fold increase for γH2AX protein levels was detected in the ChT group compared to control samples 12 and 24 hours after administrations, respectively, while both LH treatments kept protein values akin to controls (Fig. 40A-B). Regarding apoptosis, the ChT group exhibited a reduction in the Bcl2 / CC3 apoptosis protein ratio (Fig. 40C-D) at 24-hour time-point, indicating a promotion of apoptotic signals. Nevertheless, treatment with both high and low doses of LH restored this ratio to control-like levels. Likewise, chemotherapy increased ERK1/2 activation at both time-points (Fig. 40E-F), but LH treatments partially ameliorated this effect by reducing ERK1/2 phosphorylation.

3.3. DNA repair

Since cell damage and apoptosis decline through DNA repair mechanisms, we studied if LH could trigger repairing signals into the ovary in response to alkylating agents. Thus, by using WB we found that the high dose of LH prompted increased protein levels of the DNA DSB repair machinery ATM and Rad51, 12 and 24 hours after chemotherapy administration (Fig. 41A-B). Moreover, although a noteworthy activation of AKT protein was detected in ChT ovarian pools at 12 and 24 hours, both LH doses prevented this effect (Fig. 41C-D). Indeed, LH decreased the pAKT / AKT protein ratio to control-like values.

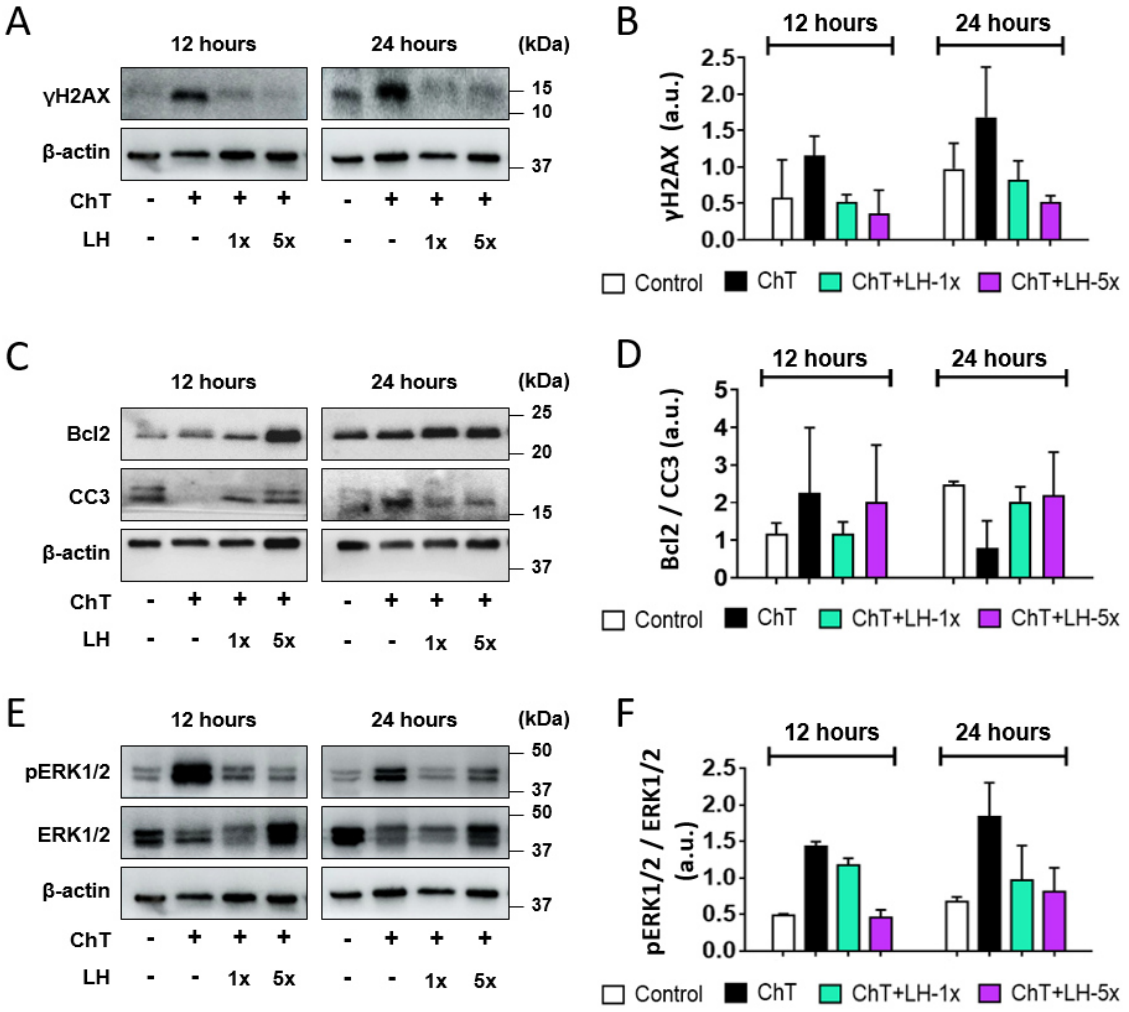

Figure 40. Ovarian damage and apoptosis assessed in ovarian lysates at 12 and 24 hours after chemotherapy administration. *(A) A representative WB for γH2AX and its (B) densitometric analysis. Both LH doses maintained the control-like levels for γH2AX preventing the increase observed in ChT group at both time-points. (C) A representative WB for the protein ratio established between the anti-apoptotic protein Bcl2 and the pro-apoptotic protein CC3, and their (D) densitometric analysis. LH treatments increased the Bcl2:CC3 ratio protecting the ovaries from chemotherapy-induced cell death at 24 hours. (E) A representative WB for the phosphorylated-ERK1/2 and ERK1/2 protein levels and their (F) densitometric analysis. Chemotherapy activated ERK1/2 signaling while both LH doses reduced this effect at 12 and 24 hours. Every WB was performed at least on two independent experiments from two pools of two ovaries each per group. Bar charts show means and SD for each experimental group.*

Furthermore, the expression of representing genes involved in key DNA repair pathways was analyzed by RT-qPCR to validate the LH mechanism. Our findings revealed that chemotherapy prompted increased mRNA transcription of DNA repair genes *Apex1, Msh6*, *Prkdc*, *Ercc3,* and *Rad51* at the 12-hour time-point, which were downregulated by 24 hours (Fig. 41E). However, ovaries from ChT+LH-1x treated mice showed an even more robust upregulation of DNA repair genes, with expression of 4 out of 5 such genes reaching levels higher than that seen with ChT

alone, and with *Rad51* overexpression being maintained to 24 hours. Unexpectedly, ChT+LH-5x ovaries showed an overall downregulation of all DNA repair genes at both time-points, excepting *Rad51* at 24 hours after treatment.

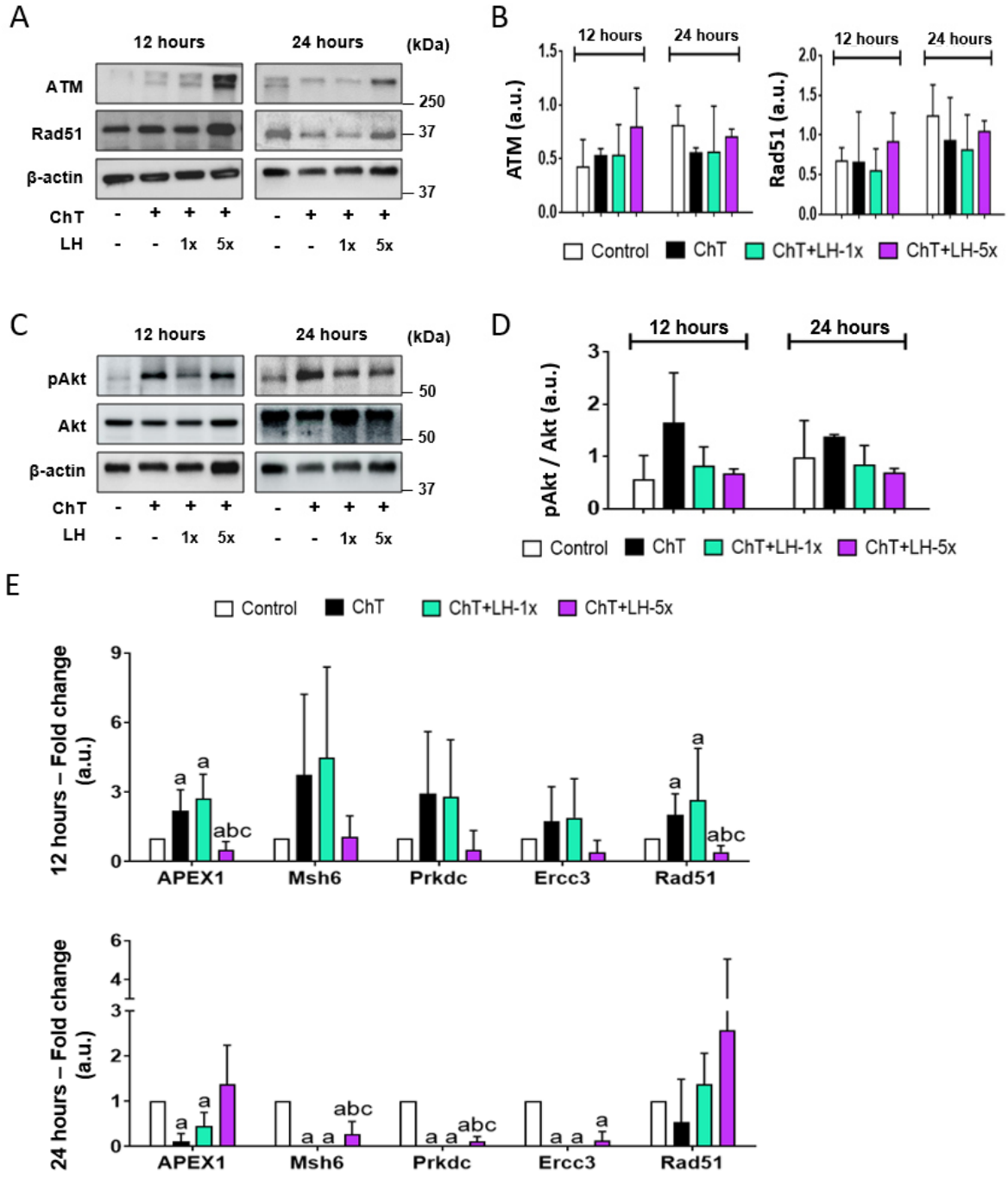

Figure 41. DNA repair signaling pathways measured in ovarian lysates at 12 and 24 hours after chemotherapy exposure. *(A) A representative WB for ATM and Rad51 proteins and their (B) densitometric analysis. LH-5x treated ovaries expressed higher levels of ATM and Rad51 than ChT-treated ovaries at both time-points. (C) A representative WB for phosphorylated-Akt and Akt proteins and their (D) densitometric analysis. Chemotherapy administration caused a notable increase of Akt activation at 12 and 24 hours, and co-treatment with LH blocked this effect showing levels similar to the control group. WBs were performed from at least two independent experiments from two pools of two ovaries each per group. (E) Analysis of mRNA transcription*

levels for the DNA repair genes Apex1, Msh6, Prkdc, Ercc3, and Rad51 in ovarian samples. At 12 hours, the expression level of all repair genes was higher in the ChT+LH-1x samples than in the ChT samples. At 24 h, all genes were downregulated in the ChT group while Rad51 was overexpressed in LH groups. Expression values were normalized to those of the control group and were expressed as fold change. Bar charts show means and SD for each experimental group. Three independent ovarian fragments per group and time-point were analyzed for qRT-PCR analysis. [a]p-value < 0.05 vs. control group; [b]p-value < 0.05 vs. ChT group; [c]p-value < 0.05 vs. ChT+LH-1x group.

4. LH effects on growing follicles exposed to alkylating agents

To validate LH-mediated gonadoprotection against chemotherapy, we used NOD-SCID mice assessing the LH effects on the already growing follicles. This strain represents a subfertile stage that may provide a suitable model to represent those patients receiving aggressive cancer therapies that compromise fertility, or already exhibiting reduced ovarian reserve, who might benefit from strategies based on growing follicle protection.

4.1. Macroscopic and histologic examination of ovaries

Macroscopic evaluation revealed that chemotherapy administration induced a 2.8- (p = 0.024) and 3.2-fold (p = 0.020) reduction in the ovarian / body weight of ChT and ChT+LH-1x groups, respectively, compared to controls (Fig. 42A). Ovarian size was also similarly decreased in ChT and ChT+LH-1x groups (p = 0.044 and 0.034, respectively; Fig. 42B-C).

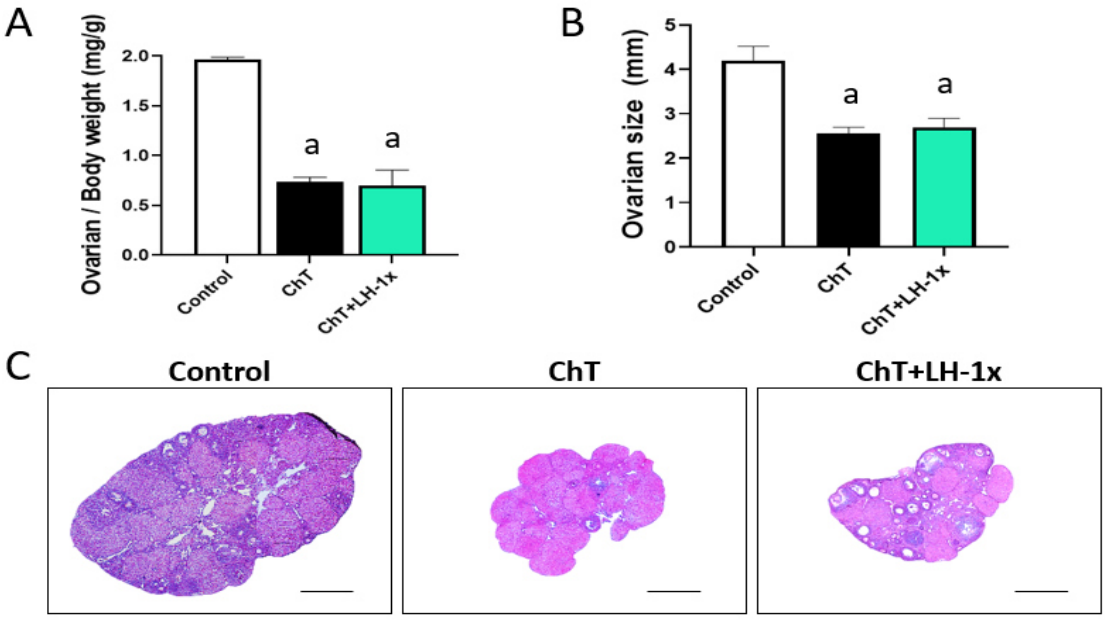

Figure 42. Macroscopic properties of ovaries in a subfertile NOD/SCID mouse model. *Mice were treated with alkylating agents with or without LH and seven days later underwent COS.*

(A) Ovarian weight normalized with bodyweight on euthanasia day. (B) Ovarian size assessed in the middle section established considering the total number of sections per ovary. (C) Representative images of ovarian sections stained with H&E (2.5x magnification; scale bars: 800 µm). ChT and ChT+LH-1x groups showed a significant reduction in the ovarian / body weight ratio and size compared to control group. Bar charts show means and SD for each experimental group (n = 3 mice for control and ChT groups while n = 4 mice for ChT+LH-1x group). [a]p-value < 0.05 vs. control group.

Stromal analysis of H&E-stained sections revealed a 3.5-fold increase in the stromal degeneration index of ChT samples compared to controls (p = 0.047; Fig. 43). Alterations identified as non-cellular regions or fibrotic areas were mainly detected in the ovarian center. On the contrary, the increase in the ChT+LH-1x group was only 1.9-fold when referred to controls (p = n.s.), indicating a significant reduction of the stromal adverse effects seen in the ChT samples (p = 0.047).

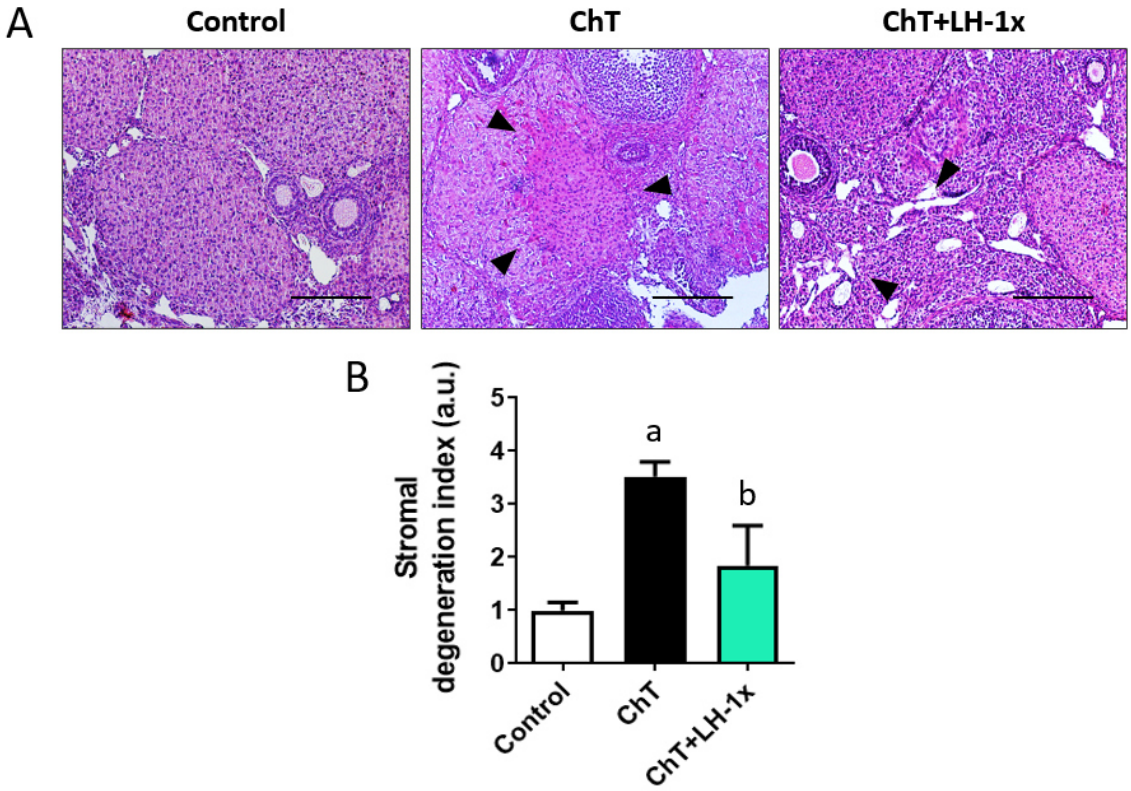

Figure 43. Evaluation of stromal degeneration in NOD/SCID mice. *(A) Representative sections stained with H&E showing the central area of ovarian stroma (10x magnification; scale bars: 200 µm). Black arrowheads indicated areas with less cell density and fibrosis. (B) Quantification of stromal degeneration index. Chemotherapy degenerated the ovarian stroma causing architecture disruption and fibrosis. LH-treated samples showed a reduction of this effect, detecting statistically significant differences with ChT samples. Bar chart shows means and SD for each experimental group (n = 3 mice for control and ChT groups while n = 4 mice for ChT+LH-1x group). [a]p-value < 0.05 vs. control group; [b]p-value < 0.05 vs. ChT group.*

4.2. Follicle endowment

NOD-SCID mice exhibited a massive follicle depletion following chemotherapy, with a 10-fold decrease in the total follicle number ($p = 0.047$; Fig. 44A) across all developmental stages (Fig. 44B). Primordial and primary populations were almost completely depleted with 96.5 % ($p = 0.036$) and 88.4 % ($p = 0.034$) reduction, respectively, compared to controls (Fig. 44C). Nevertheless, in the ChT+LH-1x group despite the observed follicle loss ($p = 0.034$), ovaries contained 31.2 % more follicles than the ChT ones. This LH protection especially benefited to primordial and primary populations, finding 83.2 % ($p = 0.034$) and 48.4 % ($p = 0.032$) more follicles, respectively, than that from ChT samples. The number of secondary, late preantral, antral and preovulatory was similar between both groups. Therefore, the percentage of quiescent follicles in ChT ovaries was reduced compared to controls ($p = 0.047$; Fig. 44D), while LH treatment blunted this chemotherapy-induced effect ($p = 0.034$) detecting control-like values in LH-treated samples.

Moreover, the number of morphologically abnormal follicles raised following chemotherapy administration with a significant increase in in both ChT and ChT+LH-1x ovaries compared to controls ($p = 0.047$ and $p = 0.034$, respectively; Fig. 44E). Abnormalities mostly affected to secondary follicles, being the ooplasm vacuolization the most frequent alteration (ChT: 52.6 ± 5.1 %, ChT+LH-1x: 47.6 ± 16.3 %; Fig. 44F).

4.3. Follicular damage

Follicular status was studied by measuring DNA damage and apoptosis on oocytes and GC by immunofluorescence. The ChT samples had more oocytes with γH2AX foci (Fig. 45A) and TUNEL-positive follicles than controls ($p = 0.047$; Fig. 45B-C). However, LH treatment resulted in a lower percentage of DNA-damaged oocytes and a significant reduction in the percentage of apoptotic follicles compared to ChT group ($p = 0.034$), being similar to control-like levels.

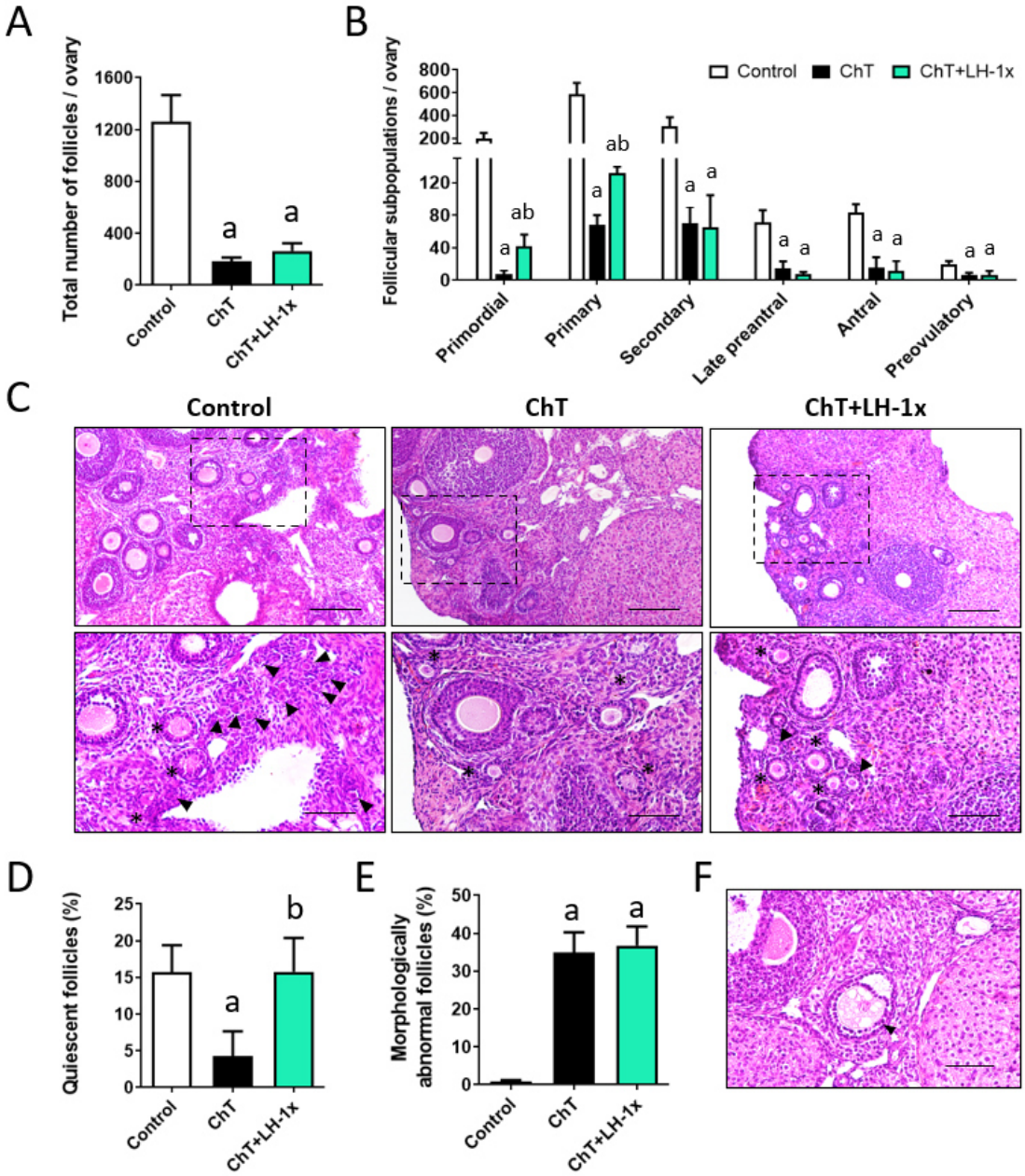

Figure 44. Assessment of ovarian reserve, follicle endowment, and morphologically follicular abnormalities in NOD/SCID ovaries. *(A) Total follicle numbers per ovary and (B) populations according to their developmental stage. LH-treated ovaries contained more follicles than ChT samples. This LH protection was most appreciable in the most undifferentiated populations of primordial and primary follicles. (C) Representative images stained with H&E of ovarian sections (10x magnification; scale bars: 200 µm) and a high magnification of the boxed regions (20x magnification; scale bars: 100 µm) showing primordial (black arrowhead) and primary (black asterisks) follicles. (D) Percentage of quiescent follicles detected in each experimental group. LH treatment preserved the percentage of quiescent follicles preventing the depletion observed in ChT ovaries. (E) Percentage of follicles presenting morphological abnormalities on oocyte and/or GC in ovaries collected 7 days after treatments. Chemotherapy increased the rate of morphologically abnormal follicles compared to control group and LH treatment was unable to reverse this effect. (F) H&E staining showing a ChT-follicle with multivacuolated ooplasm to represent the most common morphological abnormality detected in follicles (20x magnification; scale bars: 100 µm). Bar charts show means and SD for each experimental group (n = 3 mice for control and ChT groups while n = 4 mice for ChT+LH-1x group).* [a]*p-value < 0.05 vs. control group;* [b]*p-value < 0.05 vs. ChT group.*

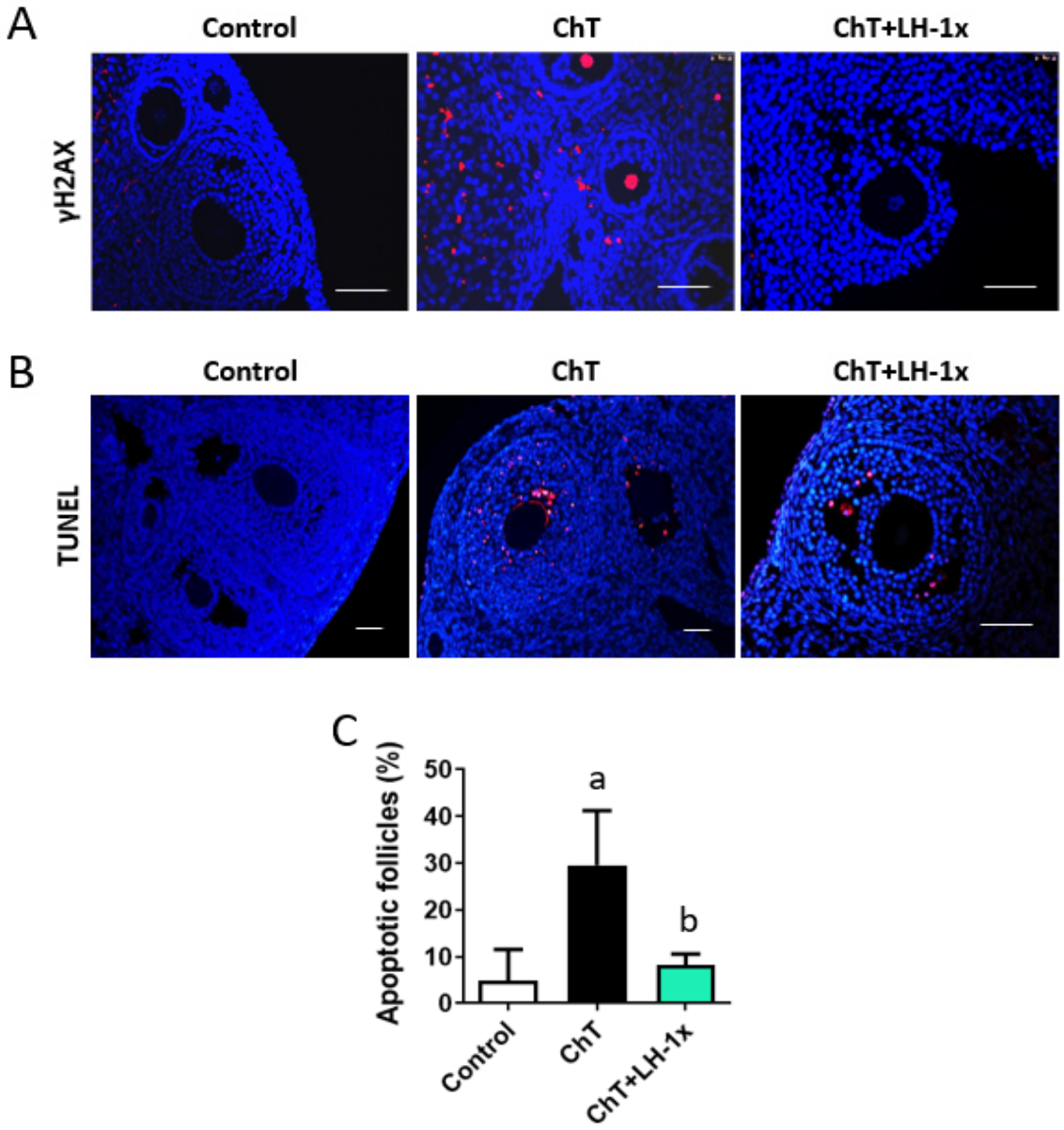

Figure 45. DNA damage and apoptosis in NOD/SCID follicles. *(A) Immunofluorescence of γH2AX protein (red) and nucleus (blue) showing follicular cells with DNA damage from all experimental groups. Scale bars: 100 µm. LH treatment protected the oocyte DNA against the DSBs induced by chemotherapy administration. (B) Representative images of TUNEL staining (red) counterstained with DAPI (blue). Scale bars: 50 µm. (C) Percentage of follicles with ≥ 20% TUNEL-positive cells. LH-treated samples showed a significant reduction of apoptotic follicles compared to ChT ovaries restoring control-like values. Bar chart shows means and SD for each experimental group (n = 3 mice for control and ChT groups while n = 4 mice for ChT+LH-1x group).* ^{a}*p-value < 0.05 vs. control group;* ^{b}*p-value < 0.05 vs. ChT group.*

4.4. Ovulation and early embryo cleavage

Chemotherapy induced a significant reduction in the number of MII oocytes (p = 0.036; Fig. 46A) and morphologically normal cleaved embryos (Fig. 46B) recovered after COS. By contrast, the

ChT+LH-1x animals ovulated similar numbers of MII oocytes as the control group, being 26.3 % higher than the ChT group. However, this protective effect was not seen for embryos.

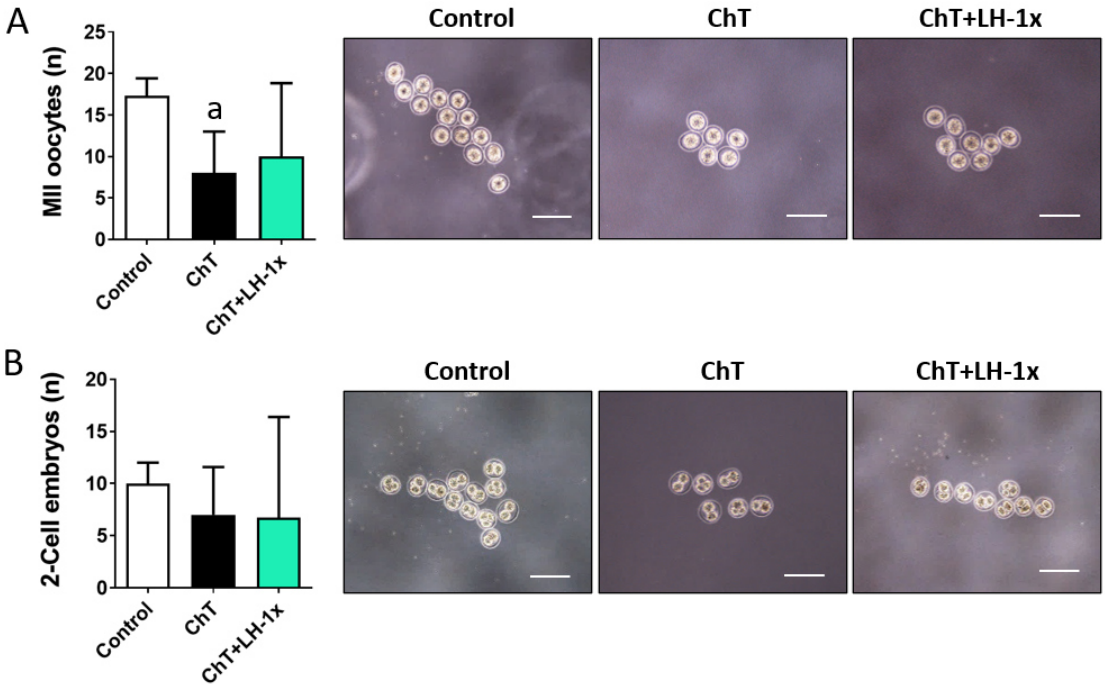

Figure 46. MII oocytes and embryos collected from NOD/SCID mice 7 days after treatments. *(A) Number of morphologically normal MII oocytes and representative images of cohorts rescued from ovarian stimulated mice (10x magnification; scale bars: 200 µm). LH-treated mice ovulated larger MII oocyte cohorts than ChT group. (B) Number of early cleavage embryos classified as good quality by morphological criteria, and representative images of cohorts collected from mated mice (10x magnification; scale bars: 200 µm). Although non-statistically significant differences were observed, both ChT and ChT+LH-1x groups showed a reduction in the number of 2-cell embryos compared to control group. Bar charts show means and SD for each experimental group (n = 3 mice for control and ChT groups while n = 4 mice for ChT+LH-1x group). [a]p-value < 0.05 vs. control group.*

4.5. Oocyte quality

The meiotic potential of recovered oocytes at the growing stage during chemotherapy exposure was analyzed by meiotic spindle and chromosome immunofluorescence to estimate their quality. The meiotic spindle was only visualized in 28.6 % of MII oocytes from the ChT group, indicating that chemotherapy induced detriments on meiotic spindle assembly (Fig. 47A). In contrast, all MII oocytes from the ChT+LH-1x group contained a well-defined and barrel-shaped spindle similar to control oocytes, reducing these non-desired effects of chemotherapy. In fact, based on our Bayesian analysis, chemotherapy administration decreased the probability of proper spindle assembly by 74.2 % relative to that of the control group. In comparison, LH treatment only

decreased by 13.3 %, indicating that LH partially recovered the probability of spindle assembly to control similar levels (Fig. 47B). Moreover, chemotherapy also reduced the spindle area of MII oocytes, being 5-fold lower in the ChT group than in controls (p = 0.001; Fig. 47C). A less severe, but still significant reduction in spindle area was also detected in oocytes from the LH-exposed group compared to controls (p = 0.030). However, the ChT+LH-1x group exhibited a 3-fold increase in spindle area relative to that of the ChT group (p = 0.049).

Subsequently, chemotherapy increased the number of MII oocytes with at least one misaligned chromosome from the metaphase plate (p = 0.035; Fig. 47D), although LH treatment significantly decreased this effect (p = 0.029), recovering control-like levels for chromosomal alignment.

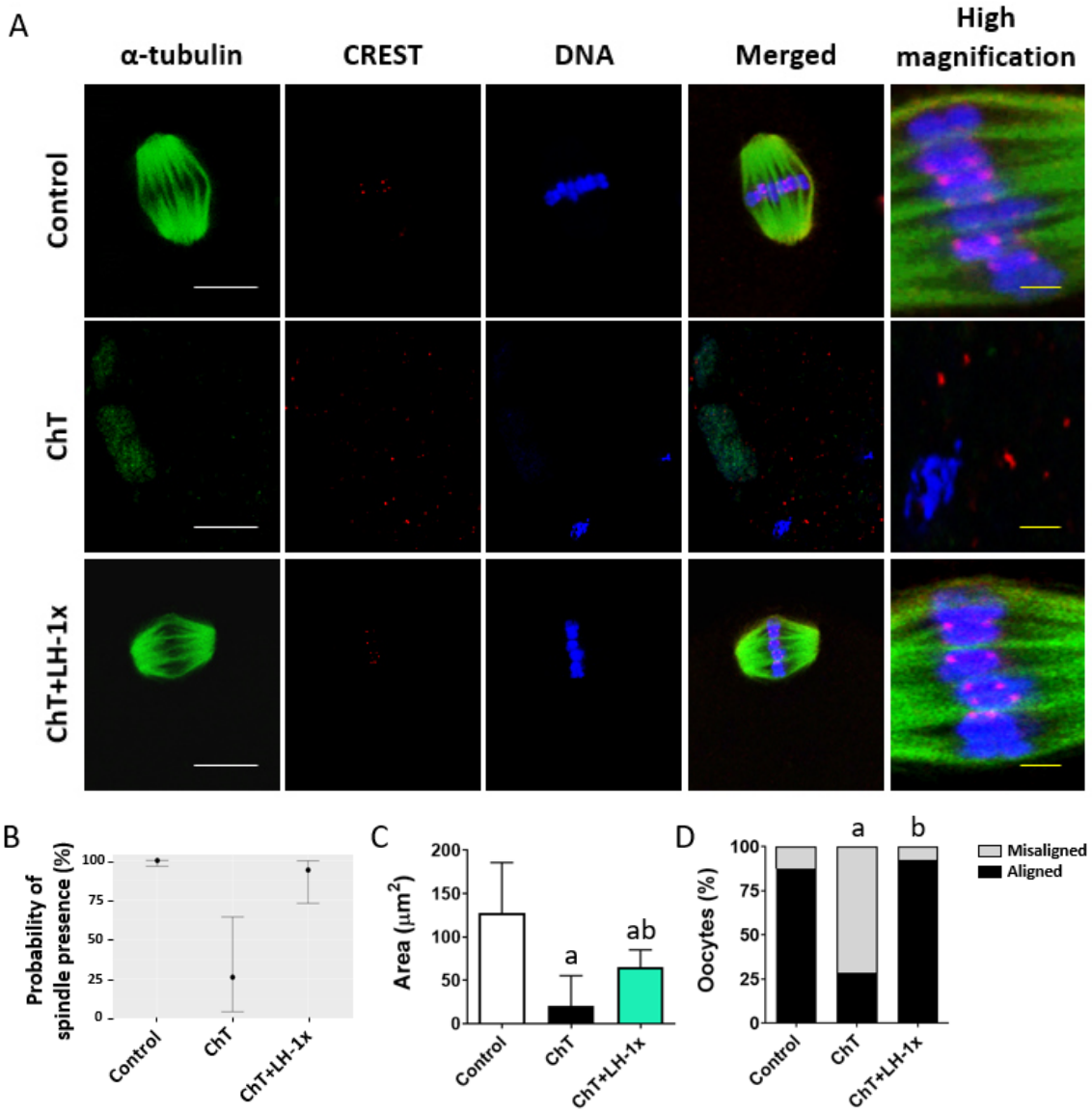

Figure 47. Examination of MII oocyte quality in NOD/SCID mice. *Analysis of MII oocytes collected 16 hours after hCG injection derived from follicles exposed to alkylating agents at the growing stage. (A) Confocal immunofluorescence images of meiotic spindles showing α-tubulin*

(green), chromosomes (blue) and CREST protein (red). The right column represents a high magnification (120x magnification) view of the equatorial plate. White scale bars: 10 μm; yellow scale bars: 2.5 μm. (B) A predictive model of spindle presence in MII oocytes calculated by Bayesian analysis using a logistic regression and a normal non-informative prior (0 ± 3 as mean ± SD). LH treatment reversed the chemotherapy-induced reduction in the probability of meiotic spindle presence promoting the spindle assembly. (C) Analysis of spindle size expressed as area units. Chemotherapy decreased the spindle area of MII oocytes and LH treatment blunted this effect with statistically significant differences. (D) Percentage of MII oocytes with proper aligned chromosomes or at least one misaligned chromosome referred to the equatorial plate. Alkylating agent administration resulted in a higher percentage of misaligned oocytes, and LH treatment reversed this effect, restoring levels similar to the control group. Bar charts show means and, where indicated, SD for each experimental group (n = 8 MII oocytes in control, n = 7 MII oocytes in ChT, and n = 13 MII oocytes in ChT+LH-1x groups were analyzed from 2 mice / group). [a]p-value < 0.05 vs. control group; [b]p-value < 0.05 vs. ChT group.

Discussion

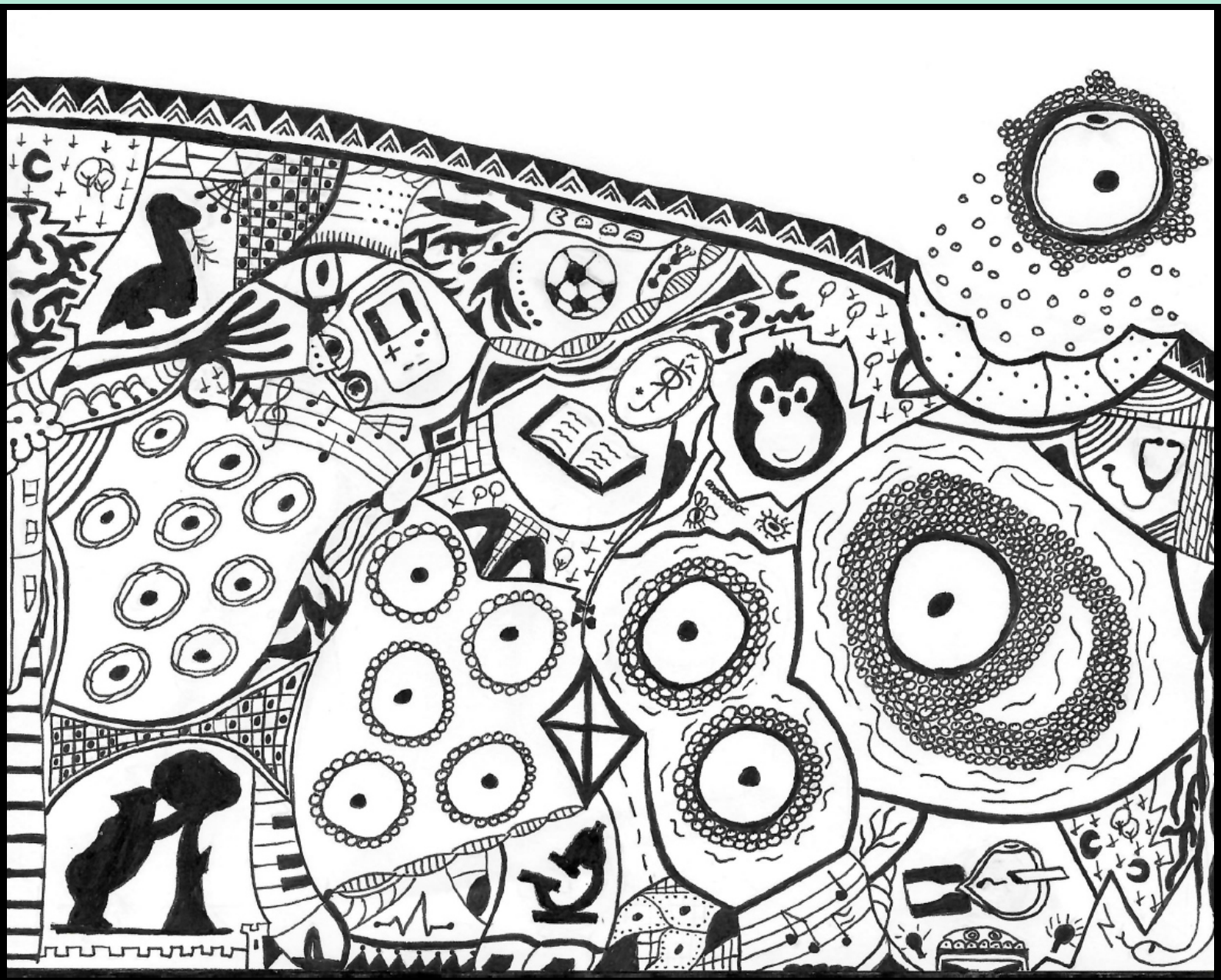

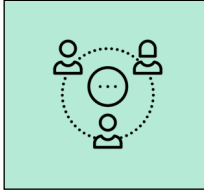

Alkylating co-adjuvant-based therapies are widely employed for the treatment of gynecologic and hematological cancers (250, 251), which represented 48.4 and 7.7 %, respectively, of the total new worldwide cancer cases in women younger than 45 years old along 2020 (88). It is important to note that the side effects of alkylating agents on female fertility are considered a primary concern for clinicians and health professionals in reproductive medicine due to their associated gonadotoxicity (108). Although there are successful techniques currently available for fertility preservation in cancer patients (182), new alternatives for the *in situ* protection of ovarian reserve are still needed. Prevention of cisplatin-induced apoptosis in prepubertal mouse oocytes by LH supplementation (132) pointed out the LH as a strong candidate for gonadoprotection against chemotherapy. For this purpose, this thesis evaluated the effect of LH treatment on 1) quiescent follicles in CD-1 mice, and 2) growing follicles in NOD-SCID subfertile mice following chemotherapy with alkylating agents at a dose equivalent to that used in cancer patients (252). In the CD-1 model, LH prevented the harmful effects of alkylating agents on ovarian reserve, follicular development, oocyte – somatic cell communication, oocyte quality, and improved breeding performance. Further, LH treatment affected DNA repair pathways, suggesting their participation in the protective effects. Similar results were seen when growing follicles were evaluated in the NOD-SCID model.

In the first experimental approach to assess LH effects on the quiescent population, samples were collected 30 days after chemotherapy and/or LH treatments since this timing is consistent with the window required for chemotherapy-exposed quiescent follicles to complete folliculogenesis in mice to ovulate a mature oocyte finally (19-22). The ovarian reserve is intimately linked with female fertility. Thereby, the size of primordial follicle pool and its status after menarche will condition the reproductive potential and lifespan of women. Our results revealed that alkylating chemotherapy induced a significant loss of follicle pool, detecting a 3-fold reduction of the total number of follicles per ovary, affecting all developmental stages. This depletion was confirmed by a decrease of MII oocytes retrieved after stimulation, suggesting that chemotherapy-treated ovaries contained a diminished number of stimulable follicles. Our findings are consistent with similar reports assessing the detrimental effects of chemotherapy on follicle endowment, including alkylating agents (134, 165, 171, 178). By contrast, a noteworthy improvement in both follicle counts and MII oocyte numbers was observed in LH-treated mice. Bearing in mind that the

analyzed follicles and MII oocytes derived from chemotherapy-exposed quiescent follicles, these results pointed out that the primordial population was the main target for the protective action of LH against alkylating agents. This effect was also confirmed in adult ovaries exposed to cisplatin (253), supporting previous observations in prepubertal mice (132) and indicating that LH could protect the ovarian reserve from multiple types of agents. Consistent with previous studies (133, 134, 167, 254, 255), we observed a close relationship between follicle loss and oocyte damage followed by chemotherapy-induced cell death. Our findings indicated that oocytes showed more DNA DSBs than GC, measured by the phosphorylation of H2AX histone (γH2AX), suggesting that oocytes were highly susceptible to DNA damage after chemotherapy with alkylating agents and a potential target to reduce the associated follicular depletion. These results supported previous findings showing that phosphoramide mustard, an active metabolite of cyclophosphamide, predominantly induced DSBs in oocyte DNA rather than in GC (142). By contrast, follicular apoptosis assessed at 12 hours after chemotherapy especially affected to GC of growing populations. It is essential to highlight that, although alkylating-like agents are not cell-cycle specific, they commonly affect to highly proliferative cells as GC (144). In fact, cyclophosphamide administration induced more apoptosis in the multilayered granulosa of secondary and antral follicles than in primordial and primary populations (133). This follicular damage was notably avoided by LH treatment that suggested a role of LH in the promotion of follicular health, being consistent with a study that described a decrease of apoptosis in GC of isolated growing follicles incubated with LH (256). LH-mediated protection on oocytes could occur, in part, through indirect signaling via somatic cells that express the LH receptor. In ovaries, the LH receptor is localized in somatic cells surrounding follicles (identified as theca cells), GC of growing follicles, and corpora lutea, but neither in oocytes nor in early follicular stages (132, 257, 258). Thus, ovarian somatic cells expressing the LH receptor may induce indirect signals in oocytes to preserve their viability. For instance, anti-apoptotic signals induced by GnRHa in oocytes may be mediated by cumulus cells expressing GnRHR-I and GnRHR-II receptors (259). Additionally, follicles became more susceptible to apoptosis and depletion upon loss of LH receptor in somatic cells after cisplatin treatment, blocking ovulation and oocyte maturation (260). Thus, the notable decrease of oocytes with γH2AX foci and apoptotic follicles observed 12 hours after low- or high-dose LH

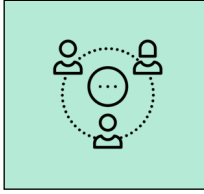

suggested that DNA damage and cell death pathways mediate the preservative effect of LH on follicle counts.

DNA damage and apoptosis are intimately connected to cell fate determination. Those cells with efficient DNA damage response or repair mechanisms are permitted to survive (261, 262). Oocytes and GC have demonstrated that they are able to transduce suitable integrated signals in response to stress and DNA damage events in order to activate repairing mechanisms that ensure follicular viability (180, 263). According to previous reports (157, 158), alkylating agents induced an early activation of DNA repair signaling systems like mismatch, base excision, NHEJ, HR, and nucleotide excision repair pathways. In general, at both 12 and 24 hours after treatments, ovaries from animals treated with LH showed higher expression of DNA repair factors than ovaries from animals treated with chemotherapy alone, indicating that LH stimulated DNA repair. Previous studies reported that LH plays a role in promoting DNA repair pathways in oocytes (132) and ovarian somatic cells (264). Overexpression of DNA repair factors like Rad51, a downstream target of the ATM pathway essential for the HR repair system, is a common mechanism by which cancer cells evade cytotoxic effects of oncologic therapies (265) and follicular cells prevent apoptosis (266, 267). Interestingly, *Rad51* mRNA was still elevated in the LH groups after 24 hours, while it was downregulated in the ChT group. DNA DSBs repair is mediated by NHEJ and HR (156), being the latter the main signaling system in oocytes with S and G2 cellular phases that correspond to those enclosed from primordial to preovulatory follicular stages (268-270). Moreover, we observed that LH treatment reduced AKT activation, a signaling pathway connecting DNA repair with DNA damage and apoptosis (271, 272). pAKT attenuates HR by inhibiting Rad51, which allows the accumulation of DNA DSBs in primordial and primary follicles (273-275). Likewise, LH treatment also reduced the chemotherapy-induced ovarian damage by restoring the expression of γH2AX, and the protein ratio between the anti-apoptotic factor Bcl2 and the pro-apoptotic CC3 to control levels. CC3 protein represents the activated and functional form of caspase-3, a specific cell death effector in oocytes and GC (276, 277). Previous studies describe that LH is able to reduce apoptosis in ovarian cells exposed to cisplatin chemotherapy (132, 278), as well as in GC by increasing the transcription of mRNA levels for Bcl2 and by reducing pro-apoptotic factors like BAX in GC (279). In addition, the increased expression of pERK1/2 protein in ChT-ovaries suggested that the ERK1/2 pathway participated in the

ovotoxicity associated with chemotherapy. Several studies have correlated the activation of ERK1/2 cascade with DNA damage response and cell death in response to various pro-death or arrest cell cycle inductors, including anti-tumor agents like ionizing radiation (280), etoposide (281), doxorubicin (282), cisplatin (283, 284) and alkylating agents (285). By contrast, LH administration reduced ERK1/2 activation as previously observed in an *in vitro* approach (132). Inhibition of ERK1/2 signaling promotes the repair of DNA DSBs (286), preventing the primordial oocytes loss induced by chemotherapy (132). Altogether, these results indicated that LH treatment promoted DNA repair mechanisms like HR to preserve the oocyte DNA integrity and to minimize the ovarian damage against alkylating agents.

The ovarian niche is crucial to generate a suitable microenvironment in the ovary and is required for maintaining both dormant and developing follicles, as well as oocyte competence and maturation (19). We found that chemotherapy affected the ovarian stroma by inducing fibrosis and several non-cellular zones that led to the loss of the tissue architecture. This effect was particularly evident in the central area of the ovaries that coincides with the medulla, which is the most vascularized section. Therefore, alkylating agents might get into the ovary via a complex vascular network deteriorating blood vessels and surrounding stroma. Degeneration of ovarian niche driven by chemotherapy, including disruption of the middle stromal region and decreased microvessel density, was reported by previous studies (150, 167, 287), which also detected a significant compromise of normal follicular morphology, oocyte maturation, and quality. However, LH treatment counteracted the chemotherapy-induced detriment to the stromal region, preserving the tissue architecture.

Furthermore, we found a significant increase of follicles with morphological abnormalities after chemotherapy, which suggested that chemotherapy compromised the development of those follicles exposed at the primordial stage, as previously reported (288). Alteration of GC and ooplasm vacuolization was the most common abnormalities detected, being associated with poor oocyte quality. Significant lower fertilization rates, as well as zygotic and embryo developmental arrest, have been identified in vacuolated oocytes, probably due to numerous and large cytosolic vacuoles interfering with meiotic spindle that might its displacement to unusual positions (194, 289, 290). LH treatment was able to reverse this effect on follicular morphology, suggesting that

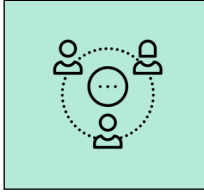

protected primordial follicles by LH would have an increased potential to initiate and maintain folliculogenesis. Interestingly, these morphological abnormalities only affected to growing populations, accumulating most of them in the secondary population in all experimental groups. The transition from primary to secondary stage comprises a large group of events, including active GC proliferation, theca cell differentiation, and blood vessel network formation (9). The need of these processes take place in a coordinated manner would become secondary follicles highly susceptible to any alteration that can affect to both germ and somatic compartments in follicles.

During follicle development, complex and continuing crosstalk between the oocytes and their surrounding GC is essential for the synchronous maturation of both germ and somatic cell compartments in ovarian follicles (246). Although oocytes coordinate follicle development by mediating GC proliferation and differentiation (22), GC constitute the primary source of molecules and metabolites used by oocytes for metabolism, growth, and maturation (291-294), pointing out the relevance of the bidirectional oocyte – GC communication. Our results indicated that growing follicles exposed to alkylating chemotherapy at the primordial stage showed altered the reciprocal intercommunication between both follicular compartments by disturbing cell junctions and secretion of growth factors at gene and protein levels. Although cell intercommunication can be affected by antineoplastic drugs in cancer (295), there are limited data regarding chemotherapy effects on cell junctions in ovaries. Our findings regarding cell junctions suggest that alkylating agents disturbed the expression of molecules involved in mechanical attachment and cytoplasm communication between oocytes and GC at gene and protein levels. Consistent with these results, cyclophosphamide dysregulated the interactions among blastomeres in preimplantation embryos by decreasing the cell-cell contacts and altering the expression of connexin and cadherin genes (296). Adherens junctions mediated by cadherins are essential in ovarian follicles (78, 297, 298). Blastomere adhesion and cell division pattern were affected in embryos derived from knockdown oocytes of E-Cadherin (299). Similar to chemotherapy effects, mouse ovaries lacking E-cadherin also resulted in a disruption of biological mechanisms controlling the primordial follicle pool that led to ovarian reserve depletion as a significant apoptotic rate (27). In addition, several studies showed a negative role of connexins in apoptosis within different cell lines and organs, including the ovary (300, 301). Thus, low expression of connexin 43 was correlated with an elevated rate of apoptotic follicles, indicating connexins act as survival factors for follicles (302-

304). Moreover, we found a reduced secretion of GDF9 and BMP15, paracrine factors predominantly produced by oocytes, in the ChT group, as previously observed in ovarian samples exposed to cyclophosphamide and busulfan (179, 288, 305), where GDF9 and BMP15 were downregulated. On the other side, our results indicated that LH treatment reversed the chemotherapy effects on the oocyte – GC communication. LH restored the expression levels of genes encoding for connexins (gap junctions), cadherins (adherens junctions), and paracrine factors (GDF9, BMP15 and specific receptors), resulting in a significant increase in protein levels similar to controls. Gonadotropin administration enhanced cell-cell contact between oocytes and GC by increasing the expression levels of connexin 37 and 43, N- and E-cadherins, and TZP to ensure the generation of mature oocytes in mice (306). Moreover, Rossi et al. noticed that LH gonadoprotection against cisplatin might be mediated by functional gap junctions through ovarian somatic cells expressing the LH receptor (132).

Chemotherapy compromises follicular development by causing atresia of growing populations and morphological alterations that lead to obtain poor-quality oocytes (307-310). Our results showed that the detrimental effects of chemotherapy on GC – oocyte communication in growing follicles were influenced by the developmental stage, particularly from the secondary to later phases. These findings suggested that primordial follicles exposed to alkylating chemotherapy depicted a reduced growth potential due to a lack of ability to establish proper bidirectional crosstalk between GC and oocytes. Primary-secondary transition in follicles represents a crucial step during folliculogenesis owing to several events taking place, such as the robust oocyte growth, the active GC proliferation, the acquisition of theca cells, and the follicle growth influenced by gonadotrophin-responsive (9, 70). In addition, secretion of paracrine factors involved in oocyte growth and GC proliferation is more evident beyond the secondary stage (311). Downregulation of connexins and cadherins disturbed the bidirectional GC – oocyte communication over the course of primary-secondary transition resulting in folliculogenesis impairment (312). GC, especially from mature follicles, mainly used gap junctions to establish their communication with each other and with oocytes, being connexins the essential protein of these intercellular channels (313). Gene knockout studies demonstrated that follicles lacking connexin 37 and 43 were unable to generate a second granulosa layer impairing follicular growth beyond the late preantral stage, as well as oocytes failed to undergo meiotic maturation (314-317). Furthermore, GDF9, BMP15

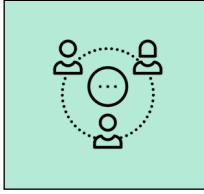

and their specific receptors are expressed in primary follicles onward (318, 319) playing synergistic roles in follicle development, cumulus expansion, antrum formation and ovulation to achieve optimal oocyte competence (86, 87, 320, 321). Nevertheless, deficient mice in GDF9 and BMP15 showed impaired follicle development beyond the secondary stage and decreased ovulation and fertilization rates (85, 87, 322, 323). By contrast, LH-treated follicles were able to achieve a gene and protein expression akin to control samples, which suggested that LH gonadoprotection prevented the far-reaching effects of chemotherapy on folliculogenesis. Hence, these results suggested that LH-treated follicles at the primordial stage preserve their ability to establish proper bidirectional communication between oocyte and surrounding GC during follicle development.

MII meiotic spindle formation can serve as a measure of oocyte quality (324, 325). Large spindle in human oocytes has correlated with an improvement in fertilization rate, blastocyst formation, and pregnancy rate, postulating spindle area as a predictive marker of embryo cleavage (326). We found that MII oocytes developed from primordial follicles exposed to chemotherapy exhibited defects in the spindle area and chromosome alignment. These could arise from the accumulation of unrepaired DNA DSBs in chemotherapy-treated oocytes that then interfere with the progression of the second meiotic division and proper spindle assembly (327). Oocytes with defects in DNA damage response and HR are more susceptible to aneuploidies due to alterations in the spindle and chromosome cohesion (328, 329). In addition, coordinated bidirectional communication between germ and somatic cell compartments during follicle development is required for oocyte meiotic properties (330). Deficient oocyte – GC communication disturbs the meiotic maturation detecting a 2-fold reduction of MII oocytes compared to wild-type condition (331). As our findings with chemotherapy, germ – somatic cell communication and oocyte competence are also compromised in other biological scenarios like aging (312, 332). Thus, the ability of LH to minimize DNA damage in oocytes, as well as to preserve reciprocal communication between oocytes and GC could underlie spindle improvements in the LH-treated oocytes. Resting follicles were therefore protected by LH to preserve their subsequent development (Fig. 48).

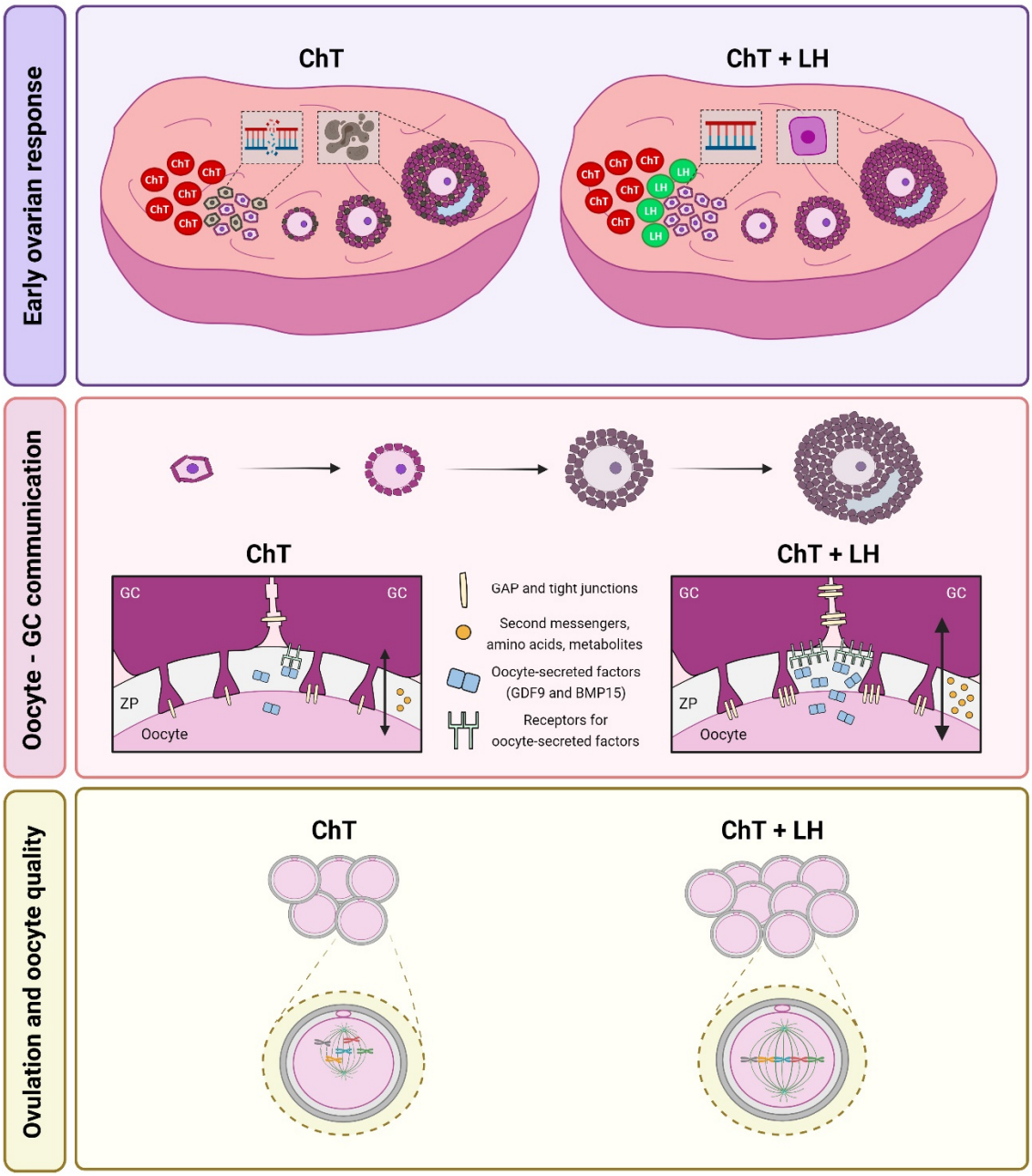

Figure 48. Mechanisms triggered by LH to confer oocyte protection against alkylating chemotherapy in adult mouse ovaries. *Chemotherapy administration damages ovarian reserve by inducing DNA DSBs in oocytes and apoptosis in GC, thereby disturbing subsequent follicular development. During primary-secondary follicle transition, oocytes exposed to chemotherapy at primordial stage reduce growth factors secretion and cell junctions between oocytes and surrounding GC that impair bidirectional communication. As a result, chemotherapy-treated mice ovulate few oocytes with reduced meiotic competence. By contrast, LH treatment protects primordial follicles by preventing the chemotherapy-induced DNA damage and apoptosis, as well as up-regulates DNA repair pathways. These positive effects are subsequently reflected on the oocyte-GC communication improvement over the course of folliculogenesis. Hence, LH ameliorates in both the quantity and the quality of ovulated oocytes.*

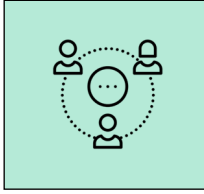

The short-term ability of LH to protect the ovarian reserve and to improve the number and quality of developing oocytes appeared to translate into long-term benefits. LH-treated mice showed a higher pregnancy rate and litter size per pregnant mouse than ChT group, leading to an increased cumulative number of pups whose weight and size were similar among experimental groups. These reproductive outcomes are consistent with previous findings in a cisplatin-treated mouse model, whereby *in vivo* administration of LH rescued fertility by increasing the number of pregnancies and pups (132). Our results also suggest that LH did not compromise the offspring's health, which might reflect the safety of this strategy during chemotherapy, being comparable to other already described fertoprotective agents (102, 165, 216, 230). The ameliorated reproductive outcomes were confirmed by the macroscopic features of stimulated ovaries collected from LH-treated mice compared to ChT group after the sixth delivery. Ovarian size correlates with follicle endowment, especially in the antral population (333); thereby changes in ovarian size are associated with follicular depletion (150). Thus, the increase in the ovarian size indicated the presence of more gonadotropin-stimulable follicles in LH-treated ovaries several months after treatments. These findings were validated by oocyte and embryo retrieval after the sixth breeding round, where LH treatment not only improved the cohort size of MII oocytes and 2-cell embryos collected, but also ameliorated their morphological quality, suggesting that *in situ* protection conferred by LH persisted at long-term. Interestingly, low-dose LH appeared to preserve better breeding performance than the high dosage, that may adversely alter other non-ovarian factors required for fertility, as previous studies reported for some drugs (334, 335). Indeed, Flaws ***et al.,*** describe that chronically supra-physiological levels of LH in plasma accelerate reproductive aging by increasing follicle loss (336). It has been reported that GnRHa administration during chemotherapy is able to improve reproductive outcomes in oncologic patients, including recovery of ovarian function, antral follicle counts, spontaneous pregnancies and the number of live births (337-339), but their efficacy as gonadoprotective agents are debated (340-343). In fact, using of GnRHa in patients undergoing gonadotoxic treatments is currently considered an experimental approach that can be offered as a complementary fertility preservation option, but should not be performed instead of the gold standard options (182, 183). A main cause of the heterogeneous effects between our proposed LH treatment and the currently used GnRHa therapies might be due to the different treatment duration and cumulative dosages. We propose an acute

administration of LH along with chemotherapy, while GnRHa therapies involve long-term repetitive treatments to suppress the reproductive axis permanently. Nevertheless, further research is still needed to determine the best dosage and timing for LH during chemotherapy regimens.

When considering options to preserve fertility, a patient's available follicle pool is a paramount concern. Patients who have received a chemotherapy cycle before undergoing fertility preservation might have reduced their ovarian reserve, so that they could benefit from therapies that protect growing follicles during an antineoplastic regimen. Using a mouse model with reduced fertility (NOD-SCID) (249), we performed COS a week (instead of 4 weeks) after chemotherapy alone or in combination with LH to assess the effects on the growing population for validating LH-mediated gonadoprotection. LH produced a significant preservation of the most undifferentiated populations (i.e., primordial and primary follicles), supporting both the results obtained in our first model and by Rossi *et al.,* (132). As a result, the ratio of primordial follicles increased in LH-treated ovaries compared to ChT group, suggesting that LH would blunt the follicular overactivation induced by chemotherapy at first glance. Previous reports have proposed that primordial follicles are directly or indirectly activated through PI3K-Akt-mTOR pathways in response to a wide range of chemotherapeutic drugs, including cyclophosphamide (102, 165, 167, 177, 260, 344). It has been suggested that ovarian reserve can be depleted driven by the burnout effect, by which a massive number of primordial follicles initiates growth following atresia when they are targeted by chemotherapy. Hence, this hypothesis entails a significant reduction of primordial follicles accompanied by an increase in the growing follicle pool that finally culminates in follicle death (102). Nevertheless, we did not document an increase in the number of growing follicles in both groups exposed to alkylating agents, suggesting that depletion of the ovarian reserve was due to other mechanisms in our NOD-SCID model. TUNEL and γH2AX assays showed that alkylating agents directly targeted oocytes and GC of all follicular stages, and LH conferred significant protection against these apoptotic effects to prevent follicle depletion. These findings confirmed that primordial follicle loss induced by chemotherapy might be due to apoptosis rather than burnout, as previously reported (133, 134, 171, 345). Thereby, adjuvant agents to counteract apoptotic events, like LH, would minimize the risk of POI. Further to this, prevention of deleterious effects on growing follicles also contributed to ovulate larger oocyte

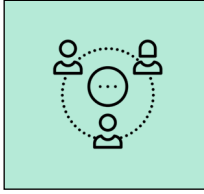

cohorts, suggesting that LH-treated ovaries contained more recruitable follicles than ChT group. Noteworthy, we noticed that chemotherapy also compromised oocyte maturation by inducing defects of spindle configuration and chromosome alignment on ovulated MII oocytes, as previously reported (346, 347). Meanwhile, MII oocytes retrieved from LH-treated mice showed a suitable meiotic competence compared to ChT samples. These findings indicated that LH treatment not only prevented the chemotherapy-driven reduction of MII oocytes, but also preserved their quality and maturation. Hence, adjuvant LH treatment would protect the ovarian reserve and already growing follicles during chemotherapy administration in our POI-induced NOD-SCID model allowing the rescue of competent MII oocytes.

Our results indicate that, despite its short serum half-life (348, 349), LH was able to protect the ovary from alkylating agents. Cyclophosphamide and its active metabolites have half-lives in plasma even shorter than that of LH (350-352), but still trigger persistent ovarian cytotoxicity for days (130, 142, 157, 255). Previous studies demonstrated that cyclophosphamide maintains for a few weeks high fertilization failure aneuploidy, miscarriage and fetus malformation rates in mice, suggesting long-term effects of cyclophosphamide on oocytes (139). Like cyclophosphamide, LH may trigger persisting effects within ovaries by activating signaling pathways and cell functions to prevent ovarian damage.

Based on our results investigating LH-mediated gonadoprotection, hCG might be another possible agent for female fertility preservation. Both gonadotrophins have equivalent roles in clinical practice and can bind the same receptor. Furthermore, the longer half-life of hCG (353) would enhance the hypothesis of hCG as a strong gonadoprotective agent. However, LH and hCG differ in the amino acid residues required for binding to their shared receptor (354). This molecular variance leads to differing activities and some biological effects. LH has demonstrated to be more effective as a proliferative and anti-apoptotic factor, while hCG has higher steroidogenic activity in human GC (355-357). Nevertheless, hCG might confer gonadoprotection against chemotherapy, thereby further research should assess this role.

Altogether, this thesis analyzed in detail the broad spectrum of protective effects elicited by LH on the ovarian reserve of adult mice during chemotherapy treatment with highly gonadotoxic agents. LH effects were investigated using several approaches designed to represent different

clinical reproductive scenarios, i.e., IVF cycles and natural conception, and uncovered possible mechanisms of action. Although these results were obtained in mice, the ability of LH to protect the mouse ovary from alkylating agents and cisplatin (132) highlights its therapeutic potential and encourages human clinical trials. In addition, in contrast with other established options for fertility preservation of patients undergoing oncologic therapies, the LH-based strategy represents a non-surgical strategy without ovarian stimulation protocols that may confer *in situ* protection of the ovarian reserve. Thus, a universal strategy with LH may be possible for fertility preservation in young female cancer patients.

Conclusions

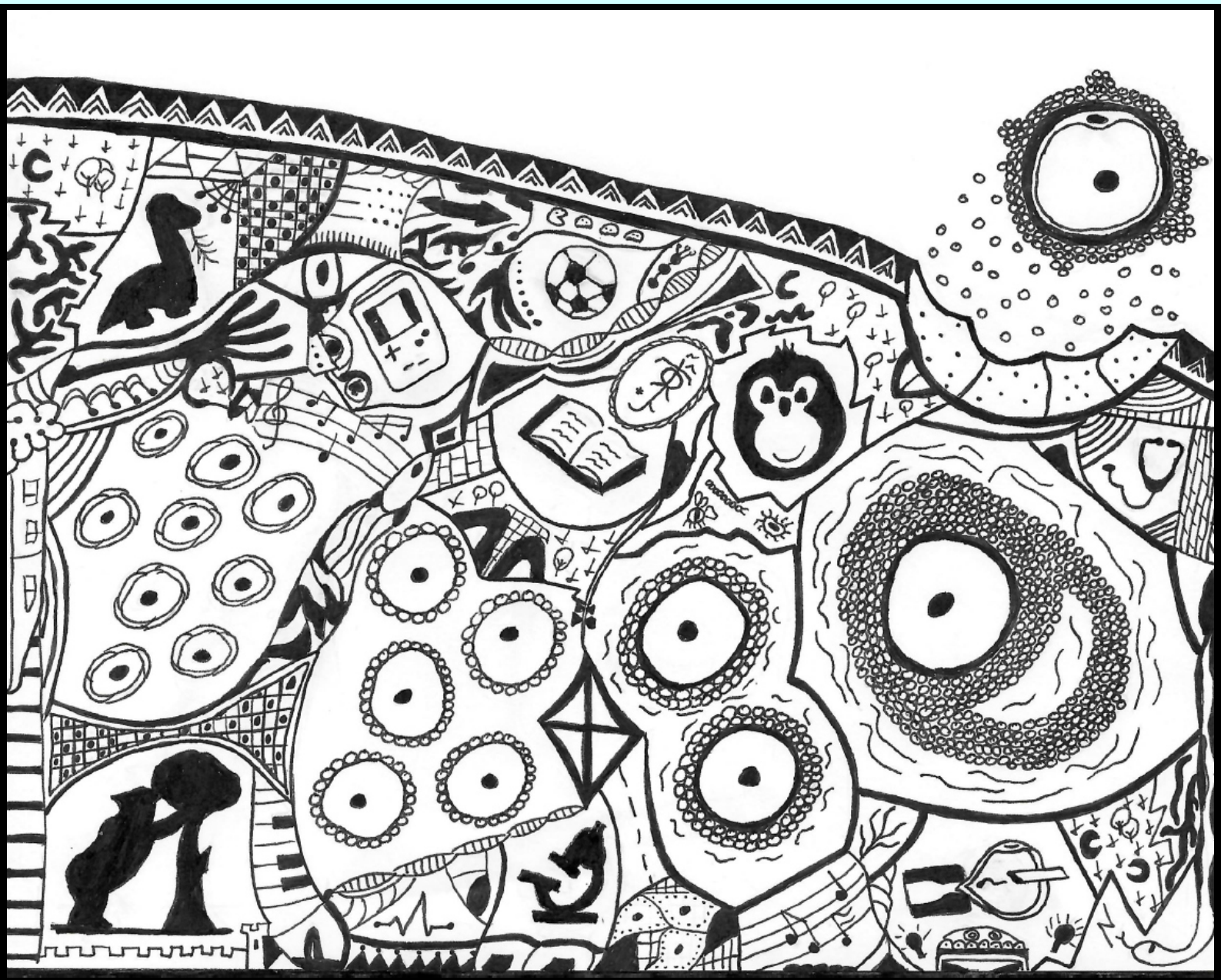

The following conclusions can be drawn from this thesis:

1. LH treatment prevents the chemotherapy-induced alteration of ovarian architecture that contributes to decrease the stromal area with non-cellular and fibrotic fields.
2. LH confers *in situ* protection of the ovarian reserve that leads to reduce the incidence of follicles with morphological abnormalities in ooplasm and GC over the course of follicular development.
3. Protection of primordial follicles by LH prevents the alteration observed after chemotherapy administration on gap and adherens junctions in the somatic and germinal compartments of follicles beyond the secondary stage, maintaining stable the oocyte – GC interaction during follicular growth.
4. LH administration counteracts the effects of chemotherapy by preserving the expression of those growth factors exchanged between oocytes and GC in follicles at advanced stages of follicular development, which promotes the maturation of both follicular compartments in order to obtain competent metaphase II oocytes.
5. Follicular protection by LH improves the number, as well as the morphological quality, the meiotic competence, and the chromosome alignment of ovulated metaphase II oocytes.
6. LH administration preserves the reproductive potential and lifespan of adult female mice without affecting the offspring's health.
7. The role of LH is mediated, at least in part, by an enhancement of DNA damage response, which triggers DNA repair mechanisms like homologous recombination, as well as generates anti-apoptotic signals during the first hours after chemotherapy exposure to maintain the follicular viability.
8. There is an optimal range of LH concentration to achieve a suitable balance between acute gonadotoxicity prevention in the short-term, and fertility preservation in the long-term.
9. LH exerts anti-apoptotic effects on the oocyte and the high proliferative GC of already growing follicles at the time of chemotherapy administration, resulting in an improvement in the quantity and quality of the resulting metaphase II oocytes.

Bibliography

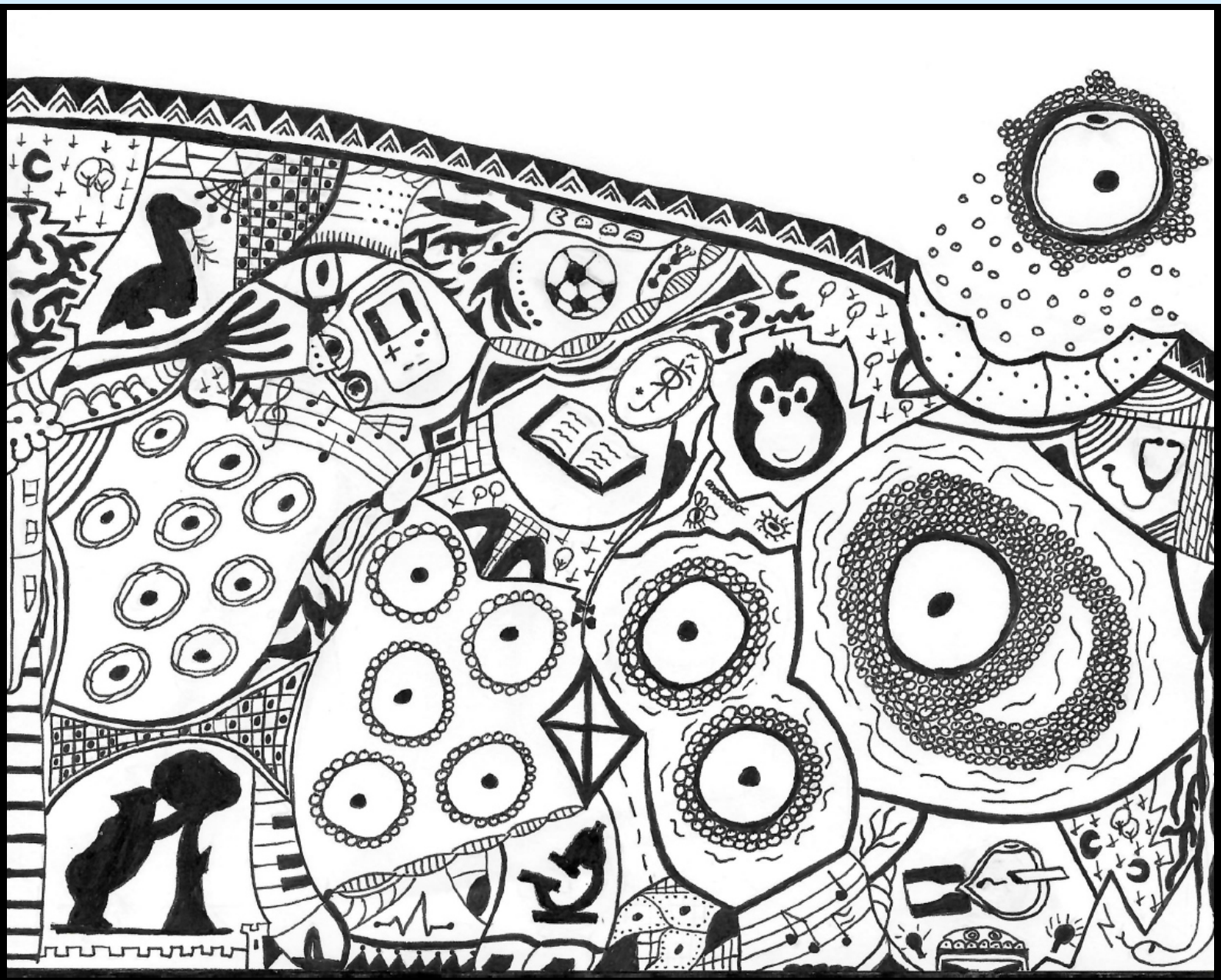

1. Smith P, Wilhelm D, Rodgers RJ. Development of mammalian ovary. J Endocrinol. 2014 Jun;221(3):R145-61.

2. Ginsburg M, Snow MH, McLaren A. Primordial germ cells in the mouse embryo during gastrulation. Development. 1990 Oct;110(2):521-8.

3. Lawson KA, Dunn NR, Roelen BA, Zeinstra LM, Davis AM, Wright CV, et al. Bmp4 is required for the generation of primordial germ cells in the mouse embryo. Genes Dev. 1999 Feb 15;13(4):424-36.

4. Ying Y, Liu XM, Marble A, Lawson KA, Zhao GQ. Requirement of Bmp8b for the generation of primordial germ cells in the mouse. Mol Endocrinol. 2000 Jul;14(7):1053-63.

5. Ying Y, Zhao GQ. Cooperation of endoderm-derived BMP2 and extraembryonic ectoderm-derived BMP4 in primordial germ cell generation in the mouse. Dev Biol. 2001 Apr 15;232(2):484-92.

6. Saitou M, Barton SC, Surani MA. A molecular programme for the specification of germ cell fate in mice. Nature. 2002 Jul 18;418(6895):293-300.

7. Molyneaux K, Wylie C. Primordial germ cell migration. Int J Dev Biol. 2004;48(5-6):537-44.

8. Farini D, La Sala G, Tedesco M, De Felici M. Chemoattractant action and molecular signaling pathways of Kit ligand on mouse primordial germ cells. Dev Biol. 2007 Jun 15;306(2):572-83.

9. Edson MA, Nagaraja AK, Matzuk MM. The mammalian ovary from genesis to revelation. Endocr Rev. 2009 Oct;30(6):624-712.

10. Sarraj MA, Drummond AE. Mammalian foetal ovarian development: consequences for health and disease. Reproduction. 2012 Feb;143(2):151-63.

11. Ford EA, Beckett EL, Roman SD, McLaughlin EA, Sutherland JM. Advances in human primordial follicle activation and premature ovarian insufficiency. Reproduction. 2020 Jan;159(1):R15-29.

12. Lei L, Spradling AC. Mouse oocytes differentiate through organelle enrichment from sister cyst germ cells. Science. 2016 Apr 1;352(6281):95-9.

13. Oktem O, Oktay K. The ovary: anatomy and function throughout human life. Ann N Y Acad Sci. 2008 Apr;1127:1-9.

14. Pepling ME, Spradling AC. Mouse ovarian germ cell cysts undergo programmed breakdown to form primordial follicles. Dev Biol. 2001 Jun 15;234(2):339-51.

15. Rajareddy S, Reddy P, Du C, Liu L, Jagarlamudi K, Tang W, et al. p27kip1 (cyclin-dependent kinase inhibitor 1B) controls ovarian development by suppressing follicle endowment and activation and promoting follicle atresia in mice. Mol Endocrinol. 2007 Sep;21(9):2189-202.

16. Rodrigues P, Limback D, McGinnis LK, Plancha CE, Albertini DF. Multiple mechanisms of germ cell loss in the perinatal mouse ovary. Reproduction. 2009 Apr;137(4):709-20.

17. Tingen CM, Bristol-Gould SK, Kiesewetter SE, Wellington JT, Shea L, Woodruff TK. Prepubertal primordial follicle loss in mice is not due to classical apoptotic pathways. Biol Reprod. 2009 Jul;81(1):16-25.

18. Kerr JB, Myers M, Anderson RA. The dynamics of the primordial follicle reserve. Reproduction. 2013 Oct 21;146(6):R205-15.

19. Clarke H. Control of mammalian oocyte development by interactions with the maternal follicular environment. Results Probl Cell Differ. 2017;63:17-41.

20. Pedersen T. Determination of follicle growth rate in the ovary of the immature mouse. J Reprod Fertil. 1970 Feb;21(1):81-93.

21. Picton HM, Harris SE, Muruvi W, Chambers EL. The in vitro growth and maturation of follicles. Reproduction. 2008 Dec;136(6):703-15.

22. Eppig JJ, Wigglesworth K, Pendola FL. The mammalian oocyte orchestrates the rate of ovarian follicular development. Proc Natl Acad Sci U S A. 2002 Mar 5;99(5):2890-4.

23. Zheng W, Zhang H, Gorre N, Risal S, Shen Y, Liu K. Two classes of ovarian primordial follicles exhibit distinct developmental dynamics and physiological functions. Hum Mol Genet. 2014 Feb 15;23(4):920-8.

24. Zheng W, Zhang H, Liu K. The two classes of primordial follicles in the mouse ovary: their development, physiological functions and implications for future research. Mol Hum Reprod. 2014 Apr;20(4):286-92.

25. Liu C, Peng J, Matzuk MM, Yao HH. Lineage specification of ovarian theca cells requires multicellular interactions via oocyte and granulosa cells. Nat Commun. 2015 Apr 28;6:6934.

26. Webb R, Garnsworthy PC, Campbell BK, Hunter MG. Intra-ovarian regulation of follicular development and oocyte competence in farm animals. Theriogenology. 2007 Sep 1;68 Suppl 1:S22-9.

27. Yan H, Wen J, Zhang T, Zheng W, He M, Huang K, et al. Oocyte-derived E-cadherin acts as a multiple functional factor maintaining the primordial follicle pool in mice. Cell Death Dis. 2019 Feb 15;10(3):160,018-1208-3.

28. Zhang H, Risal S, Gorre N, Busayavalasa K, Li X, Shen Y, et al. Somatic cells initiate primordial follicle activation and govern the development of dormant oocytes in mice. Curr Biol. 2014 Nov 3;24(21):2501-8.

29. Adhikari D, Liu K. Molecular mechanisms underlying the activation of mammalian primordial follicles. Endocr Rev. 2009 Aug;30(5):438-64.

30. Blume-Jensen P, Hunter T. Oncogenic kinase signalling. Nature. 2001 May 17;411(6835):355-65.

31. Cantley LC. The phosphoinositide 3-kinase pathway. Science. 2002 May 31;296(5573):1655-7.

32. Zheng W, Nagaraju G, Liu Z, Liu K. Functional roles of the phosphatidylinositol 3-kinases (PI3Ks) signaling in the mammalian ovary. Mol Cell Endocrinol. 2012 Jun 5;356(1-2):24-30.

33. Cecconi S, Mauro A, Cellini V, Patacchiola F. The role of Akt signalling in the mammalian ovary. Int J Dev Biol. 2012;56(10-12):809-17.

34. John GB, Gallardo TD, Shirley LJ, Castrillon DH. Foxo3 is a PI3K-dependent molecular switch controlling the initiation of oocyte growth. Dev Biol. 2008 Sep 1;321(1):197-204.

35. Ezzati MM, Baker MD, Saatcioglu HD, Aloisio GM, Pena CG, Nakada Y, et al. Regulation of FOXO3 subcellular localization by Kit ligand in the neonatal mouse ovary. J Assist Reprod Genet. 2015 Dec;32(12):1741-7.

36. Yan H, Zhang J, Wen J, Wang Y, Niu W, Teng Z, et al. CDC42 controls the activation of primordial follicles by regulating PI3K signaling in mouse oocytes. BMC Biol. 2018 Jul 5;16(1):73,018-0541-4.

37. Jang H, Na Y, Hong K, Lee S, Moon S, Cho M, et al. Synergistic effect of melatonin and ghrelin in preventing cisplatin-induced ovarian damage via regulation of FOXO3a

phosphorylation and binding to the p27(Kip1) promoter in primordial follicles. J Pineal Res. 2017 Oct;63(3):10.1111/jpi.12432. Epub 2017 Jul 18.

38. Reddy P, Liu L, Adhikari D, Jagarlamudi K, Rajareddy S, Shen Y, et al. Oocyte-specific deletion of Pten causes premature activation of the primordial follicle pool. Science. 2008 Feb 1;319(5863):611-3.
39. Tong Y, Li F, Lu Y, Cao Y, Gao J, Liu J. Rapamycin-sensitive mTORC1 signaling is involved in physiological primordial follicle activation in mouse ovary. Mol Reprod Dev. 2013 Dec;80(12):1018-34.
40. Yorino S, Kawamura K. Rapamycin treatment maintains developmental potential of oocytes in mice and follicle reserve in human cortical fragments grafted into immune-deficient mice. Mol Cell Endocrinol. 2020 Mar 15;504:110694.
41. Shimamoto S, Nishimura Y, Nagamatsu G, Hamada N, Kita H, Hikabe O, et al. Hypoxia induces the dormant state in oocytes through expression of Foxo3. Proc Natl Acad Sci U S A. 2019 Jun 18;116(25):12321-6.
42. Nagamatsu G, Shimamoto S, Hamazaki N, Nishimura Y, Hayashi K. Mechanical stress accompanied with nuclear rotation is involved in the dormant state of mouse oocytes. Sci Adv. 2019 Jun 26;5(6):eaav9960.
43. Hornick JE, Duncan FE, Shea LD, Woodruff TK. Isolated primate primordial follicles require a rigid physical environment to survive and grow in vitro. Hum Reprod. 2012 Jun;27(6):1801-10.
44. Jorge S, Chang S, Barzilai JJ, Leppert P, Segars JH. Mechanical signaling in reproductive tissues: mechanisms and importance. Reprod Sci. 2014 Sep;21(9):1093-107.
45. Parrott JA, Skinner MK. Kit-ligand/stem cell factor induces primordial follicle development and initiates folliculogenesis. Endocrinology. 1999 Sep;140(9):4262-71.
46. Jin X, Han CS, Yu FQ, Wei P, Hu ZY, Liu YX. Anti-apoptotic action of stem cell factor on oocytes in primordial follicles and its signal transduction. Mol Reprod Dev. 2005 Jan;70(1):82-90.
47. Pangas SA, Choi Y, Ballow DJ, Zhao Y, Westphal H, Matzuk MM, et al. Oogenesis requires germ cell-specific transcriptional regulators Sohlh1 and Lhx8. Proc Natl Acad Sci U S A. 2006 May 23;103(21):8090-5.

48. Liu G, Li Y, Du B, Sun Q, Qi W, Liu Y, et al. Primordial follicle activation is affected by the absence of Sohlh1 in mice. Mol Reprod Dev. 2019 Jan;86(1):20-31.

49. Choi Y, Qin Y, Berger MF, Ballow DJ, Bulyk ML, Rajkovic A. Microarray analyses of newborn mouse ovaries lacking Nobox. Biol Reprod. 2007 Aug;77(2):312-9.

50. Choi Y, Ballow DJ, Xin Y, Rajkovic A. Lim homeobox gene, lhx8, is essential for mouse oocyte differentiation and survival. Biol Reprod. 2008 Sep;79(3):442-9.

51. Ren Y, Suzuki H, Jagarlamudi K, Golnoski K, McGuire M, Lopes R, et al. Lhx8 regulates primordial follicle activation and postnatal folliculogenesis. BMC Biol. 2015 Jun 16;13:39,015-0151-3.

52. Schmidt D, Ovitt CE, Anlag K, Fehsenfeld S, Gredsted L, Treier AC, et al. The murine winged-helix transcription factor Foxl2 is required for granulosa cell differentiation and ovary maintenance. Development. 2004 Feb;131(4):933-42.

53. Nilsson EE, Skinner MK. Bone morphogenetic protein-4 acts as an ovarian follicle survival factor and promotes primordial follicle development. Biol Reprod. 2003 Oct;69(4):1265-72.

54. Lee WS, Otsuka F, Moore RK, Shimasaki S. Effect of bone morphogenetic protein-7 on folliculogenesis and ovulation in the rat. Biol Reprod. 2001 Oct;65(4):994-9.

55. Durlinger AL, Kramer P, Karels B, de Jong FH, Uilenbroek JT, Grootegoed JA, et al. Control of primordial follicle recruitment by anti-Mullerian hormone in the mouse ovary. Endocrinology. 1999 Dec;140(12):5789-96.

56. Carlsson IB, Scott JE, Visser JA, Ritvos O, Themmen AP, Hovatta O. Anti-Mullerian hormone inhibits initiation of growth of human primordial ovarian follicles in vitro. Hum Reprod. 2006 Sep;21(9):2223-7.

57. Nilsson E, Rogers N, Skinner MK. Actions of anti-Mullerian hormone on the ovarian transcriptome to inhibit primordial to primary follicle transition. Reproduction. 2007 Aug;134(2):209-21.

58. Garor R, Abir R, Erman A, Felz C, Nitke S, Fisch B. Effects of basic fibroblast growth factor on in vitro development of human ovarian primordial follicles. Fertil Steril. 2009 May;91(5 Suppl):1967-75.

59. Du XY, Huang J, Xu LQ, Tang DF, Wu L, Zhang LX, et al. The proto-oncogene c-src is involved in primordial follicle activation through the PI3K, PKC and MAPK signaling pathways. Reprod Biol Endocrinol. 2012 Aug 20;10:58,7827-10-58.

60. Nilsson EE, Kezele P, Skinner MK. Leukemia inhibitory factor (LIF) promotes the primordial to primary follicle transition in rat ovaries. Mol Cell Endocrinol. 2002 Feb 25;188(1-2):65-73.

61. Komatsu K, Koya T, Wang J, Yamashita M, Kikkawa F, Iwase A. Analysis of the Effect of Leukemia Inhibitory Factor on Follicular Growth in Cultured Murine Ovarian Tissue. Biol Reprod. 2015 Jul;93(1):18.

62. Cattanach BM, Iddon CA, Charlton HM, Chiappa SA, Fink G. Gonadotrophin-releasing hormone deficiency in a mutant mouse with hypogonadism. Nature. 1977 Sep 22;269(5626):338-40.

63. Abel MH, Wootton AN, Wilkins V, Huhtaniemi I, Knight PG, Charlton HM. The effect of a null mutation in the follicle-stimulating hormone receptor gene on mouse reproduction. Endocrinology. 2000 May;141(5):1795-803.

64. Su YQ, Wu X, O'Brien MJ, Pendola FL, Denegre JN, Matzuk MM, et al. Synergistic roles of BMP15 and GDF9 in the development and function of the oocyte-cumulus cell complex in mice: genetic evidence for an oocyte-granulosa cell regulatory loop. Dev Biol. 2004 Dec 1;276(1):64-73.

65. Peng J, Li Q, Wigglesworth K, Rangarajan A, Kattamuri C, Peterson RT, et al. Growth differentiation factor 9:bone morphogenetic protein 15 heterodimers are potent regulators of ovarian functions. Proc Natl Acad Sci U S A. 2013 Feb 19;110(8):E776-85.

66. Cheng Y, Kawamura K, Takae S, Deguchi M, Yang Q, Kuo C, et al. Oocyte-derived R-spondin2 promotes ovarian follicle development. FASEB J. 2013 Jun;27(6):2175-84.

67. Paredes A, Romero C, Dissen GA, DeChiara TM, Reichardt L, Cornea A, et al. TrkB receptors are required for follicular growth and oocyte survival in the mammalian ovary. Dev Biol. 2004 Mar 15;267(2):430-49.

68. Sato Y, Cheng Y, Kawamura K, Takae S, Hsueh AJ. C-type natriuretic peptide stimulates ovarian follicle development. Mol Endocrinol. 2012 Jul;26(7):1158-66.

69. Hsueh AJ, Kawamura K, Cheng Y, Fauser BC. Intraovarian control of early folliculogenesis. Endocr Rev. 2015 Feb;36(1):1-24.

70. Franks S, Hardy K, Conway GS. Pathophysiology of Ovarian Function in the Human Female. In: Knobil and Neill's Physiology of Reproduction. Fourth Edition ed. London: Academic Press; 2015. p. 1363-1394.

71. Zeleznik AJ, Plant TM. Control of the Menstrual Cycle. In: Knobil and Neill's Physiology of Reproduction. Fourth Edition ed. London: Academic Press; 2015. p. 1307-1361.

72. Hunzicker-Dunn M, Mayo K. Gonadotropin Signaling in the Ovary. In: Knobil and Neill's Physiology of Reproduction. Fourth Edition ed. London: Academic Press; 2015. p. 895-945.

73. Farookhi R, Desjardins J. Luteinizing hormone receptor induction in dispersed granulosa cells requires estrogen. Mol Cell Endocrinol. 1986 Sep;47(1-2):13-24.

74. Ginther OJ, Beg MA, Bergfelt DR, Donadeu FX, Kot K. Follicle selection in monovular species. Biol Reprod. 2001 Sep;65(3):638-47.

75. Yding Andersen C. Inhibin-B secretion and FSH isoform distribution may play an integral part of follicular selection in the natural menstrual cycle. Mol Hum Reprod. 2017 Jan;23(1):16-24.

76. Jeppesen JV, Kristensen SG, Nielsen ME, Humaidan P, Dal Canto M, Fadini R, et al. LH-receptor gene expression in human granulosa and cumulus cells from antral and preovulatory follicles. J Clin Endocrinol Metab. 2012 Aug;97(8):E1524-31.

77. Clarke HJ. Regulation of germ cell development by intercellular signaling in the mammalian ovarian follicle. Wiley Interdiscip Rev Dev Biol. 2018 Jan;7(1):10.1002/wdev.294. Epub 2017 Sep 11.

78. Mora JM, Fenwick MA, Castle L, Baithun M, Ryder TA, Mobberley M, et al. Characterization and significance of adhesion and junction-related proteins in mouse ovarian follicles. Biol Reprod. 2012 May 17;86(5):153, 1-14.

79. Goldberg GS, Valiunas V, Brink PR. Selective permeability of gap junction channels. Biochim Biophys Acta. 2004 Mar 23;1662(1-2):96-101.

80. Gershon E, Plaks V, Dekel N. Gap junctions in the ovary: expression, localization and function. Mol Cell Endocrinol. 2008 Jan 30;282(1-2):18-25.

81. FitzHarris G, Siyanov V, Baltz JM. Granulosa cells regulate oocyte intracellular pH against acidosis in preantral follicles by multiple mechanisms. Development. 2007 Dec;134(23):4283-95.

82. Sela-Abramovich S, Edry I, Galiani D, Nevo N, Dekel N. Disruption of gap junctional communication within the ovarian follicle induces oocyte maturation. Endocrinology. 2006 May;147(5):2280-6.

83. Vaccari S, Horner K, Mehlmann LM, Conti M. Generation of mouse oocytes defective in cAMP synthesis and degradation: endogenous cyclic AMP is essential for meiotic arrest. Dev Biol. 2008 Apr 1;316(1):124-34.

84. Shuhaibar LC, Egbert JR, Norris RP, Lampe PD, Nikolaev VO, Thunemann M, et al. Intercellular signaling via cyclic GMP diffusion through gap junctions restarts meiosis in mouse ovarian follicles. Proc Natl Acad Sci U S A. 2015 Apr 28;112(17):5527-32.

85. Dong J, Albertini DF, Nishimori K, Kumar TR, Lu N, Matzuk MM. Growth differentiation factor-9 is required during early ovarian folliculogenesis. Nature. 1996 Oct 10;383(6600):531-5.

86. Elvin JA, Clark AT, Wang P, Wolfman NM, Matzuk MM. Paracrine actions of growth differentiation factor-9 in the mammalian ovary. Mol Endocrinol. 1999 Jun;13(6):1035-48.

87. Yan C, Wang P, DeMayo J, DeMayo FJ, Elvin JA, Carino C, et al. Synergistic roles of bone morphogenetic protein 15 and growth differentiation factor 9 in ovarian function. Mol Endocrinol. 2001 Jun;15(6):854-66.

88. Sung H, Ferlay J, Siegel RL, Laversanne M, Soerjomataram I, Jemal A, et al. Global cancer statistics 2020: GLOBOCAN estimates of incidence and mortality worldwide for 36 cancers in 185 countries. CA Cancer J Clin. 2021.

89. Global Health Estimates 2020: Deaths by Cause, Age, Sex, by Country and by Region, 2000-2019 [Internet]. Geneva, Switzerland: World Health Organization, WHO; 2020 [cited June, 2021]. Available from: https://www.who.int/data/gho/data/themes/mortality-and-global-health-estimates/ghe-leading-causes-of-death.

90. Siegel RL, Miller KD, Jemal A. Cancer statistics, 2020. CA Cancer J Clin. 2020 Jan;70(1):7-30.

91. Siegel RL, Miller KD, Jemal A. Cancer statistics, 2016. CA Cancer J Clin. 2016 Jan-Feb;66(1):7-30.

92. Gold EB. The timing of the age at which natural menopause occurs. Obstet Gynecol Clin North Am. 2011 Sep;38(3):425-40.

93. Smith MA, Seibel NL, Altekruse SF, Ries LA, Melbert DL, O'Leary M, et al. Outcomes for children and adolescents with cancer: challenges for the twenty-first century. J Clin Oncol. 2010 May 20;28(15):2625-34.

94. SEER Cancer Statistics Review, 1975-2016 [Internet]. Bethesda, MD, USA: National Cancer Institute; 2020 [cited June, 2021]. Available from: https://seer.cancer.gov/csr/1975_2016.

95. Global Cancer Observatory: Cancer Today [Internet]. Lyon, France: International Agency for Research on Cancer; 2020 [cited June, 2021]. Available from: https://gco.iarc.fr/today.

96. Bhakta N, Liu Q, Ness KK, Baassiri M, Eissa H, Yeo F, et al. The cumulative burden of surviving childhood cancer: an initial report from the St Jude Lifetime Cohort Study (SJLIFE). Lancet. 2017 Dec 9;390(10112):2569-82.

97. Bedoschi G, Navarro PA, Oktay K. Chemotherapy-induced damage to ovary: mechanisms and clinical impact. Future Oncol. 2016 Oct;12(20):2333-44.

98. Codacci-Pisanelli G, Del Pup L, Del Grande M, Peccatori FA. Mechanisms of chemotherapy-induced ovarian damage in breast cancer patients. Crit Rev Oncol Hematol. 2017 May;113:90-6.

99. Anderson RA, Brewster DH, Wood R, Nowell S, Fischbacher C, Kelsey TW, et al. The impact of cancer on subsequent chance of pregnancy: A populationbased analysis. Human Reproduction. 2018;33:1281-90.

100. Newton K, Howard AF, Thorne S, Kelly MT, Goddard K. Facing the unknown: uncertain fertility in young adult survivors of childhood cancer. J Cancer Surviv. 2021 Feb;15(1):54-65.

101. Anderson RA, Themmen AP, Al-Qahtani A, Groome NP, Cameron DA. The effects of chemotherapy and long-term gonadotrophin suppression on the ovarian reserve in premenopausal women with breast cancer. Hum Reprod. 2006 Oct;21(10):2583-92.

102. Kalich-Philosoph L, Roness H, Carmely A, Fishel-Bartal M, Ligumsky H, Paglin S, et al. Cyclophosphamide triggers follicle activation and "burnout"; AS101 prevents follicle loss and preserves fertility. Sci Transl Med. 2013 May 15;5(185):185ra62.

103. Lambertini M, Del Mastro L, Pescio MC, Andersen CY, Azim HA,Jr, Peccatori FA, et al. Cancer and fertility preservation: international recommendations from an expert meeting. BMC Med. 2016 Jan 4;14:1,015-0545-7.

104. Bruning PF, Pit MJ, de Jong-Bakker M, van den Ende A, Hart A, van Enk A. Bone mineral density after adjuvant chemotherapy for premenopausal breast cancer. Br J Cancer. 1990 Feb;61(2):308-10.

105. Jeanes H, Newby D, Gray GA. Cardiovascular risk in women: the impact of hormone replacement therapy and prospects for new therapeutic approaches. Expert Opin Pharmacother. 2007 Feb;8(3):279-88.

106. Carter J, Rowland K, Chi D, Brown C, Abu-Rustum N, Castiel M, et al. Gynecologic cancer treatment and the impact of cancer-related infertility. Gynecol Oncol. 2005 Apr;97(1):90-5.

107. Howard-Anderson J, Ganz P, Bower J, Stanton A. Quality of life, fertility concerns, and behavioral health outcomes in younger breast cancer survivors: a systematic review. J Natl Cancer Inst. 2012(104(5)):386-405.

108. Meirow D, Biederman H, Anderson RA, Wallace WH. Toxicity of chemotherapy and radiation on female reproduction. Clin Obstet Gynecol. 2010 Dec;53(4):727-39.

109. Wallace WH, Thomson AB, Kelsey TW. The radiosensitivity of the human oocyte. Hum Reprod. 2003 Jan;18(1):117-21.

110. Wallace WH, Thomson AB, Saran F, Kelsey TW. Predicting age of ovarian failure after radiation to a field that includes the ovaries. Int J Radiat Oncol Biol Phys. 2005 Jul 1;62(3):738-44.

111. Meirow D, Nugent D. The effects of radiotherapy and chemotherapy on female reproduction. Hum Reprod Update. 2001 Nov-Dec;7(6):535-43.

112. Letourneau JM, Ebbel EE, Katz PP, Oktay KH, McCulloch CE, Ai WZ, et al. Acute ovarian failure underestimates age-specific reproductive impairment for young women undergoing chemotherapy for cancer. Cancer. 2012 Apr 1;118(7):1933-9.

113. Roness H, Kalich-Philosoph L, Meirow D. Prevention of chemotherapy-induced ovarian damage: possible roles for hormonal and non-hormonal attenuating agents. Hum Reprod Update. 2014 Sep-Oct;20(5):759-74.

114. Morgan S, Anderson RA, Gourley C, Wallace WH, Spears N. How do chemotherapeutic agents damage the ovary? Hum Reprod Update. 2012 Sep-Oct;18(5):525-35.

115. Petrek JA, Naughton MJ, Case LD, Paskett ED, Naftalis EZ, Singletary SE, et al. Incidence, time course, and determinants of menstrual bleeding after breast cancer treatment: a prospective study. J Clin Oncol. 2006 Mar 1;24(7):1045-51.

116. Nelson LM. Clinical practice. Primary ovarian insufficiency. N Engl J Med. 2009 Feb 5;360(6):606-14.

117. Sklar CA, Mertens AC, Mitby P, Whitton J, Stovall M, Kasper C, et al. Premature menopause in survivors of childhood cancer: a report from the childhood cancer survivor study. J Natl Cancer Inst. 2006 Jul 5;98(13):890-6.

118. Byrne J, Fears TR, Gail MH, Pee D, Connelly RR, Austin DF, et al. Early menopause in long-term survivors of cancer during adolescence. Am J Obstet Gynecol. 1992 Mar;166(3):788-93.

119. Meirow D. Reproduction post-chemotherapy in young cancer patients. Mol Cell Endocrinol. 2000 Nov 27;169(1-2):123-31.

120. Bines J, Oleske DM, Cobleigh MA. Ovarian function in premenopausal women treated with adjuvant chemotherapy for breast cancer. J Clin Oncol. 1996 May;14(5):1718-29.

121. Anderson R, Wallace W. Antimüllerian hormone, the assessment of the ovarian reserve, and the reproductive outcome of the young patient with cancer. Fertil Steril. 2013(99(6)):1469-75.

122. Taylan E, Oktay K. Fertility preservation in gynecologic cancers. Gynecol Oncol. 2019 Dec;155(3):522-9.

123. Wang S, Zheng Y, Li J, Yu Y, Zhang W, Song M, et al. Single-Cell Transcriptomic Atlas of Primate Ovarian Aging. Cell. 2020 Feb 6;180(3):585,600.e19.

124. Wagner M, Yoshihara M, Douagi I, Damdimopoulos A, Panula S, Petropoulos S, et al. Single-cell analysis of human ovarian cortex identifies distinct cell populations but no oogonial stem cells. Nat Commun. 2020 Mar 2;11(1):1147,020-14936-3.

125. Meirow D, Lewis H, Nugent D, Epstein M. Subclinical depletion of primordial follicular reserve in mice treated with cyclophosphamide: clinical importance and proposed accurate investigative tool. Hum Reprod. 1999 Jul;14(7):1903-7.

126. Oktem O, Oktay K. A novel ovarian xenografting model to characterize the impact of chemotherapy agents on human primordial follicle reserve. Cancer Res. 2007 Nov 1;67(21):10159-62.

127. Yucebilgin MS, Terek MC, Ozsaran A, Akercan F, Zekioglu O, Isik E, et al. Effect of chemotherapy on primordial follicular reserve of rat: an animal model of premature ovarian failure and infertility. Aust N Z J Obstet Gynaecol. 2004 Feb;44(1):6-9.

128. Gonfloni S, Di Tella L, Caldarola S, Cannata SM, Klinger FG, Di Bartolomeo C, et al. Inhibition of the c-Abl-TAp63 pathway protects mouse oocytes from chemotherapy-induced death. Nat Med. 2009 Oct;15(10):1179-85.

129. Kim SY, Cordeiro MH, Serna VA, Ebbert K, Butler LM, Sinha S, et al. Rescue of platinum-damaged oocytes from programmed cell death through inactivation of the p53 family signaling network. Cell Death Differ. 2013 Aug;20(8):987-97.

130. Morgan S, Lopes F, Gourley C, Anderson RA, Spears N. Cisplatin and doxorubicin induce distinct mechanisms of ovarian follicle loss; imatinib provides selective protection only against cisplatin. PLoS One. 2013 Jul 29;8(7):e70117.

131. Roti Roti EC, Leisman SK, Abbott DH, Salih SM. Acute doxorubicin insult in the mouse ovary is cell- and follicle-type dependent. PLoS One. 2012;7(8):e42293.

132. Rossi V, Lispi M, Longobardi S, Mattei M, Rella FD, Salustri A, et al. LH prevents cisplatin-induced apoptosis in oocytes and preserves female fertility in mouse. Cell Death Differ. 2017 Jan;24(1):72-82.

133. Nguyen QN, Zerafa N, Liew SH, Findlay JK, Hickey M, Hutt KJ. Cisplatin- and cyclophosphamide-induced primordial follicle depletion is caused by direct damage to oocytes. Mol Hum Reprod. 2019;25:433-44.

134. Luan Y, Edmonds ME, Woodruff TK, Kim SY. Inhibitors of apoptosis protect the ovarian reserve from cyclophosphamide. J Endocrinol. 2019;240:243-56.

135. Ben-Aharon I, Bar-Joseph H, Tzarfaty G, Kuchinsky L, Rizel S, Stemmer SM, et al. Doxorubicin-induced ovarian toxicity. Reprod Biol Endocrinol. 2010 Mar 4;8:20,7827-8-20.

136. Yeh J, Kim B, Liang YJ, Peresie J. Mullerian inhibiting substance as a novel biomarker of cisplatin-induced ovarian damage. Biochem Biophys Res Commun. 2006 Sep 22;348(2):337-44.

137. Rosendahl M, Andersen CY, la Cour Freiesleben N, Juul A, Lossl K, Andersen AN. Dynamics and mechanisms of chemotherapy-induced ovarian follicular depletion in women of fertile age. Fertil Steril. 2010 Jun;94(1):156-66.

138. Filippi F, Meazza C, Paffoni A, Raspagliesi F, Terenziani M, Somigliana E. Egg Freezing in Childhood and Young Adult Cancer Survivors. Pediatrics. 2016 Oct;138(4):10.1542/peds.2016-0291.

139. Meirow D, Epstein M, Lewis H, Nugent D, Gosden RG. Administration of cyclophosphamide at different stages of follicular maturation in mice: effects on reproductive performance and fetal malformations. Hum Reprod. 2001 Apr;16(4):632-7.

140. Barekati Z, Gourabi H, Valojerdi MR, Yazdi PE. Previous maternal chemotherapy by cyclophosphamide (Cp) causes numerical chromosome abnormalities in preimplantation mouse embryos. Reprod Toxicol. 2008 Nov-Dec;26(3-4):278-81.

141. Perez GI, Knudson CM, Leykin L, Korsmeyer SJ, Tilly JL. Apoptosis-associated signaling pathways are required for chemotherapy-mediated female germ cell destruction. Nat Med. 1997 Nov;3(11):1228-32.

142. Petrillo SK, Desmeules P, Truong TQ, Devine PJ. Detection of DNA damage in oocytes of small ovarian follicles following phosphoramide mustard exposures of cultured rodent ovaries in vitro. Toxicol Appl Pharmacol. 2011 Jun 1;253(2):94-102.

143. Soleimani R, Heytens E, Darzynkiewicz Z, Oktay K. Mechanisms of chemotherapy-induced human ovarian aging: double strand DNA breaks and microvascular compromise. Aging (Albany NY). 2011 Aug;3(8):782-93.

144. Yuksel A, Bildik G, Senbabaoglu F, Akin N, Arvas M, Unal F, et al. The magnitude of gonadotoxicity of chemotherapy drugs on ovarian follicles and granulosa cells varies depending upon the category of the drugs and the type of granulosa cells. Hum Reprod. 2015 Dec;30(12):2926-35.

145. Patel B, Meeks H, Wan Y, Johnstone EB, Glenn M, Smith KR, et al. Transgenerational effects of chemotherapy: Both male and female children born to women exposed to chemotherapy have fewer children. Cancer Epidemiol. 2018 Oct;56:1-5.

146. Di Emidio G, D'Aurora M, Placidi M, Franchi S, Rossi G, Stuppia L, et al. Pre-conceptional maternal exposure to cyclophosphamide results in modifications of DNA methylation in F1

and F2 mouse oocytes: evidence for transgenerational effects. Epigenetics. 2019 Nov;14(11):1057-64.

147. Ben-Aharon I, Shalgi R. What lies behind chemotherapy-induced ovarian toxicity? Reproduction. 2012 Aug;144(2):153-63.

148. Bar-Joseph H, Ben-Aharon I, Tzabari M, Tsarfaty G, Stemmer SM, Shalgi R. In vivo bioimaging as a novel strategy to detect doxorubicin-induced damage to gonadal blood vessels. PLoS One. 2011;6(9):e23492.

149. Ben-Aharon I, Meizner I, Granot T, Uri S, Hasky N, Rizel S, et al. Chemotherapy-induced ovarian failure as a prototype for acute vascular toxicity. Oncologist. 2012;17(11):1386-93.

150. Buigues A, Marchante M, Herraiz S, Pellicer A. Diminished Ovarian Reserve Chemotherapy-Induced Mouse Model: A Tool for the Preclinical Assessment of New Therapies for Ovarian Damage. Reproductive Sciences. 2020;8:1609-19.

151. Slater CA, Liang MH, McCune JW, Christman GM, Laufer MR. Preserving ovarian function in patients receiving cyclophosphamide. Lupus. 1999;8(1):3-10.

152. Meirow D, Dor J, Kaufman B, Shrim A, Rabinovici J, Schiff E, et al. Cortical fibrosis and blood-vessels damage in human ovaries exposed to chemotherapy. Potential mechanisms of ovarian injury. Hum Reprod. 2007 Jun;22(6):1626-33.

153. Spears N, Lopes F, Stefansdottir A, Rossi V, De Felici M, Anderson RA, et al. Ovarian damage from chemotherapy and current approaches to its protection. Hum Reprod Update. 2019;25:673-93.

154. Bolcun-Filas E, Rinaldi VD, White ME, Schimenti JC. Reversal of female infertility by Chk2 ablation reveals the oocyte DNA damage checkpoint pathway. Science. 2014 Jan 31;343(6170):533-6.

155. Tuppi M, Kehrloesser S, Coutandin DW, Rossi V, Luh LM, Strubel A, et al. Oocyte DNA damage quality control requires consecutive interplay of CHK2 and CK1 to activate p63. Nat Struct Mol Biol. 2018 Mar;25(3):261-9.

156. Khanna KK, Jackson SP. DNA double-strand breaks: signaling, repair and the cancer connection. Nat Genet. 2001 Mar;27(3):247-54.

157. Ganesan S, Keating AF. Phosphoramide mustard exposure induces DNA adduct formation and the DNA damage repair response in rat ovarian granulosa cells. Toxicol Appl Pharmacol. 2015 Feb 1;282(3):252-8.

158. Fu D, Calvo JA, Samson LD. Balancing repair and tolerance of DNA damage caused by alkylating agents. Nat Rev Cancer. 2012 Jan 12;12(2):104-20.

159. Kim SY, Nair DM, Romero M, Serna VA, Koleske AJ, Woodruff TK, et al. Transient inhibition of p53 homologs protects ovarian function from two distinct apoptotic pathways triggered by anticancer therapies. Cell Death Differ. 2019 Mar;26(3):502-15.

160. Bellusci G, Mattiello L, Iannizzotto V, Ciccone S, Maiani E, Villani V, et al. Kinase-independent inhibition of cyclophosphamide-induced pathways protects the ovarian reserve and prolongs fertility. Cell Death Dis. 2019 Sep 27;10(10):726,019-1961-y.

161. Bar-Joseph H, Ben-Aharon I, Rizel S, Stemmer SM, Tzabari M, Shalgi R. Doxorubicin-induced apoptosis in germinal vesicle (GV) oocytes. Reprod Toxicol. 2010 Dec;30(4):566-72.

162. Zhao XJ, Huang YH, Yu YC, Xin XY. GnRH antagonist cetrorelix inhibits mitochondria-dependent apoptosis triggered by chemotherapy in granulosa cells of rats. Gynecol Oncol. 2010 Jul;118(1):69-75.

163. Zhang T, He WH, Feng LL, Huang HG. Effect of doxorubicin-induced ovarian toxicity on mouse ovarian granulosa cells. Regul Toxicol Pharmacol. 2017 Jun;86:1-10.

164. Luo Q, Yin N, Zhang L, Yuan W, Zhao W, Luan X, et al. Role of SDF-1/CXCR4 and cytokines in the development of ovary injury in chemotherapy drug induced premature ovarian failure mice. Life Sci. 2017 Jun 15;179:103-9.

165. Goldman KN, Chenette D, Arju R, Duncan FE, Keefe DL, Grifo JA, et al. MTORC1/2 inhibition preserves ovarian function and fertility during genotoxic chemotherapy. Proc Natl Acad Sci U S A. 2017.

166. Chang EM, Lim E, Yoon S, Jeong K, Bae S, Lee DR, et al. Cisplatin Induces Overactivation of the Dormant Primordial Follicle through PTEN/AKT/FOXO3a Pathway which Leads to Loss of Ovarian Reserve in Mice. PLoS One. 2015 Dec 14;10(12):e0144245.

167. Wang Y, Liu M, Johnson SB, Yuan G, Arriba AK, Zubizarreta ME, et al. Doxorubicin obliterates mouse ovarian reserve through both primordial follicle atresia and overactivation. Toxicol Appl Pharmacol. 2019;381:114714.

168. Gawriluk TR, Hale AN, Flaws JA, Dillon CP, Green DR, Rucker EB,3rd. Autophagy is a cell survival program for female germ cells in the murine ovary. Reproduction. 2011 Jun;141(6):759-65.

169. Sonigo C, Beau I, Grynberg M, Binart N. AMH prevents primordial ovarian follicle loss and fertility alteration in cyclophosphamide-treated mice. FASEB Journal. 2019.

170. Kerr JB, Hutt KJ, Michalak EM, Cook M, Vandenberg CJ, Liew SH, et al. DNA damage-induced primordial follicle oocyte apoptosis and loss of fertility require TAp63-mediated induction of Puma and Noxa. Mol Cell. 2012 Nov 9;48(3):343-52.

171. Nguyen QN, Zerafa N, Liew SH, Morgan FH, Strasser A, Scott CL, et al. Loss of PUMA protects the ovarian reserve during DNA-damaging chemotherapy and preserves fertility. Cell Death Dis. 2018 May 23;9(6):618,018-0633-7.

172. Morgan S, Lopes F, Gourley C, Anderson RA, Spears N. Cisplatin and doxorubicin induce distinct mechanisms of ovarian follicle loss; imatinib provides selective protection only against cisplatin. PLoS One. 2013 Jul 29;8(7):e70117.

173. Salih SM, Ringelstetter AK, Elsarrag MZ, Abbott DH, Roti EC. Dexrazoxane abrogates acute doxorubicin toxicity in marmoset ovary. Biol Reprod. 2015 Mar;92(3):73.

174. Li X, Yang S, Lv X, Sun H, Weng J, Liang Y, et al. The mechanism of mesna in protection from cisplatin-induced ovarian damage in female rats. J Gynecol Oncol. 2013 Apr;24(2):177-85.

175. Barberino RS, Menezes VG, Ribeiro AEAS, Palheta RC,Jr, Jiang X, Smitz JEJ, et al. Melatonin protects against cisplatin-induced ovarian damage in mice via the MT1 receptor and antioxidant activity. Biol Reprod. 2017 Jun 1;96(6):1244-55.

176. Jang H, Lee OH, Lee Y, Yoon H, Chang EM, Park M, et al. Melatonin prevents cisplatin-induced primordial follicle loss via suppression of PTEN/AKT/FOXO3a pathway activation in the mouse ovary. J Pineal Res. 2016 Apr;60(3):336-47.

177. Zhou L, Xie Y, Li S, Liang Y, Qiu Q, Lin H, et al. Rapamycin Prevents cyclophosphamide-induced Over-activation of Primordial Follicle pool through PI3K/Akt/mTOR Signaling Pathway in vivo. Journal of Ovarian Research. 2017;52:161-70.

178. Pascuali N, Scotti L, Di Pietro M, Oubina G, Bas D, May M, et al. Ceramide-1-phosphate has protective properties against cyclophosphamide-induced ovarian damage in a mice model of premature ovarian failure. Hum Reprod. 2018 May 1;33(5):844-59.

179. Tan SJ, Lee LJ, Tzeng CR, Wang CW, Hsu MI, Chen CH. Targeted anti-apoptosis activity for ovarian protection against chemotherapy-induced ovarian gonadotoxicity. Reprod Biomed Online. 2014 Nov;29(5):612-20.

180. Stringer JM, Winship A, Zerafa N, Wakefield M, Hutt K. Oocytes can efficiently repair DNA double-strand breaks to restore genetic integrity and protect offspring health. Proc Natl Acad Sci U S A. 2020 May 26;117(21):11513-22.

181. McLaren JF, Bates GW. Fertility preservation in women of reproductive age with cancer. Am J Obstet Gynecol. 2012 Dec;207(6):455-62.

182. Practice Committee of the American Society for Reproductive Medicine. Electronic address: asrm@asrm.org. Fertility preservation in patients undergoing gonadotoxic therapy or gonadectomy: a committee opinion. Fertil Steril. 2019 Dec;112(6):1022-33.

183. ESHRE Guideline Group on Female Fertility Preservation, Anderson RA, Amant F, Braat D, D'Angelo A, Chuva de Sousa Lopes SM, et al. ESHRE guideline: female fertility preservation. Hum Reprod Open. 2020 Nov 14;2020(4):hoaa052.

184. Paradisi R, Macciocca M, Vicenti R, Rossi S, Morselli-Labate AM, Mastroroberto M, et al. New insights in the selection and management of cancer patients applicants for ovarian tissue cryopreservation. Gynecol Endocrinol. 2016 Nov;32(11):881-5.

185. Wallace WH, Kelsey TW, Anderson RA. Fertility preservation in pre-pubertal girls with cancer: the role of ovarian tissue cryopreservation. Fertil Steril. 2016 Jan;105(1):6-12.

186. Yee S. Factors associated with the receipt of fertility preservation services along the decision-making pathway in young Canadian female cancer patients. J Assist Reprod Genet. 2016 Feb;33(2):265-80.

187. Partridge AH, Gelber S, Peppercorn J, Sampson E, Knudsen K, Laufer M, et al. Web-based survey of fertility issues in young women with breast cancer. J Clin Oncol. 2004 Oct 15;22(20):4174-83.

188. Banerjee R, Tsiapali E. Occurrence and recall rates of fertility discussions with young breast cancer patients. Support Care Cancer. 2016 Jan;24(1):163-71.

189. Quinn GP, Vadaparampil ST, King L, Miree CA, Wilson C, Raj O, et al. Impact of physicians' personal discomfort and patient prognosis on discussion of fertility preservation with young cancer patients. Patient Educ Couns. 2009 Dec;77(3):338-43.

190. Trounson A, Mohr L. Human pregnancy following cryopreservation, thawing and transfer of an eight-cell embryo. Nature. 1983 Oct 20-26;305(5936):707-9.

191. Warner E, Glass K, Foong S, Sandwith E. Update on fertility preservation for younger women with breast cancer. CMAJ. 2020 Aug 31;192(35):E1003-9.

192. Rienzi L, Gracia C, Maggiulli R, LaBarbera AR, Kaser DJ, Ubaldi FM, et al. Oocyte, embryo and blastocyst cryopreservation in ART: systematic review and meta-analysis comparing slow-freezing versus vitrification to produce evidence for the development of global guidance. Hum Reprod Update. 2017 Mar 1;23(2):139-55.

193. Burns KC, Hoefgen H, Strine A, Dasgupta R. Fertility preservation options in pediatric and adolescent patients with cancer. Cancer. 2018 May 1;124(9):1867-76.

194. Rienzi L, Romano S, Albricci L, Maggiulli R, Capalbo A, Baroni E, et al. Embryo development of fresh 'versus' vitrified metaphase II oocytes after ICSI: a prospective randomized sibling-oocyte study. Hum Reprod. 2010 Jan;25(1):66-73.

195. Sole M, Santalo J, Boada M, Clua E, Rodriguez I, Martinez F, et al. How does vitrification affect oocyte viability in oocyte donation cycles? A prospective study to compare outcomes achieved with fresh versus vitrified sibling oocytes. Hum Reprod. 2013 Aug;28(8):2087-92.

196. Dolmans MM, Hollanders de Ouderaen S, Demylle D, Pirard C. Utilization rates and results of long-term embryo cryopreservation before gonadotoxic treatment. J Assist Reprod Genet. 2015 Aug;32(8):1233-7.

197. Cobo A, Garcia-Velasco J, Domingo J, Pellicer A, Remohi J. Elective and Onco-fertility preservation: factors related to IVF outcomes. Hum Reprod. 2018 Dec 1;33(12):2222-31.

198. Dolmans MM, Donnez J. Fertility preservation in women for medical and social reasons: Oocytes vs ovarian tissue. Best Pract Res Clin Obstet Gynaecol. 2021 Jan;70:63-80.

199. Donnez J, Dolmans MM. Fertility Preservation in Women. N Engl J Med. 2017 Oct 26;377(17):1657-65.

200. Dolmans MM, von Wolff M, Poirot C, Diaz-Garcia C, Cacciottola L, Boissel N, et al. Transplantation of cryopreserved ovarian tissue in a series of 285 women: a review of five leading European centers. Fertil Steril. 2021 May;115(5):1102-15.

201. Jensen AK, Macklon KT, Fedder J, Ernst E, Humaidan P, Andersen CY. 86 Successful Births and 9 Ongoing Pregnancies Worldwide in Women Transplanted with Frozen-Thawed Ovarian Tissue: Focus on Birth and Perinatal Outcome in 40 of these Children. J Assist Reprod Genet. 2017 Mar;34(3):325-36.

202. Oktay K, Bedoschi G, Pacheco F, Turan V, Emirdar V. First pregnancies, live birth, and in vitro fertilization outcomes after transplantation of frozen-banked ovarian tissue with a human extracellular matrix scaffold using robot-assisted minimally invasive surgery. Am J Obstet Gynecol. 2016 Jan;214(1):94.e1,94.e9.

203. Meirow D, Assad G, Dor J, Rabinovici J. The GnRH antagonist cetrorelix reduces cyclophosphamide-induced ovarian follicular destruction in mice. Hum Reprod. 2004 Jun;19(6):1294-9.

204. Tan SL, Zaidi J, Campbell S, Doyle P, Collins W. Blood flow changes in the ovarian and uterine arteries during the normal menstrual cycle. Am J Obstet Gynecol. 1996 Sep;175(3 Pt 1):625-31.

205. Faddy MJ, Gosden RG. A mathematical model of follicle dynamics in the human ovary. Hum Reprod. 1995 Apr;10(4):770-5.

206. Blumenfeld Z. How to preserve fertility in young women exposed to chemotherapy? The role of GnRH agonist cotreatment in addition to cryopreservation of embrya, oocytes, or ovaries. Oncologist. 2007(12(9)):1044-54.

207. Hasky N, Uri-Belapolsky S, Goldberg K, Miller I, Grossman H, Stemmer SM, et al. Gonadotrophin-releasing hormone agonists for fertility preservation: unraveling the enigma? Hum Reprod. 2015 May;30(5):1089-101.

208. Dolmans MM, Taylor HS, Rodriguez-Wallberg KA, Blumenfeld Z, Lambertini M, von Wolff M, et al. Utility of gonadotropin-releasing hormone agonists for fertility preservation in women receiving chemotherapy: pros and cons. Fertil Steril. 2020 Oct;114(4):725-38.

209. Lambertini M, Boni L, Michelotti A, Gamucci T, Scotto T, Gori S, et al. Ovarian Suppression With Triptorelin During Adjuvant Breast Cancer Chemotherapy and Long-term Ovarian Function, Pregnancies, and Disease-Free Survival: A Randomized Clinical Trial. JAMA. 2015 Dec 22-29;314(24):2632-40.

210. Lambertini M, Moore HCF, Leonard RCF, Loibl S, Munster P, Bruzzone M, et al. Gonadotropin-Releasing Hormone Agonists During Chemotherapy for Preservation of Ovarian Function and Fertility in Premenopausal Patients With Early Breast Cancer: A Systematic Review and Meta-Analysis of Individual Patient-Level Data. J Clin Oncol. 2018 May 2:JCO2018780858.

211. Moore HCF, Unger JM, Phillips KA, Boyle F, Hitre E, Moseley A, et al. Final Analysis of the Prevention of Early Menopause Study (POEMS)/SWOG Intergroup S0230. J Natl Cancer Inst. 2019 Feb 1;111(2):210-3.

212. Meng Y, Xu Z, Wu F, Chen W, Xie S, Liu J, et al. Sphingosine-1-phosphate suppresses cyclophosphamide induced follicle apoptosis in human fetal ovarian xenografts in nude mice. Fertil Steril. 2014 Sep;102(3):871,877.e3.

213. Kerr JB, Hutt KJ, Cook M, Speed TP, Ster A, Findlay JK, et al. Cisplatin-induced primordial follicle oocyte killing and loss of fertility are not prevented by imatinib. Nat Med. 2012 Aug;18(8):1170,2; author reply 1172-4.

214. Zamah AM, Mauro MJ, Druker BJ, Oktay K, Egorin MJ, Cedars MI, et al. Will imatinib compromise reproductive capacity? Oncologist. 2011;16(10):1422-7.

215. Kano M, Sosulski AE, Zhang L, Saatcioglu HD, Wang D, Nagykery N, et al. AMH/MIS as a contraceptive that protects the ovarian reserve during chemotherapy. Proc Natl Acad Sci U S A. 2017 Feb 28;114(9):E1688-97.

216. Roness H, Spector I, Leichtmann-Bardoogo Y, Savino AM, Dereh-Haim S, Meirow D. Pharmacological administration of recombinant human AMH rescues ovarian reserve and preserves fertility in a mouse model of chemotherapy, without interfering with anti-tumoural effects. J Assist Reprod Genet. 2019 Sep;36(9):1793-803.

217. Di Emidio G, Rossi G, Bonomo I, Alonso GL, Sferra R, Vetuschi A, et al. The Natural Carotenoid Crocetin and the Synthetic Tellurium Compound AS101 Protect the Ovary against Cyclophosphamide by Modulating SIRT1 and Mitochondrial Markers. Oxid Med Cell Longev. 2017;2017:8928604.

218. Piasecka-Srader J, Blanco FF, Delman DH, Dixon DA, Geiser JL, Ciereszko RE, et al. Tamoxifen prevents apoptosis and follicle loss from cyclophosphamide in cultured rat ovaries. Biol Reprod. 2015 May;92(5):132.

219. Ozcan P, Ficicioglu C, Yildirim OK, Ozkan F, Akkaya H, Aslan I. Protective effect of resveratrol against oxidative damage to ovarian reserve in female Sprague-Dawley rats. Reprod Biomed Online. 2015 Sep;31(3):404-10.

220. Skaznik-Wikiel ME, McGuire MM, Sukhwani M, Donohue J, Chu T, Krivak TC, et al. Granulocyte colony-stimulating factor with or without stem cell factor extends time to premature ovarian insufficiency in female mice treated with alkylating chemotherapy. Fertil Steril. 2013 Jun;99(7):2045,54.e3.

221. Pandir D, Kara O, Kara M. Protective effect of bilberry (Vaccinium myrtillus L.) on cisplatin induced ovarian damage in rat. Cytotechnology. 2014 Aug;66(4):677-85.

222. Altuner D, Gulaboglu M, Yapca OE, Cetin N. The effect of mirtazapine on cisplatin-induced oxidative damage and infertility in rat ovaries. ScientificWorldJournal. 2013 Apr 22;2013:327240.

223. Taskin MI, Yay A, Adali E, Balcioglu E, Inceboz U. Protective effects of sildenafil citrate administration on cisplatin-induced ovarian damage in rats. Gynecol Endocrinol. 2015 Apr;31(4):272-7.

224. Melekoglu R, Ciftci O, Eraslan S, Cetin A, Basak N. Beneficial effects of curcumin and capsaicin on cyclophosphamide-induced premature ovarian failure in a rat model. J Ovarian Res. 2018 Apr 26;11(1):33,018-0409-9.

225. Li F, Turan V, Lierman S, Cuvelier C, De Sutter P, Oktay K. Sphingosine-1-phosphate prevents chemotherapy-induced human primordial follicle death. Hum Reprod. 2014 Jan;29(1):107-13.

226. Akdemir A, Zeybek B, Akman L, Ergenoglu AM, Yeniel AO, Erbas O, et al. Granulocyte-colony stimulating factor decreases the extent of ovarian damage caused by cisplatin in an experimental rat model. J Gynecol Oncol. 2014 Oct;25(4):328-33.

227. Brayboy LM, Oulhen N, Witmyer J, Robins J, Carson S, Wessel GM. Multidrug-resistant transport activity protects oocytes from chemotherapeutic agents and changes during oocyte maturation. Fertil Steril. 2013 Nov;100(5):1428-35.

228. Brayboy LM, Oulhen N, Long S, Voigt N, Raker C, Wessel GM. Multidrug resistance transporter-1 and breast cancer resistance protein protect against ovarian toxicity, and are essential in ovarian physiology. Reprod Toxicol. 2017 Apr;69:121-31.

229. Ting AY, Petroff BK. Tamoxifen decreases ovarian follicular loss from experimental toxicant DMBA and chemotherapy agents cyclophosphamide and doxorubicin in the rat. J Assist Reprod Genet. 2010 Nov;27(11):591-7.

230. Kropp J, Roti Roti EC, Ringelstetter A, Khatib H, Abbott DH, Salih SM. Dexrazoxane Diminishes Doxorubicin-Induced Acute Ovarian Damage and Preserves Ovarian Function and Fecundity in Mice. PLoS One. 2015 Nov 6;10(11):e0142588.

231. Rinaldi VD, Hsieh K, Munroe R, Bolcun-Filas E, Schimenti JC. Pharmacological Inhibition of the DNA Damage Checkpoint Prevents Radiation-Induced Oocyte Death. Genetics. 2017 Aug;206(4):1823-8.

232. Tanaka Y, Kimura F, Zheng L, Kaku S, Takebayashi A, Kasahara K, et al. Protective effect of a mechanistic target of rapamycin inhibitor on an in vivo model ofcisplatin-induced ovarian gonadotoxicity. Exp Anim. 2018 Nov 1;67(4):493-500.

233. Roti Roti EC, Ringelstetter AK, Kropp J, Abbott DH, Salih SM. Bortezomib prevents acute doxorubicin ovarian insult and follicle demise, improving the fertility window and pup birth weight in mice. PLoS One. 2014 Sep 24;9(9):e108174.

234. Gremeau AS, Andreadis N, Fatum M, Craig J, Turner K, McVeigh E, et al. In vitro maturation or in vitro fertilization for women with polycystic ovaries? A case-control study of 194 treatment cycles. Fertil Steril. 2012 Aug;98(2):355-60.

235. Telfer EE, McLaughlin M, Ding C, Thong KJ. A two-step serum-free culture system supports development of human oocytes from primordial follicles in the presence of activin. Hum Reprod. 2008 May;23(5):1151-8.

236. Fasano G, Moffa F, Dechène J, Englert Y, Demeestere I. Vitrification of in vitro matured oocytes collected from antral follicles at the time of ovarian tissue cryopreservation. Reprod Biol Endocrinol. 2011;9:150.

237. Prasath EB, Chan MLH, Wong WHW, Lim CJW, Tharmalingam MD, Hendricks M, et al. First pregnancy and live birth resulting from cryopreserved embryos obtained from in vitro matured oocytes after oophorectomy in an ovarian cancer patient. Hum Reprod. 2014;29(2):276-8.

238. Hourvitz A, Yerushalmi GM, Maman E, Raanani H, Elizur S, Brengauz M, et al. Combination of ovarian tissue harvesting and immature oocyte collection for fertility preservation increases preservation yield. Reprod Biomed Online. 2015;31(4):497-505.

239. Segers I, Bardhi E, Mateizel I, Van Moer E, Schots R, Verheyen G, et al. Live births following fertility preservation using in-vitro maturation of ovarian tissue oocytes. Hum Reprod. 2020 Sep 1;35(9):2026-36.

240. Laronda MM, Rutz AL, Xiao S, Whelan KA, Duncan FE, Roth EW, et al. A bioprosthetic ovary created using 3D printed microporous scaffolds restores ovarian function in sterilized mice. Nat Commun. 2017 May 16;8:15261.

241. Saatcioglu HD, Cuevas I, Castrillon DH. Control of Oocyte Reawakening by Kit. PLoS Genet. 2016 Aug 8;12(8):e1006215.

242. Lees-Murdock DJ, Lau HT, Castrillon DH, De Felici M, Walsh CP. DNA methyltransferase loading, but not de novo methylation, is an oocyte-autonomous process stimulated by SCF signalling. Dev Biol. 2008 Sep 1;321(1):238-50.

243. Griffin J, Emery BR, Huang I, Peterson CM, Carrell DT. Comparative analysis of follicle morphology and oocyte diameter in four mammalian species (mouse, hamster, pig, and human). J Exp Clin Assist Reprod. 2006 Mar 1;3:2,1050-3-2.

244. Dath C, Van Eyck AS, Dolmans MM, Romeu L, Delle Vigne L, Donnez J, et al. Xenotransplantation of human ovarian tissue to nude mice: Comparison between four grafting sites. Human Reproduction. 2010;25:1734-43.

245. Coticchio G, Guglielmo MC, Dal Canto M, Fadini R, Mignini Renzini M, De Ponti E, et al. Mechanistic foundations of the metaphase II spindle of human oocytes matured in vivo and in vitro. Hum Reprod. 2013;28:3271-82.

246. Matzuk MM, Burns KH, Viveiros MM, Eppig JJ. Intercellular communication in the mammalian ovary: oocytes carry the conversation. Science. 2002 Jun 21;296(5576):2178-80.

247. Livak KJ, Schmittgen TD. Analysis of relative gene expression data using real-time quantitative PCR and the 2-ΔΔCT method. Methods. 2001;25:402-8.

248. Ji J, Zhang Y, Redon CE, Reinhold WC, Chen AP, Fogli LK, et al. Phosphorylated fraction of H2AX as a measurement for DNA damage in cancer cells and potential applications of a novel assay. PLoS One. 2017 Feb 3;12(2):e0171582.

249. Kumagai K, Kubota N, Saito TI, Sasako T, Takizawa R, Sudo K, et al. Generation of Transgenic Mice on an NOD/SCID Background Using the Conventional Microinjection Technique. Biol Reprod. 2011;84:682-8.

250. Brydoy M, Fossa SD, Dahl O, Bjoro T. Gonadal dysfunction and fertility problems in cancer survivors. Acta Oncol. 2007;46(4):480-9.

251. Leal AD, Van Houten H, Sangaralingham L, Freedman RA, Jemal A, Neuman HB, et al. Breast Cancer Survivorship Care Variations Between Adjuvant Chemotherapy Regimens. Clinical Breast Cancer. 2018;18:e513-e520.

252. Grigg AP, McLachlan R, Zajac J, Szer J. Reproductive status in long-term bone marrow transplant survivors receiving busulfan-cyclophosphamide (120 mg/kg). Bone Marrow Transplant. 2000;26:1089-95.

253. Del Castillo LM, Buigues A, Rossi V, Soriano MJ, Martinez J, De Felici M, et al. The cyto-protective effects of LH on ovarian reserve and female fertility during exposure to gonadotoxic alkylating agents in an adult mouse model. Hum Reprod. 2021 Aug 1;36(9):2514-28.

254. Petrillo SK, Desmeules P, Truong TQ, Devine PJ. Detection of DNA damage in oocytes of small ovarian follicles following phosphoramide mustard exposures of cultured rodent ovaries in vitro. Toxicol Appl Pharmacol. 2011;253:94-102.

255. Soleimani R, Heytens E, Darzynkiewicz Z, Oktay K. Mechanisms of chemotherapy-induced human ovarian aging: double strand DNA breaks and microvascular compromise. Aging. 2011;3:782-93.

256. Yacobi K, Wojtowicz A, Tsafriri A, Gross A. Gonadotropins enhance caspase-3 and -7 activity and apoptosis in the theca-interstitial cells of rat preovulatory follicles in culture. Endocrinology. 2004 Apr;145(4):1943-51.

257. Zhu S, Herraiz S, Yue J, Zhang M, Wan H, Yang Q, et al. 3D NIR-II Molecular Imaging Distinguishes Targeted Organs with High-Performance NIR-II Bioconjugates. Adv Mater. 2018 Mar;30(13):e1705799.

258. Yung Y, Aviel-Ronen S, Maman E, Rubinstein N, Avivi C, Orvieto R, et al. Localization of luteinizing hormone receptor protein in the human ovary. Mol Hum Reprod. 2014 Sep;20(9):844-9.

259. Scaruffi P, Stigliani S, Cardinali B, Massarotti C, Lambertini M, Sozzi F, et al. Gonadotropin Releasing Hormone Agonists Have an Anti-apoptotic Effect on Cumulus Cells. Int J Mol Sci. 2019 Nov 30;20(23):6045.

260. Chang EM, Lim E, Yoon S, Jeong K, Bae S, Lee DR, et al. Cisplatin induces overactivation of the dormant primordial follicle through PTEN/AKT/FOXO3α pathway which leads to loss of ovarian reserve in mice. PLoS ONE. 2015;10:e0144245.

261. Orren DK, Petersen LN, Bohr VA. Persistent DNA damage inhibits S-phase and G2 progression, and results in apoptosis. Mol Biol Cell. 1997;8:1129-42.

262. Biechonski S, Olender L, Zipin-Roitman A, Yassin M, Aqaqe N, Marcu-Malina V, et al. Attenuated DNA damage responses and increased apoptosis characterize human hematopoietic stem cells exposed to irradiation. Scientific Reports. 2018;8:6071.

263. Cari EL, Hagen-Lillevik S, Giornazi A, Post M, Komar AA, Appiah L, et al. Integrated stress response control of granulosa cell translation and proliferation during normal ovarian follicle development. Mol Hum Reprod. 2021 Jul 26.

264. Marcozzi S, Rossi V, Salvatore G, Di Rella F, De Felici M, Klinger FG. Distinct effects of epirubicin, cisplatin and cyclophosphamide on ovarian somatic cells of prepuberal ovaries. Aging. 2019;11:10532-56.

265. Hu J, Zhang Z, Zhao L, Li L, Zuo W, Han L. High expression of RAD51 promotes DNA damage repair and survival in KRAS-mutant lung cancer cells. BMB Reports. 2019;52(2):151-6.

266. Kujjo LL, Laine T, Pereira RJG, Kagawa W, Kurumizaka H, Yokoyama S, et al. Enhancing survival of mouse oocytes following chemotherapy or aging by targeting bax and Rad51. PLoS ONE. 2010;5:e9204.

267. Kujjo LL, Ronningen R, Ross P, Pereira RJG, Rodriguez R, Beyhan Z, et al. RAD51 Plays a Crucial Role in Halting Cell Death Program Induced by Ionizing Radiation in Bovine Oocytes1. Biol Reprod. 2012;86:76.

268. Yamamoto A, Taki T, Yagi H, Habu T, Yoshida K, Yoshimura Y, et al. Cell cycle-dependent expression of the mouse Rad51 gene in proliferating cells. Mol Gen Genet. 1996 Apr 24;251(1):1-12.

269. Goedecke W, Vielmetter W, Pfeiffer P. Activation of a system for the joining of nonhomologous DNA ends during Xenopus egg maturation. Mol Cell Biol. 1992 Feb;12(2):811-6.

270. Hagmann M, Adlkofer K, Pfeiffer P, Bruggmann R, Georgiev O, Rungger D, et al. Dramatic changes in the ratio of homologous recombination to nonhomologous DNA-end joining in oocytes and early embryos of Xenopus laevis. Biol Chem Hoppe Seyler. 1996 Apr;377(4):239-50.

271. Karimian A, Mir SM, Parsian H, Refieyan S, Mirza-Aghazadeh-Attari M, Yousefi B, et al. Crosstalk between Phosphoinositide 3-kinase/Akt signaling pathway with DNA damage response and oxidative stress in cancer. J Cell Biochem. 2019;120:10248-72.

272. Maidarti M, Anderson RA, Telfer EE. Crosstalk between PTEN/PI3K/Akt Signalling and DNA Damage in the Oocyte: Implications for Primordial Follicle Activation, Oocyte Quality and Ageing. Cells. 2020;9:200.

273. Shen WH, Balajee AS, Wang J, Wu H, Eng C, Pandolfi PP, et al. Essential Role for Nuclear PTEN in Maintaining Chromosomal Integrity. Cell. 2007;128:157-70.

274. Plo I, Laulier C, Gauthier L, Lebrun F, Calvo F, Lopez BS. AKT1 inhibits homologous recombination by inducing cytoplasmic retention of BRCA1 and RAD5. Cancer Res. 2008;68:9404-12.

275. Maidarti M, Clarkson YL, Mclaughlin M, Anderson RA, Telfer EE. Inhibition of PTEN activates bovine non-growing follicles in vitro but increases DNA damage and reduces DNA repair response. Human Reproduction. 2019;34:297-307.

276. Matikainen T, Perez GI, Zheng TS, Kluzak TR, Rueda BR, Flavell RA, et al. Caspase-3 gene knockout defines cell lineage specificity for programmed cell death signaling in the ovary. Endocrinology. 2001;142:2468-80.

277. Takai Y, Matikainen T, Jurisicova A, Kim MR, Trbovich AM, Fujita E, et al. Caspase-12 compensates for lack of caspase-2 and caspase-3 in female germ cells. Apoptosis. 2007;12:791-800.

278. Xia L, Wen H, Han X, Tang J, Huang Y. Luteinizing hormone inhibits cisplatin-induced apoptosis in human epithelial ovarian cancer cells. Oncol Lett. 2016 Mar;11(3):1943-7.

279. Wang X, Zou P, He Y, Meng K, Quan F, Zhang Y. Effect of luteinizing hormone on goat theca cell apoptosis and steroidogenesis through activation of the PI3K/AKT pathway. Anim Reprod Sci. 2018 Mar;190:108-18.

280. Lee YJ, Soh JW, Jeoung DI, Cho CK, Jhon GJ, Lee SJ, et al. PKC epsilon -mediated ERK1/2 activation involved in radiation-induced cell death in NIH3T3 cells. Biochim Biophys Acta. 2003 Feb 17;1593(2-3):219-29.

281. Tang D, Wu D, Hirao A, Lahti JM, Liu L, Mazza B, et al. ERK activation mediates cell cycle arrest and apoptosis after DNA damage independently of p53. J Biol Chem. 2002 Apr 12;277(15):12710-7.

282. Yeh PY, Chuang SE, Yeh KH, Song YC, Chang LL, Cheng AL. Phosphorylation of p53 on Thr55 by ERK2 is necessary for doxorubicin-induced p53 activation and cell death. Oncogene. 2004 Apr 29;23(20):3580-8.

283. DeHaan RD, Yazlovitskaya EM, Persons DL. Regulation of p53 target gene expression by cisplatin-induced extracellular signal-regulated kinase. Cancer Chemother Pharmacol. 2001 Nov;48(5):383-8.

284. Mukherjee S, Dash S, Lohitesh K, Chowdhury R. The dynamic role of autophagy and MAPK signaling in determining cell fate under cisplatin stress in osteosarcoma cells. PLoS One. 2017 Jun 9;12(6):e0179203.

285. Haas B, Klinger V, Keksel C, Bonigut V, Kiefer D, Caspers J, et al. Inhibition of the PI3K but not the MEK/ERK pathway sensitizes human glioma cells to alkylating drugs. Cancer Cell Int. 2018 May 4;18:69,018-0565-4. eCollection 2018.

286. Wei F, Yan J, Tang D, Lin X, He L, Xie Y, et al. Inhibition of ERK activation enhances the repair of double-stranded breaks via non-homologous end joining by increasing DNA-PKcs activation. Biochimica et Biophysica Acta - Molecular Cell Research. 2013;1833:90-100.

287. Zhang T, Yan D, Yang Y, Ma A, Li L, Wang Z, et al. The comparison of animal models for premature ovarian failure established by several different source of inducers. Regulatory Toxicology and Pharmacology. 2016;81:223-32.

288. Kim YY, Kim WO, Liu HC, Rosenwaks Z, Kim JW, Ku SY. Effects of paclitaxel and cisplatin on in vitro ovarian follicle development. Arch Med Sci. 2019 Oct;15(6):1510-9.

289. Van Blerkom J. Occurrence and developmental consequences of aberrant cellular organization in meiotically mature human oocytes after exogenous ovarian hyperstimulation. J Electron Microsc Tech. 1990 Dec;16(4):324-46.

290. Wallbutton S, Kasraie J. Vacuolated oocytes: fertilization and embryonic arrest following intra-cytoplasmic sperm injection in a patient exhibiting persistent oocyte macro vacuolization--case report. J Assist Reprod Genet. 2010 Apr;27(4):183-8.

291. Brower PT, Schultz RM. Intercellular communication between granulosa cells and mouse oocytes: existence and possible nutritional role during oocyte growth. Dev Biol. 1982 Mar;90(1):144-53.

292. Heller DT, Schultz RM. Ribonucleoside metabolism by mouse oocytes: metabolic cooperativity between the fully grown oocyte and cumulus cells. J Exp Zool. 1980 Dec;214(3):355-64.

293. Haghighat N, Van Winkle LJ. Developmental change in follicular cell-enhanced amino acid uptake into mouse oocytes that depends on intact gap junctions and transport system Gly. J Exp Zool. 1990 Jan;253(1):71-82.

294. Pelland AM, Corbett HE, Baltz JM. Amino Acid transport mechanisms in mouse oocytes during growth and meiotic maturation. Biol Reprod. 2009 Dec;81(6):1041-54.

295. Aasen T, Leithe E, Graham SV, Kameritsch P, Mayan MD, Mesnil M, et al. Connexins in cancer: bridging the gap to the clinic. Oncogene. 2019 Jun;38(23):4429-51.

296. Harrouk W, Robaire B, Hales BF. Paternal exposure to cyclophosphamide alters cell-cell contacts and activation of embryonic transcription in the preimplantation rat embryo. Biol Reprod. 2000 Jul;63(1):74-81.

297. Machell NH, Blaschuk OW, Farookhi R. Developmental expression and distribution of N- and E-cadherin in the rat ovary. Biol Reprod. 2000 Sep;63(3):797-804.

298. Machell NH, Farookhi R. E- and N-cadherin expression and distribution during luteinization in the rat ovary. Reproduction. 2003 Jun;125(6):791-800.

299. De Vries WN, Evsikov AV, Haac BE, Fancher KS, Holbrook AE, Kemler R, et al. Maternal beta-catenin and E-cadherin in mouse development. Development. 2004 Sep;131(18):4435-45.

300. Lin JH, Yang J, Liu S, Takano T, Wang X, Gao Q, et al. Connexin mediates gap junction-independent resistance to cellular injury. J Neurosci. 2003 Jan 15;23(2):430-41.

301. Plotkin LI, Manolagas SC, Bellido T. Transduction of cell survival signals by connexin-43 hemichannels. J Biol Chem. 2002 Mar 8;277(10):8648-57.

302. Chang AS, Dale AN, Moley KH. Maternal diabetes adversely affects preovulatory oocyte maturation, development, and granulosa cell apoptosis. Endocrinology. 2005 May;146(5):2445-53.

303. Johnson ML, Redmer DA, Reynolds LP, Grazul-Bilska AT. Expression of gap junctional proteins connexin 43, 32, and 26 throughout follicular development and atresia in cows. Endocrine. 1999 Feb;10(1):43-51.

304. Krysko DV, Mussche S, Leybaert L, D'Herde K. Gap junctional communication and connexin43 expression in relation to apoptotic cell death and survival of granulosa cells. J Histochem Cytochem. 2004 Sep;52(9):1199-207.

305. Park MR, Choi YJ, Kwon DN, Park C, Bui HT, Gurunathan S, et al. Intraovarian transplantation of primordial follicles fails to rescue chemotherapy injured ovaries. Sci Rep. 2013;3:1384.

306. El-Hayek S, Clarke HJ. Follicle-Stimulating Hormone Increases Gap Junctional Communication Between Somatic and Germ-Line Follicular Compartments During Murine Oogenesis. Biol Reprod. 2015 Aug;93(2):47.

307. Yuksel A, Bildik G, Senbabaoglu F, Akin N, Arvas M, Unal F, et al. The magnitude of gonadotoxicity of chemotherapy drugs on ovarian follicles and granulosa cells varies depenDing upon the category of the drugs and the type of granulosa cells. Human Reproduction. 2015.

308. Winship AL, Carpenter M, Griffiths M, Hutt KJ. Vincristine Chemotherapy Induces Atresia of Growing Ovarian Follicles in Mice. Toxicol Sci. 2019 May 1;169(1):43-53.

309. Buigues A, Marchante M, Herraiz S, Pellicer A. Diminished Ovarian Reserve Chemotherapy-Induced Mouse Model: A Tool for the Preclinical Assessment of New Therapies for Ovarian Damage. Reproductive Sciences. 2019.

310. Zhang T, Yan D, Yang Y, Ma A, Li L, Wang Z, et al. The comparison of animal models for premature ovarian failure established by several different source of inducers. Regul Toxicol Pharmacol. 2016 Nov;81:223-32.

311. Kawashima I, Kawamura K. Regulation of follicle growth through hormonal factors and mechanical cues mediated by Hippo signaling pathway. Syst Biol Reprod Med. 2018 Feb;64(1):3-11.

312. Zhang M, Bener MB, Jiang Z, Wang T, Esencan E, Scott Iii R, et al. Mitofusin 1 is required for female fertility and to maintain ovarian follicular reserve. Cell Death Dis. 2019 Jul 22;10(8):560,019-1799-3.

313. Wright CS, Becker DL, Lin JS, Warner AE, Hardy K. Stage-specific and differential expression of gap junctions in the mouse ovary: connexin-specific roles in follicular regulation. Reproduction. 2001 Jan;121(1):77-88.

314. Carabatsos MJ, Sellitto C, Goodenough DA, Albertini DF. Oocyte-granulosa cell heterologous gap junctions are required for the coordination of nuclear and cytoplasmic meiotic competence. Dev Biol. 2000 Oct 15;226(2):167-79.

315. Ackert CL, Gittens JE, O'Brien MJ, Eppig JJ, Kidder GM. Intercellular communication via connexin43 gap junctions is required for ovarian folliculogenesis in the mouse. Dev Biol. 2001 May 15;233(2):258-70.

316. Veitch GI, Gittens JE, Shao Q, Laird DW, Kidder GM. Selective assembly of connexin37 into heterocellular gap junctions at the oocyte/granulosa cell interface. J Cell Sci. 2004 Jun 1;117(Pt 13):2699-707.

317. Gittens JE, Kidder GM. Differential contributions of connexin37 and connexin43 to oogenesis revealed in chimeric reaggregated mouse ovaries. J Cell Sci. 2005 Nov 1;118(Pt 21):5071-8.

318. Silva JR, van den Hurk R, van Tol HT, Roelen BA, Figueiredo JR. Expression of growth differentiation factor 9 (GDF9), bone morphogenetic protein 15 (BMP15), and BMP receptors in the ovaries of goats. Mol Reprod Dev. 2005 Jan;70(1):11-9.

319. Sun RZ, Lei L, Cheng L, Jin ZF, Zu SJ, Shan ZY, et al. Expression of GDF-9, BMP-15 and their receptors in mammalian ovary follicles. J Mol Histol. 2010 Dec;41(6):325-32.

320. Sugiura K, Su YQ, Diaz FJ, Pangas SA, Sharma S, Wigglesworth K, et al. Oocyte-derived BMP15 and FGFs cooperate to promote glycolysis in cumulus cells. Development. 2007 Jul;134(14):2593-603.

321. Alam MH, Lee J, Miyano T. GDF9 and BMP15 induce development of antrum-like structures by bovine granulosa cells without oocytes. J Reprod Dev. 2018 Oct 12;64(5):423-31.

322. Galloway SM, McNatty KP, Cambridge LM, Laitinen MP, Juengel JL, Jokiranta TS, et al. Mutations in an oocyte-derived growth factor gene (BMP15) cause increased ovulation rate and infertility in a dosage-sensitive manner. Nat Genet. 2000 Jul;25(3):279-83.

323. Hanrahan JP, Gregan SM, Mulsant P, Mullen M, Davis GH, Powell R, et al. Mutations in the genes for oocyte-derived growth factors GDF9 and BMP15 are associated with both increased ovulation rate and sterility in Cambridge and Belclare sheep (Ovis aries). Biol Reprod. 2004 Apr;70(4):900-9.

324. Wang WH, Keefe DL. Prediction of chromosome misalignment among in vitro matured human oocytes by spindle imaging with the PolScope. Fertil Steril. 2002;78:1077-81.

325. Rama Raju GA, Prakash GJ, Krishna KM, Madan K. Meiotic spindle and zona pellucida characteristics as predictors of embryonic development: A preliminary study using PolScope imaging. Reproductive BioMedicine Online. 2007;14:166-74.

326. Tomari H, Honjo K, Kunitake K, Aramaki N, Kuhara S, Hidaka N, et al. Meiotic spindle size is a strong indicator of human oocyte quality. Reproductive Medicine and Biology. 2018;17:268-74.

327. Marangos P, Stevense M, Niaka K, Lagoudaki M, Nabti I, Jessberger R, et al. DNA damage-induced metaphase i arrest is mediated by the spindle assembly checkpoint and maternal age. Nature Communications. 2015;6:8706.

328. Watrin E, Peters JM. Cohesin and DNA damage repair. Exp Cell Res. 2006;312:2687-93.

329. Xiong B, Li S, Ai J, Yin S, OuYang Y, Sun S, et al. BRCA1 Is Required for Meiotic Spindle Assembly and Spindle Assembly Checkpoint Activation in Mouse Oocytes1. Biol Reprod. 2008;79:718-26.

330. Wigglesworth K, Lee KB, O'Brien MJ, Peng J, Matzuk MM, Eppig JJ. Bidirectional communication between oocytes and ovarian follicular somatic cells is required for meiotic arrest of mammalian oocytes. Proc Natl Acad Sci U S A. 2013 Sep 24;110(39):E3723-9.

331. Vozzi C, Formenton A, Chanson A, Senn A, Sahli R, Shaw P, et al. Involvement of connexin 43 in meiotic maturation of bovine oocytes. Reproduction. 2001 Oct;122(4):619-28.

332. El-Hayek S, Yang Q, Abbassi L, FitzHarris G, Clarke HJ. Mammalian Oocytes Locally Remodel Follicular Architecture to Provide the Foundation for Germline-Soma Communication. Curr Biol. 2018 Apr 2;28(7):1124,1131.e3.

333. Murasawa M, Takahashi T, Nishimoto H, Yamamoto S, Hamano S, Tetsuka M. Relationship between ovarian weight and follicular population in heifers. J Reprod Dev. 2005 Oct;51(5):689-93.

334. Bertoldo MJ, Listijono DR, Ho WHJ, Riepsamen AH, Goss DM, Richani D, et al. NAD+ Repletion Rescues Female Fertility during Reproductive Aging. Cell Reports. 2020;30(6):1670-81.

335. Park BK, Park MJ, Kim HG, Han SE, Kim CW, Joo BS, et al. Role of Visfatin in Restoration of Ovarian Aging and Fertility in the Mouse Aged 18 Months. Reproductive Sciences. 2020;27:681-9.

336. Flaws JA, Abbud R, Mann RJ, Nilson JH, Hirshfield AN. Chronically elevated luteinizing hormone depletes primordial follicles in the mouse ovary. Biol Reprod. 1997;57:1233-7.

337. Blumenfeld Z, Zur H, Dann EJ. Gonadotropin-Releasing Hormone Agonist Cotreatment During Chemotherapy May Increase Pregnancy Rate in Survivors. Oncologist. 2015;20:1283-9.

338. Meli M, Caruso-Nicoletti M, La Spina M, Nigro LL, Samperi P, D'Amico S, et al. Triptorelin for Fertility Preservation in Adolescents Treated with Chemotherapy for Cancer. Journal of Pediatric Hematology/Oncology. 2018;40:269-76.

339. Sinha N, Letourneau JM, Wald K, Xiong P, Imbar T, Li B, et al. Antral follicle count recovery in women with menses after treatment with and without gonadotropin-releasing hormone

agonist use during chemotherapy for breast cancer. J Assist Reprod Genet. 2018;35:1861-8.

340. Bildik G, Akin N, Senbabaoglu F, Sahin GN, Karahuseyinoglu S, Ince U, et al. GnRH agonist leuprolide acetate does not confer any protection against ovarian damage induced by chemotherapy and radiation in vitro. Hum Reprod. 2015 Dec;30(12):2912-25.

341. Horicks F, Van Den Steen G, Gervy C, Clarke HJ, Demeestere I. Both in vivo FSH depletion and follicular exposure to Gonadotrophin-releasing hormone analogues in vitro are not effective to prevent follicular depletion during chemotherapy in mice. Mol Hum Reprod. 2018 Apr 1;24(4):221-32.

342. Lambertini M, Moore HCF, Leonard RCF, Loibl S, Munster P, Bruzzone M, et al. Gonadotropin-releasing hormone agonists during chemotherapy for preservation of ovarian function and fertility in premenopausal patients with early breast cancer: A systematic review and meta-analysis of individual patient–level data. Journal of Clinical Oncology. 2018;36:1981-90.

343. Sofiyeva N, Siepmann T, Barlinn K, Seli E, Ata B. Gonadotropin-Releasing Hormone Analogs for Gonadal Protection During Gonadotoxic Chemotherapy: A Systematic Review and Meta-Analysis. Reproductive Sciences. 2019;26:939-53.

344. Shai D, Aviel-Ronen S, Spector I, Raanani H, Shapira M, Gat I, et al. Ovaries of patients recently treated with alkylating agent chemotherapy indicate the presence of acute follicle activation, elucidating its role among other proposed mechanisms of follicle loss. Fertil Steril. 2021 May;115(5):1239-49.

345. Titus S, Szymanska KJ, Musul B, Turan V, Taylan E, Garcia-Milian R, et al. Individual-oocyte transcriptomic analysis shows that genotoxic chemotherapy depletes human primordial follicle reserve in vivo by triggering proapoptotic pathways without growth activation. Sci Rep. 2021 Jan 11;11(1):407,020-79643-x.

346. Han J, Wang H, Zhang T, Chen Z, Zhao T, Lin L, et al. Resveratrol attenuates doxorubicin-induced meiotic failure through inhibiting oxidative stress and apoptosis in mouse oocytes. Aging (Albany NY). 2020 Apr 30;12(9):7717-28.

347. Xiao S, Zhang J, Liu M, Iwahata H, Rogers HB, Woodruff TK. Doxorubicin Has Dose-Dependent Toxicity on Mouse Ovarian Follicle Development, Hormone Secretion, and Oocyte Maturation. Toxicol Sci. 2017 Jun 1;157(2):320-9.

348. Santen RJ, Bardin CW. Episodic luteinizing hormone secretion in man. Pulse analysis, clinical interpretation, physiologic mechanisms. J Clin Invest. 1973 Oct;52(10):2617-28.

349. Penny R, Olambiwonnu NO, Frasier SD. Episodic fluctuations of serum gonadotropins in pre- and post-pubertal girls and boys. J Clin Endocrinol Metab. 1977 Aug;45(2):307-11.

350. Powers JF, Sladek NE. Cytotoxic activity relative to 4-hydroxycyclophosphamide and phosphoramide mustard concentrations in the plasma of cyclophosphamide-treated rats. Cancer Res. 1983 Mar;43(3):1101-6.

351. Rana S, Mohamed AR, Behnam S, Suleiman AH, Zuzana H, Moustapha H. Cyclophosphamide Pharmacokinetics in Mice: A Comparison Between Retro Orbital Sampling Versus Serial Tail Vein Bleeding. Open Pharmacol J. 2007;1:30-5.

352. Hong PS, Srigritsanapol A, Chan KK. Pharmacokinetics of 4-hydroxycyclophosphamide and metabolites in the rat. Drug Metab Dispos. 1991 Jan-Feb;19(1):1-7.

353. Norman RJ, Buchholz MM, Somogyi AA, Amato F. hCGbeta core fragment is a metabolite of hCG: evidence from infusion of recombinant hCG. J Endocrinol. 2000 Mar;164(3):299-305.

354. Galet C, Ascoli M. The differential binding affinities of the luteinizing hormone (LH)/choriogonadotropin receptor for LH and choriogonadotropin are dictated by different extracellular domain residues. Mol Endocrinol. 2005 May;19(5):1263-76.

355. Casarini L, Riccetti L, De Pascali F, Nicoli A, Tagliavini S, Trenti T, et al. Follicle-stimulating hormone potentiates the steroidogenic activity of chorionic gonadotropin and the anti-apoptotic activity of luteinizing hormone in human granulosa-lutein cells in vitro. Mol Cell Endocrinol. 2016.

356. Casarini L, Lispi M, Longobardi S, Milosa F, la Marca A, Tagliasacchi D, et al. LH and hCG Action on the Same Receptor Results in Quantitatively and Qualitatively Different Intracellular Signalling. PLoS ONE. 2012.

357. Riccetti L, Yvinec R, Klett D, Gallay N, Combarnous Y, Reiter E, et al. Human Luteinizing Hormone and Chorionic Gonadotropin Display Biased Agonism at the LH and LH/CG Receptors. Sci Rep. 2017 Apr 19;7(1):940,017-01078-8.

Appendix

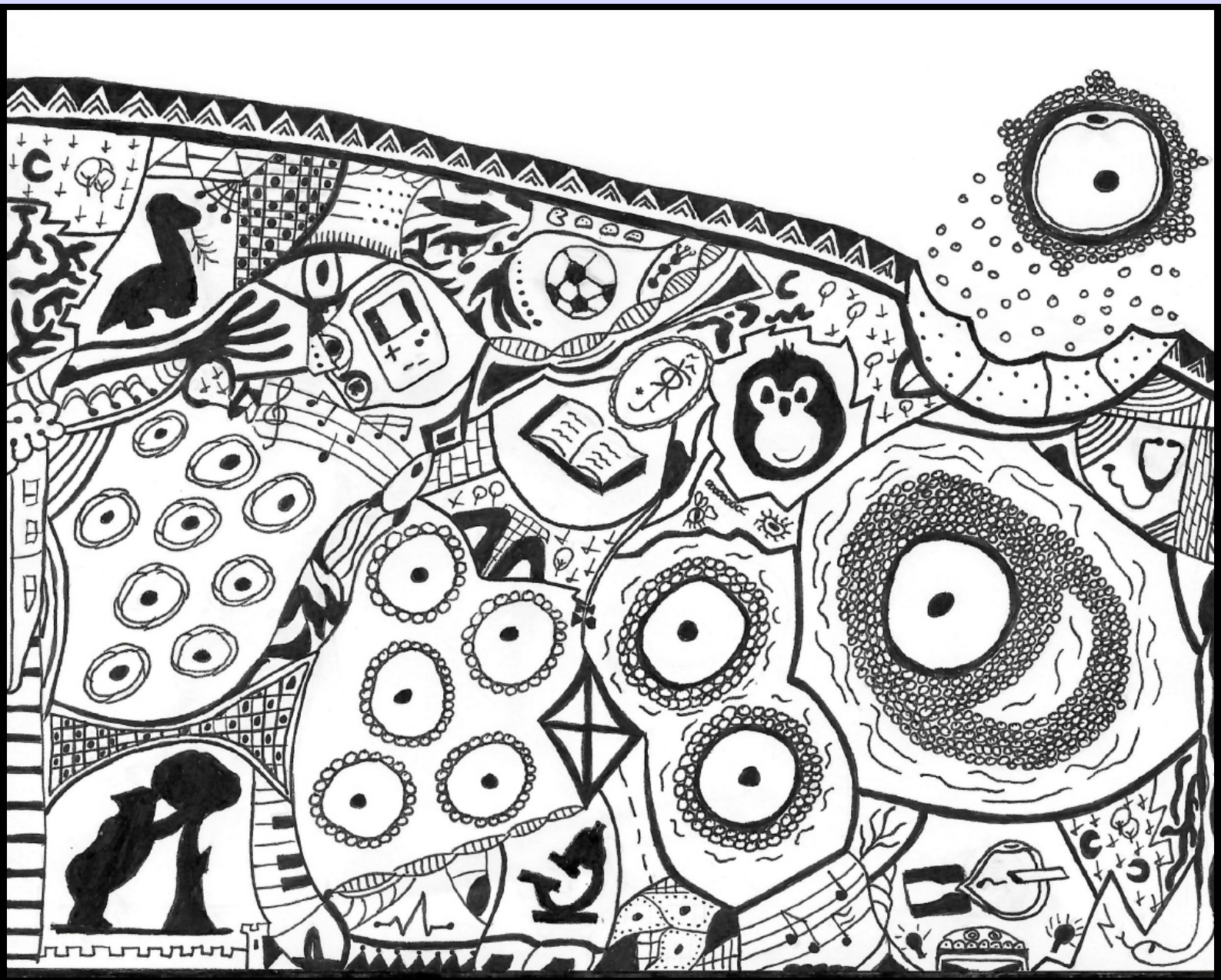

APPENDIX I. Target genes and specific primer sequences (depicted in 5' to 3' direction) used for oocyte – GC communication assessment by RT-qPCR analysis.

Gene (MGI-IDs)	Role	Sense	Primer sequence
Cx37 (95715)	Gap junction	Forward	AACGGTGCTCTTCATCTTC
		Reverse	GGGCTGTGTTACACTCAAA
Cx43 (95713)	Gap junction	Forward	CTGGGTCCTTCAGATCATATTC
		Reverse	CAGCTTCTCTTCCTTTCTCATC
E-Cad (88354)	Adherens junction	Forward	GGACAGAGAATCGCCAAAT
		Reverse	TGTTCCTGTCCCACTCATA
N-Cad (88355)	Adherens junction	Forward	CCTGCCAATCCTGATGAAA
		Reverse	AATCGAACACCAACAGAGAG
Tjp1 (98759)	Tight junction	Forward	GTCCCTCAGAGTCAGTTTAG
		Reverse	CTCTTCAGGGTCGTAATGAT
Gdf9 (95692)	Oocyte-secreted factor	Forward	GGAAGCTATTGAGGTGGAAAG
		Reverse	GAGGTTGAAGGATGCTGTAAG
Bmp15 (1316745)	Oocyte-secreted factor	Forward	AATGGTGAGGCTGGTAAAG
		Reverse	CTACCTGGTTTGATGCTAGAG
Bmpr2 (1095407)	Gdf9 and Bmp15 shared	Forward	CCATGAGGCTAACTGGAAAT
	receptor	Reverse	AGGTTCACAGCTCCTTCTA
Alk4 (1338944)	Gdf9-specific receptor	Forward	GTCCTTGACGAGACAATCAA
		Reverse	GCAATCTCCCAGTAGACAAG
Alk5 (98728)	Gdf9-specific receptor	Forward	GGCTTAGTGTTCTGGGAAAT
		Reverse	CGATGGATCAGAAGGTACAAG
Alk6 (107191)	Bmp15-specific receptor	Forward	AGGACTAGAAGGGTCAGATT
		Reverse	GGGTGGAGGTCTTTATTACAC
Rn18s (97943)	Housekeeping	Forward	CATGGCCGTTCTTAGTTGGT
		Reverse	AACGCCACTTGTCCCTCTAA

APPENDIX II. **Target genes and specific primer sequences (depicted in 5' to 3' direction) used for DNA repair assessment by RT-qPCR analysis.**

Gene (MGI-IDs)	DNA repair pathway	Sense	Primer sequence
Msh6 (1343961)	Mismatch repair	Forward	GCAGTGTTGGATGTCTTACT
		Reverse	GAAGGGATGTGTGTCTTCTC
Apex1 (88042)	Base excision repair	Forward	CTCAAGATATGCTCCTGGAAT
		Reverse	G
			CTGGTGCTTCTTCCTTTACC
Prkdc (104779)	Non-homologous end joining	Forward	CTGATCCACTGGTTGACTAAC
		Reverse	GTCAACAGGGTCCACAATAC
Ercc3 (95414)	Nucleotide excision repair	Forward	GACAGCAGATGCCACTAAA
		Reverse	CAGGAAGTCTTGGGCATATT
Rad51 (97890)	Homologous recombination	Forward	GCAGCGATGTCCTAGATAAT
		Reverse	G
			CAGTGCATACCTGGATTCTAC
Rn18s (97943)	Housekeeping	Forward	CATGGCCGTTCTTAGTTGGT
		Reverse	AACGCCACTTGTCCCTCTAA

APPENDIX III. Certificate approved for animal experimentation by the *Comité d'Experimentació i Benestar Animal* of the *Universitat de València* and by the Directorate General of Agriculture, Livestock and Fisheries, Generalitat Valenciana. Code number: 2018/VSC/PEA/0010.

GENERALITAT VALENCIANA
CONSELLERIA DE AGRICULTURA, MEDIO AMBIENTE, CAMBIO CLIMÁTICO Y DESARROLLO RURAL
DIRECCIÓN GENERAL DE AGRICULTURA, GANADERÍA Y PESCA

Unión Europea

AUTORIZACION PROCEDIMIENTO 2018/VSC/PEA/0010

Vista la solicitud realizada en fecha **26/01/18** con nº reg. entrada **2351** por D/Dª. **Pilar Campins Falcó**, Vicerrectora de Investigación y Política Científica, centro usuario **ES462500001003**, para realizar el procedimiento:

"Efecto protector de la LH sobre la reserva ovárica durante tratamiento quioterapéutico."

Teniendo en cuenta la documentación aportada, según se indica en el artículo 33, punto 5 y 6, y puesto que dicho procedimiento se halla sujeto a autorización en virtud de lo dispuesto en el artículo 31 del Real Decreto 53/2013, de 1 de febrero,

Vista la propuesta del jefe del servicio de Producción y Sanidad Animal.

AUTORIZO:

la realización de dicho procedimiento al que se le asigna el código: **2018/VSC/PEA/0010** tipo **2**, de acuerdo con las características descritas en la propia documentación para el número de animales, especie y periodo de tiempo solicitado. Todo ello sin menoscabo de las autorizaciones pertinentes, por otras Administraciones y entidades, y llevándose a cabo en las siguientes condiciones:

Usuario: **Universitat de Valencia**

Responsable del proyecto: **Sonia Herráiz Raya**

Establecimiento: **Animalario Facultad de Medicina – Campus Blasco Ibañez**

Necesidad de evaluación restrospectiva:

Condiciones específicas:

Observaciones:

Valencia a, fecha de la firma electrónica

El director general de Agricultura, Ganadería y Pesca

GENERALITAT VALENCIANA
Signat per Rogelio Llanes Ribas el 31/01/2018 14:24:27
Càrrec: Dirección General

CSV:EE7RV1HH-ZKJIU2MJ-75TYSXGK URL de validació:https://www.tramita.gva.es/csv-front/index.faces?cadena=EE7RV1HH-ZKJIUZMJ-75TYSXGK

APPENDIX IV. Certificate approved for animal experimentation by the *Comité d'Experimentació i Benestar Animal* of the *Universitat de València* and by the Directorate General of Agriculture, Livestock and Fisheries, Generalitat Valenciana. Code number: 2019/VSC/PEA/0206.

GENERALITAT VALENCIANA
Conselleria de Agricultura, Desarrollo Rural, Emergencia Climática y Transición Ecológica

Dirección General de Agricultura, Ganadería y Pesca
Ciudad Administrativa 9 de Octubre
Calle de La Democracia, 77 · 46018 Valencia
www.gva.es

UNIÓN EUROPEA

AUTORIZACION PROCEDIMIENTO 2019/VSC/PEA/0206

Vista la solicitud realizada en fecha **23/09/19** con nº reg. entrada **585464** por D/Dª. **Carlos Hermenegildo Caudevilla**, **Vicerrector de Investigación y Política Científica**, centro usuario **ES462500001003**, para realizar el procedimiento:

"Efecto protector de la LH sobre la reserva ovárica durante el tratamiento quimioterapéutico"

Teniendo en cuenta la documentación aportada, según se indica en el artículo 33, punto 5 y 6, y puesto que dicho procedimiento se halla sujeto a autorización en virtud de lo dispuesto en el artículo 31 del Real Decreto 53/2013, de 1 de febrero,

Vista la propuesta del jefe del servicio de Producción y Sanidad Animal.

AUTORIZO:

la realización de dicho procedimiento al que se le asigna el código: **2019/VSC/PEA/0206** tipo **2,** de acuerdo con las características descritas en la propia documentación para el número de animales, especie y periodo de tiempo solicitado. Todo ello sin menoscabo de las autorizaciones pertinentes, por otras Administraciones y entidades, y llevándose a cabo en las siguientes condiciones:

Usuario: **Universidad de Valencia-Estudio General**

Responsable del proyecto: **Sonia Herráiz Raya**

Establecimiento: **Animalario Unidad Central de Investigación (Fac. Medicina y Odontología) Valencia**

Necesidad de evaluación restrospectiva:

Condiciones específicas:

Observaciones:

Valencia a, fecha de la firma electrónica
El director general de Agricultura, Ganadería y Pesca

Firmado por Rogelio Llanes Ribas el 04/10/2019 13:53:10
Cargo: Dirección General

APPENDIX V. Scientific production of this doctoral thesis

1. International scientific publications

- **Del Castillo LM**, Buigues A, Rossi V, Soriano MJ, Martínez J, De Felici M, Lamsira HK, Di Rella F, Klinger FG, Pellicer A, Herraiz S. "The cyto-protective effects of luteinizing hormone on ovarian reserve and female fertility during exposure to gonadotoxic alkylating agents in an adult mouse model." Human Reproduction, Volume 36, Issue 9, pages 2514-2528, September 2021. doi.org/10.1093/humrep/deab165.
- **Del Castillo LM**, Soriano MJ, Martínez J, Pellicer A, Herraiz S. "LH preserves oocyte – granulosa cell communication in mouse follicles exposed to chemotherapy with alkylating agents at primordial stage." *In progress: manuscript prepared for submission*.

2. Works submitted to international conferences

2.1. Oral presentations

- **Del Castillo LM**, Soriano MJ, Martínez J, Pellicer A, Herraiz S. "LH prevents follicular damage and preserves the meiotic potential of oocytes exposed to chemotherapy at the primordial stage." Presentation number: O-260. Conference: ESHRE's 36th annual meeting. City of event: virtual. Dates: 05/07/2020 – 08/07/2020. Organizing entity: European Society of Human Reproduction and Embryology (ESHRE).
- **Del Castillo LM**, Buigues A, Pellegrini L, Rossi V, Klinger FG, Pellicer A, Herraiz S. "LH gonadoprotection against ovarian damage induced by alkylating drugs in adult mouse ovaries." Presentation number: O-082. Conference: ESHRE's 34th annual meeting. City of event: Barcelona (Spain). Dates: 01/07/2018 – 04/07/2018. Organizing entity: European Society of Human Reproduction and Embryology (ESHRE).

2.2. Posters

- **Del Castillo LM**, Soriano MJ, Martínez J, Pellicer A, Herraiz S. "LH preserves oocyte-granulosa cell communication in mouse ovaries exposed to chemotherapy with alkylating agents." Presentation number: P-435. Conference: ESHRE's 37th

annual meeting. City of event: virtual. Dates: 28/06/2021 – 01/07/2021. Organizing entity: European Society of Human Reproduction and Embryology (ESHRE).

- **Del Castillo LM**, Buigues A, Marchante M, Rossi V, Martínez J, Klinger FG, Pellicer A, Herraiz S. "LH in vitro treatment promotes DNA repair of mouse apoptotic follicles damaged by alkylating agents." Presentation number: P-446. Conference: ESHRE's 35th annual meeting. City of event: Vienna (Austria). Dates: 23/06/2019 – 26/06/2019. Organizing entity: European Society of Human Reproduction and Embryology (ESHRE).

APPENDIX VI. Manuscript I

Human Reproduction, Vol.00, No.0, pp. 1–15, 2021
doi:10.1093/humrep/deab165

human reproduction

ORIGINAL ARTICLE *Reproductive biology*

The cyto-protective effects of LH on ovarian reserve and female fertility during exposure to gonadotoxic alkylating agents in an adult mouse model

L.M. Del Castillo[1,2], A. Buigues[1], V. Rossi[3], M.J. Soriano[1], J. Martinez[1,2], M. De Felici[3], H.K. Lamsira[3], F. Di Rella[4], F.G. Klinger[3], A. Pellicer[1,5], and S. Herraiz [1,*]

[1]IVI Foundation—IIS La Fe, Reproductive Medicine Research Group, Valencia, Spain [2]Department of Pediatrics, Obstetrics and Gynecology, School of Medicine, University of Valencia, Valencia, Spain [3]Department of Biomedicine and Prevention, University of Rome Tor Vergata, Rome, Italy [4]Clinical and Experimental Senology, Istituto Nazionale Tumori, IRCCS, Fondazione G. Pascale, Naples, Italy [5]IVI-RMA Rome, Rome, Italy

*Correspondence address. IVI Foundation—IIS La Fe, Reproductive Medicine Research Group, Av. Fernando Abril Martorell, 106-Torre A-Planta 1, 46026 Valencia, Spain. Tel: +34-96-390-33-05; E-mail: Sonia.Herraiz@ivirma.com https://orcid.org/0000-0003-0703-6922

Submitted on February 12, 2021; resubmitted on May 7, 2021; editorial decision on June 18, 2021

STUDY QUESTION: Does LH protect mouse oocytes and female fertility from alkylating chemotherapy?

SUMMARY ANSWER: LH treatment before and during chemotherapy prevents detrimental effects on follicles and reproductive lifespan.

WHAT IS KNOWN ALREADY: Chemotherapies can damage the ovary, resulting in premature ovarian failure and reduced fertility in cancer survivors. LH was recently suggested to protect prepubertal mouse follicles from chemotoxic effects of cisplatin treatment.

STUDY DESIGN, SIZE, DURATION: This experimental study investigated LH effects on primordial follicles exposed to chemotherapy. Seven-week-old CD-1 female mice were randomly allocated to four experimental groups: Control (n = 13), chemotherapy (ChT, n = 15), ChT+LH-1x (n = 15), and ChT+LH-5x (n = 8). To induce primary ovarian insufficiency (POI), animals in the ChT and ChT+LH groups were intraperitoneally injected with 120 mg/kg of cyclophosphamide and 12 mg/kg of busulfan, while control mice received vehicle. For LH treatment, the ChT+LH-1x and ChT+LH-5x animals received a 1 or 5 IU LH dose, respectively, before chemotherapy, then a second LH injection administered with chemotherapy 24 h later. Then, two animals/group were euthanized at 12 and 24 h to investigate the early ovarian response to LH, while remaining mice were housed for 30 days to evaluate short- and long-term reproductive outcomes. The effects of LH and chemotherapy on growing-stage follicles were analyzed in a parallel experiment. Seven-week-old NOD-SCID female mice were allocated to control (n = 5), ChT (n = 5), and ChT+LH-1x (n = 6) groups. Animals were treated as described above, but maintained for 7 days before reproductive assessment.

PARTICIPANTS/MATERIALS, SETTING, METHODS: In the first experiment, follicular damage (phosphorylated H2AX histone (γH2AX) staining and terminal deoxynucleotidyl transferase-mediated dUTP nick-end labeling (TUNEL) assay), apoptotic biomarkers (western blot), and DNA repair pathways (western blot and RT-qPCR) were assessed in ovaries collected at 12 and 24 h to determine early ovarian responses to LH. Thirty days after treatments, remaining mice were stimulated (10 IU of pregnant mare serum gonadotropin (PMSG) and 10 IU of hCG) and mated to collect ovaries, oocytes, and embryos. Histological analysis was performed on ovarian samples to investigate follicular populations and stromal status, and meiotic spindle and chromosome alignment was measured in oocytes by confocal microscopy. Long-term effects were monitored by assessing pregnancy rate and litter size during six consecutive breeding attempts. In the second experiment, mice were stimulated and mated 7 days after treatments and ovaries, oocytes, and embryos were collected. Follicular numbers, follicular protection (DNA damage and apoptosis by H2AX staining and TUNEL assay, respectively), and ovarian stroma were assessed. Oocyte quality was determined by confocal analysis.

MAIN RESULTS AND THE ROLE OF CHANCE: LH treatment was sufficient to preserve ovarian reserve and follicular development, avoid atresia, and restore ovulation and meiotic spindle configuration in mature oocytes exposed at the primordial stage. LH improved the cumulative pregnancy rate and litter size in six consecutive breeding rounds, confirming the potential of LH treatment to preserve fertility. This protective effect appeared to be mediated by an enhanced early DNA repair response, via homologous recombination, and generation of anti-apoptotic signals in the ovary a few hours after injury with chemotherapy. This response ameliorated the chemotherapy-induced increase in DNA-damaged oocytes and apoptotic granulosa cells. LH treatment also protected growing follicles from chemotherapy. LH reversed the chemotherapy-induced depletion of primordial and primary follicular subpopulations, reduced oocyte DNA damage and granulosa cell apoptosis, restored mature oocyte cohort size, and improved meiotic spindle properties.

LARGE SCALE DATA: N/A.

LIMITATIONS, REASONS FOR CAUTION: This was a preliminary study performed with mouse ovarian samples. Therefore, preclinical research with human samples is required for validation.

WIDER IMPLICATIONS OF THE FINDINGS: The current study tested if LH could protect the adult mouse ovarian reserve and reproductive lifespan from alkylating chemotherapy. These findings highlight the therapeutic potential of LH as a complementary non-surgical strategy for preserving fertility in female cancer patients.

STUDY FUNDING/COMPETING INTEREST(S): This study was supported by grants from the Regional Valencian Ministry of Education (PROMETEO/2018/137), the Spanish Ministry of Science and Innovation (CP19/00141), and the Spanish Ministry of Education, Culture and Sports (FPU16/05264). The authors declare no conflict of interest.

Key words: fertility preservation / follicle protection / ovoprotection / cancer / chemotherapy / LH / DNA repair

Introduction

The female reproductive lifespan is widely thought to depend on the number of non-renewable primordial follicles, constituting the ovarian reserve that progressively decreases with age (Macklon and Fauser, 1999). External factors, such as chemotherapy treatment, can accelerate follicular depletion and menopause onset. Cytotoxic treatments cause a spectrum of effects on the ovary ranging from partial damage, to premature ovarian insufficiency (POI) and loss of fertility (Koyama *et al.*, 1977; Kalich-Philosoph *et al.*, 2013; Spears *et al.*, 2019). Notably, oncologic treatments cause a 38% reduction in the likelihood that patients will achieve pregnancy (Anderson *et al.*, 2018).

This is a growing problem worldwide, with over 1.9 million women of reproductive age (15–49 years old) newly diagnosed with cancer in 2018 alone (Ferlay *et al.*, 2018). Among young women who are nulliparous, the 5-year cancer survival rate can be as high as 75% (Howlader *et al.*, 2019). Thus, a growing number of female patients will experience the undesired gonadotoxic side effects associated with oncologic treatments, highlighting the relevance of fertility preservation.

Patient age and type and dose of chemotherapeutic agent are the main factors determining the degree of ovarian damage (Kalich-Philosoph *et al.*, 2013), with older patients being more susceptible to POI after treatment. Among chemotherapeutic drugs, alkylating agents, like cyclophosphamide and busulfan, associate with the highest risk of inducing follicular depletion leading to POI (Meirow *et al.*, 2010). Although the precise mechanism for follicle depletion by alkylating agents remains unclear, these cytotoxic drugs derive their anticancer properties by inducing inter- and intra-strand DNA crosslinking that leads to apoptosis and cell death.

The ability to respond to DNA insults is critical to ensure follicular viability. In meiotic cells (e.g. oocytes), homologous recombination promoted by the ataxia telangiectasia-mutated pathway (ATM), is the primary mechanism for accurate double-strand break (DSB) repair (Kujjo *et al.*, 2010; Kujjo *et al.*, 2012; Winship *et al.*, 2018). Also, agents like cyclophosphamide damage growing follicles, thereby inducing the over-activation of dormant follicles, known as the burnout effect, that finally results in loss of the ovarian reserve (Kalich-Philosoph *et al.*, 2013).

LH, a gonadotropin with a complex role in folliculogenesis, was recently proposed to protect the follicle pool of prepubertal mice from cisplatin. LH was proposed to prevent the chemotherapy-induced reduction of primordial follicles by stimulating anti-apoptotic signals from a subset of somatic cells expressing the LH receptor (LHR) (Rossi *et al.*, 2017). Although these results are encouraging, further research is required because cisplatin only associates with a moderate risk of inducing POI (Meirow *et al.*, 2010), and prepubertal ovaries lack late preantral and antral follicles, precluding evaluation of how over-activation contributes to follicular exhaustion. Furthermore, the developmental potential of LH-preserved oocytes and the underlying protective mechanisms remain unclear. We, thus, aimed to assess the effects of LH in protecting the adult mouse ovary, containing all follicle populations, from the most gonadotoxic alkylating agents. The competence of the LH-protected follicles was also analyzed.

Material and methods

Animal procedures

All animal experiments in this study were approved and performed according to the Institutional Review Board and the Ethics Committee in Experimental Research of the University of Valencia, Valencia, Spain (2018/VSC/PEA/0010 and 2019/VSC/PEA/0206).

Study design

This was an experimental study (study design summarized in Supplementary Fig. S1) to investigate LH effects on primordial follicles that were exposed to chemotherapy. Seven-week-old CD-1 female mice were randomly allocated to four experimental groups: Control

(n = 13), chemotherapy (ChT, n = 15), ChT+LH-1x (n = 15), and ChT+LH-5x (n = 8). Mice receiving chemotherapy were intraperitoneally injected with 120 mg/kg of cyclophosphamide and 12 mg/kg of busulfan in dimethyl sulfoxide (DMSO) (all from Sigma-Aldrich, St. Louis, Missouri, MO, USA), as previously described (Buigues *et al.*, 2020), while controls were injected with saline. For LH treatments, the ChT+LH-1x and ChT+LH-5x mice were dosed with 1 (2.3 ng/ml) or 5 (11.5 ng/ml) IU of LH (Luveris, Merck Serono, Darmstadt, Germany), respectively, before chemotherapy and then again with chemotherapy 24 h later. After treatments, the early ovarian response to LH and both the short- and long-term reproductive outcomes were assessed.

In a parallel experiment to analyze LH effects on growing follicles exposed to chemotherapy, 7-week-old NOD-SCID female mice were allocated to control (n = 5), ChT (n = 5), and ChT+LH-1x (n = 6) groups. Mice were treated as described above and maintained for 7 days.

Effects on quiescent follicles

To evaluate the LH effects on follicles at the dormant primordial stage during chemotherapy exposure (Supplementary Fig. S1A), 31 seven-week-old CD-1 female mice randomly allocated to control, chemotherapy (ChT) and chemotherapy with LH (ChT+LH-1x) groups and treated as described above were maintained for 30 days. These mice were then subjected to controlled ovarian stimulation (COS) to recover oocytes and embryos derived from follicles damaged at the primordial stage. Two mice from each group were euthanized 16 h after hCG administration to collect mature oocytes, while the remaining were housed with males immediately after hCG injection and euthanized 40 h later to collect ovaries, oocytes, and early cleavage-stage embryos. To assess the long-term effects of LH, 30 days after treatments 4 mice/group were housed with fertile males for 6 months to allow continuous breeding. For long-term assessment, an additional group treated with a high-dose, i.e. 5 IU, of LH (11.5 ng/ml) was included (ChT+LH-5x).

To analyze the protective early response to LH, a complementary experiment was performed on 16 CD-1 female mice treated with LH and alkylating agents as described above and euthanized 12 and 24 h after ChT and/or LH treatment to evaluate ovarian samples (Supplementary Fig. S1B).

An *in vivo* experiment was performed with cisplatin to determine if the protective effects of LH depended on the type of chemotherapy agent. Twenty-four 7-week-old CD-1 female mice were allocated to four experimental groups (n = 6/group): control, cisplatin (Cs), LH, and cisplatin with LH (Cs+LH). Mice received a single dose of 5 mg/kg of cisplatin, 1 IU of LH, or saline solution as a control. The fourth group received 1 IU of LH together with 5 mg/kg of cisplatin. Ovaries were collected 5 days after treatment to count follicles.

Effects on growing oocyte populations

Finally, to test if LH can also protect the growing follicle population, NOD/SCID female mice were used. These mice represent a worst-case ovarian scenario as they are considerably less fertile than the CD-1 strain (Kumagai *et al.*, 2011). Sixteen 7-week-old NOD-SCID female mice were randomly allocated to control, ChT, and ChT+LH-1x groups, and treatments administered as described above. Seven days after treatment, mice underwent COS to ensure that any collected oocytes were derived from growing-stage follicles exposed to chemotherapy. Two mice per group were euthanized 16 h after hCG injection to collect oocytes, while remaining mice were mated with males immediately after hCG injection and euthanized 40 h later to collect ovaries, metaphase II (MII) ovulated oocytes, and early cleavage-stage embryos from oviducts (Supplementary Fig. S1C).

Histological evaluation and follicle count

Formalin-fixed ovarian samples were paraffin-embedded and cut into 4-µm thick sections. Every fifth section was stained with hematoxylin and eosin (H&E) for morphological evaluation and follicle count. Follicular counts were performed blindly by three observers (L.M.C., A.B., and J.M.), and only follicles with a visible nucleus were counted to avoid double counting. Developmental stages were classified according to standard criteria (Dath *et al.*, 2010). The following follicles were considered morphologically abnormal: presence of two or more oocytes in the same follicle, multiple vesicles on ooplasm, disruption of granulosa layers, or complete degeneration (Supplementary Fig. S2). Stromal degeneration was assessed over the whole ovary in representative H&E sections with a bright-field microscope, identified as the presence of fibrotic non-cellular or tissue absent regions embedded in ovarian stroma. A degenerated area index was quantified as the disrupted area/total tissue area of each sample using ImageJ software (National Institutes of Health, Bethesda, MD, USA). For each treatment group, mean stromal degeneration indices were calculated, normalized to the index of the control group, and expressed as fold-changes.

Oocytes and early cleavage-stage embryo collection

Dissected reproductive tracts were placed in a small petri dish containing flushing media (Origio, Måløv, Denmark) at 37°C and oviducts carefully isolated by removing ovaries and uteri with a sterilized blade. Oocytes and embryos were flushed from the oviducts by expelling flushing media from a 30-gauge needle inserted into the infundibulum. To determine an oocyte's maturation stage, cumulus–oocyte complexes were denudated with 300 µg/ml hyaluronidase (Sigma-Aldrich) for 30–60 s. Oocytes and embryos were classified according to morphological criteria under a binocular loupe (SZX2, Olympus, Tokyo, Japan).

Meiotic spindle staining and chromosome assessment

MII-oocytes obtained 16 h after hCG administration from CD-1 (n = 33) and NOD-SCID (n = 28) mice were processed and stained according to Coticchio *et al.* (2013) with minor modifications. Briefly, for microtubule and centromere staining, fixed oocytes were incubated with anti µ-Tubulin conjugated with fluorescein isothiocyanate (FITC) (1:50 dilution; F2168—Sigma-Aldrich) and anti-centromere proteins (CREST, 1:20 dilution; 15-234—Antibodies Incorporated, Davis, CA, USA) primary antibodies overnight at 4°C inside a dark humidified chamber. Then, oocytes were incubated with an Alexa Fluor 594 secondary antibody (1:1000 dilution; A-11014—Invitrogen, Carlsbad, CA, USA) for 1 h at room temperature (RT). Chromosomes were labeled using 20 µg/ml Hoechst fluorescent stain (H33342—Sigma-Aldrich) for

20 min at RT. High-resolution images were captured with a confocal microscope (Leica TCS SP8, Leica Microsystems GmbH, Wetzlar, Germany) and LAS X image software (Leica Microsystems GmbH). Total spindle areas and chromosome alignments were analyzed for each oocyte using ImageJ software (National Institutes of Health). Oocytes were classified as misaligned when at least one chromosome diverged by ≥2 µm from the equatorial plate as previously described (Coticchio et al., 2013).

Cell damage

DNA damage and apoptosis in follicles were examined by immunofluorescence for phosphorylated H2AX histone (γH2AX), a specific marker of DSBs, and by terminal deoxynucleotidyl transferase-mediated dUTP nick-end labeling (TUNEL) assay, respectively. For γH2AX immunostaining, samples were incubated overnight at 4°C with a monoclonal rabbit anti-γH2AX antibody (1:400 dilution; 9718—Cell Signaling, Danvers, MA, USA) followed by a 1 h incubation at RT with a biotinylated goat anti-rabbit IgG secondary antibody (1:500 dilution; BA-1000—Vector Laboratories, Burlingame, CA, USA). Fluorescence staining was performed using streptavidin-conjugated Alexa Fluor 594 (1:1000 dilution; S32356—Invitrogen) for 45 min at RT. Samples were mounted with Fluoroshield mounting medium with DAPI (Abcam, Cambridge, UK). For TUNEL assay, DNA fragmentation was assessed by a TMR red in situ cell death detection kit (Roche Diagnostics, Basel, Switzerland), following the manufacturer's instructions.

Stained sections were examined and high-magnification images obtained using a fluorescence microscope with an attached digital camera (Leica DM4000B and DFC450C, Leica Microsystems GmbH). Oocytes containing positive γH2AX-labeled foci were considered damaged, and the DNA damage index calculated as γH2AX-positive/total oocytes for each sample. TUNEL-positive labelling was quantified by Image ProPlus 6.0 software (Media Cybernetics Inc., Rockville, MD, USA), and follicles were considered apoptotic when showing ≥ 20% TUNEL-positive granulosa cells.

Western blotting

Frozen ovaries were homogenized in RIPA lysis buffer (50 mM Tris-HCl, 150 mM NaCl, 4% NP-40, 0.5% sodium deoxycholate, 0.1% sodium dodecyl sulfate (SDS), pH 7.4) containing phosphatase (PhospSTOP EASYpack, Roche Diagnostics) and protease (cOmplete tablets EDTA-free EASY-pack, Roche Diagnostics) inhibitors. Protein content was determined by Bradford assay. Subsequently, 30 µg of protein from each sample were separated on 8–12% SDS-polyacrylamide gels and transferred to polyvinylidene difluoride (PVDF) membranes. Blots were blocked using 5% bovine serum albumin (BSA, Sigma-Aldrich) or non-fat powdered milk dissolved in Tris-Buffered saline with 0.1% Tween 20 (TBST) for 1 h at RT and then exposed to primary antibodies—ataxia-telangiectasia mutated kinase (ATM, 1:2000 dilution; ab78), RAD51 recombinase (Rad51, 1:5000 dilution; ab133534—both from Abcam), cleaved Caspase-3 (CC3, 1:1000 dilution; 9661), phospho-extracellular signal-regulated Kinase 1 and 2 (pERK1/2, 1:1000 dilution; 4370), ERK1/2 (1:1000 dilution; 4695), phospho- serine/threonine-protein Kinase 1 (pAkt, 1:1000 dilution; 4060), Akt (1:500 dilution; 4691—all five from Cell Signaling), B-cell lymphoma-2 (Bcl2, 1:200 dilution; sc7382) or β-Actin (1:2000 dilution; sc47778—both from Santa Cruz Biotechnology, Dallas, TX, USA)—overnight at 4°C. After washing in TBST, membranes were incubated with appropriate Horseradish peroxidase (HRP)-conjugated secondary antibodies for 1 h at RT. Following incubation with a chemiluminescence detection reagent (ThermoFisher, Waltham, MA, USA), protein bands were visualized by Amersham Imager 680 (GE HealthCare Life Sciences, Marlborough, MA, USA). Integrated light intensity of each band was determined by ImageJ software (National Institutes of Health). Signal intensities were normalized to the intensity of the housekeeping protein β-Actin.

Relative gene expression

Total RNA was obtained from ovaries collected 12 and 24 h after chemotherapy administration using the RNeasy micro kit (Qiagen, Hilden, Germany), according to the manufacturer's instructions, and complementary cDNA synthesized from 0.5 µg of RNA per sample using the PrimeScript RT reagent kit (Takara Bio Inc., Kusatsu, Japan). Real-time quantitative PCR (RT-qPCR) was performed with specific primers for DNA repair associated genes (Supplementary Table SI) using PoweUp Sybr Green (ThermoFisher) and a StepOnePlus system (Applied Biosystems, Foster City, CA, USA). All PCR reactions were run in triplicate, and the relative gene expression was calculated by the CT method (Livak and Schmittgen, 2001) using 18S ribosomal (Rn18s) as a housekeeping gene.

Statistics

Data are presented as mean and standard deviation (mean±SD). Sample size was estimated with R statistical programming language (pwr package; R Core Team, Vienna, Austria). Two-by-two comparisons between experimental groups were performed with the non-parametric Mann-Whitney test using SPSS v.22.0 (IBM, Chicago, IL, USA). For spindle assessment data, multiple comparisons between groups were performed using the Turkey all-pair comparisons method (multcomp R package) with the R statistical programming language. The spindle dichotomic variable (presence/absence) was analyzed by Bayesian analysis using a logistic regression and a normal non-informative prior (0 ± 3 as mean±SD). The quality of the Bayesian model was checked for 1000 simulations. Spindle area was analyzed by linear regression and the remaining variables by logistic regression. A P-value <0.05 was considered statistically significant.

Results

Protective effects of LH on quiescent follicles

Follicle endowment and ovarian stroma

Ovaries from mice treated with alkylating agents exhibited 69.8% ($P = 0.025$) fewer follicles than controls, particularly affecting the primordial, primary, and secondary populations ($P = 0.024$, $P = 0.025$ and $P = 0.034$, respectively; Fig. 1A and B). LH-treated samples had 53.8% fewer follicles than controls, but this difference was not statistically significant ($P = 0.063$, Fig. 1A). LH treatment ameliorated the chemotherapy-induced follicle loss and increased the number of primordial, primary, antral, and preovulatory follicles by 38.1%, 36.1%,

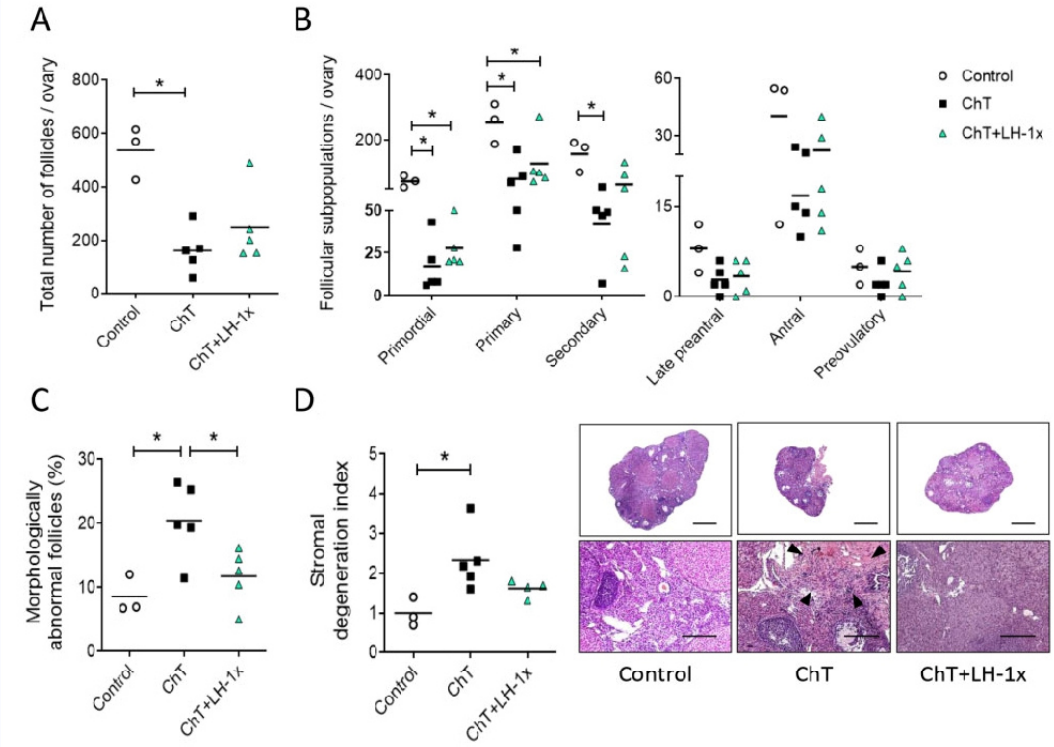

Figure 1. LH treatment prevented follicular depletion, atresia, and stromal degeneration induced by chemotherapy. Alkylating agents were administered with or without LH and ovaries analyzed 30 days later. (**A**) Chemotherapy (ChT) treatment reduced the number of total follicles assessed in hematoxylin and eosin (H&E) stained sections, and LH co-administration blunted this effect. (**B**) All follicular subpopulations were higher in the LH-cotreated group than in the ChT group. (**C**) Percentages of morphologically abnormal follicles were similar in the LH and control group, but the ChT group showed a significant increase in atretic follicles. (**D**) Stromal degeneration index (fibrotic non-cellular or tissue absent area/total tissue area of each sample, normalized to control group index), and representative images at 2.5× (top, scale bar = 800 μm) and 10× (bottom, scale bar = 200 μm) magnification showing that LH preserves stromal morphology. Disrupted regions were identified as fibrotic areas and are indicated with black arrows in 10× images. Scatter plots show individual data and means for all groups (n = 3 in control and n = 5 in ChT and chemotherapy with LH (ChT+LH-1×) groups). Statistical significance was determined by two-tailed Mann–Whitney *U* test; **P*-values <0.05 were considered statistically significant.

25.0%, and 52.4% of ChT follicle numbers, respectively, although these differences were not statistically significant due to high variability between samples. Relative to the control group, the ChT treatment group had more morphologically abnormal follicles ($P = 0.049$), while LH prevented this effect, with the LH group showing similar numbers of abnormal follicles as the control group and significantly fewer than the ChT group ($P = 0.047$; Fig. 1C).

ChT treatment also disrupted the structure of the ovarian stroma, with fibrotic areas localized in the center of the stroma being the most common alteration in ovaries from the ChT group. The mean stromal degeneration index of the ChT group was 2.3-fold higher than that of the control group ($P = 0.025$). Ovaries from the ChT+LH-1× group had well-preserved morphologies and exhibited only a slight 1.6-fold increase in their stromal degeneration index relative to that of controls ($P = 0.077$; Fig. 1D). Thus, LH treatment blunted this chemotherapy-induced effect; albeit not statistically significant differences were found between ChT and ChT+LH-1× samples ($P = 0.086$).

Ovulation and early embryo cleavage

Relative to control mice, mice treated 30 days previously with alkylating agents yielded fewer MII-oocytes after COS ($P = 0.04$). LH treatment blunted this effect. The number of MII-oocytes collected from LH-treated mice was statistically similar ($P = 0.329$; Fig. 2A) to that of control mice and was 25.0% higher than that of ChT-treated mice. However, the ChT+LH-1× group had significantly fewer normal 2-cell embryos than the control group (Fig. 2B).

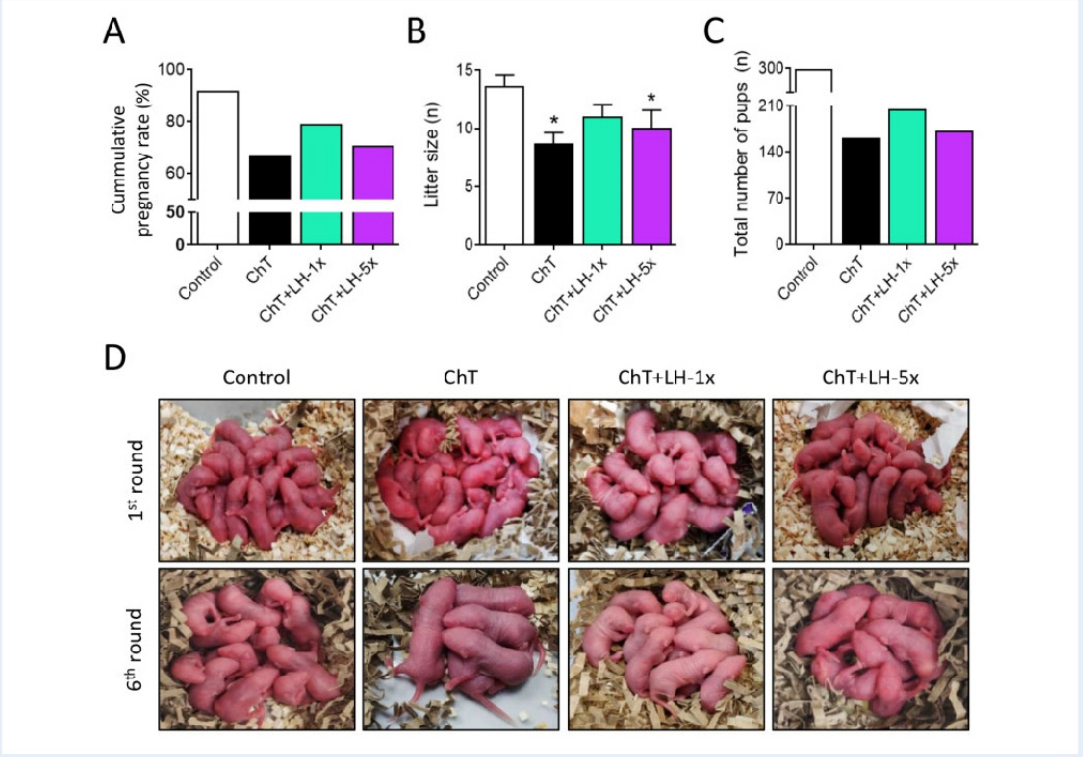

Figure 3. LH co-administration improved breeding outcomes and extended reproductive lifespan. Mice were treated with alkylating agents with or without LH and 1 month later tested for breeding performance in six consecutive mating attempts. (**A**) ChT (black) reduced the cumulative pregnancy rate and LH treatment reversed this, with the 1× dose (green) being more effective than the 5× dose (purple). (**B**) ChT reduced the mean litter size and LH-1× reversed this effect. (**C**) ChT reduced the total number of pups and LH-1××x ameliorated this effect. (**D**) Representative first and last litters from all experimental groups. Graphs show means and, where indicated, SD for each experimental group (n = 4 animals/group). Statistical significance for litter size was determined by two-tailed Mann–Whitney *U* test; **P*-values <0.05 compared with the control group were considered statistically significant.

Twelve hours after treatment, there was an acute increase in the percent of apoptotic follicles (by TUNEL) in the ChT ($P = 0.034$) and ChT+LH-1× ($P = 0.034$) groups compared to controls. LH treatment protected ovaries from ChT-induced apoptosis in a dose-dependent manner, with a 1.6- and 6.7-fold reduction in apoptotic follicles in the ChT+LH-1× group ($P = 0.043$) and ChT+LH-5× ($P = 0.020$), respectively, when compared to the ChT group. The high-dose LH group had similar levels of apoptosis as controls (Fig. 4B). Growing follicles were the most susceptible population to apoptosis, but both the high and low doses of LH protected them from damage, resulting in a significantly lower TUNEL signal than that of the ChT group (Control: 2.0 ± 1.7%, ChT: 10.3 ± 1.6%, ChT+LH-1×: 5.6 ± 2.1% $P = 0.021$, ChT+LH-5×: 1.5 ± 1.7% $P = 0.020$). TUNEL-positive oocytes were not detected in any experimental group.

Additionally, the Bcl2/CC3 apoptosis protein ratio was similar in all groups (data not shown) twelve hours after treatments. However, at the 24 h timepoint the ChT group exhibited a reduction in the Bcl2/CC3 apoptosis protein ratio, and treatment with both high and low doses of LH restored this ratio to control-like levels (Fig. 4C and Supplementary Fig. S3A). Chemotherapy also increased ERK1/2 activation at both 12 and 24 h. Treatment with LH partially ameliorated this effect by reducing ERK1/2 phosphorylation (Fig. 4D and Supplementary Fig. S3B).

Finally, the high dose of LH increased the levels of the DNA DSB repair machinery ATM and Rad51 proteins (Fig. 4E and Supplementary Fig. S3C). Chemotherapy activated Akt, and treatment with both LH doses prevented this effect, reducing the pAkt/Akt ratio to control-like values at 12 and 24 h (Fig. 4F and Supplementary Fig. S3D). Chemotherapy also increased mRNA transcription of the DNA repair genes apurinic/apyrimidinic endodeoxyribonuclease 1 *(Apex1)*, mutS homolog 6 *(Msh6)*, protein kinase DNA-activated catalytic subunit *(Prkdc)*, excision repair cross-complementation group 3 *(Ercc3)*, and *Rad51* at the 12-h timepoint, which were downregulated by 24 h (Fig. 4G). Ovaries from ChT+LH-1×-treated mice showed an even more

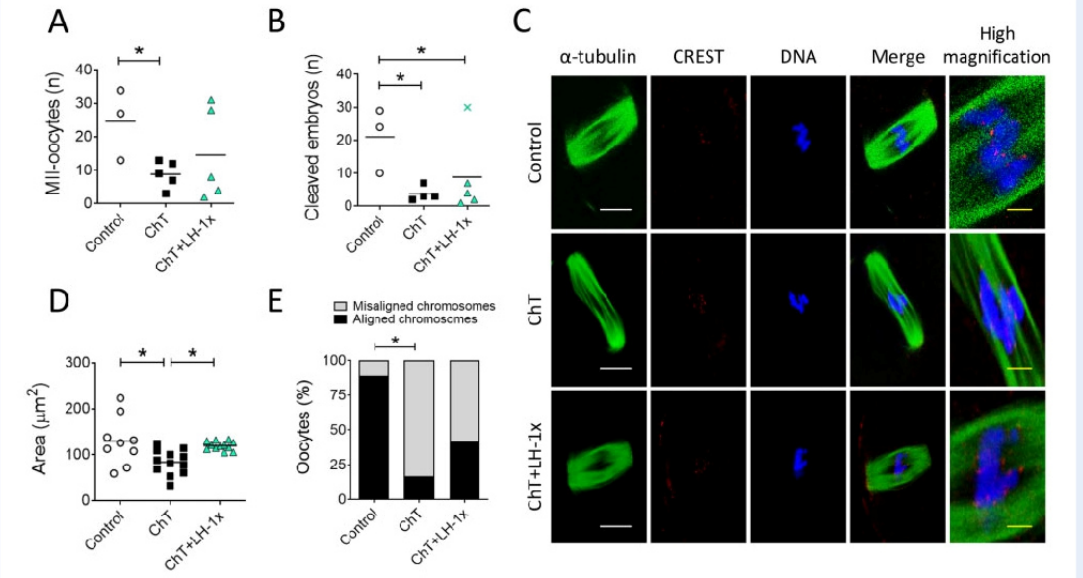

Figure 2. LH treatment ameliorated the effects of alkylators on oocyte quantity and quality. Alkylating agents were administered with or without LH and controlled ovarian stimulation (COS) performed 30 days later to release oocytes that had been exposed to chemotherapy during their quiescent stage. (**A**) Number of morphologically normal metaphase II (MII) oocytes recovered after COS from all experimental groups. LH-treated mice ovulated greater numbers of MII-oocytes than ChT-treated mice (**B**) Number of 2-cell stage embryos. (**C**) Representative confocal images of meiotic spindles from MII-oocytes (n = 9 in control, and n = 12 in ChT and in ChT+LH groups). α-tubulin staining (green) (showing spindles), chromosomes (blue), and CREST-centromere proteins (red) were visualized to evaluate chromosome alignment and microtubule–chromosome attachment. The right column shows high magnification images of merged optical sections. White scale bar = 10 μm; yellow scale bar = 1.25 μm. (**D**) Calculated spindle areas. LH treatment reversed the chemotherapy-induced reduction in spindle area. (**E**) Chromosomal alignment with reference to the metaphase plate. The LH-treated group had a lower percentage of misaligned chromosomes than the ChT group. Scatter plots indicate individual data and means of all analyzed mice (n = 5 in controls, and n = 7 in ChT and ChT+LH-1× groups). Outliers are indicated by a cross. Statistical significance was determined by two-tailed Mann–Whitney *U* test (A and B) or linear (D) and logistic (E) regressions; **P*-values <0.05 were considered statistically significant.

Oocyte quality

Thirty-three MII-oocytes, all with meiotic spindles, were recovered from all experimental groups (Fig. 2C). The mean spindle area of oocytes from the ChT group was 35.3% less than the mean control spindle area ($P = 0.019$), but the mean spindle area of the LH-treated group was similar to that of controls and 31.1% higher than that of the ChT group ($P = 0.035$; Fig. 2D). Furthermore, the ChT group had more misaligned MII-oocytes than the control group ($P = 0.019$; Fig. 2E), and LH treatment ameliorated that effect, i.e. the number of misaligned MII oocytes were similar in the ChT+LH-1× and control groups.

Breeding trials

Reproductive lifespans of treated mice were assessed by breeding performance during six mating attempts (Fig. 3). As maternal age increased, pregnancy rates and litter sizes progressively decreased in all experimental groups. This decline was accelerated in the ChT group, with reduced cumulative pregnancy rate and litter size per delivery (Fig. 3A–C) resulting in a 45.8% reduction in the number of live births relative to controls (Fig. 3D). In contrast, both LH-treated groups had better reproductive outcomes than the ChT group. In particular, the low-dose LH group had 21% more healthy pups than the ChT group.

The ovarian protective mechanism of LH

Twelve hours after chemotherapy treatment, DSBs were identified by γH2AX staining in oocytes at all follicular stages. All groups receiving chemotherapy had significantly higher percentages of γH2AX-positive oocytes than controls ($P = 0.034$ in all cases), but both the high and low LH-treated samples had significantly lower γH2AX expression levels than the ChT samples ($P = 0.021$ and $P = 0.020$, respectively, Fig. 4A). Growing follicles were the most affected population showing the highest percentage of γH2AX-positive oocytes after chemotherapy (Control: 22.4 ± 1.8%, ChT: 69.4 ± 13.6%, $P = 0.034$), although both LH dosages significantly reduced the chemotherapy-induced DNA damage (ChT+LH-1×: 45.7 ± 4.8%, ChT+LH-5×: 39.4 ± 5.7%; $P = 0.021$ in both cases).

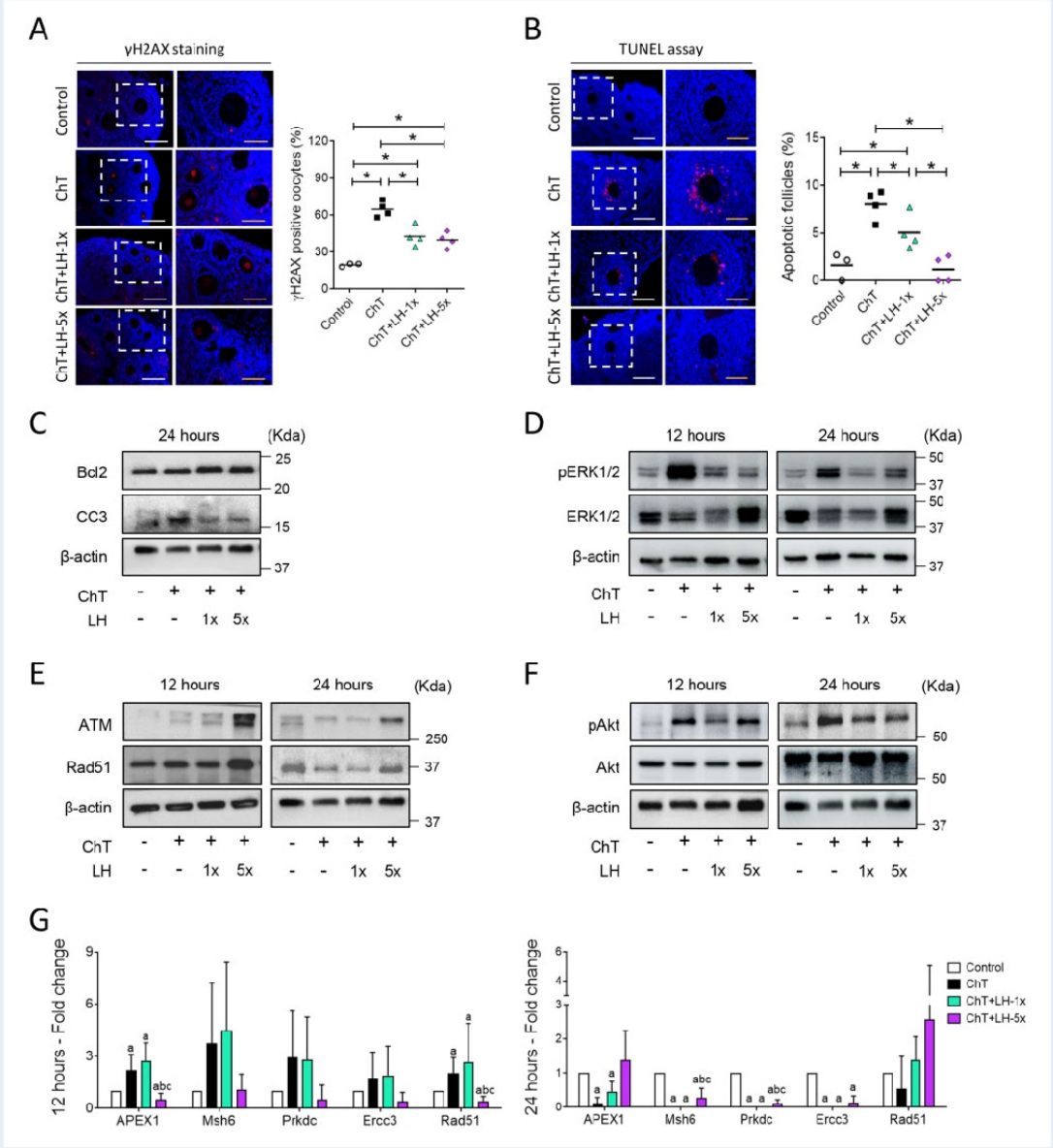

Figure 4. LH promoted DNA repair and cell survival and reduced the deleterious effects of chemotherapy on ovarian tissue. Alkylating agents were administered with or without LH and ovaries assessed 12 and 24 h after (**A**) phosphorylated H2AX histone (γH2AX) immunofluorescence (red) counterstained with DAPI (blue) of ovarian samples collected 12 h after treatments with alkylating agents with or without a low (1×) or high (5×) dose of LH (n = 3 in controls, and n = 4 in ChT, ChT+LH-1×, and ChT+LH-5× groups). Images on the left are at 20× (white scale bar = 100 μm) and on the right at 40× (yellow scale bar = 50 μm). The percentages of follicles showing γH2AX positive oocytes were quantified. The LH-treated groups had lower percentages of follicles with double-strand breaks (DSB) than the ChT group. (**B**) Terminal deoxynucleotidyl transferase-mediated dUTP nick-end labeling (TUNEL) assay (red) counterstained with DAPI (blue) was performed on ovarian sections 12 h after treatments. Magnifications and scale bars are as described in (A). Both LH-treated groups had a lower percentage of apoptotic follicles than the ChT group. (**C**) Representative western blots (WB) showing the levels of the anti-apoptotic protein B-cell lymphoma-2 (Bcl2) and the pro-apoptotic protein cleaved caspase-3 (CC3). Both doses of LH increased the Bcl2: CC3 ratio protecting the ovaries from ChT-induced cell death at 24 h.

robust upregulation of DNA repair genes, with expression of 4 out of 5 such genes reaching levels higher than that seen with ChT alone and with *Rad51* overexpression being maintained to 24 h. Unexpectedly, ChT+LH-5× ovaries showed an overall downregulation of DNA repair genes at both time-points, excepting *Rad51* at 24 h after treatment.

LH treatment protects ovaries from cisplatin

Cisplatin treatment similarly depleted the follicular pool by affecting all oocyte developmental stages (Supplementary Fig. S4). LH treatment prevented the cisplatin effects on the primordial and primary follicle populations, yielding 33.4% ($P=0.041$) and 38.2% ($P=0.009$) more follicles, respectively, than seen in the cisplatin-treated group.

Effects on growing follicles

LH treatment efficacy in a subfertile mouse model

We also assessed NOD-SCID mice, which are subfertile and therefore may provide a model for patients with aggressive cancers or already exhibiting reduced ovarian reserve. Here, NOD-SCID mice exhibited a 10-fold decrease of the follicular pool ($P=0.050$; Fig. 5A) across all developmental stages (Fig. 5B) following chemotherapy. LH-treated ovaries contained 31.2% more follicles than the ChT-treated ovaries, with particular improvement in primordial and primary populations ($P=0.034$ and $P=0.032$, respectively). Indeed, the percentage of quiescent follicles in the ChT+LH-1× group was restored to control levels (Fig. 5C and D). Nevertheless, chemotherapy promoted follicular atresia, with increases in the number of morphologically abnormal follicles in both ChT and ChT+LH-1× ovaries compared to controls ($P=0.050$ and $P=0.034$, respectively; Fig. 5E). Furthermore, a 3.5-fold increase in the stromal degeneration index was detected in ChT samples ($P=0.050$), while the increase in the ChT+LH-1× group was only 1.85-fold when referred to controls, indicating a reduction of the stromal negative effects seen in the ChT samples ($P=0.047$; Fig. 5F).

Additionally, the ChT group had more γH2AX-positive oocytes (Fig. 5G) and TUNEL-positive follicles than controls ($P=0.050$; Fig. 5H). However, LH treatment resulted in a lower percentage of DNA-damaged oocytes and a significant reduction in the percentage of apoptotic follicles ($P=0.034$).

Chemotherapy also reduced the number of MII-oocytes ($P=0.036$) and morphologically normal 2-cell embryos recovered after COS. However, the ChT+LH-1× group produced similar numbers of MII-oocytes as the control group and 26.3% more than the ChT group (Fig. 6A). This protective effect was not seen for 2-cell embryos (Fig. 6B).

Oocyte quality was then assessed in a total of 28 MII-oocytes. Meiotic spindle was only detected in 28.6% of MII-oocytes from the ChT group; in contrast and similar to the controls, all MII-oocytes from the ChT+LH-1× group contained a well-defined spindle (Fig. 6D). LH treatment increased the probability of proper spindle assembly by 60.9% relative to that of the ChT group (Fig. 6C). Chemotherapy also reduced the spindle area of MII-oocytes, with the spindle area of the ChT group being 5-fold lower than that of the control group ($P=0.001$). A less severe, but still significant reduction in spindle area was also detected in oocytes from the LH-exposed group ($P=0.030$, compared to controls). However, the LH-group exhibited a 3-fold increase in spindle area relative to that of the ChT group ($P=0.049$; Fig. 6E). The ChT group also had more MII-oocytes with misaligned chromosomes than the control group ($P=0.035$), but the ChT+LH-1× group had similar numbers as the controls and significantly fewer than the ChT group ($P=0.029$; Fig. 6F).

Discussion

This study tested the effect of LH treatment on ovarian reserve in (i) quiescent follicles in CD-1 mice and (ii) growing follicles in NOD-SCID subfertile mice following chemotherapy with alkylating agents at a dose equivalent to that used in cancer patients (Grigg *et al.*, 2000). In the CD-1 model, LH prevented the negative effects of alkylating agents on ovarian reserve, follicular development, and oocyte quality and improved breeding performance. Further, LH treatment affected DNA repair pathways, suggesting these pathways may participate in the protective effects. Similar results were seen for growing follicles in the NOD-SCID model.

The effects of 1 IU of LH on both follicle count and MII-oocyte numbers four weeks after chemotherapy and LH treatment indicate that primordial follicles were the main target for the protective action of LH, since the timing is consistent with the window required for chemotherapy-exposed quiescent follicles to complete folliculogenesis (Clarke, 2017). This finding was confirmed in adult ovaries exposed to cisplatin, supporting previous observations in prepubertal mice (Rossi *et al.*, 2017) and indicating that LH can protect the ovarian reserve

Figure 4. Continued

(**D**) Representative WB showing phosphorylated-extracellular signal-regulated Kinase 1 and 2 (pERK1/2) and ERK1/2 protein levels. ChT activated ERK1/2 signaling and LH treatments reduced this effect at 12 and 24 h. (**E**) Representative WB for ataxia-telangiectasia mutated kinase (ATM) and RAD51 recombinase (Rad51) proteins. LH-5×-treated ovaries expressed higher levels of ATM and Rad51 than ChT-treated ovaries at 12 and 24 h. (**F**) Representative WB for phosphorylated-serine/threonine-protein Kinase 1 (pAkt) and Akt proteins. Chemotherapy caused a notable increase of Akt activation at both time-points, and cotreatment with LH blocked this effect. All WBs were performed from at least two independent experiments from two pools of two ovaries each per group. (**G**) mRNA expression levels of the indicated DNA repair genes at 12 (left) and 24 h (right). At 12 h, the expression levels of all repair genes were higher in the ChT+LH-1× samples than in the ChT samples. At 24 h, Rad51 expression was higher in both LH groups than in the ChT group. Three independent ovarian fragments per group and time-point was analyzed, and expression levels were normalized to those of the control group. Scatter plots indicate individual data and means; bar charts display means and SDs. Statistical significance was determined by two-tailed Mann–Whitney *U* test; *P*-values <0.05 were considered statistically significant. $^{*}P<0.05$ or $^{a}p<0.05$, $^{b}P<0.05$ and $^{c}P<0.05$ indicating statistical differences from the control, ChT, and ChT+LH-1× group, respectively.

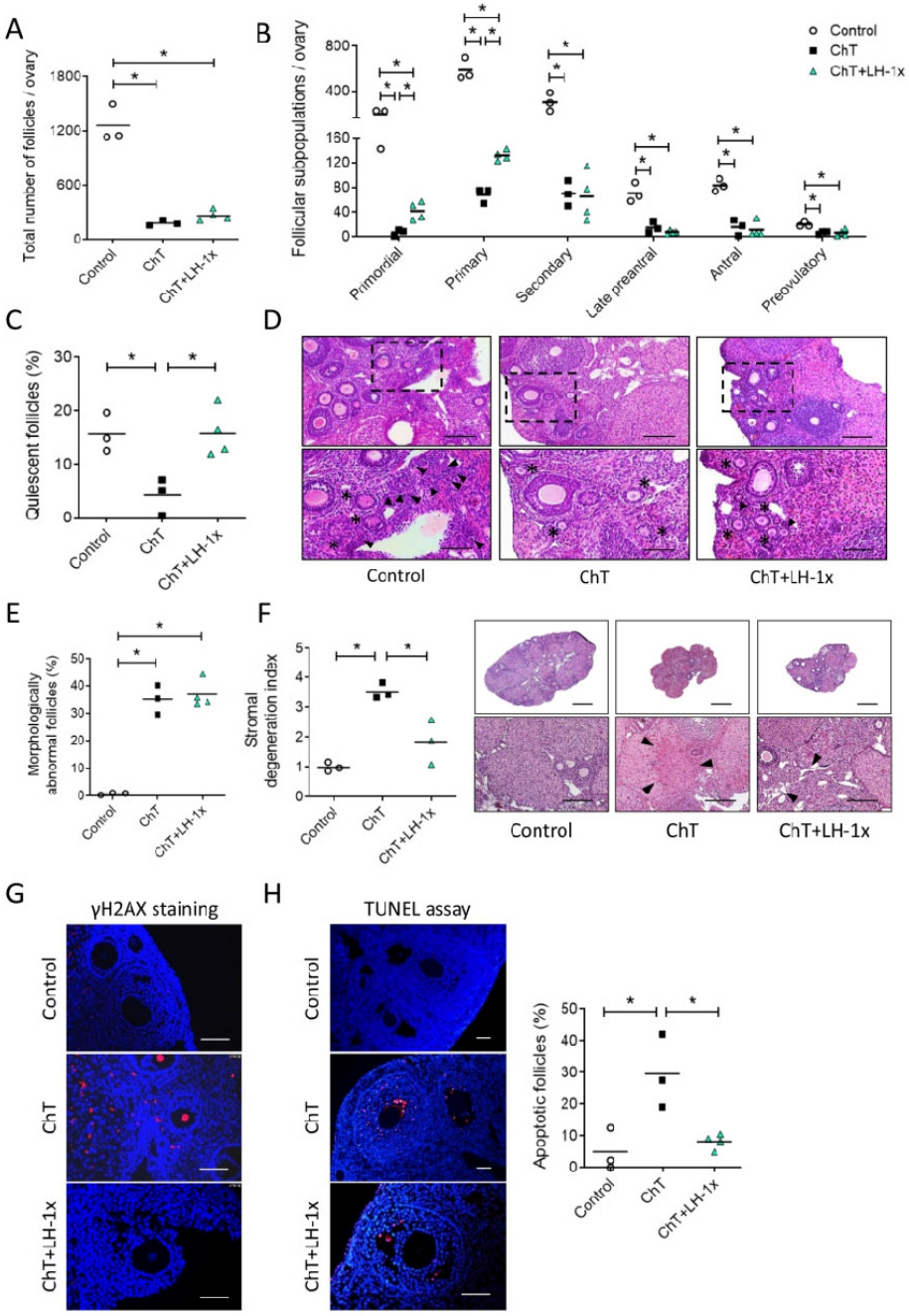

Figure 5. LH treatment protected the ovarian reserve and stromal architecture and prevented ChT-induced follicular damage in a subfertile NOD/SCID mouse model. Mice were treated with alkylating agents with or without LH and seven days later underwent COS. Ovaries were harvested and examined for follicle numbers, DNA damage, and apoptosis. (**A**) Total follicle numbers. (**B**) Follicle subpopulations.

from multiple types of agents. Consistent with previous studies (Petrillo *et al.*, 2011; Soleimani *et al.*, 2011; Luan *et al.*, 2019; Nguyen *et al.*, 2019; Wang, *et al.*, 2019), we observed a close relationship between follicle loss and oocyte damage followed by chemotherapy induced-cell death. Thus, the notable decrease of oocytes with γH2AX foci and apoptotic follicles observed 12 h after low- or high-dose LH suggests that DNA damage and cell death pathways mediate the preservative effect of LH on follicle counts.

DNA damage and apoptosis are intimately connected to cell fate determination in that cells with efficient DNA damage response or repair mechanisms are permitted to survive (Orren *et al.*, 1997; Biechonski *et al.*, 2018). In general, at both 12 and 24 h after treatment, ovaries from animals treated with LH had higher expression of DNA repair factors such as Rad51 than ovaries from animals treated with alkylating agents alone, indicating that LH stimulates DNA repair as previously suggested (Rossi *et al.*, 2017; Marcozzi *et al.*, 2019). In fact, overexpression of Rad51, a downstream target of the ATM pathway essential for the homologous recombination repair process, is a common mechanism by which cancer cells evade cytotoxic effects of oncologic therapies (Hu *et al.*, 2019) and follicular cells prevent apoptosis (Kujjo *et al.*, 2010, 2012). We also observed that LH treatment reduced Akt activation, a signaling pathway connecting DNA repair (Karimian *et al.*, 2019; Maidarti *et al.*, 2020) and DSB accumulation in primordial and primary follicles by inhibiting Rad51 (Shen *et al.*, 2007; Plo *et al.*, 2008; Maidarti *et al.*, 2019). Moreover, our findings suggested that LH decreases apoptosis by restoring CC3 levels, a specific cell death effector in oocytes and granulosa (Matikainen *et al.*, 2001; Takai *et al.*, 2007), and prevents ERK1/2 activation (Wei *et al.*, 2013; Rossi *et al.*, 2017).

MII meiotic spindle formation can serve as a measure of oocyte quality (Wang and Keefe, 2002; Rama *et al.*, 2007; Tomari *et al.*, 2018). We found that MII-oocytes that developed from primordial follicles exposed to chemotherapy exhibited defects in spindle area and chromosome alignment. Unrepaired DSBs in oocytes interfere with progression of the second meiotic division, proper spindle assembly, and chromosome cohesion (Watrin and Peters, 2006; Xiong *et al.*, 2008; Marangos *et al.*, 2015). Hence, the ability of LH to attenuate chemotherapy-induced DNA damage could underlie the improvements observed in spindle and chromosome alignment. Resting follicles were therefore protected by LH to preserve their subsequent development.

Bidirectional somatic-germ cell communication is crucial to generate a suitable microenvironment in the ovary and is required for oocyte competence and maturation. We found that chemotherapy affected the ovarian niche by degenerating the ovarian stroma and impairing oocyte maturation and quality, as previously reported (Zhang *et al.*, 2016; Wang *et al.*, 2019; Buigues *et al.*, 2020). However, treatment with LH reduced the deleterious effects on ovarian stromal cells and architecture. The protective LH effects on oocytes could occur, in part, via ovarian somatic cells that express the LH receptor (Chang *et al.*, 2015).

The short-term ability of LH to protect the ovarian reserve and improve the number and quality of developing oocytes appeared to translate into long-term benefits for reproductive performance. ChT-LH-treated mice had higher pregnancy rates and more pups than the ChT group, consistent with findings in cisplatin-treated mice (Rossi *et al.*, 2017). Interestingly, low-dose LH appeared to better preserve breeding performance. High LH dosage could adversely alter factors required for fertility, as previously described (Flaws *et al.*, 1997), and reported for some drugs (Bertoldo *et al.*, 2020; Park *et al.*, 2020). Administering gonadotropin-releasing hormone agonists (GnRHa) during chemotherapy can improve reproductive outcomes in oncologic patients (Blumenfeld *et al.*, 2015; Meli *et al.*, 2018; Sinha *et al.*, 2018), but their efficacy as gonadoprotective agents is controversial (Bildik *et al.*, 2015; Horicks *et al.*, 2018; Lambertini *et al.*, 2018; Sofiyeva *et al.*, 2019). The effects induced by our proposed LH treatment and the GnRHa therapies currently in use mainly differ in terms of treatment duration and cumulative dosage. We propose an acute administration of LH along with chemotherapy, but GnRHa therapies involve long-term repetitive treatments to achieve permanent suppression of the reproductive axis. Nevertheless, further research is needed to determine the best dosage and timing for LH during chemotherapy regimens.

When considering regimens to preserve fertility, a patient's ovarian pool is an important consideration. Patients with aggressive cancer and who have already received a chemotherapeutic cycle before undergoing fertility preservation are likely to already have diminished reserves and could benefit from therapies that can protect growing follicle populations. Using a mouse model with reduced fertility (NOD-SCID) (Kumagai *et al.*, 2011), we performed COS one week (instead of 4 weeks) after chemotherapy with or without LH treatment. LH significantly protected the most undifferentiated subpopulations (i.e.

Figure 5. Continued
The LH group had more total follicles than the ChT group. This effect was most appreciable in the primordial and primary populations, (**C**) ChT depleted the quiescent population and LH blocked this effect. (**D**) Representative H&E stained images captured at 10× (top, scale bar = 200 μm) and magnified images of the boxed regions at 20× (bottom, scale bar = 100 μm) showing primordial (black arrows) and primary (black asterisks) follicles. (E) LH treatment was unable to reverse the ChT-induced increase in the percentage of morphologically abnormal follicles. (**F**) Stromal degeneration index and representative images of lesions visualized at 2.5× (top, scale bar = 800 μm) and 10× (bottom, scale bar = 200 μm). Fibrotic areas are indicated with black arrows in 10x images. LH treatment protected ovaries from ChT-induced stromal degeneration. (**G**) Representative images of γH2AX (red) immunofluorescence counterstained with DAPI (blue). LH treatment protects cells from ChT-induced double-strand breaks. Scale bar = 100 μm. (**H**) Representative images of TUNEL-staining (red) counterstained with DAPI (blue). Scale bar = 50 μm. Apoptotic follicles (≥ 20% labeled cells) were quantified. ChT treatment increased the percentage of apoptotic follicles, and LH treatment reversed this effect. Scatter plots indicate individual data and means of all analyzed mice (n = 3 in Control and ChT, and n = 4 in ChT+LH-1× groups). Statistical significance was determined by two-tailed Mann–Whitney *U* test; **P*-values <0.05 were considered statistically significant.

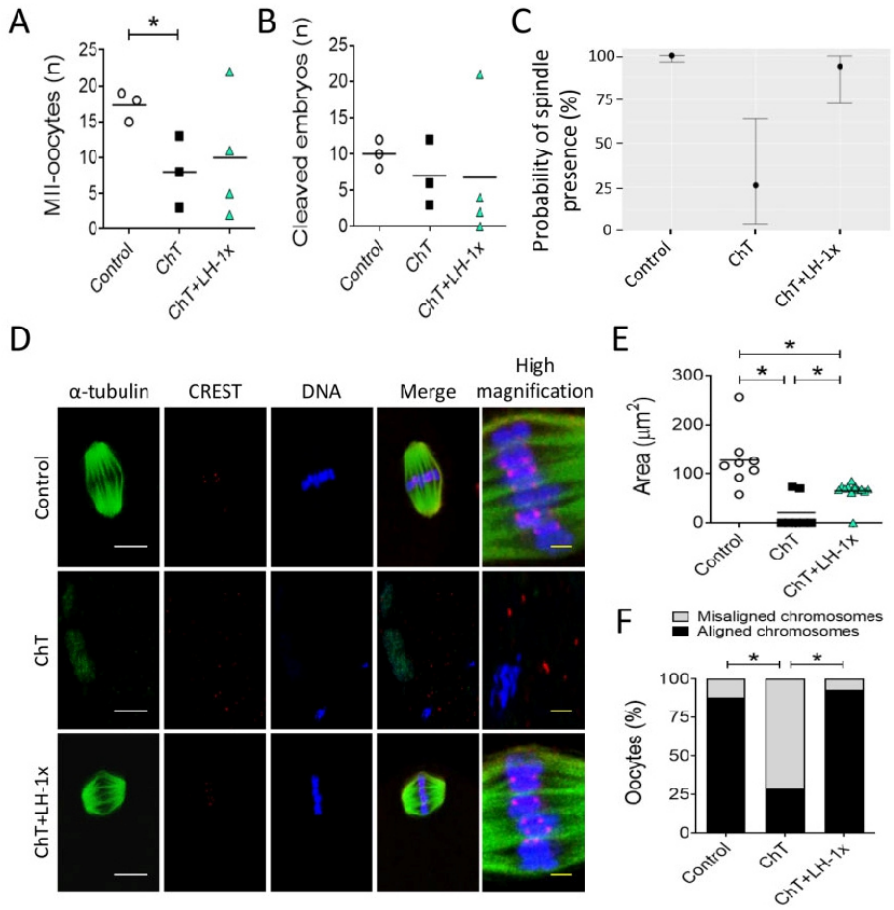

Figure 6. LH treatment ameliorated the effects of alkylators on oocyte quality in NOD/SCID mice. Mice were treated with alkylating agents with or without LH and 7 days later underwent COS to release oocytes that had been exposed to chemotherapy during their growth stage. (**A**) ChT reduced the number of healthy MII-oocytes ovulated after COS, and LH blunted this effect. (**B**) ChT decreased the number of early-cleavage stage embryos, and LH was unable to block this effect. (**C**) Bayesian model predicting the probability of spindle presence in MII-oocytes. LH treatment promoted spindle assembly during chemotherapy. (**D**) Representative images of meiotic spindles from ovulated MII-oocytes (n = 8 in Control, n = 7 in ChT, and n = 13 in ChT+LH-1× groups) and a high magnification view of the equatorial plate. α-tubulin staining (green), chromosomes (blue), and CREST-protein centromeres (red) were visualized. White scale bar = 10 μm; yellow scale bar = 1.25 μm. (**E**) Analysis of spindle area indicates LH treatment can ameliorate the effects of ChT. (**F**) Percentage of MII-oocytes with at least one misaligned chromosome as referred to the equatorial plate. ChT treatment resulted in a higher percentage of oocytes with misaligned chromosomes and LH treatment reversed this effect. Scatter plots indicated individual data and means of all analyzed mice (n = 5 in Control and ChT, and n = 6 in ChT+LH-1× groups). Statistical significance was determined by two-tailed Mann–Whitney *U* test (A and B), Bayesian analysis (C), linear (E) and logistic (F) regressions; **P*-values <0.05 were considered statistically significant.

primordial and primary follicles), supporting both the results obtained in our first model and by other authors (Rossi *et al.*, 2017). This effect may reflect reduced DNA damage in oocytes and/or diminished burnout effect (Kalich-Philosoph *et al.*, 2013; Chang *et al.*, 2015; Wang *et al.*, 2019). Treatment with LH also blocked the deleterious effects of chemotherapy on growing oocyte populations, rescuing spindle defects and restoring suitable meiotic competence.

Altogether, these results indicate that, despite its short half-life (Santen and Bardin, 1973; Penny *et al.*, 1977), LH is able to protect the ovary from alkylating agents. Cyclophosphamide and its active

metabolites have half-lives in plasma even shorter than that of LH (Powers and Sladek, 1983; Hong *et al.*, 1991; Rana *et al.*, 2007) but still trigger persistent cytotoxicity. Like cyclophosphamide, LH may trigger persisting effects by activating signaling pathways and cell functions.

LH and hCG have equivalent roles in clinical practice and can bind the same receptor; hCG has a longer half-life (Norman *et al.*, 2000), making it a strong candidate for gonadoprotection. However, LH and hCG differ in the amino acid residues required for binding to their shared receptor (Galet and Ascoli, 2005). This molecular variance leads to differing activities. LH is more effective as a proliferative and anti-apoptotic factor, while hCG has higher steroidogenic activity (Casarini *et al.*, 2016; Riccetti *et al.*, 2017). Nevertheless, hCG may be gonadoprotective, and further research should assess this.

In conclusion, this is the first study to analyze, in detail, the broad spectrum of protective effects elicited by LH on the ovarian reserve of adult mice during chemotherapy treatment with highly gonadotoxic agents. Mechanistically, LH appeared to prevent follicular depletion by reducing DNA damage in oocytes and by decreasing apoptosis and follicular atresia. We found that LH triggers an early DNA damage response after chemotherapy, which likely improves ovulation and oocyte competence. Treatment with LH also had long-term reproductive benefits, improving fertility and extending the reproductive lifespans of mice exposed to chemotherapy. Our research investigated LH effects using several approaches designed to represent different clinical reproductive scenarios, e.g. IVF cycles and natural conception, and uncovered possible mechanisms of action. Although these results were obtained in mice, the ability of LH to protect the mouse ovary from alkylating agents and cisplatin (Rossi *et al.*, 2017) highlights its therapeutic potential encouraging human clinical trials. Thus, a universal LH-based strategy may be possible for in situ ovarian reserve protection in female cancer patients.

Supplementary data

Supplementary data are available at *Human Reproduction* online.

Data availability

The data underlying this article will be shared on reasonable request to the corresponding author.

Acknowledgements

The authors would like to thank Sonia Priego and microscopy service (UCIM, University of Valencia, Valencia, Spain) for technical assistance in oocyte analysis. The authors are also grateful to Merck Serono for providing the LH.

Authors' roles

L.M.C. conducted experimental studies, analyzed results, and wrote the manuscript; A.B. performed experiments and analyzed results; V.R., M.J.S., H.K.L., and J.M. contributed to performing the experiments; F.G.K., M.D.F., and F.D.R. designed and supervised the research and critically reviewed the manuscript; A.P. designed, supervised, coordinated, and funded the study and critically revised the manuscript; S.H. designed, coordinated, and conducted experiments, funded the research, and wrote the manuscript.

Funding

This study was supported by grants from the Regional Valencian Ministry of Education (PROMETEO/2018/137), the Spanish Ministry of Science and Innovation (CP19/00141), and the Spanish Ministry of Education, Culture and Sports (FPU16/05264).

Conflict of interest

The authors declare no conflict of interest.

References

Anderson RA, Brewster DH, Wood R, Nowell S, Fischbacher C, Kelsey TW, Wallace WH. The impact of cancer on subsequent chance of pregnancy: a population based analysis. *Hum Reprod* 2018;**33**:1281–1290.

Bertoldo MJ, Listijono DR, Ho WHJ, Riepsamen AH, Goss DM, Richani D, Jin XL, Mahbub S, Campbell JM, Habibalahi A. *et al.* NAD+ repletion rescues female fertility during reproductive aging. *Cell Rep* 2020;**30**:1670–1681.

Biechonski S, Olender L, Zipin-Roitman A, Yassin M, Aqaqe N, Marcu-Malina V, Rall-Scharpf M, Trottier M, Meyn MS, Wiesmüller L. *et al.* Attenuated DNA damage responses and increased apoptosis characterize human hematopoietic stem cells exposed to irradiation. *Sci Rep* 2018;**8**:6071.

Bildik G, Akin N, Senbabaoglu F, Sahin GN, Karahuseyinoglu S, Ince U, Taskiran C, Selek U, Yakin K, Guzel Y. *et al.* GnRH agonist leuprolide acetate does not confer any protection against ovarian damage induced by chemotherapy and radiation in vitro. *Hum Reprod* 2015;**30**:2912–2925.

Blumenfeld Z, Zur H, Dann EJ. Gonadotropin-releasing hormone agonist cotreatment during chemotherapy may increase pregnancy rate in survivors. *Oncologist* 2015;**20**:1283–1289.

Buigues A, Marchante M, Herraiz S, Pellicer A. Diminished ovarian reserve chemotherapy-induced mouse model: a tool for the preclinical assessment of new therapies for ovarian damage. *Reprod Sci* 2020;**27**:1609–1619.

Casarini L, Riccetti L, De Pascali F, Nicoli A, Tagliavini S, Trenti T, La Sala GB, Simoni M. Follicle-stimulating hormone potentiates the steroidogenic activity of chorionic gonadotropin and the anti-apoptotic activity of luteinizing hormone in human granulosa-lutein cells in vitro. *Mol Cell Endocrinol* 2016;**422**:103–114.

Chang EM, Lim E, Yoon S, Jeong K, Bae S, Lee DR, Yoon TK, Choi Y, Lee W. Cisplatin induces overactivation of the dormant primordial follicle through PTEN/AKT/FOXO3α pathway which leads to loss of ovarian reserve in mice. *PLoS One* 2015;**10**:e0144245.

Clarke H. Control of mammalian oocyte development by interactions with the maternal follicular environment. *Results Probl Cell Differ* 2017;**63**:17–41.

Coticchio G, Guglielmo MC, Dal Canto M, Fadini R, Mignini Renzini M, De Ponti E, Brambillasca F, Albertini DF. Mechanistic

foundations of the metaphase II spindle of human oocytes matured in vivo and in vitro. *Hum Reprod* 2013;**28**:3271–3282.

Dath C, Van Eyck AS, Dolmans MM, Romeu L, Delle Vigne L, Donnez J, Van Langendonckt A. Xenotransplantation of human ovarian tissue to nude mice: comparison between four grafting sites. *Hum Reprod* 2010;**25**:1734–1743.

Ferlay J, Ervik J, Lam F, Colombet M, Mery L, Piñeros M, Znaor A, Soerjomataram BF. *Global Cancer Observatory: Cancer Today 2020*. Lyon, France: International Agency for Research on Cancer; 2018.

Flaws JA, Abbud R, Mann RJ, Nilson JH, Hirshfield AN. Chronically elevated luteinizing hormone depletes primordial follicles in the mouse ovary. *Biol Reprod* 1997;**57**:1233–1237.

Galet C, Ascoli M. The differential binding affinities of the luteinizing hormone (LH)/choriogonadotropin receptor for LH and choriogonadotropin are dictated by different extracellular domain residues. *Mol Endocrinol* 2005;**19**:1263–1276.

Grigg AP, McLachlan R, Zaja J, Szer J. Reproductive status in long-term bone marrow transplant survivors receiving busulfan-cyclophosphamide (120 mg/kg). *Bone Marrow Transplant* 2000;**26**: 1089–1095.

Hong PS, Srigritsanapol A, Chan KK. Pharmacokinetics of 4-hydroxy-cyclophosphamide and metabolites in the rat. *Drug Metab Dispos* 1991;**19**:1–7.

Horicks F, Van Den Steen G, Gervy C, Clarke HJ, Demeestere I. Both in vivo FSH depletion and follicular exposure to Gonadotrophin-releasing hormone analogues in vitro are not effective to prevent follicular depletion during chemotherapy in mice. *Mol Hum Reprod* 2018;**24**:221–232.

Howlader N, Noone AM, Krapcho M, Miller D, Brest A, Yu M, Ruhl J, Tatalovich Z, Mariotto A, Lewis DR. SEER cancer statistics review. *Natl Cancer Inst* 2019;1975–2016. 2020.

Hu J, Zhang Z, Zhao L, Li L, Zuo W, Han L. High expression of RAD51 promotes DNA damage repair and survival in KRAS-mutant lung cancer cells. *BMB Rep* 2019;**52**:151–156.

Kalich-Philosoph L, Roness H, Carmely A, Fishel-Bartal M, Ligumsky H, Paglin S, Wolf I, Kanety H, Sredni B, Meirow D. Cyclophosphamide triggers follicle activation and "burnout "; AS101 prevents follicle loss and preserves fertility. *Sci Transl Med* 2013;**5**:185ra62. ra62.

Karimian A, Mir SM, Parsian H, Refieyan S, Mirza-Aghazadeh-Attari M, Yousefi B, Majidinia M. Crosstalk between Phosphoinositide 3-kinase/Akt signaling pathway with DNA damage response and oxidative stress in cancer. *J Cell Biochem* 2019;**120**:10248–10272.

Koyama H, Wada T, Nishizawa Y, Iwanaga T, Aoki Y, Terasawa T, Kosaki G, Yamamoto T, Wada A. Cyclophosphamide-induced ovarian failure and its therapeutic significance in patients with breast cancer. *Cancer* 1977;**39**:1403–1409.

Kujjo LL, Laine T, Pereira RJG, Kagawa W, Kurumizaka H, Yokoyama S, Perez GI. Enhancing survival of mouse oocytes following chemotherapy or aging by targeting bax and Rad51. *PLoS One* 2010;**5**:e9204.

Kujjo LL, Ronningen R, Ross P, Pereira RJG, Rodriguez R, Beyhan Z, Goissis MD, Baumann T, Kagawa W, Camsari C. *et al.* RAD51 plays a crucial role in halting cell death program induced by ionizing radiation in bovine oocytes1. *Biol Reprod* 2012;**86**:76.

Kumagai K, Kubota N, Saito TI, Sasako T, Takizawa R, Sudo K, Kurokawa M, Kadowaki T. Generation of transgenic mice on an NOD/SCID background using the conventional microinjection technique. *Biol Reprod* 2011;**84**:682–688.

Lambertini M, Moore HCF, Leonard RCF, Loibl S, Munster P, Bruzzone M, Boni L, Unger JM, Anderson RA, Mehta K. *et al*. Gonadotropin-releasing hormone agonists during chemotherapy for preservation of ovarian function and fertility in premenopausal patients with early breast cancer: a systematic review and meta-analysis of individual patient–level data. *J Clin Oncol* 2018;**36**: 1981–1990.

Livak KJ, Schmittgen TD. Analysis of relative gene expression data using real-time quantitative PCR and the 2-ΔΔCT method. *Methods* 2001;**25**:402–408.

Luan Y, Edmonds ME, Woodruff TK, Kim SY. Inhibitors of apoptosis protect the ovarian reserve from cyclophosphamide. *J Endocrinol* 2019;**240**:243–256.

Macklon NS, Fauser BCJM. Aspects of ovarian follicle development throughout life. *Horm Res* 1999;**52**:161–170.

Maidarti M, Clarkson YL, Mclaughlin M, Anderson RA, Telfer EE. Inhibition of PTEN activates bovine non-growing follicles in vitro but increases DNA damage and reduces DNA repair response. *Hum Reprod* 2019;**34**:297–307.

Maidarti M, Anderson RA, Telfer EE. Crosstalk between PTEN/PI3K/Akt signalling and DNA damage in the oocyte: implications for primordial follicle activation. *Oocyte Quality Ageing. Cells* 2020;**9**: 200.

Marangos P, Stevense M, Niaka K, Lagoudaki M, Nabti I, Jessberger R, Carroll J. DNA damage-induced metaphase i arrest is mediated by the spindle assembly checkpoint and maternal age. *Nat Commun* 2015;**6**:8706.

Marcozzi S, Rossi V, Salvatore G, Di Rella F, De Felici M, Klinger FG. Distinct effects of epirubicin, cisplatin and cyclophosphamide on ovarian somatic cells of prepuberal ovaries. *Aging (Albany NY)* 2019;**11**:10532–10556.

Matikainen T, Perez GI, Zheng TS, Kluzak TR, Rueda BR, Flavell RA, Tilly JL. Caspase-3 gene knockout defines cell lineage specificity for programmed cell death signaling in the ovary. *Endocrinology* 2001; **142**:2468–2480.

Meirow D, Biederman H, Anderson RA, Wallace WH. Toxicity of chemotherapy and radiation on female reproduction. *Clin Obstet Gynecol* 2010;**53**:727–739.

Meli M, Caruso-Nicoletti M, La Spina M, Nigro LL, Samperi P, D'Amico S, Bellia F, Miraglia V, Licciardello M, Cannata E. *et al*. Triptorelin for fertility preservation in adolescents treated with chemotherapy for cancer. *J Pediatr Hematol Oncol* 2018;**40**:269–276.

Nguyen QN, Zerafa N, Liew SH, Findlay JK, Hickey M, Hutt KJ. Cisplatin- and cyclophosphamide-induced primordial follicle depletion is caused by direct damage to oocytes. *Mol Hum Reprod* 2019; **25**:433–444.

Norman RJ, Buchholz MM, Somogyi AA, Amato F. hCGbeta core fragment is a metabolite of hCG: evidence from infusion of recombinant hCG. *J Endocrinol* 2000;**164**:299–305.

Orren DK, Petersen LN, Bohr VA. Persistent DNA damage inhibits S-phase and G2 progression, and results in apoptosis. *Mol Biol Cell* 1997;**8**:1129–1142.

Park BK, Park MJ, Kim HG, Han SE, Kim CW, Joo BS, Lee KS. Role of visfatin in restoration of ovarian aging and fertility in the mouse aged 18 months. *Reprod Sci* 2020;**27**:681–689.

Penny R, Olambiwonnu NO, Frasier SD. Episodic fluctuations of serum gonadotropins in pre- and post-pubertal girls and boys. *J Clin Endocrinol Metab* 1977;**45**:307–311.

Petrillo SK, Desmeules P, Truong TQ, Devine PJ. Detection of DNA damage in oocytes of small ovarian follicles following phosphoramide mustard exposures of cultured rodent ovaries in vitro. *Toxicol Appl Pharmacol* 2011;**253**:94–102.

Plo I, Laulier C, Gauthier L, Lebrun F, Calvo F, Lopez BS. AKT1 inhibits homologous recombination by inducing cytoplasmic retention of BRCA1 and RAD5. *Cancer Res* 2008;**68**:9404–9412.

Powers JF, Sladek NE. Cytotoxic activity relative to 4-hydroxycyclophosphamide and phosphoramide mustard concentrations in the plasma of cyclophosphamide-treated rats. *Cancer Res* 1983;**43**:1101–1106.

Rama RG, Prakash GJ, Krishna KM, Madan K. Meiotic spindle and zona pellucida characteristics as predictors of embryonic development: a preliminary study using PolScope imaging. *Reprod BioMed Online* 2007;**14**:166–174.

Rana S, Mohamed AR, Behnam S, Suleiman AH, Zuzana H, Moustapha H. Cyclophosphamide pharmacokinetics in mice: a comparison between retro orbital sampling versus serial tail vein bleeding. *Open Pharmacol J* 2007;**1**:30–35.

Riccetti L, Yvinec R, Klett D, Gallay N, Combarnous Y, Reiter E, Simoni M, Casarini L, Ayoub MA. Human luteinizing hormone and chorionic gonadotropin display biased agonism at the LH and LH/CG receptors. *Sci Rep* 2017;**7**:940.

Rossi V, Lispi M, Longobardi S, Mattei M, Rella FD, Salustri A, De Felici M, Klinger FG. LH prevents cisplatin-induced apoptosis in oocytes and preserves female fertility in mouse. *Cell Death Differ* 2017;**24**:72–82.

Santen RJ, Bardin CW. Episodic luteinizing hormone secretion in man. Pulse analysis, clinical interpretation, physiologic mechanisms. *J Clin Invest* 1973;**52**:2617–2628.

Shen WH, Balajee AS, Wang J, Wu H, Eng C, Pandolfi PP, Yin Y. Essential role for nuclear PTEN in maintaining chromosomal integrity. *Cell* 2007;**128**:157–170.

Sinha N, Letourneau JM, Wald K, Xiong P, Imbar T, Li B, Harris E, Mok-Lin E, Cedars MI, Rosen MP. Antral follicle count recovery in women with menses after treatment with and without gonadotropin-releasing hormone agonist use during chemotherapy for breast cancer. *J Assist Reprod Genet* 2018;**35**:1861–1868.

Sofiyeva N, Siepmann T, Barlinn K, Seli E, Ata B. Gonadotropin-releasing hormone analogs for gonadal protection during gonadotoxic chemotherapy: a systematic review and meta-analysis. *Reprod Sci* 2019;**26**:939–953.

Soleimani R, Heytens E, Darzynkiewicz Z, Oktay K. Mechanisms of chemotherapy-induced human ovarian aging: double strand DNA breaks and microvascular compromise. *Aging (Albany NY)* 2011;**3**:782–793.

Spears N, Lopes F, Stefansdottir A, Rossi V, De Felici M, Anderson RA, Klinger FG. Ovarian damage from chemotherapy and current approaches to its protection. *Hum Reprod Update* 2019;**25**:673–693.

Takai Y, Matikainen T, Jurisicova A, Kim MR, Trbovich AM, Fujita E, Nakagawa T, Lemmers B, Flavell RA, Hakem R. *et al.* Caspase-12 compensates for lack of caspase-2 and caspase-3 in female germ cells. *Apoptosis* 2007;**12**:791–800.

Tomari H, Honjo K, Kunitake K, Aramaki N, Kuhara S, Hidaka N, Nishimura K, Nagata Y, Horiuchi T. Meiotic spindle size is a strong indicator of human oocyte quality. *Reprod Med Biol* 2018;**17**:268–274.

Wang WH, Keefe DL. Prediction of chromosome misalignment among in vitro matured human oocytes by spindle imaging with the PolScope. *Fertil Steril* 2002;**78**:1077–1081.

Wang Y, Liu M, Johnson SB, Yuan G, Arriba AK, Zubizarreta ME, Chatterjee S, Nagarkatti M, Nagarkatti P, Xiao S. Doxorubicin obliterates mouse ovarian reserve through both primordial follicle atresia and overactivation. *Toxicol Appl Pharmacol* 2019;**381**:114714.

Watrin E, Peters JM. Cohesin and DNA damage repair. *Exp Cell Res* 2006;**312**:2687–2693.

Wei F, Yan J, Tang D, Lin X, He L, Xie Y, Tao L, Wang S. Inhibition of ERK activation enhances the repair of double-stranded breaks via non-homologous end joining by increasing DNA-PKcs activation. *Biochim Biophys Acta* 2013;**1833**:90–100.

Winship AL, Stringer JM, Liew SH, Hutt KJ. The importance of DNA repair for maintaining oocyte quality in response to anti-cancer treatments, environmental toxins and maternal ageing. *Hum Reprod Update* 2018;**24**:119–134.

Xiong B, Li S, Ai J, Yin S, OuYang Y, Sun S, Chen D, Sun Q. BRCA1 is required for meiotic spindle assembly and spindle assembly checkpoint activation in mouse oocytes1. *Biol Reprod* 2008;**79**:718–726.

Zhang T, Yan D, Yang Y, Ma A, Li L, Wang Z, Pan Q, Sun Z. The comparison of animal models for premature ovarian failure established by several different source of inducers. *Regul Toxicol Pharmacol* 2016;**81**:223–232.

APPENDIX VII. Manuscript II

Title

LH preserves oocyte – granulosa cell communication in mouse follicles exposed to chemotherapy with alkylating agents at primordial stage

Running title

LH preserves somatic-germ crosstalk from chemotherapy

Authors

L.M. Del Castillo1,2, M.J. Soriano1, J. Martinez1,2, A. Pellicer1,3, S. Herraiz1*

1. IVI Foundation – IIS La Fe, Reproductive Medicine Research Group, Valencia, Spain.
2. Departament de Pediatria, Obstetrícia i Ginecologia, Facultat de Medicina i Odontologia, Universitat de València, Valencia, Spain.
3. IVI-RMA Rome, Rome, Italy.

***Address correspondence to:**

Sonia Herraiz, PhD

IVI Foundation, Valencia, Spain.

Av. Fernando Abril Martorell, 106-Torre A- Planta1. 46026 Valencia, Spain.

Phone number: +34 96 390 33 05

Sonia.Herraiz@ivirma.com

ORCID iD: 0000-0003-0703-6922

Abstract

Study question: Does LH preserve the bidirectional communication between germ and somatic compartments of mouse follicles exposed to chemotherapy at the primordial stage?

Summary answer: LH treatment prevents the chemotherapy-induced effects on the oocyte-granulosa cells (GC) crosstalk during the folliculogenesis.

What is known already: Follicular growth and oocyte maturation can be disturbed after chemotherapy, which finally leads to poor quality oocytes and infertility. Reciprocal communication between oocytes and GC over the course of folliculogenesis is required for a proper follicular development and oocyte competence. LH was recently proposed to protect the quality of metaphase II oocytes derived from primordial follicles exposed to chemotherapy in mice.

Study design, size, duration: This was an experimental study where adult seven-week-old CD-1 female mice were randomly allocated to control (n=3), chemotherapy (ChT, n=5) and ChT+LH (n=5) groups. Primary ovarian insufficiency (POI) was induced in ChT and ChT+LH groups by intraperitoneally administrating 120 mg/kg of cyclophosphamide and 12 mg/kg of busulfan, while animals in control group only received vehicle. ChT+LH group was also treated with 1 international unit (IU) of LH 24 hours before chemotherapy administration, followed by a second 1 IU injection of LH simultaneously with the chemotherapy. Animals were stimulated after 30 days of housing with 10 IU of pregnant mare serum gonadotropin (PMSG) and 10 IU of hCG. Mice was euthanized 48 hours after hCG injection to collect ovaries.

Participants/materials, setting, methods: Follicles were mechanically isolated by puncture from one frozen-thawed ovary per mouse. Isolated follicles were counted and classified according to their diameter in primordial/primary (<100 µm) or secondary/later developmental stages (≥100 µm). Follicles measuring ≥100 µm were selected, keeping intact half of them (FOL), while remaining were decumulated to obtain denuded oocytes (OO) and GC. Total RNA and protein contents were extracted from FOL, OO and GC, and analyzed by qRT-PCR and western blot to evaluate key molecules involved in oocyte-GC junctions (Cx37, E-Cad, Cx43, N-Cad, Tjp1) and paracrine factors (Gdf9, Bmp15, Bmpr2, Alk4, Alk5, Alk6). Intercellular junctions and oocyte-secreted factors were subsequently visualized by confocal microscopy to validate the molecular outcomes.

Main results and the role of chance: LH improved the follicle content of ovaries exposed to chemotherapy by specially protecting the smallest ones, which correspond with the primordial and primary populations. LH treatment reverted the chemotherapy-induced impairment of oocyte-GC communication at gene and protein expression levels in secondary and later developmental follicles exposed to chemotherapy at primordial phase . This LH-mediated protection seemed to be similarly conferred to the both germ and somatic compartments. LH also restored the already decreased levels of immunofluorescence signal on ChT-samples up to control-like values for the Cx37, E-Cad and Cx43 mediated cell junctions, as well as the oocyte-secreted factors GDF9 and BMP15. The alteration of signal intensity by chemotherapy was detected beyond the secondary stage, suggesting that the attenuation of oocyte-GC crosstalk might be happened during the primary-secondary transition.

Limitations, reasons for caution: This was an animal model study performed with a reduced sample size that should be validated in larger studies with human samples.

Wider implications of the findings: Our results suggest that LH-treated primordial follicles retain the ability to properly establish oocyte-GC interactions and crosstalk during follicular growth. Thus, these findings represent a novel mechanism triggered by LH treatment that would explain the protective effects of LH on the oocyte quality and female fertility seen in previous studies.

Study funding/competing interest(s): This research was funded by the Regional Valencian Ministry of Education (PROMETEO/2018/137), the Spanish Ministry of Science and Innovation (CP19/00141), and the Spanish Ministry of Education, Culture and Sports (FPU16/05264). The authors declare no conflict of interest.

Trial registration number: N/A.

Key words

Fertility preservation, folliculogenesis, follicle development, somatic-germ cell interactions, chemotherapy, LH.

Introduction

Oocytes and their neighboring granulosa cells (GC) establish a reciprocal communication over the course of folliculogenesis, essential to produce a healthy egg. By this crosstalk, oocytes are supplied by GC with second messengers, amino-acids, peptides, and molecules to support the oocyte metabolic activity and growth, while the oocyte sends signals to the somatic cells that regulate their differentiation, proliferation and help create a suitable microenvironment that ensure the oocyte maturation (Clarke, 2018). Oocytes and GC are physically interconnected throughout thin cytoplasmic projections, called transzonal projections (TZP), that extend from GC to oocyte membrane and carry out two major functions. On the one hand, TZP preserve the granulosa-oocyte complex integrity maintaining the adhesion between both compartments. This task is performed, at least in part, by adherens and tight junctions, where epithelial and neural cadherins (E-Cad and N-Cad, respectively), and tight junction protein 1 (TJP1) play key roles (Mora et al., 2012). On the other hand, TZP tips harbor gap junctions, which consist of intercellular channels composed of transmembrane proteins, termed connexins, that allow the rapid exchange of molecules up to 1 kDa in size between the coupled cells (Goldberg et al., 2004). Connexin 37 and 43 (Cx37 and Cx43, respectively) are the most abundant in mammals and indispensable for follicular development and oocyte growth (Gershon et al., 2008). Moreover, gap junctions allow the oocyte regulate its pH (FitzHarris et al., 2007), as well as control the meiotic status of developing oocytes by mediating the transfer of cyclic adenosine monophosphate (cAMP) and cyclic guanosine monophosphate (cGMP) from GC into the oocytes to maintain the meiotic arresting, up to the luteinizing hormone (LH) surge, and the subsequent meiotic resumption (Sela-Abramovich et al., 2006, Vaccari et al., 2008, Shuhaibar et al., 2015). However, signals sent by oocytes to the surrounding GC are not depending on gap junctions. Oocyte-derived factors, like GDF9 and BMP15, are secreted as homo- or hetero-dimers that bind to receptor dimers expressed on GC membrane that are composed of BMP receptor 2 (BMPR2) and activin A receptor type 1B (ALK4), BMPR2 – ALK4, or by BMPR2 and TGF-β receptor 1 (ALK5), BMPR2 – ALK5, to trigger SMAD2/3 signal after GDF9 binding, while BMP15 binds to BMP receptor type 1B (ALK6), BMPR2 – ALK6, to trigger SMAD1/5/8 activation (Peng et al., 2013, Clarke, 2018). These oocyte-secreted factors play a synergistic role to promote follicle development influencing

oocyte – GC interactions, somatic cell differentiation and proliferation, cumulus expansion and oocyte competence (Dong et al., 1996, Elvin et al., 1999, Yan et al., 2001, Su et al., 2004,).

LH, a gonadotropin involved in ovulation and maintenance of corpus luteum, has recently been proposed as an encouraging candidate to preserve the female fertility from moderate and high gonadotoxic chemotherapy associated to cisplatin and alkylating agents, respectively (Rossi et al., 2017, Del Castillo et al., 2021). These studies reported that LH treatment is able to protect mouse ovarian reserve resulting in an improvement of subsequent fertility and reproductive lifespan. LH protection on oocytes might be mediated indirectly by somatic cells expressing LH receptor to promote early DNA damage response triggering DNA repair and anti-apoptotic signals that partially prevent the chemotherapy-induced follicle death. As a result, not only follicle pool was preserved, but also quality of ovulated oocytes exposed to chemotherapy at primordial stage. These findings indicated that primordial follicles treated with LH presumably have an ameliorated potential for developing over the course of folliculogenesis to finally release a mature metaphase II oocyte. Bearing in mind the paramount role of a suitable communication between the oocyte and the surrounding GC for follicle development and oocyte competence (Matzuk et al., 2002), the improvement of germ – somatic cell crosstalk can be one of the underlying mechanisms to explain LH protection. Hence, this study aimed to investigate whether LH might preserve the ability of follicles exposed to alkylating chemotherapy at primordial stage to establish a proper bidirectional oocyte – GC communication during folliculogenesis.

Materials and methods

Animals

Seven-week-old female CD-1 mice (Charles River Laboratories, Saint-Germain-Nuelles, France) were used in this experimental study. The animals were housed free access to standard diet and water ad libitum, and housed in controlled temperature and humidity standard conditions in an environmentally controlled rooms with 12:12 hour light-dark cycle. Animal procedures were approved and carried out according to the Institutional Review Board and the *Comité d'Experimentació i Benestar Animal* of the *Universitat de València*, Valencia, Spain (2018/VSC/PEA/0010 and 2019/VSC/PEA/0206).

Study design

Adult female mice were randomly allocated to control (n = 3), chemotherapy (ChT, n = 5) and chemotherapy with LH (ChT+LH, n = 5) experimental groups. Control mice were intraperitoneally (i.p.) injected with saline followed by a second injection of dimethyl sulfoxide (DMSO, chemotherapy vehicle, from Sigma-Aldrich, St. Louis, MO, USA) 24 hours later. ChT group received saline followed by 120 mg/kg of cyclophosphamide and 12 mg/kg of busulfan (both from Sigma-Aldrich) in DMSO. ChT+LH mice were i.p. injected with 1 international unit (IU) of LH (2.3 ng/mL, Luveris, Merck Serono, Darmstadt, Germany) followed by 1 IU of LH simultaneously with chemotherapy 24 hours later. This regimen should activate LH-associated protective mechanisms and pathways before chemotherapy-induced insult. Mice were maintained for 30 days to ensure that the analyzed oocytes and GC derived from follicles damaged at primordial stage. Animals were then synchronized for ovulation to ensure that all ovaries harbored follicles at late developmental stages. With this aim, a controlled ovarian stimulation (COS) was performed with 10 IU of pregnant mare serum gonadotropin (PMSG, Sigma-Aldrich) and 10 IU of hCG (Ovitrelle, Merck Serono) 48 hours later. Animals were euthanized 40 hours later collecting both ovaries. One ovary per mouse was fixed in buffered 4% formaldehyde for immunofluorescence evaluation, while remaining ones were frozen for follicle isolation and further molecular analysis.

Follicle isolation

Follicles were mechanically isolated from frozen-thawed ovaries by puncturing with 30 G needles (Braun Vetcare, S.A., Spain) on a plastic dish containing Leibovitz's L-15 medium (Gibco, Fisher Scientific, Hampton, NH, USA) under SZX2 binocular loupe (Olympus, Tokyo, Japan). Minced tissue was carefully revised to detect any isolated follicle by using Leica DMI 3000B inverted bright floor microscope attached to Leica DFC450C digital camera (Leica Microsystems GmbH, Wetzlar, Germany). The number of isolated follicles was normalized with the ovarian weight to express the isolation yield. Every isolated follicle was classified with the LAS v4.13 software (Leica Microsystems GmbH) according to follicular diameter in follicles <100 µm, that correspond to primordial and primary stages, and follicles ≥100 µm, that represent the secondary, late preantral, antral and preovulatory subpopulations. Those follicles measuring ≥100 µm were selected and placed on a plastic dish containing phosphate-buffered saline (PBS) with calcium and magnesium

(Gibco, Fisher Scientific) drops. Half of follicles ≥100 µm were kept intact, hereafter complete follicles (FOL), while the remaining were decumulated by using a decreasing diameter series of Flexipet pipettes (170, 140 and 80 µm) adjusted to a Flexipet handle (all from Cook Medical, Bloomington, IN, USA) to obtain denuded oocytes (OO) and GC released. Subsequently, FOL, OO and GC of each experimental group were pooled and placed on separated microtubes, followed by a 10 minute centrifugation at 2500 RPM at 4°C. Finally, the supernatants were carefully discarded and the pellets containing the samples were stored at -80°C for further analysis.

Gene expression

Interactions between oocyte and GC were evaluated on isolated samples from follicles ≥100 µm at the gene level by analyzing the expression of key genes encoding for cell junctions (Cx37, Cx43, E-Cad, N-Cad and TJP1), and oocyte-secreted factors (GDF9 and BMP15) including their specific receptor components (BMPR2, ALK4, ALK5 and ALK6). Total RNA was extracted from the pooled isolated FOL (at least n = 47 /group), OO (at least n = 38 /group) and GC released (from at least n = 41 follicles ≥100 µm/group) by using a Quick-RNA micropep kit (Zymo Research, Irvine, CA, USA) following manufacturer's instructions. RNA concentration was measured by NanoDrop One/OneC Spectrophotometer (ThermoFisher, Waltham, MA, USA). Complementary cDNA was synthesized from 2 µg of RNA using the High-Capacity cDNA reverse transcription kit (Applied Biosystems, Foster City, CA, USA), according to manufacturer's instructions, and real-time PCR (RT-PCR) was performed in a T3000 thermocycler (Biometra GmbH, Göttingen, Germany). Resulting cDNA samples were diluted with DNase/RNase -free water up to a final concentration of 100 ng cDNA/µL. Every quantitative PCR (RT-qPCR) reaction was run in triplicate with specific primers (Supplementary Table SI) using PowerUp Sybr Green (ThermoFisher), at MicroAmp Optical 384 well plates (Applied Biosystems) in a ViiA 7 Real-Time PCR System (Applied Biosystems). The relative gene expression was calculated by the cycle threshold (CT) method (Livak and Schmittgen, 2001) using 18S ribosomal (Rn18s) as a housekeeping gene.

Western blotting

Pooled isolated FOL (at least n = 103 /group), OO (at least n = 100 /group) and GC (from at least n = 108 follicles ≥100 µm /group) were homogenized in radioimmunoprecipitation assay (RIPA) buffer (50 mM Tris-HCl, 150 mM NaCl, 4% Nonidet P-40, 0.5% sodium deoxycholate, 0.1% sodium dodecyl sulfate (SDS), pH 7.4) containing phosphatase (PhospSTOP EASYpack, Roche Diagnostics, Switzerland) and protease (cOmplete tablets EDTA-free EASY-pack, Roche Diagnostics, Switzerland) inhibitors and maintained on ice for 30 minutes. After incubation, samples were centrifuged for 20 minutes at 13000 RPM at 4°C. Protein content was determined by a colorimetric assay based on the Bradford method using Protein Assay Dye Reagent Concentrate (Bio-Rad, Hercules, CA, USA) and a SpectraMax 190 Microplate Reader (Molecular Devices, San José, CA, USA). Subsequently, 15 µg of protein from each sample was separated on 10% SDS-polyacrylamide gels and transferred to polyvinylidene difluoride (PVDF) membranes (Bio-Rad). Blots were blocked using 5% Bovine Serum Albumin (BSA, Sigma-Aldrich) or non-fat powdered milk dissolved in Tris-buffered saline with 0.1% Tween 20 (TBST) for 1 hour at room temperature (RT), and then exposed to primary antibodies at the following dilutions – Cx37 (1:500 dilution; 40-4300 – Invitrogen, Carlsbad, CA, USA), Cx43 (1:5000 dilution; C6219 – Sigma-Aldrich), E-Cad (1:1000 dilution; 3195 – Cell Signaling, Danvers, MA, USA), GDF9 (1:1000 dilution; ab93892 – Abcam, Cambridge, UK), BMP15 (1:1000 dilution; PA5-95615 – Invitrogen), and β-Actin (1:2000 dilution; sc47778 – Santa Cruz Biotechnology, Dallas, TX, USA) – overnight (O/N) on an orbital shaker at 4°C. Membranes were then incubated with the appropriate anti-mouse or anti-rabbit horseradish peroxidase (HRP)-conjugated secondary antibodies (sc-516102 and sc-2004; 1:2000 dilution for both; Santa Cruz Biotechnology) for 1 hour at RT. After washing in TBST, membranes were incubated with a chemiluminescence detection reagent (Super Signal West Femto Maximum Sensitivity Substrate, ThermoFisher) and protein bands visualized by chemiluminescence imaging using Amersham Imager 680 (GE HealthCare Life Sciences, Marlborough, MA, USA). Integrated light intensity of each band was determined by ImageJ software (National Institutes of Health, Bethesda, MD, USA). Signal intensities were normalized to the intensity of the housekeeping protein β-Actin. Albeit all molecules were analyzed on FOL samples, factors were only assessed on OO or GC attending to their predominant expression by one follicular compartment.

Immunofluorescence staining

Fixed ovaries were paraffin-embedded, and then cut into 4-µm thick sections. Five representative ovarian sections per sample and target protein were deparaffined and rehydrated. Antigen retrieval was performed incubating sections with Envision FLEX Target retrieval solution High pH (Dako Denmark A/S, Glostrup, Denmark) in a pressure cooker for 3 minutes at 125°C and 1.5 atm. After cooling at RT, samples were blocked for 1 hour at RT in PBS supplemented with 3% BSA (Sigma-Aldrich), 2% Goat Normal Serum (GNS, Vector Laboratories, Burlingame, CA, USA) and 0.01% Triton X-100 (Sigma-Aldrich). Subsequently, samples were incubated O/N at 4ºC with the primary antibodies used on the western blotting section: Cx37 (1:50 dilution), Cx43 (1:200 dilution), E-Cad (1:200 dilution), GDF9 (1:100 dilution), and BMP15 (1:100 dilution). Then, sections were incubated for 1 hour at RT with biotinylated anti-mouse or anti-rabbit IgG secondary antibodies (1:500 dilution for both; BA-9200 and BA-1000, respectively – Vector Laboratories). Immunofluorescence staining was performed using streptavidin-conjugated Alexa Fluor 488 or 594 (1:500 dilution for both; S32354 and S32356, respectively – Invitrogen) for 45 minutes at RT. Slides were mounted and nucleus were stained using Vectashield Vibrance antifade mounting medium with DAPI (Vector Laboratories). Leica TCS SP8 and LAS X software (Leica Microsystems GmbH) were used for confocal microscopy, and image collection was performed with 1.3 numerical aperture x40 oil immersion objective at 405 nm (for DAPI), and 488 or 594 nm (for target proteins). For each follicle, high-resolution image was captured at the Z-axis point where the highest fluorescence intensity was detected. Relative intensity quantification of targeted proteins was determined by using ImageJ software (National Institutes of Health) in all the visualized follicles. For each treatment group (ChT and ChT+LH), mean relative intensities were normalized to the control levels and expressed as fold-change.

Statistics

GraphPad Prism 8.3.0 (GraphPad Software, San Diego, CA, USA) was used for statistical data analysis and graphic generation. Data are presented as mean and standard deviation (Mean ± SD). Any statistically significant difference between the experimental groups were identified

through two-by-two comparisons with the non-parametric Mann-Whitney test for unpaired samples. A p-value <0.05 was considered statistically significant.

Results

LH prevented follicle depletion

Ovaries collected from ChT group harbored 2.1-fold less follicles than controls (Control: 37.6 ± 9.4 follicles/mg, ChT: 17.8 ± 5.1 follicles/mg; p = 0.036), affecting this reduction similarly to follicles with both diameters (p = 0.036 in both cases). However, LH-treated ovaries showed control-like values for the total number of isolated follicles and avoided the chemotherapy-induced reduction (ChT+LH: 28.9 ± 5.5 follicles/mg; p = 0.032). The LH action against chemotherapy specially preserved the number of follicles measuring <100 µm (p = 0.016), that correspond to primordial and primary stages.

LH preserved gene expression of factors involved in oocyte – GC communication

Analysis of isolated FOL revealed an overall downregulation pattern in ChT samples compared to controls for all those genes involved in cell interactions and growth factors (Fig. 1A). This downregulation particularly affected to Cx37, involved in gap junctions, and the oocyte-secreted factor GDF9. By contrast, LH treatment maintained gene expression values akin to control group for ten out of eleven genes, restoring the reduced fold changes of ChT group. LH associated improvement against chemotherapy significantly benefitted to the expression of Cx37, E-Cad, Cx43, GDF9 and ALK5 genes. In addition, OO and GC were subsequently analyzed to investigate whether the gene expression differences affected to a particular follicular compartment. Results revealed a global downregulation in ChT samples compared to control group for both follicular compartments, finding statistically significant differences for N-Cad and GDF9 in OO (Fig. 1B), and for Cx43, Cx37, BMP15 and BMPR2 in GC (Fig. 1C). By contrast, LH-treated samples showed expression levels similar to controls for most genes, increasing the values observed in both ChT-OO and -GC. This LH effect against chemotherapy substantially affected to Cx37, N-Cad, GDF9 and ALK5 in OO, and to Cx43, GDF9, BMP15, BMPR2 and ALK5 in GC. E-Cad was not expressed on GC for any experimental group. Afterwards, these gene expression differences between groups were confirmed at the protein level, finding a noteworthy reduction of the

differentially expressed factors Cx37, E-Cad, Cx43, GDF9 and BMP15 on FOL of ChT group (Fig. 1D), while LH restored the protein expression of such molecules up to control-like values. Likewise, further analysis of OO (Fig. 1E) and GC (Fig. 1F) samples showed that LH counteracted the chemotherapy effects on both follicular compartments preventing the significant reduction of protein levels observed on ChT samples.

LH promoted interactions between oocyte and GC beyond the secondary stage

Fluorescence signal for Cx37 was localized in GC and oocytes of each follicular stage with a stronger signal in the germ compartment, where Cx37 was detected in the ooplasm and nucleus (Fig. 2A). E-Cad expression was only detected in oocytes, where this factor was restricted to the outermost cell boundaries in all follicle populations with a similar intensity among developmental stages (Fig. 2A). In addition, although Cx43 expression was visualized in stroma, this factor was predominantly detected in GC, where seemed to be differentially expressed depending on the developmental stage. Thus, primary follicles showed a weak fluorescence restricted to few GC, while secondary follicles contained a strong Cx43-signal by many GC (Fig. 2A), and late preantral to antral follicles exhibited the strongest intensity expressed by most of their GC. It is important to note that Cx43 was also found with a strong signal on the outermost edge of ooplasm from late preantral populations. Comparing groups, a significant reduction of Cx37 ($p = 0.036$), E-Cad ($p = 0.035$), and Cx43 ($p = 0.036$) signals were detected on ChT-follicles compared to controls. These alterations particularly appeared in the primary-secondary transition, with control-like intensity in primary population for the three factors, but reduced values beyond the secondary stage (Fig. 2B-D). By contrast, LH-treated follicles showed a fluorescence pattern akin to controls in all follicular populations, thereby enhancing the three molecule signals compared to ChT group with statistically significant differences from secondary to antral stages.

LH enhanced oocyte – GC crosstalk beyond the secondary stage

GDF9 and BMP15 were mainly visualized on the ooplasm of all follicle populations, albeit some GC also showed positive signals (Fig 3A). No differences were found among follicular stages from control samples when signal intensity was quantified . However, a 1.7-fold ($p = 0.036$) and more than 2-fold ($p = 0.018$) reductions of signal were observed in ChT samples for GDF9 and BMP15,

respectively. These alterations for both factors were similarly detected from the secondary population in ChT group (Fig. 3B-C). On the other side, follicles in ChT+LH group showed fluorescence levels for GDF9 and BMP15 akin to controls for all follicle populations that avoided the chemotherapy-induced effects with statistically significant differences ($p = 0.008$ in both cases). Indeed, a significant increase on the signal of both factors was found in ChT+LH sections compared to ChT group for all growing populations excluding the primary stage.

Discussion

This study evaluated whether LH treatment was able to preserve the ability of mouse follicles exposed to alkylating chemotherapy at the primordial stage to establish a suitable crosstalk between germ and somatic compartments over the course of folliculogenesis. We found that 1 IU of LH administered before and together with the gonadotoxic treatment prevented the chemotherapy-induced detriments on the follicle pool and oocyte – GC communication by prompting an enhancement of cell interactions and expression of growth factors.

Our results regarding follicle isolation indicated that LH administration reversed the chemotherapy effects on follicle pool by preventing the loss of quiescent and growing populations. Bearing in mind that the pool of growing stages in our samples derived from primordial follicles during chemotherapy, LH would preserve the ovarian reserve mainly composed of quiescent follicles. These findings were in line with previous studies that reported a significant protection of the most undifferentiated follicular stages against cisplatin and alkylating agents by promoting DNA repairing mechanisms and anti-apoptotic signals (Rossi et al., 2017, Del Castillo et al., 2021). Co-adjuvant administration of LH-releasing hormone agonists during chemotherapy was observed to confer some protection of ovarian function and fertility in oncologic patients (Blumenfeld et al., 2015, Lambertini et al., 2015, Meli et al., 2018, Sinha et al., 2018), albeit their effectiveness and the precise molecular mechanism to prevent follicle loss remains unclear (Dolmans et al., 2020).

Complex and continuing crosstalk between the oocytes and their surrounding GC during follicle development is essential for the synchronous maturation of both germ and somatic cell compartments in ovarian follicles (Matzuk et al., 2002). Although oocytes coordinate follicle development by mediating GC proliferation and differentiation (Eppig et al., 2002), GC constitute the main source of molecules and metabolites used by oocytes for metabolism, growth, and

maturation (Heller and Schultz, 1980, Brower and Schultz, 1982, Haghighat and Van Winkle, 1990, Pelland et al., 2009), pointing out the relevance of the bidirectional oocyte – GC communication. Our results indicated that growing follicles exposed to alkylating chemotherapy at primordial stage showed altered the reciprocal intercommunication between both follicular compartments by disturbing cell junctions and secretion of growth factors at both gene and protein levels. Although cell intercommunication can be affected by antineoplastic drugs in cancer (Aasen et al., 2019), there are limited data regarding chemotherapy effects on cell junctions in ovaries. In that sense, our findings suggest that alkylating agents disturbed the expression of molecules involved in mechanical attachment, such as cadherins, and cytoplasm communication, mediated by connexins, between oocytes and GC at gene and protein levels . Consistent with these results, cyclophosphamide dysregulated the interactions among blastomeres in preimplantation embryos by decreasing the cell-cell contacts and altering the expression of connexin and cadherin genes (Harrouk et al., 2000). Adherens junctions mediated by cadherins are essential in ovarian follicles, playing important roles during early follicular growth and corpus luteum formation (Machell et al., 2000, Machell and Farookhi, 2003, Mora et al., 2012). Blastomere adhesion and cell division pattern were affected in embryos derived from knockdown oocytes of E-Cadherin (De Vries et al., 2004). Similar to chemotherapy effects, mouse ovaries lacking E-cadherin also resulted in a disruption of biological mechanisms controlling primordial follicle pool that led to ovarian reserve depletion as a significant apoptotic rate (Yan et al., 2019). In addition, several studies showed a negative role of connexins in apoptosis within different cell lines and organs, including the ovary (Lin et al., 2003, Plotkin et al., 2002). Thus, low expression of connexin 43 was correlated with elevated rate of apoptotic follicles, indicating that connexins act as survival factors for follicles (Johnson et al., 1999, Krysko et al., 2004, Chang et al., 2005). Moreover, we found a reduced secretion of GDF9 and BMP15, paracrine factors predominantly produced by oocytes, on the ChT group, as previously observed in ovarian samples exposed to cyclophosphamide and busulfan (Park et al., 2013, Tan et al., 2014, Kim et al., 2019), where GDF9 and BMP15 were downregulated. On the other side, our results indicated that LH treatment reversed the chemotherapy effects on the oocyte – GC communication. LH restored the expression levels of genes encoding for connexins (gap junctions), cadherins (adherens junctions) and paracrine factors (GDF9, BMP15 and specific receptors), resulting in a significant increase of protein levels

similar to controls. Gonadotropin administration enhanced cell-cell contact between oocytes and GC by increasing the expression levels of connexin 37 and 43, N- and E-cadherins, and transzonal projections to ensure generation of mature oocytes in mice (El-Hayek and Clarke, 2015). Moreover, Rossi et al. noticed that LH gonadoprotection against cisplatin might be mediated by gap junctions through ovarian somatic cells expressing LH receptor (Rossi et al., 2017).

Chemotherapy compromises follicular development by causing atresia of growing populations and morphological alterations that lead to obtain poor-quality oocytes (Yuksel et al., 2015, Zhang, T. et al., 2016, Buigues et al., 2019, Winship et al., 2019). Our results showed that the detrimental effects of chemotherapy on GC – oocyte communication in growing follicles were influenced by the developmental stage, particularly from the secondary to later phases. These findings suggested that primordial follicles exposed to alkylating agents depicted a reduced potential of growth due to a lack on the ability to establish a proper bidirectional crosstalk between GC and oocytes in next developmental stages. Primary-secondary transition represents a crucial step during folliculogenesis owing to several events take place, such as the robust oocyte growth, the active GC proliferation, the acquisition of theca cells, and the follicular growth influenced by gonadotrophin-responsive (Edson et al., 2009, Franks et al., 2015). In addition, secretion of paracrine factors involved in oocyte growth and GC proliferation is more evident beyond the secondary stage (Kawashima and Kawamura, 2018). Downregulation of connexins and cadherins disturbed the bidirectional GC – oocyte communication over the course of primary-secondary transition resulting in impaired folliculogenesis (Zhang et al., 2019). GC, especially from mature follicles, relied on gap junctions to establish their communication with each other and with oocytes, being connexins the essential protein of these intercellular channels (Wright et al., 2001). Gene knockout studies demonstrated that follicles lacking of connexin 37 and 43 were unable to generate a second granulosa layer impairing follicular growth beyond the late preantral stage, as well as oocytes failed to undergo meiotic maturation (Carabatsos et al., 2000, Ackert et al., 2001, Veitch et al., 2004, Gittens and Kidder, 2005). Furthermore, GDF9, BMP15 and their specific receptors are expressed in primary follicles onward (Silva et al., 2005, Sun et al., 2010) playing synergistic roles in follicle development, cumulus expansion, antrum formation and ovulation to achieve an optimal oocyte competence (Elvin et al., 1999, Yan et al., 2001, Sugiura et al., 2007,

Alam et al., 2018). Nevertheless, deficient mice in GDF9 and BMP15 showed impaired follicle development beyond the secondary stage and decreased ovulation and fertilization rates (Dong et al., 1996, Galloway et al., 2000, Yan et al., 2001, Hanrahan et al., 2004). By contrast, LH-treated follicles were able to achieve a gene and protein expression akin to control samples, which suggested that LH gonadoprotection prevented the far-reaching effects of chemotherapy in folliculogenesis. In this line, a recent study reported that concomitant LH treatment with alkylating chemotherapy decreased the rate of morphologically abnormal follicles leading to not only an improvement of the quantity of metaphase II oocytes, but also the oocyte competence (Del Castillo et al., 2021).

Altogether, this is a very first study analyzing the implications of alkylating chemotherapy and LH co-administration on the GC – oocyte communication during the folliculogenesis. This study suggests that LH-treated follicles at primordial stage would maintain the ability to establish a proper bidirectional crosstalk between oocyte and surrounding GC when initiate their development to finally ovulate a competent and fertilizable oocyte. Hence, maintenance of GC – oocyte interactions might be one of the underlying mechanisms triggered by LH to confer the ovarian reserve protection against chemotherapy. These findings encourage further research assessing the feasibility of LH treatment to counteract the gonadotoxicity induced by chemotherapeutic drugs. Therefore, our research highlights the potential use of LH as a novel candidate for female fertility preservation in cancer patients undergoing chemotherapy.

Data availability

The data underlying this article will be shared on reasonable request to the corresponding author.

Authors' roles

L.M.C. conducted experimental studies, analyzed results, and wrote the manuscript; M.J.S. and J.M. contributed to perform the experiments; A.P. designed, coordinated, funded the research, and critically revised the manuscript; S.H. designed, supervised, coordinated, funded the study, and wrote the manuscript.

Acknowledgements

We would like to thank *Servei de Microscòpia* and laboratory animal facility from the *Unitat Central d'Investigació de Medicina* (*UCIM*, *Universitat de València*, Valencia, Spain) for their technical assistance, support and the use of their facilities. The authors thank Merck Serono for providing the LH.

Funding

This study was supported by grants from the Regional Valencian Ministry of Education (PROMETEO/2018/137), the Spanish Ministry of Science and Innovation (CP19/00141), and the Spanish Ministry of Education, Culture and Sports (FPU16/05264).

Conflict of Interest

The authors declare no conflict of interest.

References

Aasen T, Leithe E, Graham SV, Kameritsch P, Mayan MD, Mesnil M, Pogoda K, Tabernero A. Connexins in cancer: bridging the gap to the clinic. Oncogene 2019;38:4429-4451.

Ackert CL, Gittens JE, O'Brien MJ, Eppig JJ, Kidder GM. Intercellular communication via connexin43 gap junctions is required for ovarian folliculogenesis in the mouse. Dev Biol 2001;233:258-270.

Alam MH, Lee J, Miyano T. GDF9 and BMP15 induce development of antrum-like structures by bovine granulosa cells without oocytes. J Reprod Dev 2018;64:423-431.

Blumenfeld Z, Zur H, Dann EJ. Gonadotropin-Releasing Hormone Agonist Cotreatment During Chemotherapy May Increase Pregnancy Rate in Survivors. Oncologist 2015;20:1283-1289.

Brower PT, Schultz RM. Intercellular communication between granulosa cells and mouse oocytes: existence and possible nutritional role during oocyte growth. Dev Biol 1982;90:144-153.

Buigues A, Marchante M, Herraiz S, Pellicer A. Diminished Ovarian Reserve Chemotherapy-Induced Mouse Model: A Tool for the Preclinical Assessment of New Therapies for Ovarian Damage. Reproductive Sciences 2019;.

Carabatsos MJ, Sellitto C, Goodenough DA, Albertini DF. Oocyte-granulosa cell heterologous gap junctions are required for the coordination of nuclear and cytoplasmic meiotic competence. Dev Biol 2000;226:167-179.

Chang AS, Dale AN, Moley KH. Maternal diabetes adversely affects preovulatory oocyte maturation, development, and granulosa cell apoptosis. Endocrinology 2005;146:2445-2453.

Clarke HJ. Regulation of germ cell development by intercellular signaling in the mammalian ovarian follicle. Wiley Interdiscip Rev Dev Biol 2018;7:10.1002/wdev.294. Epub 2017 Sep 11.

De Vries WN, Evsikov AV, Haac BE, Fancher KS, Holbrook AE, Kemler R, Solter D, Knowles BB. Maternal beta-catenin and E-cadherin in mouse development. Development 2004;131:4435-4445.

Del Castillo LM, Buigues A, Rossi V, Soriano MJ, Martinez J, De Felici M, Lamsira HK, Di Rella F, Klinger FG, Pellicer A et al. The cyto-protective effects of LH on ovarian reserve and female fertility during exposure to gonadotoxic alkylating agents in an adult mouse model. Hum Reprod 2021;.

Dolmans MM, Taylor HS, Rodriguez-Wallberg KA, Blumenfeld Z, Lambertini M, von Wolff M, Donnez J. Utility of gonadotropin-releasing hormone agonists for fertility preservation in women receiving chemotherapy: pros and cons. Fertil Steril 2020;114:725-738.

Dong J, Albertini DF, Nishimori K, Kumar TR, Lu N, Matzuk MM. Growth differentiation factor-9 is required during early ovarian folliculogenesis. Nature 1996;383:531-535.

Edson MA, Nagaraja AK, Matzuk MM. The mammalian ovary from genesis to revelation. Endocr Rev 2009;30:624-712.

El-Hayek S, Clarke HJ. Follicle-Stimulating Hormone Increases Gap Junctional Communication Between Somatic and Germ-Line Follicular Compartments During Murine Oogenesis. Biol Reprod 2015;93:47.

Elvin JA, Clark AT, Wang P, Wolfman NM, Matzuk MM. Paracrine actions of growth differentiation factor-9 in the mammalian ovary. Mol Endocrinol 1999;13:1035-1048.

500 Eppig JJ, Wigglesworth K, Pendola FL. The mammalian oocyte orchestrates the rate of ovarian
501 follicular development. Proc Natl Acad Sci U S A 2002;99:2890-2894.

502 FitzHarris G, Siyanov V, Baltz JM. Granulosa cells regulate oocyte intracellular pH against
503 acidosis in preantral follicles by multiple mechanisms. Development 2007;134:4283-4295.

504 Franks S, Hardy K, Conway GS. Pathophysiology of Ovarian Function in the Human Female.
505 Anonymous Knobil and Neill's Physiology of ReproductionFourth Edition edn, 2015. Academic
506 Press, London, pp. 1363-1394.

507 Galloway SM, McNatty KP, Cambridge LM, Laitinen MP, Juengel JL, Jokiranta TS, McLaren RJ,
508 Luiro K, Dodds KG, Montgomery GW et al. Mutations in an oocyte-derived growth factor gene
509 (BMP15) cause increased ovulation rate and infertility in a dosage-sensitive manner. Nat Genet
510 2000;25:279-283.

511 Gershon E, Plaks V, Dekel N. Gap junctions in the ovary: expression, localization and function.
512 Mol Cell Endocrinol 2008;282:18-25.

513 Gittens JE, Kidder GM. Differential contributions of connexin37 and connexin43 to oogenesis
514 revealed in chimeric reaggregated mouse ovaries. J Cell Sci 2005;118:5071-5078.

515 Goldberg GS, Valiunas V, Brink PR. Selective permeability of gap junction channels. Biochim
516 Biophys Acta 2004;1662:96-101.

517 Haghighat N, Van Winkle LJ. Developmental change in follicular cell-enhanced amino acid uptake
518 into mouse oocytes that depends on intact gap junctions and transport system Gly. J Exp Zool
519 1990;253:71-82.

520 Hanrahan JP, Gregan SM, Mulsant P, Mullen M, Davis GH, Powell R, Galloway SM. Mutations in
521 the genes for oocyte-derived growth factors GDF9 and BMP15 are associated with both increased
522 ovulation rate and sterility in Cambridge and Belclare sheep (Ovis aries). Biol Reprod
523 2004;70:900-909.

524 Harrouk W, Robaire B, Hales BF. Paternal exposure to cyclophosphamide alters cell-cell contacts
525 and activation of embryonic transcription in the preimplantation rat embryo. Biol Reprod
526 2000;63:74-81.

Heller DT, Schultz RM. Ribonucleoside metabolism by mouse oocytes: metabolic cooperativity between the fully grown oocyte and cumulus cells. J Exp Zool 1980;214:355-364.

Johnson ML, Redmer DA, Reynolds LP, Grazul-Bilska AT. Expression of gap junctional proteins connexin 43, 32, and 26 throughout follicular development and atresia in cows. Endocrine 1999;10:43-51.

Kawashima I, Kawamura K. Regulation of follicle growth through hormonal factors and mechanical cues mediated by Hippo signaling pathway. Syst Biol Reprod Med 2018;64:3-11.

Kim YY, Kim WO, Liu HC, Rosenwaks Z, Kim JW, Ku SY. Effects of paclitaxel and cisplatin on in vitro ovarian follicle development. Arch Med Sci 2019;15:1510-1519.

Krysko DV, Mussche S, Leybaert L, D'Herde K. Gap junctional communication and connexin43 expression in relation to apoptotic cell death and survival of granulosa cells. J Histochem Cytochem 2004;52:1199-1207.

Lambertini M, Boni L, Michelotti A, Gamucci T, Scotto T, Gori S, Giordano M, Garrone O, Levaggi A, Poggio F et al. Ovarian Suppression With Triptorelin During Adjuvant Breast Cancer Chemotherapy and Long-term Ovarian Function, Pregnancies, and Disease-Free Survival: A Randomized Clinical Trial. JAMA 2015;314:2632-2640.

Lin JH, Yang J, Liu S, Takano T, Wang X, Gao Q, Willecke K, Nedergaard M. Connexin mediates gap junction-independent resistance to cellular injury. J Neurosci 2003;23:430-441.

Livak KJ, Schmittgen TD. Analysis of relative gene expression data using real-time quantitative PCR and the 2-ΔΔCT method. Methods 2001;25:402-408.

Machell NH, Blaschuk OW, Farookhi R. Developmental expression and distribution of N- and E-cadherin in the rat ovary. Biol Reprod 2000;63:797-804.

Machell NH, Farookhi R. E- and N-cadherin expression and distribution during luteinization in the rat ovary. Reproduction 2003;125:791-800.

Matzuk MM, Burns KH, Viveiros MM, Eppig JJ. Intercellular communication in the mammalian ovary: oocytes carry the conversation. Science 2002;296:2178-2180.

553 Meli M, Caruso-Nicoletti M, La Spina M, Nigro LL, Samperi P, D'Amico S, Bellia F, Miraglia V,
554 Licciardello M, Cannata E et al. Triptorelin for Fertility Preservation in Adolescents Treated with
555 Chemotherapy for Cancer. Journal of Pediatric Hematology/Oncology 2018;40:269-276.

556 Mora JM, Fenwick MA, Castle L, Baithun M, Ryder TA, Mobberley M, Carzaniga R, Franks S,
557 Hardy K. Characterization and significance of adhesion and junction-related proteins in mouse
558 ovarian follicles. Biol Reprod 2012;86:153, 1-14.

559 Park MR, Choi YJ, Kwon DN, Park C, Bui HT, Gurunathan S, Cho SG, Song H, Seo HG, Min G
560 et al. Intraovarian transplantation of primordial follicles fails to rescue chemotherapy injured
561 ovaries. Sci Rep 2013;3:1384.

562 Pelland AM, Corbett HE, Baltz JM. Amino Acid transport mechanisms in mouse oocytes during
563 growth and meiotic maturation. Biol Reprod 2009;81:1041-1054.

564 Peng J, Li Q, Wigglesworth K, Rangarajan A, Kattamuri C, Peterson RT, Eppig JJ, Thompson
565 TB, Matzuk MM. Growth differentiation factor 9:bone morphogenetic protein 15 heterodimers are
566 potent regulators of ovarian functions. Proc Natl Acad Sci U S A 2013;110:E776-85.

567 Plotkin LI, Manolagas SC, Bellido T. Transduction of cell survival signals by connexin-43
568 hemichannels. J Biol Chem 2002;277:8648-8657.

569 Rossi V, Lispi M, Longobardi S, Mattei M, Rella FD, Salustri A, De Felici M, Klinger FG. LH
570 prevents cisplatin-induced apoptosis in oocytes and preserves female fertility in mouse. Cell
571 Death Differ 2017;24:72-82.

572 Sela-Abramovich S, Edry I, Galiani D, Nevo N, Dekel N. Disruption of gap junctional
573 communication within the ovarian follicle induces oocyte maturation. Endocrinology
574 2006;147:2280-2286.

575 Shuhaibar LC, Egbert JR, Norris RP, Lampe PD, Nikolaev VO, Thunemann M, Wen L, Feil R,
576 Jaffe LA. Intercellular signaling via cyclic GMP diffusion through gap junctions restarts meiosis in
577 mouse ovarian follicles. Proc Natl Acad Sci U S A 2015;112:5527-5532.

578 Silva JR, van den Hurk R, van Tol HT, Roelen BA, Figueiredo JR. Expression of growth
579 differentiation factor 9 (GDF9), bone morphogenetic protein 15 (BMP15), and BMP receptors in
580 the ovaries of goats. Mol Reprod Dev 2005;70:11-19.

581 Sinha N, Letourneau JM, Wald K, Xiong P, Imbar T, Li B, Harris E, Mok-Lin E, Cedars MI, Rosen
582 MP. Antral follicle count recovery in women with menses after treatment with and without
583 gonadotropin-releasing hormone agonist use during chemotherapy for breast cancer. J Assist
584 Reprod Genet 2018;35:1861-1868.

585 Su YQ, Wu X, O'Brien MJ, Pendola FL, Denegre JN, Matzuk MM, Eppig JJ. Synergistic roles of
586 BMP15 and GDF9 in the development and function of the oocyte-cumulus cell complex in mice:
587 genetic evidence for an oocyte-granulosa cell regulatory loop. Dev Biol 2004;276:64-73.

588 Sugiura K, Su YQ, Diaz FJ, Pangas SA, Sharma S, Wigglesworth K, O'Brien MJ, Matzuk MM,
589 Shimasaki S, Eppig JJ. Oocyte-derived BMP15 and FGFs cooperate to promote glycolysis in
590 cumulus cells. Development 2007;134:2593-2603.

591 Sun RZ, Lei L, Cheng L, Jin ZF, Zu SJ, Shan ZY, Wang ZD, Zhang JX, Liu ZH. Expression of
592 GDF-9, BMP-15 and their receptors in mammalian ovary follicles. J Mol Histol 2010;41:325-332.

593 Tan SJ, Lee LJ, Tzeng CR, Wang CW, Hsu MI, Chen CH. Targeted anti-apoptosis activity for
594 ovarian protection against chemotherapy-induced ovarian gonadotoxicity. Reprod Biomed Online
595 2014;29:612-620.

596 Vaccari S, Horner K, Mehlmann LM, Conti M. Generation of mouse oocytes defective in cAMP
597 synthesis and degradation: endogenous cyclic AMP is essential for meiotic arrest. Dev Biol
598 2008;316:124-134.

599 Veitch GI, Gittens JE, Shao Q, Laird DW, Kidder GM. Selective assembly of connexin37 into
600 heterocellular gap junctions at the oocyte/granulosa cell interface. J Cell Sci 2004;117:2699-2707.

601 Winship AL, Carpenter M, Griffiths M, Hutt KJ. Vincristine Chemotherapy Induces Atresia of
602 Growing Ovarian Follicles in Mice. Toxicol Sci 2019;169:43-53.

603 Wright CS, Becker DL, Lin JS, Warner AE, Hardy K. Stage-specific and differential expression of
604 gap junctions in the mouse ovary: connexin-specific roles in follicular regulation. Reproduction
605 2001;121:77-88.

606 Yan C, Wang P, DeMayo J, DeMayo FJ, Elvin JA, Carino C, Prasad SV, Skinner SS, Dunbar BS,
607 Dube JL et al. Synergistic roles of bone morphogenetic protein 15 and growth differentiation factor
608 9 in ovarian function. Mol Endocrinol 2001;15:854-866.

609 Yan H, Wen J, Zhang T, Zheng W, He M, Huang K, Guo Q, Chen Q, Yang Y, Deng G et al.
610 Oocyte-derived E-cadherin acts as a multiple functional factor maintaining the primordial follicle
611 pool in mice. Cell Death Dis 2019;10:160-018-1208-3.

612 Yuksel A, Bildik G, Senbabaoglu F, Akin N, Arvas M, Unal F, Kilic Y, Karanfil I, Erylmaz B, Yilmaz
613 P et al. The magnitude of gonadotoxicity of chemotherapy drugs on ovarian follicles and granulosa
614 cells varies depenDing upon the category of the drugs and the type of granulosa cells. Human
615 Reproduction 2015;.

616 Zhang M, Bener MB, Jiang Z, Wang T, Esencan E, Scott Iii R, Horvath T, Seli E. Mitofusin 1 is
617 required for female fertility and to maintain ovarian follicular reserve. Cell Death Dis 2019;10:560-
618 019-1799-3.

619 Zhang T, Yan D, Yang Y, Ma A, Li L, Wang Z, Pan Q, Sun Z. The comparison of animal models
620 for premature ovarian failure established by several different source of inducers. Regul Toxicol
621 Pharmacol 2016;81:223-232.

622

623 **Tables**

624 **Supplementary Table SI.** Target genes and specific primer sequences (depicted in 5' to 3'
625 direction) used for oocyte – GC communication assessment by RT-qPCR analysis.

Gene abbreviation (MGI-IDs)	Forward primer sequence	Reverse primer sequence
Cx37 (95715)	AACGGTGCTCTTCATCTTC	GGGCTGTGTTACACTCAAA
Cx43 (95713)	CTGGGTCCTTCAGATCATATTC	CAGCTTCTCTTCCTTTCTCATC
E-Cad (88354)	GGACAGAGAATCGCCAAAT	TGTTCCTGTCCCACTCATA

N-Cad (88355)	CCTGCCAATCCTGATGAAA	AATCGAACACCAACAGAGAG
Tjp1 (98759)	GTCCCTCAGAGTCAGTTTAG	CTCTTCAGGGTCGTAATGAT
Gdf9 (95692)	GGAAGCTATTGAGGTGGAAAG	GAGGTTGAAGGATGCTGTAAG
Bmp15 (1316745)	AATGGTGAGGCTGGTAAAG	CTACCTGGTTTGATGCTAGAG
Bmpr2 (1095407)	CCATGAGGCTAACTGGAAAT	AGGTTCACAGCTCCTTCTA
Alk4 (1338944)	GTCCTTGACGAGACAATCAA	GCAATCTCCCAGTAGACAAG
Alk5 (98728)	GGCTTAGTGTTCTGGGAAAT	CGATGGATCAGAAGGTACAAG
Alk6 (107191)	AGGACTAGAAGGGTCAGATT	GGGTGGAGGTCTTTATTACAC
Rn18s (97943)	CATGGCCGTTCTTAGTTGGT	AACGCCACTTGTCCCTCTAA

MGI: Mouse genome informatics database

Figures

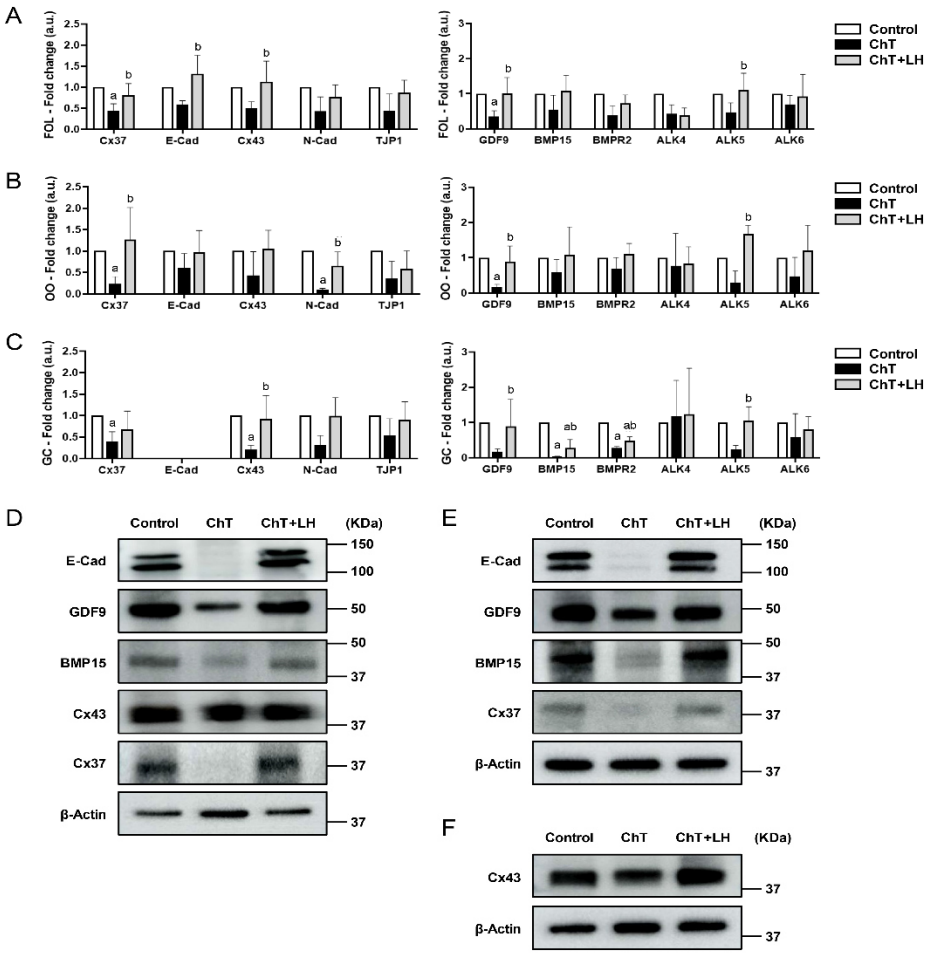

Figure 1. Gene and protein expression of cell junctions and oocyte-secreted factors expressed by follicles. Analysis of mRNA transcription levels for Cx37, E-Cad, Cx43, N-Cad

and TJP1 involved in cell junctions and for GDF9, BMP15, BMPR2, ALK4, ALK5 and ALK6 in (A) FOL isolated from ovaries collected 30 days after treatments, in (B) OO and in (C) GC obtained from isolated follicles measuring ≥ 100 µm. Expression values were normalized to those of the control group and were expressed as fold change. Bar charts showed means and SD for each experimental group. Representative western blots showing the levels of Cx37, E-Cad, Cx43, GDF9 and BMP15 in (D) FOL, (E) OO, and (F) GC retrieved from follicles with a diameter ≥100 µm. LH treatment reversed the chemotherapy-induced downregulation at gene and protein level of factors involved in oocyte – GC communication, protecting both follicular compartments. Pooled samples from n = 3 mice for control group and n = 5 mice for ChT and ChT+LH-1x groups were analyzed. ap-value < 0.05 vs. control group; bp-value < 0.05 vs. ChT group.

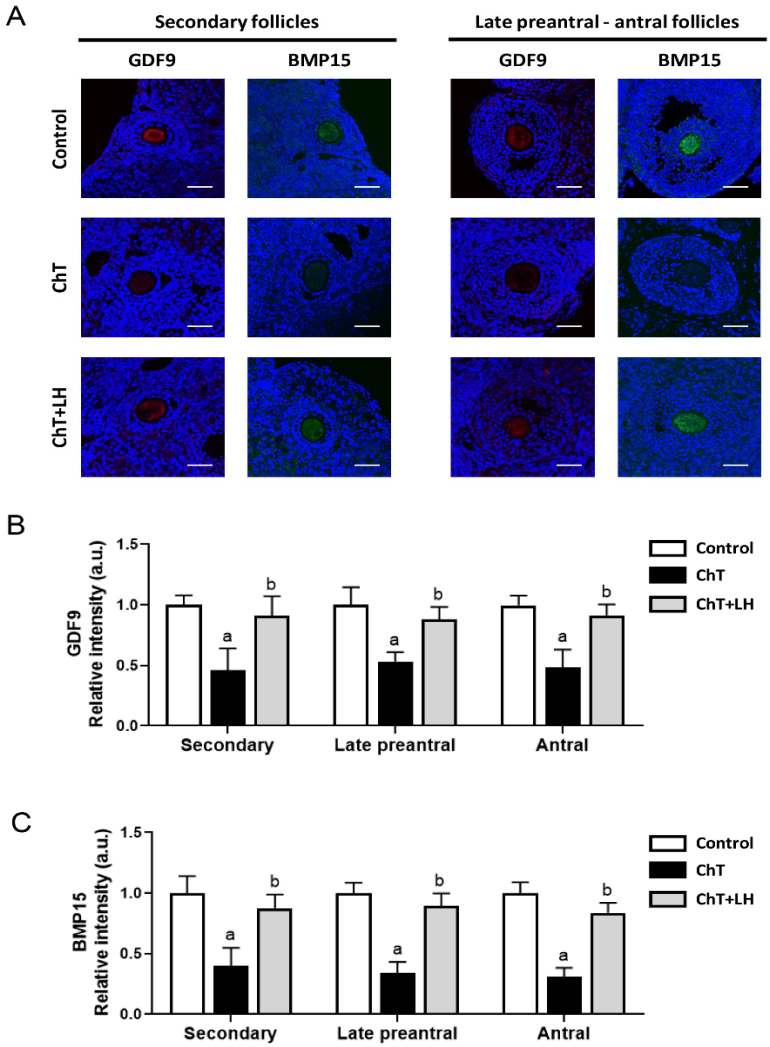

Figure 2. Immunofluorescence staining of key proteins involved in cell junctions. (A) Representative confocal images showing secondary (left panel) and late preantral or antral

follicles (right panel) stained with blue signal for nucleus (DAPI), connexin 37 (Cx37) and connexin 43 (Cx) labelled with green signal, and epithelial cadherin (E-Cad) in red signal. Scale bars: 50 μm. Quantitative analysis of fluorescence intensity for (B) Cx37, (C) E-Cad, and (D) Cx43 proteins on each developmental stage. LH treatment prevented the significant chemotherapy-induced reduction of three proteins beyond the secondary stage. Bar charts showed means and SD for each experimental group. Samples from n = 3 mice for control group and n = 5 mice for ChT and ChT+LH groups were analyzed. ap-value < 0.05 vs. control group; bp-value < 0.05 vs. ChT group.

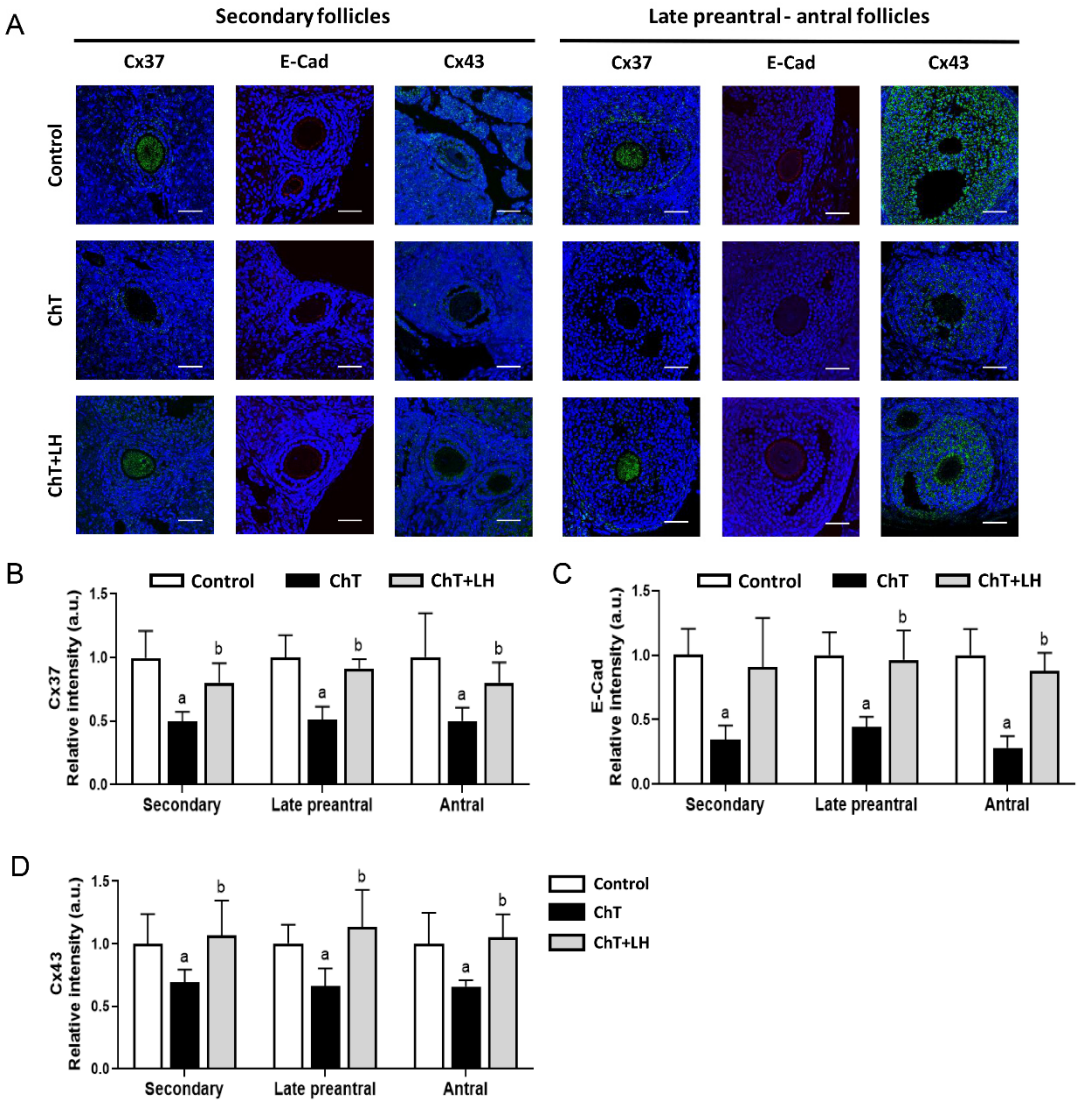

Figure 3. Immunofluorescence staining of the oocyte secreted factors GDF9 and BMP15. (A) Representative confocal images of secondary follicles on the left panel, and late preantral and antral follicles on the right one. Fluorescence staining showed nucleus in blue signal and the targeted molecules GDF9 and BMP15 in red and green signals, respectively. Scale bars: 50 μm.

Quantitative analysis of fluorescence intensity for (B) GDF9 and (C) BMP15 in late growing follicles. LH treatment avoided the decrease of fluorescence intensity induced by alkylating agents on both oocyte-secreted factors from the secondary stage. Bar charts showed means and SD for each experimental group. Samples from n = 3 mice for control group and n = 5 mice for ChT and ChT+LH groups were analyzed. ap-value < 0.05 vs. control group; bp-value < 0.05 vs. ChT group.

APPENDIX VII. PhD student's scientific contributions indirectly related to this thesis

1. International scientific publications

- Soriano MJ, **Del Castillo LM**, Subirá J, Herera A, Guerrero A, Gavilá J, Santaballa A, Herraiz S, Díaz-García C. "New insights into gene expression profiling of breast cancer tumours in patients undergoing ovarian stimulation for fertility preservation purposes." *In progress: manuscript prepared for submission*.
- Soriano MJ, **Del Castillo LM**, Martínez J, Lopez R, Subirá J, Herraiz S, Díaz-García C. "New approaches to assess the safety of letrozole supplementation during controlled ovarian stimulation for oocyte vitrification in early-stage hormone-sensitive breast cancer tumours." *In progress: manuscript prepared for submission*.

2. Works submitted to international conferences

2.1. Oral presentations

- Lopez R, Francés-Herrero E, Rodríguez-Eguren A, **Del Castillo LM**, Faus A, Pellicer A, Herraiz S, Cervelló I. "Murine Oocyte Maturation and Developmental Competence Using Biocompatible Hydrogel Based on Decellularized Bovine Ovarian Cortex." Presentation number: O-046. Conference: SRI 69th annual scientific meeting. City of event: Denver, CO (USA). Dates: 15/03/2022 – 19/03/2022. Organizing entity: Society for Reproductive Investigation (SRI).

2.2. Posters

- Soriano MJ, **Del Castillo LM**, Subirá J, Herera A, Guerrero A, Gavilá J, Santaballa A, Díaz-García C. "Characterization of the gene expression profile of breast cancer tumours in patients undergoing ovarian stimulation for fertility preservation purposes." Presentation number: P-481. Conference: ESHRE's 38th annual meeting. City of event: Milan (Italy). Dates: 03/07/2022 – 06/07/2022. Organizing entity: European Society of Human Reproduction and Embryology (ESHRE).
- Soriano MJ, **Del Castillo LM**, Martínez J, Herraiz S, Díaz-García C. "Controlled ovarian stimulation protocols for oocyte vitrification induce differential gene expression profiles in primary tumours of breast cance." Presentation number: P-446. Conference: ESHRE's 37th annual meeting. City of event: virtual. Dates:

28/06/2021 – 01/07/2021. Organizing entity: European Society of Human Reproduction and Embryology (ESHRE).

- Soriano MJ, **Del Castillo LM**, Lozoya V, Molina I, Díaz-García C. "Post-wash total motile sperm count as the most accurate predictor for live birth after intrauterine insemination." Presentation number: P-056. Conference: ESHRE's 35th annual meeting. City of event: Vienna (Austria). Dates: 23/06/2019 – 26/06/2019. Organizing entity: European Society of Human Reproduction and Embryology (ESHRE).